Automation in Architectural Photogrammetry

Line-Photogrammetry for the Reconstruction from Single and Multiple Images

Cover by Axel Smits

This PhD thesis is published under the same title in the series:

Publications on Geodesy 54
ISBN 90 6132 281 2
NCG, Netherlands Geodetic Commission
Delft, The Netherlands
www.ncg.knaw.nl

Automation in Architectural Photogrammetry – Line-Photogrammetry for the Reconstruction from Single and Multiple Images

Proefschrift

ter verkrijging van de graad van doctor
aan de Technische Universiteit Delft,
op gezag van de Rector Magnificus prof.dr.ir. J.T. Fokkema,
voorzitter van het College voor Promoties,
in het openbaar te verdedigen
op maandag 15 september 2003 om 10.30 uur
door

Franciscus Antonius VAN DEN HEUVEL

geodetisch ingenieur

geboren te Heerlen

Dit proefschrift is goedgekeurd door de promotor:
Prof.dr.ir. M.G. Vosselman

Samenstelling promotiecommissie:

Rector Magnificus, voorzitter
Prof.dr.ir. M.G. Vosselman, Technische Universiteit Delft, promotor
Prof.Dr.-Ing. W. Förstner, University of Bonn
Prof.Dr. L. van Gool, Katholieke Universiteit Leuven
Prof.Dr.habil. H.-G. Maas, Dresden University of Technology
Prof.dr.ir. P.J.G. Teunissen, Technische Universiteit Delft
Prof.dr.ir. M. Molenaar, International Institute for Geo-Information Science and Earth Observation (ITC)

Het paard draaft zijn manen vochtig

De vogel vliegt zijn vleugels vol

De mens sterft dorstig

Lucebert

Contents

Abstract

Automation in Architectural Photogrammetry –
Line-Photogrammetry for the Reconstruction from Single and Multiple Images

Frank van den Heuvel

Architectural photogrammetry has been practised for more than a century with the documentation of cultural heritage as its main objective. Since the introduction of the computer, and later the digital camera, research in photogrammetry aims at automation. This thesis reports on research on automation in architectural photogrammetry for efficient reconstruction of detailed building models from one or more – possibly widely separated – digital close-range images. This research is on the fringes of photogrammetry and computer vision. It treats topics frequently studied in computer vision in a photogrammetric way and offers new solutions. This approach is characterised by:

- Robust and direct solutions for approximate value computation
- Statistical testing of consistency of redundant information
- Integral least-squares adjustment of all information for optimal parameter estimation
- Quality control by statistical testing and error propagation
- Semi-automatic processing, aiming at a reliable solution with a minimum of user interaction
- Pre-calibration of the camera's used
- Exploitation of generic knowledge of the object shape
- Use of image lines as the basic type of observations

The research is presented in the form of a collection of papers published between 1997 and 2002. Furthermore, the methods described in the papers have also been applied to a reference set of images. The results of these experiments are presented in a separate chapter.

The demand for models of the built environment has increased due to the development of computer applications such as virtual and augmented reality, and computer games. In these applications the required accuracy of the models is not as high as in traditional applications of architectural photogrammetry, such as documentation of cultural heritage. Emphasis in research has shifted towards efficient production of computer models that show a high level of realism.

In this study, full automation of reconstruction from images is not aimed at. The reason is that for many years to come it is expected that user-interaction will be required for the reconstruction of well-structured building models. Therefore, a semi-automatic approach is chosen that exploits knowledge of the characteristics of the application. These characteristics can be summarised as regularities in the shape of the object, such as planar façades, rectangular and repeating structures in the form of windows, and shape symmetries. As a result many object edges will be straight and often their projections in the images show good contrast, which facilitates their automated extraction using image processing techniques. The automatically or manually extracted straight image line features are the main observations in the line-photogrammetric approaches presented in this thesis. Furthermore, the methods developed are characterised by the use of robust direct solutions for approximate value computation, followed by least-squares adjustment in which the knowledge of the shape of the building is processed together with the image line observations. This integral adjustment provides optimal estimates for the object model parameters and facilitates quality assessment.

A significant part of the research is on single image processing for object reconstruction and camera calibration. With the use of shape knowledge it is often possible to partially reconstruct a building from line observations in a single image. A method has been developed in which the conditions on the image line observations that result from knowledge on the related edges in object space are adjusted. The adjusted observations are used for reconstruction. This method is of importance because of the possibility to test the consistency of the acquired information during interactive modelling, even before object reconstruction. However, a disadvantage is the separate step for object reconstruction that complicates error propagation. Therefore, a line-photogrammetric bundle adjustment has been developed that allows the integral adjustment of image line observations of a single or multiple images in combination with object shape constraints. The point and plane parameters of a polyhedral boundary representation are the parameters in the mathematical model, while the object constraints that result from the object topology are simultaneously enforced.

It is common in photogrammetry to work with a calibrated camera. However, this is not possible when just one or a few historic images of a building are available, because information on the interior orientation is usually missing. Fortunately, it is often possible to derive important camera information using the conditions on the image lines that result from the object shape knowledge. A method that exploits parallelism and orthogonality of object edges has been developed for the estimation of parameters of interior orientation including lens distortion from one or more images. The least-squares adjustment applied allows for assessment of the precision of the estimates and their correlations. The precision of interior orientation parameters estimated using a single image is low compared to conventional multi-image calibration methods. The quality of the parameters considerably improves when image lines of multiple images are used, while correspondence between the images is not required for this method as is the case in conventional calibration methods.

Finding approximate image orientation is a major topic in photogrammetry. Two fundamentally different methods have been developed for image orientation. The first one makes use of the partial object reconstruction obtained from manual measurements in a single image as described previously. This reconstruction can be limited to one rectangle in object space. A direct solution for reconstruction from the projection of a rectangle in a single image has been investigated. When correspondence between two partial reconstructions is available, relative orientation between the two related images can be established, again with a direct solution. Similarly, exterior orientation of a single image can be established when sufficient object co-ordinates are known.

The second method for relative orientation is a highly automated one. It derives the rotations of the image relative to the object through edge extraction followed by vanishing point detection. Then a search procedure establishes correspondence and the relative position of two images in one step. This method has shown to be successful for highly convergent imagery of buildings and thus is a solution to the wide-baseline stereo problem. However, repeating structures in the building such as identical windows in combination with considerable differences in image scale for corresponding parts of the building may hinder a reliable correspondence detection. A few manually established correspondences may then be required.

Vanishing point detection uses clustering of image lines based on statistical tests of the intersection of three interpretation planes, i.e. the planes through the image lines and the projection centre. This method exploits both parallelism of object edges as well as orthogonality, and automatically labels image lines according to their orientation in object space. The success rate depends on the characteristics of the building and on factors such as the orientation of the image relative to the object. Vanishing point detection results have

been used for estimation of interior and relative orientation parameters. With the detection of at least two orthogonal object orientations an ambiguous rotation of the image relative to the building is found. The automated method for relative orientation resolves this ambiguity. This method exploits coplanarity of object features and detects object planes. In fact, a partial and approximate object reconstruction is retrieved as a by-product. Therefore, it is to be regarded as a first step towards automated reconstruction of a structured object model.

Future research in the direction of automated reconstruction has to aim at refining the object model by the detection of multiple object planes and their topologic relations. In such an approach the edges and points of the object model result from the intersection of object planes, while in the manual reconstruction approach the object edges and points result primarily from the intersection of interpretation planes.

The processing of images of the CIPA reference data set has demonstrated the capabilities and limitations of the developed methods for camera calibration, image orientation, and object reconstruction. Calibration of the camera was performed semi-automatically with five images of the reference data set. The results were compared with the camera information available from the reference data set. The maximum parameter difference was three times its standard deviation.
The two different methods for image orientation have been applied on four images taken at the corners of the building. The first one is based on the reconstruction of rectangles from a single image. Resulting orientations differ less than 4 degrees from the adjusted values derived in a bundle adjustment. With the second more automated method a correct approximate solution was obtained for all image pairs using two or three manually measured corresponding points. Full automation of relative orientation was not possible for all image pairs due to the repeating structures in the façades and for imagery where image scale differences were large.
An object model was reconstructed based on a line-photogrammetric bundle adjustment of manual line measurements in the same four images. Geometric object constraints made the reconstruction of occluded object points possible, improved regularity of the building model and strengthened the geometry of the network.

The research presented in this thesis contributes to the fields of photogrammetry and computer vision. However, emphasis is on photogrammetry where manual or semi-automatic measurement methods prevail and least-squares adjustment is the tool commonly applied for parameter estimation. The developed line-photogrammetric bundle adjustment model that allows the incorporation of object shape knowledge is the main contribution to this field. Computer vision is generally more focussed on automation, single image processing, and the use of uncalibrated cameras. Therefore, the methods developed for vanishing point detection, used for image orientation and camera calibration, and the methods developed for reconstruction from a single image are primarily in the field of computer vision. In conclusion, this thesis contributes to bringing photogrammetry and computer vision closer together, which will be beneficial to both fields.

Samenvatting

Automatisering in de architectuurfotogrammetrie –
Lijnfotogrammetrie voor de reconstructie uit enkele en meerdere beelden

Frank van den Heuvel

Architectuurfotogrammetrie wordt al meer dan een eeuw toegepast met als belangrijkste doel de documentatie van ons cultureel erfgoed. Sinds de introductie van de computer – en later de digitale camera – richt het onderzoek in de fotogrammetrie zich op automatisering. Dit proefschrift rapporteert over onderzoek naar automatisering in de architectuur-fotogrammetrie voor een efficiënte reconstructie van gedetailleerde gebouwmodellen met behulp van een of meer digitale beelden. Dit onderzoek bevindt zich op het grensvlak van fotogrammetrie en computer vision. Onderwerpen die in de computer vision vaak bestudeerd worden, worden hier op een fotogrammetrische manier benaderd. Deze aanpak wordt gekarakteriseerd door:

- robuuste en directe oplossingen voor de berekening van benaderde waarden;
- statistische toetsing op consistentie van redundante informatie;
- integrale kleinste-kwadraten vereffening van alle informatie voor een optimale parameterschatting;
- kwaliteitscontrole door statistische toetsing en foutenvoortplanting;
- semi-automatische verwerking, gericht op het verkrijgen van een betrouwbare oplossing met een minimum aan interventie door de operateur;
- het kalibreren van de camera voorafgaand aan de reconstructie;
- gebruik van generieke kennis van de objectvorm;
- gebruik van lijnen in de beelden als het belangrijkste waarnemingstype.

Het onderzoek wordt gepresenteerd als een verzameling artikelen die gepubliceerd zijn in de periode van 1997 tot en met 2002. Bovendien zijn de in de artikelen beschreven methodes toegepast op een referentiedataset met opnamen van het stadhuis in Zürich. De resultaten hiervan worden in een apart hoofdstuk besproken.

De vraag naar computermodellen van de bebouwde omgeving is toegenomen als gevolg van computertoepassingen zoals *virtual reality*, *augmented reality* en computerspelletjes. De benodigde precisie is in deze toepassingen niet zo hoog als in de traditionele toepassingen van de architectuurfotogrammetrie, zoals de documentatie van historische gebouwen. Het zwaartepunt in het hedendaags onderzoek is daarom verschoven naar methoden voor de efficiënte productie van computermodellen die er zo realistisch mogelijke uitzien.

In het onderzoek dat onderwerp is van dit proefschrift wordt niet gestreefd naar volledige automatisering. De reden is dat niet verwacht mag worden dat binnen een aantal jaren de volledig automatische reconstructie van goed gestructureerde gebouwmodellen mogelijk wordt. Daarom richt het onderzoek zich op een semi-automatische aanpak waarbij gebruik gemaakt wordt van kennis over de karakteristieken van de toepassing. Deze karakteristieken zijn bijvoorbeeld de regelmatigheden in de objectvorm zoals het vlak zijn van gevels, rechthoekige en herhalende structuren in ramen en deuren en vorm-symmetrieën. Veel gebouwlijnen zullen recht zijn en vaak een goed contrast in de beelden laten zien wat de automatische extractie met behulp van beeldverwerkingstechnieken vergemakkelijkt. De automatisch of handmatig geëxtraheerde rechte beeldlijnen vormen het belangrijkste waarnemingstype in de lijnfotogrammetrische benadering in dit proefschrift. Bovendien worden de methoden gekenmerkt door het gebruik van robuuste, directe oplossingen voor de berekening van benaderde waarden gevolgd door een kleinste-

kwadraten vereffening waarin de kennis over de gebouwvorm samen met de lijnwaarnemingen wordt verwerkt. Deze integrale vereffening levert optimale schattingen voor de modelparameters.

Een belangrijk deel van het onderzoek richt zich op het gebruik van een enkele opname voor de objectreconstructie en de camerakalibratie. Door het gebruik van vormkennis is het vaak mogelijk om een gebouw gedeeltelijk te reconstrueren op basis van lijnmetingen in een enkele foto. Hiervoor is een methode ontwikkeld waarin de voorwaarden op de lijnmetingen die volgen uit de kennis over de gerelateerde lijnen van het object worden vereffend. De vereffende waarnemingen worden vervolgens gebruikt voor de reconstructie. Het belang van deze methode ligt vooral in de mogelijkheid om op meetfouten te controleren gedurende het interactief modelleren, nog voordat de objectreconstructie mogelijk is. Een nadeel is echter dat er een aparte stap nodig is voor de reconstructie, zodat de foutenvoortplanting complexer wordt. De later ontwikkelde lijnfotogrammetrische bundelvereffening kent dit nadeel niet. Met deze methode is de integrale vereffening mogelijk van lijnmetingen van een enkele of meerdere opnamen en vormvoorwaarden. De punt- en vlakparameters van een veelvlakbeschrijving (*B-rep*) zijn de objectparameters van het wiskundige model, terwijl de voorwaarden die het gevolg zijn van de objecttopologie in de vorm van waarnemingen in het model opgenomen zijn.

In de fotogrammetrie is het gebruikelijk om met een gekalibreerde camera te werken. Dit is echter niet mogelijk wanneer er slechts een of enkele historische opnamen van een gebouw beschikbaar zijn, omdat dan informatie over de camera meestal ontbreekt. Echter, vaak kan belangrijke informatie over de camera afgeleid worden uit de voorwaarden op de lijnmetingen die volgen uit de beschikbare of veronderstelde objectkennis. De hiervoor ontwikkelde methode maakt gebruik van parallellisme en orthogonaliteit van objectlijnen voor de schatting van inwendige oriënteringsparameters, inclusief lensvertekening. De toegepaste kleinste-kwadraten vereffening maakt een schatting van de precisie van de parameters mogelijk. Wordt de methode met een enkele opname toegepast dan blijkt de precisie van de parameters laag te zijn in vergelijking met conventionele kalibratiemethoden. De ontwikkelde methode kan ook met meerdere beelden gebruikt worden. De precisie van de geschatte parameters verbetert dan aanzienlijk, terwijl correspondentie tussen de beelden niet nodig is.

Het vinden van de stand en de positie van beelden – het oriënteren – is een belangrijk onderwerp in de fotogrammetrie. Twee nieuwe methoden voor het oriënteren worden in dit proefschrift beschreven. De eerste maakt gebruik van gedeeltelijke objectreconstructie op basis van handmatige metingen in één opname. Deze reconstructie kan zich beperken tot een enkele rechthoek. Wanneer correspondentie tussen uit twee beelden gereconstrueerde rechthoeken bekend is, kan de relatieve oriëntering van beide opnamen worden bepaald. Ook is het mogelijk om de uitwendige oriëntering van een opname te bepalen wanneer de rechthoek in 3D bekend is.

De tweede, geautomatiseerde methode voor oriënteren bepaalt eerst de oriëntatie van een opname ten opzichte van het object met behulp van lijnextractie en verdwijnpuntdetectie. Vervolgens worden de relatieve positie en correspondentie gelijktijdig gevonden met een zoekprocedure. Deze methode is succesvol gebleken voor sterk convergente opnamen van gebouwen en biedt daarmee een oplossing voor het vraagstuk dat in de computer vision bekend staat als *wide-baseline stereo.* Wel kunnen herhalende structuren in de gevels, zoals identieke ramen in combinatie met grote schaalverschillen tussen de opnamen, een betrouwbare oplossing in de weg staan. Dan zijn enkele handmatig verkregen correspondenties nodig.

De ontwikkelde methode voor verdwijnpuntdetectie groepeert rechte lijnen in beelden op basis van statistische toetsen van snijdingsvoorwaarden van drie zogenaamde

interpretatievlakken. Dit zijn de vlakken die opgespannen worden door de beeldlijnen en het projectiecentrum van de opname. Deze methode gebruikt parallellisme en orthogonaliteit van objectlijnen en groepeert de lijnen naar hun oriëntatie in de objectruimte. Het succes hangt af van de karakteristieken van het gebouw en van andere factoren zoals de oriëntatie van de opname ten opzichte van het gebouw. Verdwijnpuntdetectie is gebruikt in de hiervoor genoemde methoden voor het schatten van inwendige en uitwendige oriënterings-parameters. Met de detectie van tenminste twee loodrechte objectrichtingen wordt een meerduidige rotatie van de opname ten opzichte van het gebouw gevonden. De automatische methode voor relatief oriënteren lost deze meerduidigheid op en gebruikt de coplanariteit van lijnen in een gevel om gevelvlakken te detecteren. In feite wordt een gedeeltelijke, benaderde objectreconstructie verkregen als een bijproduct. Daarom kan deze methode voor relatief oriënteren gezien worden als een eerste stap naar de automatische reconstructie van een gestructureerd objectmodel.

Toekomstig onderzoek naar automatische reconstructie dient zich te richten op het detailleren van het objectmodel door de detectie van meerdere objectvlakken en hun topologische relaties. In een dergelijke aanpak worden de hoeken van het objectmodel gevonden door het snijden van objectvlakken, terwijl in een handmatige reconstructie de hoeken in de eerste plaats worden gevonden door het snijden van interpretatievlakken.

Het verwerken van de beelden van de referentiedataset heeft de mogelijkheden en beperkingen van de ontwikkelde methoden voor camerakalibratie, beeldoriëntatie en objectreconstructie gedemonstreerd. Camerakalibratie werd semi-automatisch uitgevoerd met vijf beelden. De resultaten werden vergeleken met de camerainformatie van de referentiedataset en lieten een goede overeenstemming zien.
De twee methoden voor oriënteren zijn toegepast op vier beelden die op de hoeken van het gebouw genomen waren. De eerste oriënteringsmethode maakt gebruik van met een enkele foto gereconstrueerde rechthoeken. De gevonden oriënteringen verschilden minder dan 4 graden van de waarden gevonden in een lijnfotogrammetrische bundelvereffening. Met de tweede, meer automatische methode werd een goede benaderde oplossing gevonden voor alle beeldparen met gebruikmaking van twee of drie handmatig gemeten corresponderende punten. Volledige automatisering van de relatieve oriëntering bleek niet mogelijk voor alle beeldparen als gevolg van de zich herhalende structuren in de gevels en grote schaalverschillen tussen en in de beelden.
Een gebouwmodel werd gereconstrueerd op basis van een lijnfotogrammetrische bundelvereffening van handmatige lijnmetingen in dezelfde vier beelden. Geometrische objectvoorwaarden maakten de reconstructie van verdekte objectpunten mogelijk, verbeterden de regelmatigheid van het gebouwmodel en versterkten de geometrie van het netwerk.

Het in dit proefschrift gepresenteerde onderzoek draagt bij aan zowel de fotogrammetrie als de computer vision. De nadruk ligt op de fotogrammetrie waar handmatige of semi-automatische meetmethoden de overhand hebben en de kleinste-kwadraten vereffening de standaardmethode is voor parameterschatting. De ontwikkelde lijnfotogrammetrische bundelvereffening die de verwerking van kennis over de objectvorm mogelijk maakt, is de belangrijkste bijdrage op dit vakgebied. Computer vision is meer gericht op automatisering, enkelbeeldverwerking en het gebruik van ongekalibreerde camera's. Daarom zijn de methoden ontwikkeld voor verdwijnpuntdetectie, gebruikt voor oriënteren en camera-kalibratie, en de methoden ontwikkeld voor de reconstructie op basis van één beeld, in eerste instantie tot de computer vision te rekenen. Concluderend kan gesteld worden dat dit proefschrift bijdraagt tot het nader tot elkaar brengen van de twee disciplines, wat beide ten goede komt.

1 Introduction

1.1 Scope and premises

Architectural photogrammetry is the oldest branch of photogrammetry. It was practised by Alfred Meydenbauer (1834-1921) more than a century ago (Luhmann, 2000), (Albertz and Wiedemann, 1997). Many of his photographic plates are still kept in the Meydenbauer Archives near Berlin. These glass plates have a size of up to 40 by 40 centimetre and were used for the extraction of metric information, and more general, for the documentation of historic buildings. At that time the efficiency and safety of the data acquisition were considered as the main advantages of photogrammetry for this application. The restitution was performed mainly graphically, simplified by vertical orientation of the plates during photography.

Although Meydenbauers methods became outdated with the introduction of the stereo plotter, only in the last decade did the potential for efficiency improvement in architectural photogrammetry increase significantly due to the advent of digital photography. There are two main reasons for this potential. Firstly, image acquisition with a digital camera is quick and cheap. However, resolution cannot (yet) compete with the Meydenbauer glass plates. Secondly, with images directly available in a computer, digital image processing can be applied to support the extraction of the required information. Especially in the case of object modelling, the image acquisition phase is much less labour-intensive than the information extraction phase, and thus research is to concentrate on the second phase. The research topic of this thesis is the automation of architectural photogrammetry aiming at efficiency in modelling of buildings from images. When developments in this field result in a considerable cost reduction, numerous applications for this technique come in view. Examples are virtual and augmented reality applications for maintenance, education, or facility management, and computer games, additional to a more extensive use for documentation of cultural heritage.

Before formulating the objectives of this study more precisely in the next section, the scope of the research is detailed with a presentation of the premises that relate to the camera used, the images and their configuration, and the object and 3D model characteristics.

Camera
There are no requirements for the digital camera, as long as it is pre-calibrated, or the developed procedures presented in this thesis allow an estimation of the interior orientation parameters to a sufficient level of precision. Depending on the application at hand, this level might not be reached when using a video camera. Two important error sources typical for video imagery are not addressed here. They are image scale difference between the column and row direction, and interlacing effects (line jitter). Also resolution of video imagery is low (0.3×10^6 pixels). Resolution of the digital images used in the experiments described in chapter 2 and 3 is in the order of 1.5×10^6 pixels. Also digitised analogue imagery could be used. However, image plane deformations are not accounted for and are to be removed in a pre-processing step, as far as possible. Depending on the characteristics of the imagery, focal length, principle point, and lens distortion can be estimated using the image data.

Image configuration
Images are assumed to be taken with a handheld camera. In practice images are often taken at eye-level, which is between 1.5 and 2 meters above the ground, although this is not a requirement. However, for the procedure developed for automated relative orientation the angle between the optical axis and the vertical direction is assumed to be at least 45 degree (Heuvel, 2002). Procedures have been developed for the camera calibration and reconstruction from a single image. The information that can be extracted from a single

image is dependent on its orientation relative to the object. More than one image is required for the reconstruction of a complete all-around object model. It is also advisable to use more than one image because of the improvement in quality (especially reliability), image interpretation, reduced occlusions, and improved texture mapping. A minimum image configuration is one with an image at every corner of the building, each image showing the whole building. This type of configuration is examined in the case study described in chapter 3. In general, the number of images to process is to be minimised because of efficiency considerations (see the next section). This implies strongly convergent imagery.

Object characteristics
Although architectural photogrammetry is the topic of this thesis, the methods described are not only suitable for image-based reconstruction of buildings, but also for the reconstruction of other man-made objects that have the following interrelated characteristics:
- Straight, parallel, perpendicular, and coplanar object edges
- Repeating structure and shape symmetries
- Adequate object description through a polyhedral model

These shape characteristics are to be inferred from the imagery at hand, in an automatic or manual way, and result in the formulation of hypotheses. These hypotheses are to be statistically tested and utilised for the reconstruction through their integration in a photogrammetric bundle adjustment that facilitates the assessment of the quality of the 3D model. For the architectural application the use of the above-mentioned shape characteristics implies the use of basic knowledge and assumptions on the construction of the building.

Object model
For the requirements for the reconstructed computer model, the following premises have been adopted:
- The 3D reconstruction is represented by a polyhedral boundary representation (B-rep) in a model co-ordinate system.
- The reconstruction is highly structured; one or a few faces in the boundary representation represent entities such as façades, doors, and windows of the building.
- No control, i.e. no a priori object co-ordinates are available. Possibly orientation information is available, such as the assumption that the walls are vertical. Furthermore, application of a scale factor or its estimation from known distances in order to scale the model is optional.

Architectural photogrammetry is a branch of photogrammetry with applications ranging from documentation of historic sites to modelling for virtual reality. In the first application the emphasis is on accuracy and completeness while in the second application realism of the model plays a more important role. With the extensive use of object shape knowledge, this research concentrates on efficient creation of building models and does not aim for the highest accuracy possible. However, the assessment of the quality of the model is important in virtually all applications because it allows using a minimum amount of information for reaching a preset quality level.

1.2 Objective

The overall objective of the research reported in this thesis is formulated as follows:

To improve the efficiency of the photogrammetric reconstruction of polyhedral object models of buildings and assess the quality of these models. Efficiency improvement is sought through the integration of generic object knowledge in a line-photogrammetric approach for reconstruction.

The terms used in the above formulation of the objective are discussed hereafter in order to clarify the objective.

Efficiency
Automation of object reconstruction is a goal frequently encountered in the field of photogrammetry and computer vision. However, a highly structured reconstruction, as is aimed for in this study, is very difficult to obtain in an automatic way and therefore we cannot expect to be able to do without image interpretation by a human operator. Use of object knowledge implies use of additional information that reduces the required number of images for reconstruction on a pre-set quality level. A reduction of the number of images improves the efficiency of the reconstruction, assuming that inferring the object knowledge semi-automatically is more efficient than manually processing additional images. Only when a fully automatic procedure is applied the number of images used is almost irrelevant. However, full automation can only be achieved when an unstructured reconstruction is aimed at. An example of a successful approach for automated unstructured reconstruction from an image sequence is found in (Pollefeys et al., 2000).

Photogrammetric reconstruction
The term *photogrammetric* points to the use of images taken with a pre-calibrated metric camera or a camera with a stable interior orientation of which the calibration parameters are determined using the same imagery as available for the reconstruction, either in a pre-processing step or simultaneously with the metric reconstruction (so-called self-calibration). Furthermore, the term *photogrammetric* implies the use of least-squares adjustment of redundant information, and an assessment of the quality achieved. The reconstruction is virtual, i.e. in the form of a computer model derived from the images of the real object.

Line-photogrammetric
This specification of the photogrammetric approach points to the use of lines in image space as the basic type of observations. Here only the use of straight image lines – represented by two endpoints – is investigated. This is in contrast with traditional photogrammetric approaches that are point-based. Often the term line-photogrammetry also implies the use of a parameterisation for the edges in object space. This is not the case here. Here the 3D-co-ordinates of points and possibly the parameters of planes are stored together with the object model topology.

Polyhedral object models
The research is limited to applications where a polyhedral object model in the form of a boundary representation describes the object well enough for practical use. The research concentrates on architectural photogrammetry; an application field where this is generally true. The use of polyhedral object models is to be regarded as applying a form of object knowledge.

Generic object knowledge
Many man-made objects have a shape that is not only polyhedral, but very regular as well. This kind of information on the shape generally improves the quality of the reconstruction considerably and can even be essential for the reconstruction. A layman can infer it from images of the object, although an operator with specific domain knowledge is expected to be more effective.

Quality
Quality is quantified by precision and reliability parameters. Quality is to be assessed in order to verify that a certain required quality level is reached. This is especially important when reconstruction from a few images or even one image is investigated.

1.3 Related research

The scope and objective presented in the previous sections direct the search for related research. Related research is found in the fields of photogrammetry and computer vision.

Photogrammetry
The use of object shape knowledge is the main characteristic of this research. Other characteristics are related to the use of object knowledge; the assumption of straight object edges leads to the use of lines in image space because straight object edges project to straight image lines as long as lens and image plane distortions can be neglected. The presence of geometric relations between the object edges directs the research to topics such as vanishing point detection and single image reconstruction. These topics are not frequently studied in the photogrammetric community. This was observed more than ten years ago by Williamson and Brill (Williamson and Brill, 1990) and is confirmed by the contents of recent textbooks in photogrammetry. Single image processing is often limited to image rectification (e.g. (Kasser and Egels, 2002), section 4.1; (Mikhail et al., 2001), section 4.1) or resection using known 3D-co-ordinates of points (e.g. (Schenk, 1999), section 15.2.1; (Mikhail et al., 2001), section 5.3). This is also reflected in textbooks in the field of close-range photogrammetry (Luhmann, 2000), (Atkinson, 1996). However, in (Luhmann, 2000) section 4.5 the use of straight lines is explicitly discussed, while in (Schenk, 1999) lines – not necessarily straight – are used as features for image orientation. In appendix D of (Mikhail et al., 2001) a mathematical description of line features in image and object space is presented. In this book also the vanishing point is defined (section 2.3). In (Kraus, 1997) section 4.7.2 the use of line features for the determination of interior and relative orientation using object shape knowledge is discussed.

In 1988 the interest of the photogrammetric community for the use of line features was revived with papers published at the ISPRS (International Society for Photogrammetry and Remote Sensing) congress in Kyoto (Mulawa and Mikhail, 1988), (Tommaselli and Lugnani, 1988). In fact, this interest in line features stems from the early days of photogrammetry when graphical methods were used for restitution. Since the 1980's line-photogrammetry for aerial as well as close-range applications was studied more frequently and by researchers all over the world (Zielinski, 1993), (McGlone and Shufelt, 1994), (Petsa and Patias, 1994), (Gülch, 1995), (Patias et al., 1995), (Heikkinen, 1995), (Schwermann, 1995), (Wiman and Axelsson, 1996), (Mikhail and Weerawong, 1997), (Chen and Shibasaki, 1998), (Streilein, 1999), (Vosselman and Veldhuis, 1999), (Smith and Park, 2000), (Tommaselli, 2000), (Grussenmeyer and Khalil, 2002), (Habib et al., 2002b).

In many of these line-photogrammetric approaches, the use of object knowledge, such as geometric relations between object edges, is accommodated. However, not much photogrammetric research is conducted on other topics discussed in this thesis, such as the use of object shape knowledge for single image camera calibration and reconstruction. Single image reconstruction is investigated in (Braun, 1994) and recently in (Khalil and Grussenmeyer, 2002). In several approaches single image reconstruction is possible as part of a multiple image approach (Vosselman and Veldhuis, 1999), (Lang and Förstner, 1996). These approaches introduce the object shape knowledge in the form of parameterised object models. In many cases the model parameters (apart from scale) can be estimated from measurements in a single image. In (El-Hakim, 2000) object shape constraints, such as perpendicularity and symmetry are applied for reconstruction from a single close-range image. Single image camera calibration is treated in (Ethrog, 1984), while multiple image camera calibration using straight-line features is presented in (Habib et al., 2002a). Automation of image orientation is an important research topic in photogrammetry. In the review paper by Heipke (Heipke, 1997) three approaches for automation of relative

orientation that make use of line features are described. None of them is implemented in a commercial system and only one approach can cope with close-range imagery (Wang, 1998).

In conclusion, a trend towards the use of linear features is observed in photogrammetry. However these features are not yet frequently used in photogrammetric practice and especially their use for camera calibration, image orientation, and object reconstruction in combination with geometric object information is still a popular research topic.

Computer vision

In the field of computer vision the use of line features, single image object modelling, single image camera calibration[1], and vanishing point detection are popular topics. This is reflected in textbooks (Hartley and Zisserman, 2000), (Faugeras, 1993) as well as in the number of papers on these topics. In the last decade the fields of computer vision and photogrammetry have come closer. In recent conferences of ISPRS, researchers from the computer vision community have made significant contributions (e.g. (Gool et al., 2002), (Pollefeys et al., 2002), (Fua et al., 2002), (Navab, 2002), (Appel and Förstner, 2002)). Photogrammetrists study and contribute to methods developed in computer vision (e.g. (Förstner, 2000), (Grussenmeyer and Khalil, 2002)). These methods are based on projective geometry where the relation between image and object space co-ordinate systems is usually formulated in homogeneous co-ordinates. This formulation has not been adopted in this thesis, however, in all formulations image space is treated as a 3D space where an image point is represented by a 3D vector with the projection centre as the origin. A rigorous least-squares adjustment of the observations and error propagation to assess the precision of the model parameters is applied. Least-squares bundle adjustment is not the most common optimisation technique in computer vision, although it's benefits were recently recognised (El-Hakim, 2002).

Automation in reconstruction of buildings is a frequent research topic in computer vision. The reconstruction of an unstructured object model from a sequence of uncalibrated (video) images is considered to be a solved problem (Gool et al., 2002), (Pollefeys et al., 2000). Research challenges are now found in the development of wide-baseline approaches in which a few still images are used that differ considerable in viewing angle (in contrast to the use of image sequences with short baselines between consecutive images) (Matas et al., 2000), (Lourakis et al., 2000), (Schaffalitzky and Zisserman, 2001), (Pritchett and Zisserman, 1998), (Tuytelaars and Gool, 2000), (Baumberg, 2000). Looking at research into image-based reconstruction of architecture, semi-automatic or interactive approaches are most frequent (Debevec et al., 1996), (Shum et al., 1998), (El-Hakim, 2002). Research on single image reconstruction is found in (Brauer-Burchardt and Voss, 1999), (Criminisi et al., 1999), (Sturm and Maybank, 1999), (Guillou et al., 2000), (Jelinek and Taylor, 2001). The next step is to automatically derive a structured object model from single or widely separated views. Research in this direction is presented in (Dick et al., 2000), (Bartoli et al., 2001), (Werner and Zisserman, 2002).

Single image camera calibration is more frequently studied in computer vision than in photogrammetry. Examples of approaches of single image camera calibration from the computer vision field using geometric constraints on object edges can be found in (Brauer-Burchardt and Voss, 2000) and (Eelaart and Hendriks, 1999). Camera calibration is often studied in combination with object reconstruction (Guillou et al., 2000), (Wilczkowiak et al., 2001). Vanishing point detection has a long history as a topic in its own right (Collins and Weiss, 1990), (Straforini et al., 1990), (Brauer-Burchardt and Voss, 2001), (Rother, 2002), or

[1] Here the photogrammetric meaning of the term *camera calibration* is used, i.e. the determination of interior orientation (intrinsic) camera parameters.

is investigated in combination with its use for camera calibration, image orientation, or object reconstruction.

In conclusion, especially in the last years the research topic of automation in reconstruction of architecture from uncalibrated images has drawn considerable interest from the computer vision community. This implies interest in topics such as automated camera calibration, image orientation, and use of a priori knowledge on the object's shape as well. Research in photogrammetry is mostly concentrated on aerial imagery. Close-range photogrammetry is overlapping computer vision as far as the applications are concerned. Observing the contributions of computer vision to aerial photogrammetry (Faugeras et al., 1998); (Baillard et al., 1999), computer vision can be distinguished from photogrammetry mainly by the approach chosen. This leads to the conclusion that this thesis deals with topics that primarily belong to the computer vision field, but the approach – presented in the next section – is primarily a photogrammetric one.

1.4 Approach

The improvement in efficiency of the modelling using images is strived for by automating the photogrammetric process. In this section the importance of a priori knowledge for automation is explained, as well as the reason for concentrating on the automation of image orientation rather than object modelling. Furthermore, the choice is discussed for using image line features as the basic type of observation, instead of image points as used in conventional photogrammetric methods.

The level of automation possible depends on the a priori knowledge available
Exploiting the characteristics of the application increases the level of automation. Although in architectural photogrammetry the images are generally well structured, it is not expected that full automation of the reconstruction of a structured object model is possible. This is in contrast to other application fields in which artificial targets or textured light are applied, as in some industrial or medical applications of photogrammetry. In general, the level of automation possible increases with the amount of a priori knowledge available. This can be knowledge on the design of an artificial target, as well as knowledge about the objects to be modelled, for instance in the form of a database with CAD models.

Automation of modelling is more difficult than automation of image orientation
As in aerial photogrammetry, the image orientation step of the photogrammetric process has better chances for being automated than the object modelling itself. For automatic modelling a higher level of image understanding is required than for image orientation. The image features required for modelling, such as the edges of a polyhedral object, are difficult to extract automatically because these features often do not show good contrast in the images, and usually they drown in an abundance of features of which most are not suitable for modelling. However, a large percentage of these features can be used for automating image orientation and camera calibration.

Through image interpretation the operator is able to select and extract (measure) those features from the images that relate directly to the features of the object model. In conventional photogrammetry the operator is looking for corner points in the images that directly relate to vertices of the boundary representation that is being constructed. In this thesis the emphasis is on line features that relate to object edges. However, the principle is the same. Close examination of architectural imagery leads to the conclusion that many of these edges show poor contrast in the images, while many other edges – that do not relate to features of the object description the operator has in mind – are clearly visible (see the example in Figure 1). The latter type of edges is likely to be extracted by image processing

(an edge detector). These automatically extracted line features are the major input to the procedures for image orientation described in this thesis.

Figure 1: Original image (left). Image overlaid with automatically extracted lines (right). Note the low image contrast on the corner edge where the two façades meet.

Why choose a feature-based approach?

The choice for a feature-based approach instead of an area-based approach is supported by the characteristics of the application. The façade of a building is planar in principle, but looked at in detail there are many deviations from a single plane. For instance, windows and doors are usually not in the plane of the façade itself. In fact, these deviations, although small relative to the dimensions of the building, often lead to good contrast in the images in the form of straight lines. This is an important reason for the presence of line features in images of buildings. Most buildings do not have many edges, i.e. corners where façades meet, and these edges regularly do not show good contrast in the images. They can be measured manually, however, an edge detector will often fail to extract these image lines. Therefore, the automatic procedures presented in this thesis use extracted line features that are expected to relate to object edges in or close to a façade.

The discontinuities in the shape of the façades are a major reason for the presence of linear features in the images. At the same time the object discontinuities make an area-based approach less suitable because in such an approach the object surface is assumed to be continuous and often locally approximated by a plane. When the baseline between two images is relatively small – like in a stereo configuration – an area-based approach is still possible depending on the size of the discontinuities and the adopted base-height ratio. In case of a video image sequence the base-height ratio is so small that area-based approaches are preferred. Here we aim at the use of a few convergent images with a base-height ratio in the order of 1. Projective transformation – or affine transformation, often used as an approximation of a projective transformation – cannot be used for relating the content of consecutive images due the discontinuities in the object shape. Line and point features are invariant to projective transformation. However, only a subset of the automatically extracted line features in consecutive images corresponds, due to the fact that edges visible

in one image can be occluded in another. Occlusion is also the reason for considerable differences in contrast of the same object edge in different images (Figure 2, edges on the right side of the windows).

Figure 2: Parts of an image from the left (top) and one from the right (bottom), note the image scale difference. Automatically extracted image lines of the two windows in the upper left corner of the images are shown on the right.

Why prefer line to point features?

Above, the presence and use of line features was emphasised. There are several reasons for preferring line features to point features:

- A line is represented by more pixels than a point feature and thus more precisely located in the direction perpendicular to it.
- In contrast to a point, a line contains information on the object topology; an edge connects object points.
- In contrast to a point, a line contains orientation information of the related object edge.
- Edges have to be only partly visible in the images. Object points can be occluded; occlusion of object edges is often only partial.

- Different parts of an object edge can be measured in different images. The correspondence requirement of points is therefore relaxed in the case of lines.

The (interrelated) disadvantages of line features compared to point features are:
- A line is not precisely located in the direction parallel to it, while the precision of image point location is much more homogeneous.
- There is no redundancy in the intersection of two interpretation planes, while there is in the intersection of two rays.
- Although an unbounded image line and a point are both represented by two parameters, a network with image point observations is geometrically stronger than one with image lines.

These disadvantages apply when individual edges are reconstructed in 3D. However, they vanish when constraints on the intersection of object lines are applied, as is the case in the reconstruction methods described in this thesis. In conclusion, line features are favoured over point features in the application at hand.

Automation of the image orientation steps

As stated previously, it is not realistic to expect that full automation of the reconstruction of a highly structured description of the building will be possible. Therefore, the automation concentrates on the first steps of the photogrammetric reconstruction, i.e. the orientation of the images. The orientation process distinguishes interior, relative, and exterior orientation. Interior orientation involves camera calibration; the determination of the focal length, principle point, and elimination of lens distortion.

Relative orientation between two images involves five parameters, three for the rotation of the second image relative to the first, and two parameters for relative position (the distance between the two images, i.e. scale, remains undetermined). The approach for determining relative orientation presented in this thesis is based on vanishing points and therefore rotations are determined for each image relative to the three main orientations of the building. Thus, the rotation part of the relative orientation can be regarded as absolute.

The last orientation step – the exterior orientation – includes six parameters, the five parameters of relative orientation and scale as the sixth parameter. Although we aim at an unscaled object model, exterior orientation (relative to this model) is to be determined for any other image needed to extend and improve the model.

The methods presented in this thesis are capable of determining the photogrammetric orientations described above in a highly automatic way. As a by-product, parts of the object faces are detected and reconstructed. With the orientations performed, the operator can concentrate on the image interpretation for modelling. Furthermore, approximate values are available that are required for the least-squares bundle adjustment.

Manual line measurements for modelling

The procedures that have been developed for image orientation result in a partial and coarse object model. Such a model is derived in a highly automated way, however, it cannot be expected to meet the requirements of most projects. Apart from the fact that a good starting point has been reached for future research in automated modelling of buildings from close-range imagery, we have to fall back on manual measurements and image interpretation in order to obtain a model of sufficient quality. Advantages of using image lines have been listed above. For an operator it is an advantage to measure edges at locations in the images where they show good contrast. A semi-automatic approach is to be investigated in which the operator selects automatically extracted edges, or guides the image line extraction by roughly indicating the location of the lines. The operator should also have the possibility to measure points when they are sufficiently well defined and visible in the images.

Development from manual to (semi-)automatic processing

In an application as architectural photogrammetry fully automated procedures will not be successful in all cases. This is true not only for the reconstruction of a structured object

model, but also for the image orientation, especially when using widely separated views. The main reasons are the presence of repeating structures in the scene and occlusions. Therefore, the research started off with the development of procedures that make use of manual measurement. In a later stage automation of several procedures was investigated, however, manual interaction for correction of automatically derived results, or for supplying additional information is incorporated in these (semi-) automatic procedures.

Development from single image to multiple image processing.
A considerable part of the research has been devoted to information extraction from a single image. Especially when using object knowledge, information about the camera, its orientation relative to the object, or a partial object model can be derived from a single image. However, to meet the requirements of most projects – such as a certain level of precision or a complete object model – multiple images are needed. In order to be able to fully exploit the geometric information in images when object shape knowledge is available, it is considered important to investigate single image as well as multiple image processing. The approach from single to multiple image processing is also found in (Hartley and Zisserman, 2000).

1.5 Overview

The research is presented in this thesis as a collection of nine selected papers published between 1997 and 2002. These papers make up chapter 2. In chapter 3 the results of the application of the methods presented in the papers on a reference data set are presented. Chapter 4 contains a discussion on future work and the conclusions. In this section the papers and the relations between them are outlined in chronological order.

The research in architectural photogrammetry reported in this thesis started off with an investigation into methods for image orientation using geometric object knowledge, in particular using the image of a rectangular structure in object space (Heuvel, 1997) (thesis section 2.1). Here, the interior orientation of the image is assumed to be known. Already in this stage of the research the potential of line measurements in a single image in combination with object shape information for tasks such as image orientation, object reconstruction, and camera calibration was apparent. A direct solution for the computation of the focal length from an image of a rectangle was investigated.

Next, approaches for modelling of buildings from multiple images were investigated where both interior orientation and image orientation were considered to be known at least approximately (Heuvel and Vosselman, 1997) (thesis section 2.2). This research concentrated on the geometric modelling technique, the object parameterisation, and the mathematical model to apply. A polyhedral B-rep (Boundary representation) and CSG (Constructive Solid Geometry) were both considered for object modelling. However, a choice for object parameterisation is avoided in the mathematical model because this model uses condition equations with image observations only. This approach has several advantages, but also disadvantages. Advantages are the absence of parameters in the model and therefore there is no need for approximate values. Furthermore, it allows least-squares adjustment and statistical testing in an early stage of the modelling process, without the requirement that the object model be reconstructed. However, disadvantages such as the requirement of a separate step for object model computation from adjusted observations, and the fact that the formulation of a complete set of independent condition equations can be problematic, speak against a mathematical model with condition equations only.

Straight image edge extraction and vanishing point detection are considered to be crucial first steps towards automation of image orientation and object reconstruction in applications

where parallel object edges are dominant (Heuvel, 1998b) (thesis section 2.3). It can also be regarded as a procedure for the detection of parallelism of object edges. Later, also the use of vanishing point detection for automated camera calibration as well as relative orientation were explored (Heuvel, 1999a), (Heuvel, 2002). The developed procedure for vanishing point detection is built on the image line grouping based on statistical tests of the intersection of three interpretation planes. This is in contrast to other procedures often based on grouping of intersections of two interpretation planes (or image lines). The developed procedure avoids the choice of a parameter space and the parameters involved in its binning. Another characteristic of the procedure is the use of the assumption that three perpendicular main object orientations are present. This greatly improves the detection of the second and third vanishing point. However, it can only be used in cases where the interior orientation of the image is known. In section 3.2 a procedure is presented for semi-automatic use of the vanishing point detection method for camera calibration.

The direct solution for the reconstruction of a parallelogram from a single image presented in (Heuvel, 1997) results in a rectangle after the adjustment of the observations using a single rectangularity condition. This idea was further developed for the reconstruction of more complex polyhedral shapes from a single image (Heuvel, 1998a) (thesis section 2.4). Condition equations result from the object topology (for instance, three object edges meeting in one corner point), as well as from geometric object constraints (for instance, parallelism of object edges; this condition is identical to the corner point condition). Many condition equations have been formulated, however, a complete set of conditions is required for a unique object reconstruction. In contrast to the direct solution in (Heuvel, 1997), this object reconstruction from adjusted observations is sequential; first the orientation of object edges and planes is derived, then planes and points are positioned in an iterative manner. Currently a unique reconstruction cannot be guaranteed in all cases because not all required condition equations have been implemented. A mathematical model with object parameters avoids the problem of finding a complete set of independent condition equations – expected to be even more difficult for a multi image reconstruction – and simplifies the error propagation and quality assessment. Therefore, research continued with the development of a more conventional model with parameters. The approach for reconstruction from a single image is still of importance for two reasons. First, it is suitable for approximate value computation in case of (single image) reconstruction using a mathematical model with parameters. Second, it is to be regarded as an extension of the procedure for image orientation using a single rectangle; the relative orientation of images that contain the same part of a building is found through the similarity transformation between the reconstructed models of that part.

In (Heuvel, 1999b) (thesis section 2.5) the mathematical model that allows the direct least-squares estimation of object parameters is presented. The main characteristics of this model for so-called line-photogrammetric bundle adjustment are:

- The parameterisation is free of degeneracies.
- Point and plane parameters of the polyhedral B-rep are estimated simultaneously; the incorporation of plane parameters simplifies the formulation of many object shape constraints.
- Shape constraints are incorporated in the form of weighted observation equations.
- The model is non-linear in the parameters as well as in the observations (i.e. the image lines).

Because of the last characteristic approximate values are needed for both parameters and observations. For the observations the original observations are used as approximate values. To obtain approximate values of the parameters the model is set up with only linear equations where exterior orientation parameters are treated as constants. Exterior orientation parameters are assumed to be derived with one of the procedures discussed previously. The solution is reached iteratively in two steps. First, only the parameters are updated. After convergence has been reached, both parameters and observations are

updated. In this way a bias in the solution resulting from low quality approximate values is avoided.

Experiments confirmed that an adjustment model of considerable redundancy can be obtained with only a few overlapping images, due to the incorporation of many different types of shape constraints. The reduction in the number of images required to reach a certain level of quality improves the efficiency of the reconstruction because in this approach image interpretation and measurement is a manual task. The procedure for vanishing point detection discussed above could be used for the detection of parallelism and perpendicularity constraints, however this has not been tested. In later research the automatic determination of the approximate values of exterior orientation was investigated (Heuvel, 2002).

As mentioned before, vanishing points contain information on the interior orientation of the image. This information has been exploited for camera calibration from a single image (Heuvel, 1999a) (thesis section 2.6). The condition equations for the least-squares adjustment of parallelism and perpendicularity constraints have been linearised with respect to the focal length, principle point, and lens distortion parameters. Precision of the estimated parameters is computed by error propagation. As expected, the precision of the focal length and principle point is generally low and strongly depends on the orientation of the image relative to the object. However, when interior orientation is assumed stable within a set of images, their condition equations can be combined in one adjustment. The precision of the parameters improves considerably when image orientation differs from image to image. Note that there is no correspondence between the images required, and vanishing point detection can be highly automated. In several single image experiments full convergence could not be obtained for all parameters at once (without adjusting the observations). This is due to errors in the observations that deteriorate the coefficients. In these cases a two-step approach is required in which first the lens distortion is estimated. Then focal length and principle point are estimated using the adjusted observations from the first step. Statistical testing of observations is performed in the first step, assessment of the parameter precision in the second step.

As suggested in (Heuvel, 2000) (thesis section 2.7), the estimation of camera calibration parameters could also be integrated in the model for line-photogrammetric bundle adjustment presented in (Heuvel, 1999b). This so-called self-calibration approach has not been implemented. Furthermore, in (Heuvel, 2000) the advantages of using image lines for reconstruction are stressed and the pros and cons of least-squares adjustment with and without parameters are discussed. The main conclusion is that a model without parameters – i.e. condition equations with observations only – is beneficial for use during interactive modelling where the model can be continuously updated with new information and results of statistical testing are presented to the user. A final line-photogrammetric bundle adjustment integrating image and object information is to be performed to estimate the object parameters and assess their quality.

In the paper (Heuvel, 2001) (thesis section 2.8) a case study is presented that demonstrates the potential of the developed procedures for the reconstruction from a single image. The image is a scanned glass plate from the Meydenbauer archives of which interior orientation was unknown. The photograph was taken in 1911 with a camera of which the lens was shifted along the y-axis of the camera system. The resulting shift of the principle point was estimated together with the focal length using the method described in (Heuvel, 1999a). The shift of the principle point in camera x-direction could not be estimated due to the vertical orientation of the image plane. The line-photogrammetric bundle adjustment method presented in (Heuvel, 1999b) was used to estimate the object parameters of a B-rep from the manual line measurements together with the object knowledge, such as topology and

shape information, inferred from the image. The relative precision achieved varied between 0.1% and 1% of the object dimensions.

In pursuing automation in architectural photogrammetry vanishing point detection plays a central role in this research. In (Heuvel, 2002) (thesis section 2.9) an automatic procedure for image orientation is presented that builds on the vanishing point detection in two ways. First, image line extraction and vanishing point detection constitute the first step of the procedure. This step results in an ambiguous rotation matrix for each image and a set of image lines labelled according to their orientation in space. Second, the same principles that are used for the vanishing point detection are being used for the detection of the relative position of two images. This is possible because of the similarities between an epipole (found by intersection of epipolar planes) and a vanishing point (found by intersection of interpretation planes). This relation is visualised in Figure 3 of (Heuvel, 2002). The procedure groups possible correspondences based on statistical tests of all combinations of two corresponding image points. The points are created by intersection of the extracted lines. The computational burden of the procedure can be high, depending on the number of possible correspondences that in turn depends on the characteristics of the images and the parameter settings. In the example of chapter 3 the computational burden is reduced by manual measurement of two corresponding points per image pair. This semi-automatic approach also eliminates ambiguous solutions. This procedure for image orientation requires the presence of coplanar object points and detects the planes in which these points reside. In this way parts of the building façades are detected as a by-product.

References

Albertz, J. and Wiedemann, A. (Editors), 1997. Architekturphotogrammetrie gestern - heute - morgen. T.U. Berlin.

Appel, M. and Förstner, W., 2002. Scene constraints for direct single image orientation with selfdiagnosis, Photogrammetric Computer Vision. International Archives of Photogrammetry and Remote Sensing, Vol. 34 part 3A, Graz, Austria, pp. 42-49.

Atkinson, K.B. (Editor), 1996. Close Range Photogrammetry and Machine Vision. Whittles Publishing, Scotland.

Baillard, C., Schmid, C., Zisserman, A. and Fitzgibbon, A. W., 1999. Automatic line matching and 3D reconstruction of buildings from multiple views. International Archives of Photogrammetry and Remote Sensing, Vol. 32 part 3-2W5, München, pp. 69-80.

Bartoli, A., Sturm, P. and Horaud, R., 2001. Projective structure and motion from two views of a piecewise planar scene, 8th International Conference on Computer Vision, Vancouver, Canada, pp. 593-598.

Baumberg, A., 2000. Reliable feature matching across widely separated views, Computer Vision and Pattern Recognition CVPR2000, pp. 774-781.

Brauer-Burchardt, Ch. and Voss, K., 1999. Monocular 3D-reconstruction of buildings, VMV'99, pp. 109-116.

Brauer-Burchardt, Ch. and Voss, K., 2000. Automatic lens distortion calibration using single views, DAGM-symposium Mustererkennung 2000. Springer, Kiel, Germany, pp. 187-194.

Brauer-Burchardt, Ch. and Voss, K., 2001. Robust vanishing point determination in noisy images, CVGIP: Image Understanding. Springer, Vol. 54, pp. 289-300.

Braun, C., 1994. Interpretation von Einzelbildern zur Gebäuderekonstruktion. PhD Thesis, Rheinischen Friedrich-Wilhelms Universität, Bonn, Germany.

Chen, T. and Shibasaki, R.S., 1998. Determination of camera's orientation parameters based on line features, Vol. 32 part 5, Hakodate, Japan, pp. 23-28.

Collins, R.T. and Weiss, R.S., 1990. Vanishing Point Calculation as a Statistical Inference on the Unit Sphere, IEEE third int. Conference on Computer Vision, pp. 400-403.

Criminisi, A., Reid, I. and Zisserman, A., 1999. Single view metrology, 7th International Conference on Computer Vision, Corfu, Greece, pp. 434-442.

Debevec, P., Taylor, C. and Malik, J., 1996. Modeling and rendering architecture from photographs: a hybrid geometry- and image-based approach, proceedings SIGGRAPH'96, pp. 11-20.

Dick, A., Torr, Ph. and Cipolla, R., 2000. Automatic 3D modelling of architecture, 11th British Machine Vision Conference, Bristol, UK, pp. 372-381.

Eelaart, I. van de and Hendriks, E.A., 1999. A flexible camera calibration system that uses straight lines in a 3D scene to calculate the lens distortion, fifth annual conference of the Advanced School for Computing and Imaging (ASCI), Heijen, The Netherlands, pp. 443-448.

El-Hakim, S.F., 2000. A practical approach to creating precise and detailed 3D models from single and multiple views. International Archives of Photogrammetry and Remote Sensing, Vol. 33 part 5A, Amsterdam, Netherlands, pp. 202-209.

El-Hakim, S.F., 2002. Semi-automatic 3D reconstruction from widely separated views, Close-range imaging, long-range vision. International Archives of Photogrammetry and Remote Sensing, Vol. 34 part 5, Corfu, Greece, pp. 143-148.

Ethrog, U., 1984. Non-metric camera calibration and photo orientation using parallel and perpendicular lines of the photographed objects. Photogrammetria, 39(1984): 13-22.

Faugeras, O., 1993. Three-dimensional computer vision. The MIT Press, Cambridge, Massachusetts; London, England.

Faugeras, O. et al., 1998. 3-D reconstruction of urban scenes from image sequences. Computer Vision and Image Understanding, 69(3): 292-309.

Förstner, W., 2000. New orientation procedures, ISPRS congress. International Archives of Photogrammetry and Remote Sensing, Vol. 33 part 3, Amsterdam, pp. 297-304.

Fua, P., Grün, A., D'Apuzzo, N. and Plänkers, R., 2002. Markerless full body shape and motion capture from video sequences. International Archives of Photogrammetry and Remote Sensing, Vol. 34 part 5, Corfu, Greece, pp. 256-261.

Gool, L. van et al., 2002. 3D modeling and registration under wide baseline conditions, Photogrammetric Computer Vision. International Archives of Photogrammetry and Remote Sensing, Vol. 34 part 3A, Graz, Austria, pp. 3-14.

Grussenmeyer, P. and Khalil, O.A., 2002. Solutions for exterior orientation in photogrammetry: a review. Photogrammetric Record, 17(100): 615-634.

Guillou, E., Meneveaux, D., Maisel, E. and Bouatouch, K., 2000. Using vanishing points for camera calibration and coarse 3D reconstruction from a single image. The visual computer, 16: 396-410.

Gülch, E., 1995. Line photogrammetry: a tool for precise localization of 3D points and lines in automated object reconstruction, Integrating Photogrammetric Techniques with Scene Analysis and Machine Vision II. SPIE, Vol. 2486, Orlando, USA, pp. 2-12.

Habib, A.F., Morgan, M. and Lee, Y.-R., 2002a. Bundle adjustment with self-calibration using straight lines. Photogrammetric Record, 17(100): 635-650.

Habib, A.F., Shin, S.W. and Morgan, M., 2002b. Automatic pose estimation of imagery using free-form control linear features, Photogrammetric computer vision. International Archives of Photogrammetry and Remote Sensing, Vol. 34 part 3, Graz, Austria, pp. 150-155.

Hartley, R. and Zisserman, A., 2000. Multiple view geometry in computer vision. Cambridge University Press, Cambridge.

Heikkinen, J., 1995. Three-dimensional modeling from moving images with help of linear features, Videometrics IV. SPIE, Vol. 2598, Philadelphia, USA, pp. 255-263.

Heipke, C., 1997. Automation of interior, relative, and absolute orientation. ISPRS J. of Photogrammetry and Remote Sensing, 52: 1-19.

Heuvel, F.A. van den, 1997. Exterior Orientation using Coplanar Parallel Lines, 10th Scandinavian Conference on Image Analysis (SCIA'97), Lappeenranta, Finland, pp. 71-78.

Heuvel, F.A. van den, 1998a. 3D reconstruction from a single image using geometric constraints. ISPRS J. of Photogrammetry and Remote Sensing, 53(6): 354-368.

Heuvel, F.A. van den, 1998b. Vanishing point detection for architectural photogrammetry. H. Chikatsu and E. Shimizu (Editors). International Archives of Photogrammetry and Remote Sensing, Vol. 32 part 5, Hakodate, Japan, pp. 652-659.

Heuvel, F.A. van den, 1999a. Estimation of interior orientation parameters from constraints on line measurements in a single image. P. Patias (Editor). International Archives of Photogrammetry and Remote Sensing, Vol. 32 part 5W11, Thessaloniki, Greece, pp. 81-88.

Heuvel, F.A. van den, 1999b. A Line-photogrammetric mathematical model for the reconstruction of polyhedral objects. S.F. El-Hakim (Editor), Videometrics VI. proceedings of SPIE, Vol. 3641, San Jose, USA, pp. 60-71.

Heuvel, F.A. van den, 2000. Line-photogrammetry and its application for reconstruction from a single image, 19. Jahrestagung der DGPF. Deutschen Gesellschaft fuer Photogrammetrie und Fernerkundung, Vol. 8, Essen, pp. 255-263.

Heuvel, F.A. van den, 2001. Object reconstruction from a single architectural image taken with an uncalibrated camera. Photogrammetrie Fernerkundung Geoinformation, 2001(4): 247-260.
Heuvel, F.A. van den, 2002. Towards automatic relative orientation for architectural photogrammetry. P. Patias (Editor). International Archives of Photogrammetry and Remote Sensing, Vol. 34 part 5, Corfu, Greece, pp. 227-232.
Heuvel, F.A. van den and Vosselman, G., 1997. Efficient 3D modeling of buildings using a priori geometric object information. S.F. El-Hakim (Editor), Videometrics V. proceedings of SPIE, Vol. 3174, San Diego, USA, pp. 38-49.
Jelinek, D. and Taylor, C.J., 2001. Reconstruction of linearly parameterized models from single images with a camera of unknown focal length. IEEE Trans. on PAMI, 23(7): 767-773.
Kasser, M. and Egels, Y., 2002. Digital Photogrammetry. Taylor & Francis, New York.
Khalil, O.A. and Grussenmeyer, P., 2002. Single image and topology approaches for modeling buildings, Close-range imaging, long-range vision. International Archives of Photogrammetry and Remote Sensing, Vol. 34 part 5, Corfu, Greece, pp. 131-136.
Kraus, K., 1997. Photogrammetry - Volume 2 - Advanced Methods and Applications, 2. F. Duemmler Verlag, Bonn.
Lang, F. and Förstner, W., 1996. 3D-city modeling with a digital one-eye stereo system. International Archives of Photogrammetry and Remote Sensing, Vol. 31 part B4, Vienna, Austria, pp. 261-265.
Lourakis, M. I. A. , Halkidis, S. T. and Orphanoudakis, S. C., 2000. Matching disparate views of planar surfaces using projective invariants. Image and Vision Computing, 18(9): 673-683.
Luhmann, T., 2000. Nahbereichsphotogrammetrie - Grundlagen, Methoden und Anwendungen. Herbert Wichmann Verlag, Heidelberg.
Matas, J., Urban, M. and Pajdla, T., 2000. Unifying view for wide-baseline stereo matching. B. Likar (Editor), Computer Vision Winter Workshop, pp. 214-222.
McGlone, J.Ch. and Shufelt, J.A., 1994. Projective and object space geometry for monocular building extraction, IEEE Computer Society Conference on Computer Vision and Pattern Recognition. IEEE, Seattle, USA, pp. 54-61.
Mikhail, E.M., Bethel, J.S. and McGlone, J.Ch., 2001. Introduction to Modern Photogrammetry. John Wiley & Sons, Inc., New York.
Mikhail, E.M. and Weerawong, K., 1997. Exploitation of linear features in surveying and photogrammetry. Journal of Surveying Engineering, 123(1): 32-47.
Mulawa, D.C. and Mikhail, E.M., 1988. Photogrammetric treatment of linear features, Vol. 27 part B10, Kyoto, Japan, pp. 383-393.
Navab, N., 2002. Canonical representation and three view geometry of cylinders, Photogrammetric Computer Vision. International Archives of Photogrammetry and Remote Sensing, Vol. 34 part 3A, Graz, Austria, pp. 218-224.
Patias, P., Petsa, E. and Streilein, A., 1995. Digital line photogrammetry - concepts, formulation, degeneracies, simulations, algorithms, practical examples, Eidgenössische Technische Hochschule (ETH), Zürich, Switserland.
Petsa, E. and Patias, P., 1994. Formulation and assessment of straight line based algorithms for digital photogrammetry, Vol. 30 part 5, Melbourne, Australia, pp. 310-317.
Pollefeys, M. , Koch, R. , Vergauwen, M. and Van Gool, L., 2000. Automated reconstruction of 3D scenes from sequences of images. ISPRS J. of Photogrammetry and Remote Sensing, 55(4): 251-267.
Pollefeys, M. et al., 2002. Video-to-3D. International Archives of Photogrammetry and Remote Sensing, Vol. 34 part 5, Corfu, Greece, pp. 579-584.
Pritchett, P. and Zisserman, A., 1998. Wide baseline stereo matching, Sixth International Conference on Computer Vision, pp. 754 -760.
Rother, C., 2002. A new approach to vanishing point detection in architectural environments. Image-and-Vision-Computing, 20(9-10): 647-655.
Schaffalitzky, F. and Zisserman, A., 2001. Viewpoint invariant texture matching and wide baseline stereo, Eighth IEEE International Conference on Computer Vision (ICCV), Vol. 2, pp. 636-643.
Schenk, T., 1999. Digital Photogrammetry. TerraScience, Laurelville, USA.
Schwermann, R., 1995. Geradengestützte Bildorientierung in der Nahbereichsphotogrammetrie. PhD Thesis, Rheinisch-Westfälischen Technischen Hochschule, Aachen, Germany.
Shum, H.-Y., Szeliski, R., Baker, S., Han, M. and Anandan, P., 1998. Interactive 3D modeling from multiple images using scene regularities, European Workshop on 3D Structure from Multiple Images of Large-scale Environments (at ECCV '98).

Smith, M.J. and Park, D.W.G., 2000. Absolute and exterior orientation using linear features. International Archives of Photogrammetry and Remote Sensing, Vol. 33 part B3, Amsterdam, Netherlands, pp. 850-857.

Straforini, M., Coelho, C. and Campani, M., 1990. A fast and precise method to extract vanishing points, Close-range photogrammetry meets machine vision. SPIE, Vol. 1395, Zurich, pp. 266-274.

Streilein, A., 1999. Digitale Photogrammetrie und CAAD. PhD Thesis, Eidgenössische Technische Hochschule (ETH), Zürich, Switserland.

Sturm, P. and Maybank, S.J., 1999. A method for interactive 3D reconstruction of piecewise planar objects from single images, 10th British Machine Vision Conference, Nottingham, England, pp. 265-274.

Tommaselli, A.M.G., 2000. Orientation and reconstruction of close-range images using lines. International Archives of Photogrammetry and Remote Sensing, Vol. 33 part B5, Amsterdam, Netherlands, pp. 838-845.

Tommaselli, A.M.G. and Lugnani, J.B., 1988. An alternative mathematical model to the collinearity equation using straight features, Vol. 27, Kyoto, Japan, pp. 765-774.

Tuytelaars, T. and Gool, L. van, 2000. Wide Baseline Stereo Matching based on Local, Affinely Invariant Regions, British Machine Vision Conference BMVC'2000, pp. 412-422.

Vosselman, G. and Veldhuis, H., 1999. Mapping by Dragging and Fitting of Wireframe Models. PE&RS, 65(7): 769-776.

Wang, Y., 1998. Principles and applications of structural image matching. ISPRS J. of Photogrammetry and Remote Sensing, 53: 154-165.

Werner, T. and Zisserman, A., 2002. New techniques for automated architectural reconstruction from photographs, ECCV 2002. Springer-Verlag, pp. 541-555.

Wilczkowiak, M., Boyer, E. and Sturm, P., 2001. Camera calibration and 3D reconstruction from single images using parallelepipeds, IEEE-International-Conference-on-Computer-Vision, Vol. 1, pp. 142-148.

Williamson, J.R. and Brill, M.H., 1990. dimensional analysis through perspective - a reference manual. American Society for Photogrammetry and Remote Sensing.

Wiman, H. and Axelsson, P., 1996. Finding 3D-structures in multiple aerial images using lines and regions. International Archives of Photogrammetry and Remote Sensing, Vol. 31 part B3, Vienna, Austria, pp. 953-959.

Zielinski, H., 1993. Object reconstruction with digital line photogrammetry. PhD Thesis, Royal Institute of Technology, Stockholm, Sweden.

2 Papers

This chapter contains a selection of nine papers that were published in proceedings and journals between 1997 and 2002. They have only been edited to remove minor errors and meet layout requirements. An overview of the content of the papers and their coherence is presented in section 1.5.

The paper titles are listed below:

2.1

Exterior Orientation using Coplanar Parallel Lines[1]

[1] Reference: Heuvel, F.A. van den, 1997. **Exterior Orientation using Coplanar Parallel Lines.** Proceedings of the 10th Scandinavian Conference on Image Analysis (Lappeenranta, Finland), ISBN 951-764-145-1, pp.71-78.

Exterior Orientation using Coplanar Parallel Lines

Frank A. van den Heuvel

Delft University of Technology
Faculty of Civil Engineering and Geosciences
Thijsseweg 11, 2629 JA Delft, The Netherlands

Abstract

In this paper an efficient direct solution for the determination of the exterior orientation parameters of an image is presented. The method requires two sets of parallel lines in object space that are coplanar (a parallelogram). The need for this method arises in applications where parallelograms or rectangles are common object features. This is especially true for 3D modelling of (most) buildings, currently a popular application of photogrammetry and computer vision.
The procedure consists of two steps. In the first step the ratios of the distances from the projection centre to the corner points of the parallelogram are computed using only parallelism information. With the results of the first step model coordinates (3D-coordinates in the camera system at arbitrary scale) can be computed. In the second step an object coordinate system is introduced in order to determine the exterior orientation parameters of the image in this system.
The advantages of this procedure are the absence of singularities (as long as the four points are not on (or close to) one line in the image) and its efficiency. This makes it a suitable procedure for pose estimation in real-time applications.
The first step of this method is successfully applied for 3D-reconstruction of (parts of) a building from single images.

1 Introduction

The exterior orientation procedure described in this paper has been developed as a part of a research project in the field of close-range photogrammetry applied to 3D modelling of buildings. The need for computer models of buildings is apparent in Computer Aided Architectural Design (CAAD). Architects want to show their designs and how they fit in the existing environment using computer animations [4]. Computer models are not only used in architectural design but for maintenance and renovation purposes as well. Of most of the existing buildings there is no computer model available mostly because they were not designed with the help of a CAD-system. Here the demand for reverse engineering arises. This holds for detailed models of one or a few buildings as well as for models that cover several blocks of houses or even complete cities. These city models are often derived from aerial photographs and are usually restricted to "2½D" i.e. for each position in the ground plane exactly one height is available. There is a difference in required precision between the two types of models. Architectural models usually require a precision in the order of 1 to several centimetres while for city models the precision is at a level between 0.1 and 1 meter.

The applicability of the method discussed in this paper is not restricted to modelling for architectural purposes but is suitable for all applications where polyhedral objects with parallel edges are involved. As the approximate orientation of aerial images is quite straightforward, this method is primarily developed for close-range photogrammetry and computer vision.

Especially in architectural photogrammetry the objects (buildings) show many straight edges. As these edges or parts of them are often well visible in the images, lines are used more and more in the photogrammetric applications where they appear. Buildings are often designed with the use of only a few basic shapes. The shape that is occurring in almost every building is the rectangle. It is the most common shape of windows, doors and of course of the building itself. The rectangular shape of building features is an example of geometric information that can aid in the 3D-reconstruction.

One of the bottlenecks of the 3D-reconstruction process is the initial orientation of the images. Therefore the direct solution for the exterior orientation parameters that is presented in this paper has been developed. This solution exploits available knowledge or assumptions about the object geometry. The information required for this method consists of two sets of (coplanar) parallel lines in object space for the reconstruction of model coordinates in the camera coordinate system (step 1 of the exterior orientation) and at least 7 parameters for the definition of the object coordinate system in order to compute the parameters of the exterior orientation (step 2).

The detection and precise positioning of the lines in the image that correspond to parallel edges of the object is assumed to be successfully accomplished, let it be manually or automatically through image analysis techniques. The detection of lines in the image that are parallel in object space is equivalent to vanishing point detection. On this topic quite some research has been undertaken [13]. This is even more true for edge detection that can be applied for the precise positioning of the lines in the image.

Before going into detail we give a short overview of related research on exterior orientation and pose estimation in the next section. Then the first step of the exterior orientation procedure is discussed. An alternative to the method of the first step is presented in section 4 and the results of the two methods are proven to be identical. The second step of the procedure in which the exterior orientation parameters are determined follows. In section 6 it is shown that the method for exterior orientation can be modified for relative orientation of two images. The paper finishes with a discussion of several tests where the first step of the procedure is applied to 3D-reconstruction in the camera coordinate system.

2 Related research

Exterior orientation in photogrammetry and pose estimation as it is mostly called in computer vision is a popular research subject. The exterior orientation problem can be described in a general way as follows:

What is the position and orientation of an image in space relative to (parts of) an object, based on the perspective projection of the object in the image and geometric object information?

In computer vision the problem is often stated the other way around. Starting with a known position and orientation of the image one is searching for the position and orientation of the object relative to the image. This is called pose estimation. There is no fundamental distinction between the two perspectives. The research in this field aims at a direct solution to the problem, as it is usually difficult to find approximate values needed for an iterative approach. A secondary goal is to require only a minimum amount of object information.

The geometric information of the object can be diverse. Most of the research has been directed towards a solution for the problem with a minimum set of three points of which the

position is known in space. This is called the perspective three-point problem. An extensive review of six different (but sometimes quite similar) direct solutions of which the first dates back to 1841, is given in [8]. Most of the solutions show singularities and sometimes considerable numerical instability. Usually additional information (read points) is needed to select the correct solution from the set of computed solutions.

Some research has concentrated on the perspective n-point problem with n greater than 3. Mostly the perspective four-point problem is attacked (see [9] and [1]). Constraints on the position of the points in space can be imposed, like in [7] and [12] where the exterior orientation is based on a rectangle in space. It is clear that additional points or constrained positions of the points in space make a considerable simplification of the formulation possible with all its benefits with respect to numerical stability and the reduction in the number of solutions possible.

The object information can be specified at a higher level than coordinates of points namely in the form of line information which is especially suitable for polyhedral objects, and at an even higher level in the form of primitives like spheres or cylinders (see [5]). In these studies line-to-line correspondence (line photogrammetry) replaces point-to-point correspondence.
Line information can consist of a full specification of the position and orientation of the lines in space like in [14] and [11] or consist of relations between the lines like perpendicularity and parallelism as in [5]. In the latter case the exterior orientation can only be completed after the introduction of an object coordinate system.

Especially in the field of computer vision often the pose estimation is combined with the estimation of interior orientation parameters (focal length and principal point) and camera calibration parameters (lens distortion) like in [2].

In our approach to the space resection problem the object information consists of two sets of lines that are coplanar and parallel in object space. The four lines make up a parallelogram and thus our space resection problem is a special case of the perspective four-point problem. Lens distortion is assumed to be absent (or corrected for) and interior orientation parameters are known unless stated otherwise.

First the distance ratios from the projection centre to the corner points of the parallelogram are derived from the perspective projection of the four lines of the parallelogram. This is the first step in the exterior orientation procedure. In the second step the exterior orientation parameters can be computed with the introduction of an object coordinate system.

3 Step 1: computation of the distance ratios

The measurements that define 4 lines in the image are the input for the first step of the exterior orientation procedure. These lines are assumed to correspond to lines in object space that are coplanar and parallel, in other words they form a parallelogram. The image coordinates of the 4 corner points of the parallelogram are input to the algorithm. To arrive at these coordinates manual measurements can be performed or some kind of (straight) edge detection can be applied, followed by line intersection. The detection of the edges that make up the parallelogram can be performed manually, although research in automating this task has been undertaken. As interior orientation and camera calibration are assumed to be known, we will not differentiate between image and camera coordinates. In other words the vector that is built from the image coordinates (x,y) and the focal length (c) is assumed to correspond to a direction vector in object space. In the camera system this is the vector $(x,y,-c)$.

The algorithm for the computation of the distance ratios is based on [1]. We call it the volumetric approach because it involves the computation of volumes of the tetrahedrons that consist of 3 of the 4 points of the parallelogram and the projection centre (see figure 1). The volumes of the 4 tetrahedrons (the 4 combinations of 3 corner points) can be computed in two ways:

1. From the 3 vectors defined by the image coordinates, the focal length and the distances to the 3 corner points (the focal length will cancel out in the computation of the distance ratios; see below).
2. From object information i.e. the area (A) of the triangle formed by the 3 corner points and the distance (h) of the projection centre to the plane of this triangle.

Elimination of A and h results in 3 equations in which only the 4 distances between the projection centre and the corner points are unknown. From these equations the 3 distance ratios can be derived.

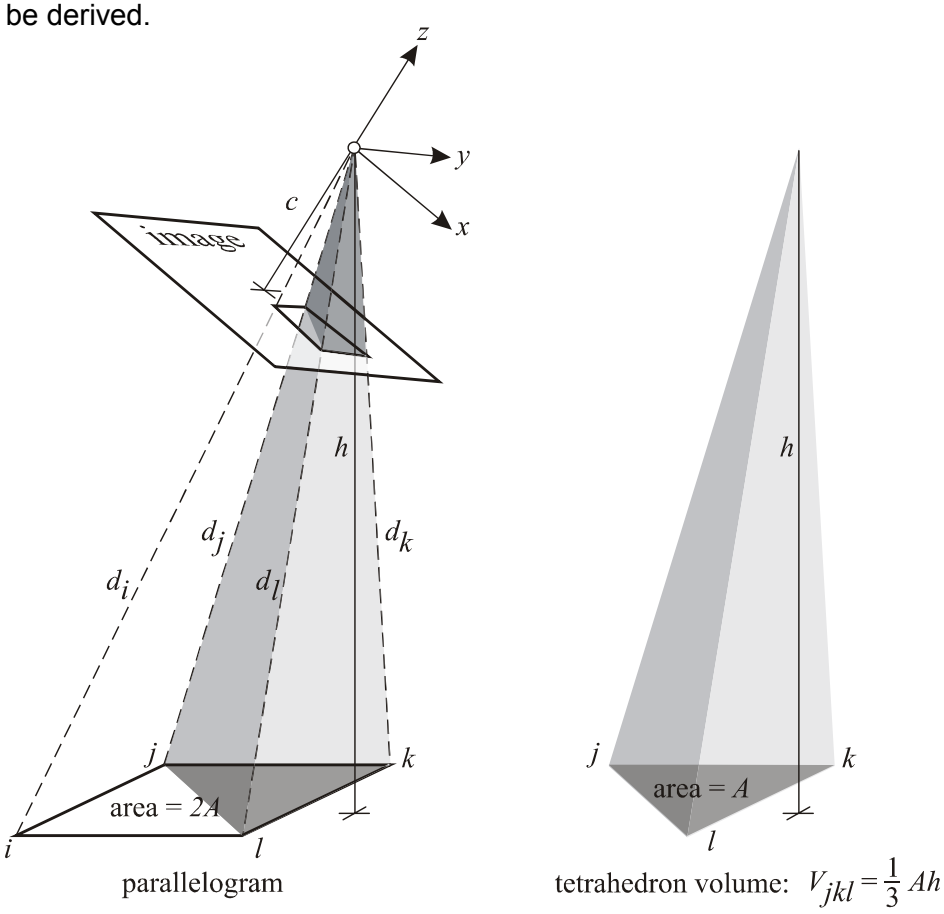

Figure 1: Parallelogram i,j,k,l and volume V of a tetrahedron.

Volume of the tetrahedron (V_{ijk}) computed from vectors of image coordinates ($x_.$), focal length (c) and distances ($d_.$):

$$V_{ijk} = \frac{d_i d_j d_k |[\mathbf{i},\mathbf{j},\mathbf{k}]|}{6\,|\mathbf{i}||\mathbf{j}||\mathbf{k}|} \quad \text{with:} \quad [\mathbf{i},\mathbf{j},\mathbf{k}] = \det(\mathbf{i},\mathbf{j},\mathbf{k}), \quad \mathbf{x}_i = \mathbf{i} = (x_i, y_i, -c) \tag{1}$$

Notation:

- *In formulas where the letters i, j, k, l are used, a cyclic permutation of the 4 points is allowed. For instance the identifier i+1 can be substituted by j (and l+1 by i, etc.). The cyclic order of the points is not to be changed.*

- *Matrices and vectors are printed in bold.*
- *For coordinate(vector)s in object space capitals are used.*

The volume of the same tetrahedron can be computed from its area in the plane of the parallelogram (A_{ijk}) and the distance from this plane to the projection center (h):

$$V_{ijk} = A_{ijk}\frac{h}{3} \tag{2}$$

A_{ijk} is the area of triangle ijk and could only be computed if object coordinates of the corner points were available. But as we will see in the sequel in step 1 of the exterior orientation there is no need to introduce an object coordinate system. This is due to the fact that we assume the 4 lines to build a parallelogram in object space. Because of the parallelism a diagonal of the parallelogram always splits its area in 2 equal parts. And thus the areas A_{ijk} of the 4 triangles in the plane of the parallelogram are all equal. As the same holds for the distance h of the projection centre to the plane of the parallelogram it follows that the volumes of the 4 tetrahedrons are identical. Combining (1) and (2):

$$(2Ah =)\frac{d_i d_j d_k\,|[\mathbf{i},\mathbf{j},\mathbf{k}]|}{|\mathbf{i}||\mathbf{j}||\mathbf{k}|} = \frac{d_j d_k d_l\,|[\mathbf{j},\mathbf{k},\mathbf{l}]|}{|\mathbf{j}||\mathbf{k}||\mathbf{l}|} = \frac{d_k d_l d_i\,|[\mathbf{k},\mathbf{l},\mathbf{i}]|}{|\mathbf{k}||\mathbf{l}||\mathbf{i}|} = \frac{d_l d_i d_j\,|[\mathbf{l},\mathbf{i},\mathbf{j}]|}{|\mathbf{l}||\mathbf{i}||\mathbf{j}|} \tag{3}$$

These are the 3 equations where only the four distances d_i are unknown.
The distance ratios C_{ij} can be written as follows:

$$C_{ij} = \frac{d_j|\mathbf{i}|}{d_i|\mathbf{j}|} = \frac{[\mathbf{k},\mathbf{l},\mathbf{i}]}{[\mathbf{j},\mathbf{k},\mathbf{l}]}\ \left(= \frac{[\mathbf{x}_{j+1},\mathbf{x}_{j+2},\mathbf{x}_{j+3}]}{[\mathbf{x}_{i+1},\mathbf{x}_{i+2},\mathbf{x}_{i+3}]}\right) \tag{4}$$

The following remarks have to be made:

1. In the computation of the determinants the focal length is a constant factor. In the division of two determinants it will cancel out. This is why the distance ratios are independent of the focal length as stated before.
2. The sign of the determinant depends on the order of the corner point vectors. The sign is positive if they are ordered clockwise as seen from the projection centre. Otherwise it will be negative. In (4) the sign cancels out in the same way as the focal length.
3. The determinants may not be (close to) zero. In other words the projections of the corner points may not be (close to) one line in the image. It is obvious that the precision of the distance ratios increases with an increasing area of the parallelogram in the image.

The computation of distance ratios is the first step in the derivation of the exterior orientation parameters of the camera. In the second step a 3D-coordinate system is introduced with (at least) 7 coordinates of the corner points of the parallelogram. Then the 6 parameters of the exterior orientation are computed. This step can be seen as the absolute orientation of a mono model. Model coordinates ($\mathbf{X}_i^m$) can be written as a function of one distance d_i that defines the scale of the model:

$$\mathbf{X}_i^m = \frac{d_i}{|\mathbf{x}_i|}\mathbf{x}_i\left(= \frac{d_i}{|\mathbf{i}|}\mathbf{i}\right) = \lambda_i\mathbf{x}_i, \quad \mathbf{X}_j^m = \lambda_i C_{ij}\mathbf{x}_j \tag{5}$$

4 Step 1: the non-volumetric approach

The results of the previous section can be verified with a different approach, which we call the non-volumetric approach. This method uses the fact that the direction of two parallel lines in the camera system is defined by the perspective projection of the two lines in the image [3]. This is depicted in figure 2 for two sets of parallel lines. The normal vector of the plane of the parallelogram ($\mathbf{n}$) is found with the two direction vectors ($\mathbf{r}_1$ and $\mathbf{r}_2$):

$$\begin{aligned} &\mathbf{r}_1 = (\mathbf{j}\times\mathbf{k})\times(\mathbf{i}\times\mathbf{l}), \quad \mathbf{r}_2 = (\mathbf{i}\times\mathbf{j})\times(\mathbf{l}\times\mathbf{k}) \\ &\mathbf{n} = \mathbf{r}_1\times\mathbf{r}_2 \end{aligned} \tag{6}$$

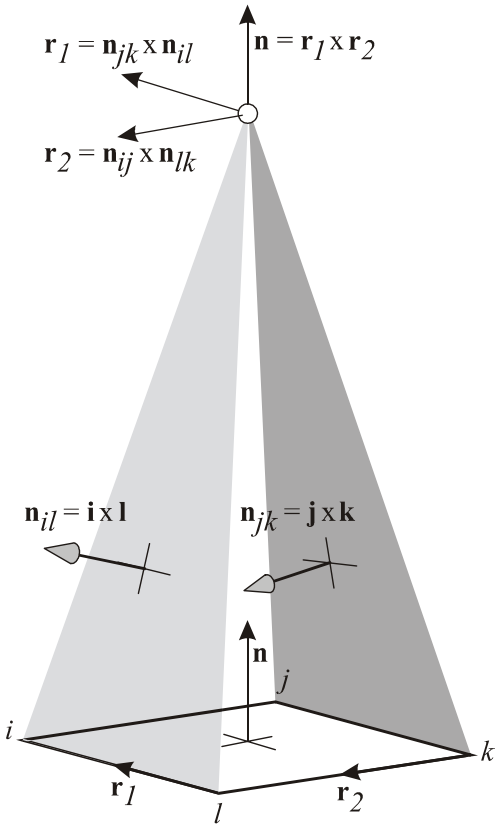

Figure 2: The vectors in the non-volumetric approach

The distances to the corner points ($d_.$) can be expressed as a function of the distance from the projection centre to the plane of the rectangle (h):

$$d_i = h\frac{|\mathbf{i}||\mathbf{n}|}{|\mathbf{i}\cdot\mathbf{n}|} \tag{7}$$

The normal vector resulting from (6) is directed towards the projection centre. In the expression for the distance ratios (C_{ij}) the sign of the dot product in (7) cancels out:

$$C_{ij} = \frac{d_j|\mathbf{i}|}{d_i|\mathbf{j}|} = \frac{\mathbf{i}\cdot\mathbf{n}}{\mathbf{j}\cdot\mathbf{n}} = \frac{[\mathbf{i},\mathbf{r}_1,\mathbf{r}_2]}{[\mathbf{j},\mathbf{r}_1,\mathbf{r}_2]} \tag{8}$$

Obviously this is a more complicated expression than (4). In the sequel it is proven that the two approaches lead to the same result.

Combining (4) and (8) we get:

$$C_{ij} = \frac{[\mathbf{i}, \mathbf{r}_1, \mathbf{r}_2]}{[\mathbf{j}, \mathbf{r}_1, \mathbf{r}_2]} = \frac{[\mathbf{i}, \mathbf{k}, \mathbf{l}]}{[\mathbf{j}, \mathbf{k}, \mathbf{l}]} \tag{9}$$

$\mathbf{r}_1$ and $\mathbf{r}_2$ can be written as the sum of two products [18]:

$$\mathbf{r}_1 = (\mathbf{j} \times \mathbf{k}) \times (\mathbf{i} \times \mathbf{l}) = [\mathbf{j},\mathbf{k},\mathbf{l}]\,\mathbf{i} - [\mathbf{j},\mathbf{k},\mathbf{i}]\,\mathbf{l} = [\mathbf{i},\mathbf{l},\mathbf{j}]\,\mathbf{k} - [\mathbf{i},\mathbf{l},\mathbf{k}]\,\mathbf{j} \tag{10}$$

$$\mathbf{r}_2 = (\mathbf{i} \times \mathbf{j}) \times (\mathbf{l} \times \mathbf{k}) = [\mathbf{i}, \mathbf{j}, \mathbf{k}]\mathbf{l} - [\mathbf{i}, \mathbf{j}, \mathbf{l}]\mathbf{k} \tag{11}$$

And so the normal vector to the plane of the parallelogram becomes:

$$\mathbf{n} = \mathbf{r}_1 \times \mathbf{r}_2 = [\mathbf{j},\mathbf{k},\mathbf{l}][\mathbf{i},\mathbf{j},\mathbf{k}](\mathbf{i} \times \mathbf{l}) - [\mathbf{j},\mathbf{k},\mathbf{l}][\mathbf{i},\mathbf{j},\mathbf{l}](\mathbf{i} \times \mathbf{k}) + [\mathbf{j},\mathbf{k},\mathbf{i}][\mathbf{i},\mathbf{j},\mathbf{l}](\mathbf{l} \times \mathbf{k}) \tag{12}$$

or:

$$\mathbf{n} = \mathbf{r}_1 \times \mathbf{r}_2 = -[\mathbf{i},\mathbf{l},\mathbf{k}][\mathbf{i},\mathbf{j},\mathbf{k}](\mathbf{j} \times \mathbf{l}) + [\mathbf{i},\mathbf{l},\mathbf{k}][\mathbf{i},\mathbf{j},\mathbf{l}](\mathbf{j} \times \mathbf{k}) + [\mathbf{i},\mathbf{l},\mathbf{j}][\mathbf{i},\mathbf{j},\mathbf{k}](\mathbf{k} \times \mathbf{l}) \tag{13}$$

Substituting (12) and (13) in (8) we get:

$$\mathbf{i} \cdot \mathbf{n} = [\mathbf{j}, \mathbf{k}, \mathbf{i}][\mathbf{i}, \mathbf{j}, \mathbf{l}][\mathbf{i}, \mathbf{l}, \mathbf{k}], \quad \mathbf{j} \cdot \mathbf{n} = [\mathbf{i}, \mathbf{l}, \mathbf{j}][\mathbf{i}, \mathbf{j}, \mathbf{k}][\mathbf{j}, \mathbf{k}, \mathbf{l}] \tag{14}$$

and:

$$\frac{\mathbf{i} \cdot \mathbf{n}}{\mathbf{j} \cdot \mathbf{n}} = \frac{[\mathbf{i}, \mathbf{k}, \mathbf{l}]}{[\mathbf{j}, \mathbf{k}, \mathbf{l}]} \tag{15}$$

Which proves (4).

5 The parameters of the parallelogram

The shape of the parallelogram is defined by the image coordinates of the four points and the distance ratios between the projection centre and the corner points of the parallelogram. Two parameters are needed to describe the shape of a parallelogram. The first parameter is the ratio of the distances between the parallel lines or the width-height ratio. The angle between the two directions in object space is the second parameter (see figure 3).

The parameters of the parallelogram depend on the focal length [10]. As a result the focal length can be determined if one of the parameters is known. In practice the focal length will strongly depend on the noise in the image coordinates and not be estimable at all if the optical axis is perpendicular to the plane of the parallelogram.

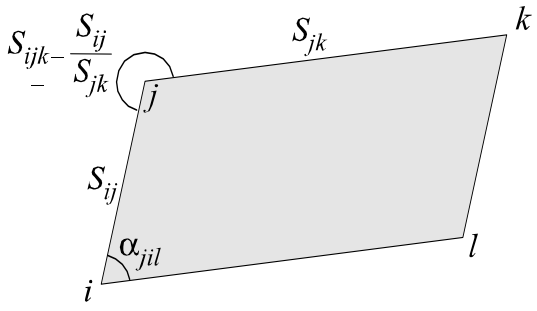

Figure 3: The shape parameters S_{ijk} en α_{jil} of the parallelogram.

The distance between point i and j is computed from the model coordinates (5):

$$S_{ij}^2 = (\mathbf{X}^m{}_j - \mathbf{X}^m{}_i) \cdot (\mathbf{X}^m{}_j - \mathbf{X}^m{}_i = \lambda^2{}_i (C_{ij}\,\mathbf{x}_j - \mathbf{x}_i) \cdot (C_{ij}\,\mathbf{x}_j - \mathbf{x}_i) \tag{16}$$

Then the width-height ratios S_{ijk} become:

$$S_{ijk}^2 = \frac{S_{ij}^2}{S_{jk}^2} = \frac{(C_{ij}\mathbf{x}_j - \mathbf{x}_i)\cdot(C_{ij}\mathbf{x}_j - \mathbf{x}_i)}{(C_{ik}\mathbf{x}_k - C_{ij}\mathbf{x}_j)\cdot(C_{ik}\mathbf{x}_k - C_{ij}\mathbf{x}_j)} \tag{17}$$

The number of possible distance ratios is 12 (including diagonals). In other words: there are 12 different combinations of ijk to compute this shape parameter.

The distance ratios C_{ij} do not depend on the focal length but this does not hold for the model coordinates. So if the distance ratio S_{ij}/S_{ik} is known it is possible to compute the focal length from (17):

$$c^2 = \frac{(C_{ij}x_j - x_i)^2 + (C_{ij}y_j - y_i)^2 - \frac{S_{ij}^2}{S_{ik}^2}((C_{ik}x_k - x_i)^2 + (C_{ik}y_k - y_i)^2)}{\frac{S_{ij}^2}{S_{ik}^2}(1 - C_{ik})^2 - (1 - C_{ij})^2}$$

Again there are 12 permutations of ijk possible. From this formula it is clear that c cannot be computed if C_{ij}=1 and C_{ik}=1, that is if the optical axis is perpendicular to the plane of the parallelogram.

The angle between the two directions in object space of the parallelogram is computed from the model coordinates as follows:

$$\cos\alpha_{jil} = \frac{(\mathbf{X}_j - \mathbf{X}_i)\cdot(\mathbf{X}_l - \mathbf{X}_i)}{|\mathbf{X}_j - \mathbf{X}_i||\mathbf{X}_l - \mathbf{X}_i|} = \frac{(C_{ij}\mathbf{x}_j - \mathbf{x}_i)\cdot(C_{il}\mathbf{x}_l - \mathbf{x}_i)}{|C_{ij}\mathbf{x}_j - \mathbf{x}_i||C_{il}\mathbf{x}_l - \mathbf{x}_i|} \tag{18}$$

From the 8 observations in the image ((*x,y*) of 4 points) the 2 parameters of the shape of the parallelogram can be computed and the 6 parameters of the exterior orientation as explained in the next section. So there is no redundancy for the determination of these 8 parameters. If the two directions of the parallelogram are (assumed to be) perpendicular we deal with a rectangle in object space. The known angle gives the possibility to determine the focal length. In case of rectangularity the focal length results from:

$$c^2 = \frac{(C_{ij}x_j - x_i)(C_{il}x_l - x_i) + (C_{ij}y_j - y_i)(C_{il}y_l - y_i)}{(C_{ij} - 1)(C_{il} - 1)} \tag{19}$$

Again the focal length cannot be calculated if the optical axis is perpendicular to the plane of the rectangle. If the focal length is known (19) can be converted into a condition equation:

$$0 = (C_{ij}\mathbf{x}_j - \mathbf{x}_i)\cdot(C_{il}\mathbf{x}_l - \mathbf{x}_i) \tag{20}$$

If rectangularity is assumed the condition (20) can be used for testing this assumption. In case of acceptance the condition is imposed on the observations. The adjusted observations and the derived distance ratios are input to the second step of the procedure: the computation of the exterior orientation parameters.

6 Step 2: exterior orientation parameters

For the second step of the exterior orientation procedure an object coordinate system is introduced by supplying at least 7 (suitable) object coordinates. This step consists of the computation of the position and orientation of the image in the object system. As we have computed distance ratios in the first step, scale is not yet introduced and has to be determined in this step of the procedure. In this way step 2 is fully identical with a three dimensional similarity transformation for which 7 parameters have to be determined. In photogrammetric terminology an absolute orientation of the model represented by (5) has to be performed. The direct solution for this transformation is based on [6].

The similarity transformation can be written as follows:

$$\begin{aligned} \lambda\, \mathbf{R}\, \mathbf{x}_i &= \mathbf{X}_i - \mathbf{X}^0 \\ \lambda\, \mathbf{R}\, C_{ij}\, \mathbf{x}_j &= \mathbf{X}_j - \mathbf{X}^0 \end{aligned} \tag{21}$$

where:

λ	scale factor (= λ_i)
$\mathbf{R}$	rotation matrix
C_{ij}	distance ratio projection centre - points i and j from step 1
$\mathbf{x}_.$	image coordinates
$\mathbf{X}_.$	the available coordinates in the object system
$\mathbf{X}^0$	the coordinates of the projection centre

The second step of the exterior orientation is split in 2 parts:

1. Computation of the scale factor λ
2. Computation of the parameters of the rotation matrix $\mathbf{R}$ and the location of the projection centre $\mathbf{X}^0$

The scale factor is computed as the ratio of a distance in object space and the corresponding distance in model space:

$$\lambda\, (= \lambda_i) = \frac{|\mathbf{X}_i - \mathbf{X}_j|}{|\mathbf{x}_i - C_{ij}\, \mathbf{x}_j|} \tag{22}$$

With (21) and (5) equation (21) can be written as:

$$(\mathbf{I} + \mathbf{S})\, \mathbf{X}_i^m = (\mathbf{I} - \mathbf{S})(\mathbf{X}_i - \mathbf{X}^0) \tag{23}$$

Where the rotation matrix $\mathbf{R}$ is written as the product of two skew-symmetric matrices. $\mathbf{S}$ is built from the normalised quaternion elements $q_.$:

$$\mathbf{R} = (\mathbf{I} - \mathbf{S})^{-1}(\mathbf{I} + \mathbf{S}), \quad \text{with:} \quad \mathbf{S} = \begin{pmatrix} 0 & -q_3 & q_2 \\ q_3 & 0 & -q_1 \\ -q_2 & q_1 & 0 \end{pmatrix} \tag{24}$$

The quaternion elements $\mathbf{q}$ can be related to Euler angles.
Equation (23) can be rewritten as:

$$\mathbf{X}_i^m - \mathbf{X}_i = \mathbf{M}_i\, \mathbf{q} - \mathbf{w} \tag{25}$$

with:

$$\mathbf{M}_i = \begin{pmatrix} 0 & -Z_i^m - Z_i & Y_i^m + Y_i \\ Z_i^m + Z_i & 0 & -X_i^m - X_i \\ -Y_i^m - Y_i & X_i^m + X_i & 0 \end{pmatrix}, \quad \mathbf{q} = \begin{pmatrix} q_1 \\ q_2 \\ q_3 \end{pmatrix} \text{ and } \mathbf{w} = (\mathbf{I} - \mathbf{S})\mathbf{X}^0 \tag{26}$$

This is a system of equations that is linear in the normalised quaternion elements $\mathbf{q}$ and the auxiliary vector $\mathbf{w}$. The vector $\mathbf{X}^0$ can be computed from (26) after $\mathbf{w}$ is solved from (25). These parameters can be computed if at least six object coordinates $\mathbf{X}_i$ are known. The known coordinates cannot be an arbitrary set of object coordinates, as they will have to define the parameters. If the number of available object coordinates exceeds 7 the equation (25) will become an over determined system of equations. The parameters can then be solved through least squares. In such a case of redundancy the scale factor λ has to be determined iteratively through the use of adjusted camera coordinates in (22) (assuming the redundancy applies to the scale factor).

7 Relative orientation

The procedure for the exterior orientation as described in the previous sections can be modified for relative orientation. Then the same parallelogram has to be present in the images for which the relative orientation is to be determined.

The first step of the procedure, the computation of the distance ratios, remains unchanged. In the second step the model coordinates (represented by equation (5)) of the two images are related through a similarity transformation. For the relative orientation equation (21) becomes (superscripts are used for the image number):

$$\lambda \mathbf{R}\, C_{ij}^1 \mathbf{x}_j^1 = C_{ij}^2 \mathbf{x}_j^2 - \mathbf{X}^0 \quad \text{with} \quad \lambda = \frac{\lambda_i^1}{\lambda_i^2} \tag{27}$$

The scale factor λ is the ratio between the unknown scale factors of the two models (λ_i^1 and λ_i^2). λ can be computed from a distance in the two model systems:

$$\lambda = \frac{|\mathbf{x}_i^2 - C_{ij}^2 \mathbf{x}_j^2|}{|\mathbf{x}_i^1 - C_{ij}^1 \mathbf{x}_j^1|} \tag{28}$$

Because the width-height ratio of the parallelogram is redundantly determined by two images, two (slightly) different values for λ can be computed. For practical purposes such as initial (approximate) value computation the average of the two can be used in the remaining part of the procedure. For an optimum result in terms of precision an adjustment can be applied. Therefore a condition equation can be derived using equation (17). With the adjusted observations there is only one solution for λ. The second parameter of the parallelogram, the angle between the two object directions, is redundantly determined in the same way. Its corresponding condition equations can be found with (19).

Once λ is computed the parameters of $\mathbf{R}$ and $\mathbf{X}^0$ are determined as in the previous section. Here the vector $\mathbf{X}^0$ is defined in the model system of image 2 and thus defined up to a scale factor (λ_i^2). $\mathbf{R}$ and $\mathbf{X}^0$ contain the 5 independent parameters of the relative orientation.

8 Conclusions

The presented method for exterior orientation is applicable when a perspective projection of a parallelogram in object space is available. It is a direct solution that is free of singularities as long as the four corner points of the parallelogram are not on or close to one line in the image. Apart from the parameters of the exterior orientation the two shape parameters of the parallelogram can be computed directly from the observations. If a rectangle in object space is used instead of a parallelogram a constraint has to be imposed on the observations. This leads to an improvement of the orientation parameters.

If the same parallelogram is present in several images the relative orientation of the images can be computed with a method that is very similar to the one for the exterior orientation. Then the shape parameters of the parallelogram are redundantly determined and no other object information apart from the parallelism is required.

References

[1] Abidi, M.A.; Chandra, T., 1995. A new efficient and direct solution for pose estimation using quadrangular targets: algorithm and evaluation. IEEE transactions on pattern analysis and machine intelligence, Vol.17, No.5, pp.534-538

[2] Abidi, M.A.; Chandra, T., 1990. Pose estimation for camera calibration and landmark tracking. Proceedings 1990 IEEE int.conf. Robotics and Automation, pp.420-426

[3] Braun, C., 1994. Interpretation von Einzelbildern zur Gebaeuderekonstruktion. Dissertation Bonn University, Druckerei Schwarzbold, Germany

[4] Coyne, R.; McLaughlin, S.; Newton, S., 1996. Information technology and praxis: a survey of computers in design practice. Environment and Planning B: Planning and Design, Vol.23, No.5, pp. 515-552

[5] Ferri, M.; Mangili, F.; Viano, G., 1993. Projective pose estimation of linear and quadratic primitives in monocular computer vision. CVGIP: Image understanding Vol.58, No.1, July, pp. 66-84

[6] Grafarend, E.W., Lohse, P., Schaffrin, B., 1989. Drei-dimensionaler Ruekwaerts-einschnitt. ZfV, Vol.114, pp.61-67,127-137,172-175,225-234,278-287

[7] Haralick R.M., 1989. Determining Camera Parameters from the perspective projection of a rectangle. Pattern Recognition, Vol.22 No.3 pp.225-230

[8] Haralick R.M.; Lee, C-N.; Ottenberg, K.; Noelle, M., 1994. Review and analysis of solutions of the three point perspective pose estimation problem. Int. Journal of Computer Vision, 13, 3, pp.331-356

[9] Horaud, R.; Conio, B.; Leboullieux, O., 1989. An analytic solution for the perspective 4-point problem. Computer Vision, Graphics, and Image Processing 47, pp.33-44

[10] Katani, K., 1993. Geometric Computation for Machine Vision. Clarendon Press, Oxford, ISBN 0-19-856385-X, pp.63-65

[11] Lee, C-N.; Haralick, R.M., 1996. Statistical estimation for exterior orientation from line-to-line correspondences. Image and Vision Computing 14, pp.379-388

[12] Lee, R.; Lu, P-C.; Tsai, W-H., 1990. Robot Location Using Single Views of Rectangular Shapes. PE&RS, Vol.56, No.2, pp.231-238

[13] McLean, G.F.; Kotturi, D., 1995. Vanishing Point Detection by Line Clustering. IEEE Transactions on PAMI Vol.17, No.11, pp.1090-1095

[14] Petsa, E.; Patias, P., 1994. Formulation and assessment of straight line based algorithms for digital photogrammetry. Proceedings ISPRS Commission V Intercongress Symposium Melbourne pp.310-317

[15] Tan, T.N.; Sullivan, G.D.; Baker, K.D., 1996. Closed-form algorithms for object pose and scale recovery in constrained scenes. Pattern Recognition, Vol. 29, No. 3, pp.449-461

[16] Tommaselli, A.M.G.; Tozzi, C.L., 1996. A Recursive Approach to Space Resection Using Straight Lines PE&RS, Vol.62, No.1, pp.57-66

[17] Wen, W.; Yuan, B., 1995. Structure inference and pose estimation based on symmetry of object. proceedings Frontiers of computer technology IEEE Region 10's Annual Int. Conf., Vol.2, pp.766-770

[18] Wylie, C.R.; Barrett, L.C., 1982. Advanced Engineering Mathematics. McGraw-Hill, Inc., fifth ed.ition, pp.768-769

[19] Zeng, Z.; Wang, X., 1992. A general solution of a closed-form space resection. PE&RS, Vol.58, No.3, pp.327-338

2.2

Efficient 3D modelling of buildings using a priori geometric object information[1]

[1] Reference: Heuvel, F.A. van den, Vosselman, M.G., 1997. **Efficient 3D modelling of buildings using a priori geometric object information.** in Videometrics V (San Diego), Sabry F. El-Hakim (ed.), Proceedings of SPIE Vol. 3174, pp. 38-49.

Efficient 3D modelling of buildings using a priori geometric object information

Frank A. van den Heuvel, George Vosselman

Delft University of Technology
Department of Geodetic Engineering
Thijsseweg 11, 2629 JA Delft, The Netherlands

Abstract

The subject of this paper is the research that aims at efficiency improvement of acquisition of 3D building models from digital images for Computer Aided Architectural Design (CAAD). The results do not only apply to CAAD, but to all applications where polyhedral objects are involved. The research is concentrated on the integration of a priori geometric object information in the modelling process. Parallelism and perpendicularity are examples of the a priori information to be used. This information leads to geometric constraints in the mathematical model. This model can be formulated using condition equations with observations only. The advantage is that the adjustment does not include object parameters and the geometric constraints can be incorporated in the model sequentially. As with the use of observation equations statistical testing can be applied to verify the constraints. For the initial values of orientation parameters of the images we use a direct solution based on a priori object information as well. For this method only two sets of (coplanar) parallel lines in object space are required.

The paper concentrates on the mathematical model with image lines as the main type of observations. Advantages as well as disadvantages of a mathematical model with only condition equations are discussed. The parameterisation of the object model plays a major role in this discussion.

Keywords: close-range photogrammetry, computer vision, line photogrammetry, geometric modelling, topology, geometric constraints, mathematical model, sequential adjustment, object reconstruction, CAAD

1 Introduction

When acquiring 3D computer models of buildings we have to be aware of the requirements set by the user of these models. A first distinction can be made between so-called city models and architectural models. The first type of model usually covers (a part of) a city and contains relatively simple house models. Often aerial images are used which leads to an emphasis on modelling of the roofs of the buildings. As there is an increasing demand for city models the amount of research on the efficient acquisition of these models is considerable.[2-4, 8] The second type of model generally contains only one building or a single block of buildings and will usually show detail in the shape of the façades. Now close-range imagery is needed and the models are more complex. The increase in complexity of the building model is the reason why we do not want to work with only a limited number of predefined basic shapes called primitives (see section 3). These primitives are often used to build the model in the approaches for the acquisition of city models. Here the idea is that the operator can construct new primitives in interaction with the images and then reuses these shapes in order to increase efficiency. Predefined primitives with a parametric representation are used in other approaches for the acquisition of architectural models as

well.[1, 9] In our approach a shape is represented by topological relations and geometric constraints between object features (points, lines and planes) because we can not expect the operator to supply a parametric representation of the new shape without constraints. The mathematical model we adopted is based on condition equations with observations and does not contain parameters apart from image pose parameters in case the position and orientation of the images are only approximately known (section 4). The main advantage of a mathematical model with only conditions on the observations is that there is no need for parameterisation of the object (or primitive) and as a result there is no need for the computation of approximate values for these parameters. Furthermore the data supplied by the operator can be processed sequentially (see section 6) resulting in an early detection of possible errors. Disadvantages are the formulation and the choice of (independent) condition equations (section 5) and the fact that the object model has to be computed from the adjusted observations in a separate step (section 7). In the next section the starting-points of the research are elucidated and some basic choices are explained.

2 Premises and approach

The research focuses on close-range photogrammetry for buildings but we want the results to be applicable to all objects that can be represented as a polyhedral shape. This is true for most of the man-made objects like buildings. Another important feature of these polyhedral man-made objects is that they often show repetitive patterns. In the case of buildings a multitude of examples can be supplied such as vertical walls or identical windows. In the next section the geometric modelling of the polyhedral objects will be discussed.

The geometry of the image will depend on the camera. We assume interior orientation parameters to be known and as a result for each location in the image the corresponding direction in object space is known in the camera system.

The relation between the camera system and the object system is supplied by the exterior orientation parameters. The mathematical model is formulated in such a way that two approaches are possible. In the first approach the exterior orientation parameters are known approximately. To arrive at approximate values the procedure outlined in section 4.3 can be used. This method relies on a priori geometric object information in the form of parallel lines. In this case the exterior orientation parameters will have to be improved by adjustment. The second approach assumes the exterior orientation parameters to be known to a sufficient degree. Then the exterior orientation parameters can be eliminated from the mathematical model.

The system concepts presented here do not rely on an automated image interpretation or segmentation. As many others we believe that real-life imagery requires a semi-automated approach.[1-4] In fact it should be possible to perform the interpretation and the measurements of the images fully manual. But since efficiency improvement is our goal, automation of image analysis tasks is the aim for the long-term. The system presented here is designed for manual processing of the results of low-level feature extraction. The extracted image features can be straight lines or image points. The research effort in image feature extraction is considerable; see e.g. Ref. 5 and 6. Relations between the image features are not assumed to be present beforehand. The topology is to be supplied by the operator through image interpretation. Apart from the topology the operator has to measure missing image features and can supply geometric constraints such as parallel object lines or perpendicular object planes. Efficiency is definitely improved when the operator can make use of Constructive Solid Geometry (CSG).[7] Then the object representation is built from geometric primitives selected by the operator. A primitive is a relatively simple shape such as a box and allows many object topology relations and geometry constraints to be supplied

in one go. But we do not want to be limited to the use of predefined primitives. The operator should be able to build new primitives by specifying topology and constraints. It is clear that the need for operator interaction with the imagery as well as with the 3D-model under construction demands for a seamless integration of photogrammetric image processing functionality and CAD-functionality within one graphical user interface.

3 Geometric modelling

In this section the adopted geometric image-object model is discussed. An explicit distinction is made between topology and geometry. Furthermore the choice of parameterisation of the geometric features is presented.

Although in the next section a mathematical model is formulated in which the parameterisation of the object model does not play a role, we cannot do without geometric modelling. A choice has to be made for the representation of the object model and thus for the data structure to be used. The need for a data structure does not only arise in the object reconstruction phase, but in the image interpretation phase as well. In the image interpretation phase the projection of a wire frame is to be superimposed on the images in order to visualize the established relations between the images and the object model.

As in many advanced CAD systems we adopt a hybrid geometric modelling approach in the sense that we want to combine a boundary representation (B-rep) and a CSG approach. The operator then can work in two modes. The first mode is the B-rep mode in which mode the operator can construct object features (points, lines or planes in space) by combining point and line features in the images. Geometric constraints can be added to these object features. In this mode solids can be constructed as a combination of planes (and thereby lines and points) in space. B-reps of solids have to be validated. The boundary of a valid solid must be closed, orientable, non-self-intersecting, bounding and connected.[10] These solids then can act as primitives in the second mode, i.e. the CSG mode. In this mode primitives can be combined using Boolean operations resulting in a binary CSG tree where the leaf nodes represent the primitives and the branch nodes are the Boolean operators (union, difference and intersection). CSG modelling will be supported by specialized software, a so-called solid modelling kernel. The CSG mode will increase productivity considerably, especially when the object shows many repeating elements. For instance for windows in buildings this will be true. It is important to note that in this approach the primitives constructed by the operator do not have a parametric representation. They are represented by their topology in combination with geometric constraints.

The geometric model chosen (Figure 1) is based on the Formal Data Structure (FDS) presented in Ref.11. In this graph-based model there is a clear distinction between topology and geometry. This is important because the emphasis in the image interpretation process is on topology. The operator links the edges in the images to the edges in object space. Edges in object space are linked to faces and faces again to solids. On the geometry side of the geometric model the relations between the points and lines in the image and the points, lines and planes in object space are depicted. It has to be noted that lines and planes in object space can be features representing the object (then the *projection* relation holds) or features that relate image and object geometry (then the *defines* relation hold).

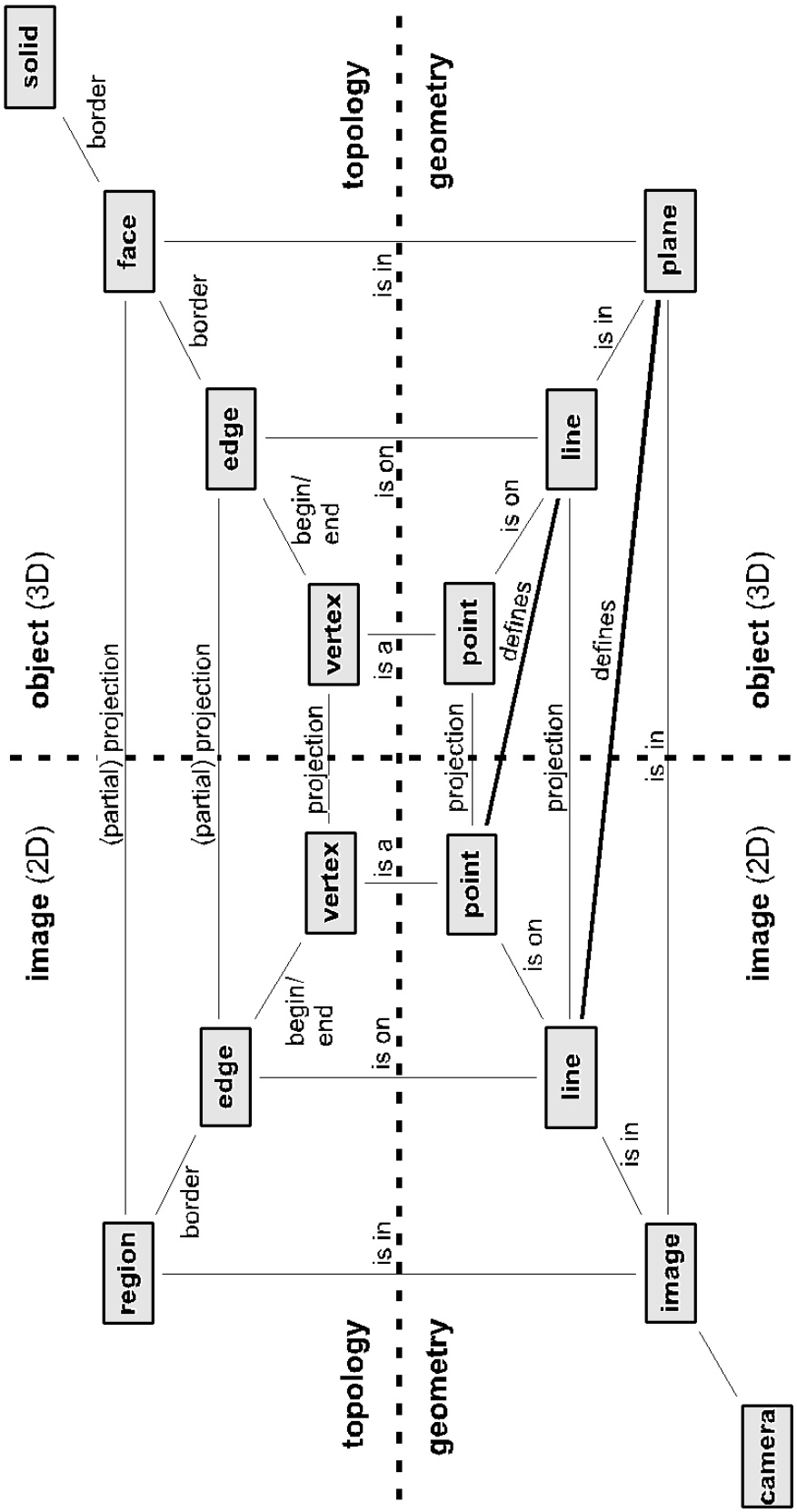

Figure 1: Geometric image-object model

Entity	*Image (2D)*	*Object (3D)*	*Remarks*
Point	2	3	see Table 2
Line	2	4	see Table 2
(Image) plane	(6 : exterior orientation)	3	see Table 2
Vertex	2	3	point parameters
Edge	4	6	e.g. parameters of begin and end points
Region / face	2 · (# edges)	3 + 2 · (# edges)	e.g. parameters of bordering lines (+ 3D-constraints)
Solid	-	3 · (# faces)	e.g. parameters of bordering planes

Table 1: Number of parameters of the entities of the geometric model

The image itself and the camera that is used to take the image are added to the geometric model for completeness. The minimum number of parameters associated with each entity is listed in Table 1. The parameterisation itself is chosen similar to the one used by Kanatani.[12] The parameterisation of points, lines and planes is listed in Table 2.

Entity	*Direction*	*Position*	*Constraints*
Point		$\mathbf{x} = (x, y, z)$, $l_{\mathbf{x}}$	$\lvert\mathbf{x}\rvert = \sqrt{x^2 + y^2 + z^2} = 1$
Line (image point)	$\mathbf{d} = (x, y, z)_{\mathbf{d}}$	$\mathbf{p} = (x, y, z)_{\mathbf{p}}$, $l_{\mathbf{p}}$	$\lvert\mathbf{d}\rvert = \lvert\mathbf{p}\rvert = 1$, $\mathbf{d} \cdot \mathbf{p} = 0$
Plane (image line)	$\mathbf{n} = (x, y, z)_{\mathbf{n}}$	$l_{\mathbf{n}}$	$\lvert\mathbf{n}\rvert = 1$

Table 2: Parameterisation of points, lines and planes in space

To avoid the singularities that can arise when a line or a plane passes through the origin a direction vector of unit length is used in combination with a parameter (*l*) that specifies the distance to the origin of the coordinate system. This singularity does not occur for the position vector of a point. For uniformity a unit vector and a separate length parameter is used for the point parameterisation as well. In this way the duality between point and plane representation is preserved. The parameterisation is visualized in Figure 2. The same parameterisation is used for the image features as well. Then only the *direction* (and *constraints*) column of Table 2 apply and $l_{\mathbf{p}}$ and $l_{\mathbf{n}}$ are zero for the representation of image features in the camera system.

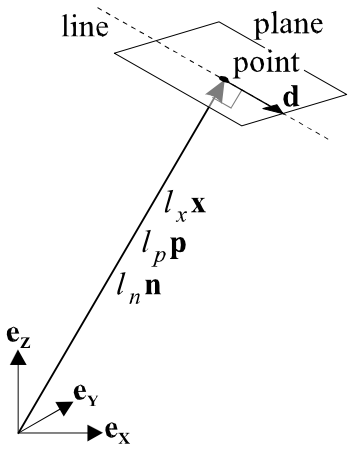

Figure 2: Parameterisation of point, line and plane

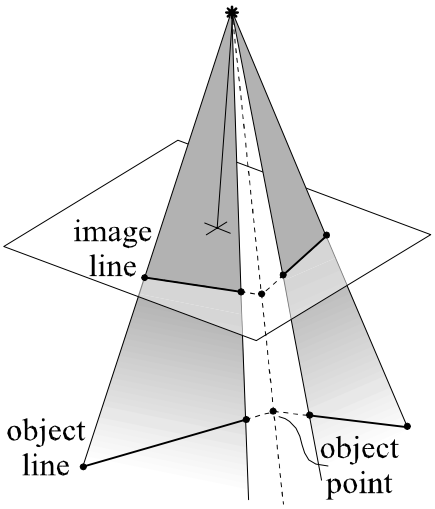

Figure 3: Image and object points and lines

4 A mathematical model for line photogrammetry

In this section we present a mathematical model that differs from commonly adopted models in the sense that the model does not include object parameters. The exterior orientation parameters of the images can be eliminated from the model so a mathematical model results with condition equations with observations only. With this approach parameterisation of the object does not play a role during the interactive modelling process. At the same time geometric object constraints can be examined and processed one by one. First the observation vectors are discussed and their transformation to the coordinate system of the exterior orientation parameters. Then the choice between parameters and constraints is made.

4.1 The observations

The mathematical model aims at the adjustment of automatically extracted or manually measured straight line features in the image. The line features are the main type of observations. Lines in the image can be intersected resulting in image points (Figure 3). These points do not belong to the group of image point observations because they fully depend on the lines in the image that have priority in the line-photogrammetric approach presented here.

The image point observations are represented by the direction vector $\mathbf{d} = \frac{(x, y, -c)}{|(x, y, -c)|}$ where (x, y) is the location of the point in the camera system (relative to the principal point) and c is the focal length. The line features in the image all have a begin and end point, possibly on the border of the image. But these points do not have to correspond to vertices of the object. This is probably not the case if the lines result from automatic feature extraction and no segmentation is performed, i.e. the topology is unknown. This is the reason why each line feature is represented in the model by the normal vector $\mathbf{n}$ of the plane through the line and the projection centre. If the begin and end point of the line are stored the plane in space (and thereby the corresponding line in object space) can be bordered if needed. The normal vector can be computed from the direction vectors of begin and end point through their cross product: $\mathbf{n} = \frac{\mathbf{d}^i \times \mathbf{d}^j}{\left|\mathbf{d}^i \times \mathbf{d}^j\right|}$. In principle only one type of observations exists namely the direction vector in space corresponding to a point or a line feature in the image, respectively a line or a plane in object space.

By using a three-element direction vector we have over-parameterised the observations because a direction in space is defined by only two parameters. In relation, the covariance matrix of the observations is singular if the focal length is assumed to be a non-stochastic constant. For the point observations the focal length could be eliminated as an observed quantity but for the normal vectors that represent the image line observations this is not the case. In order to solve this, a constraint is introduced in the model for each observation vector (Table 2). The advantage of the over-parameterisation in combination with a condition is the absence of singularities that can be encountered in other approaches.[13]

Up to this point the observation vectors are specified in the camera system. To be able to combine the observations of different images the camera systems of these images have to be transformed to a common system through their exterior orientation parameters. The transformation of a normal vector $\mathbf{n}$ and a direction vector $\mathbf{d}$ are listed in Table 3.

	Direction	*Position*	*Constraints*
Exterior orientation	$\mathbf{R}$ (rotation matrix)	$\mathbf{r}$, $l_{\mathbf{r}}$	$\lvert\mathbf{r}\rvert = 1$
Line direction $\mathbf{d}$ (image point)	$\mathbf{Rd}$	$\mathbf{p} = \frac{\mathbf{Rd} \times (\mathbf{r} \times \mathbf{Rd})}{\lvert\mathbf{Rd} \times (\mathbf{r} \times \mathbf{Rd})\rvert}$, $l_{\mathbf{p}} = l_{\mathbf{r}}(\mathbf{r} \cdot \mathbf{p})$	$\lvert\mathbf{d}\rvert = 1$, if $\lvert\mathbf{r} \times \mathbf{Rd}\rvert = 0$ then $l_{\mathbf{p}} = 0$ and e.g. $\mathbf{p} = \frac{(y_{\mathbf{r}}, -x_{\mathbf{r}}, 0)}{\lvert(y_{\mathbf{r}}, -x_{\mathbf{r}}, 0)\rvert}$
Plane normal $\mathbf{n}$ (image line)	$\mathbf{Rn}$	$l_{\mathbf{n}} = l_{\mathbf{r}}(\mathbf{r} \cdot \mathbf{Rn})$	$\lvert\mathbf{n}\rvert = 1$

Table 3: Transformation of observation vectors to a common coordinate system

4.2 Parameters or constraints?

In this section the choice between a mathematical model with object parameters and a model with constraints on the observations is discussed. The model with object parameters is treated first.

Two types of parameters can be distinguished. First there are the parameters that describe the position and orientation of the images, the so-called exterior orientation parameters. Secondly we have the object parameters that describe the geometry of the object. There are many options for the parameterisation of the object geometry. Commonly object geometry is built from points, lines and planes and the parameters of only one type of these object features are used to specify the geometry. The choice for a point, line or plane parameterisation is discussed next. In principle parameterisation with a mixtures of the three is possible but seems unpractical and will not be considered here.

In case of a parameterisation of the object by points or lines constraints have to be applied. In a point parameterisation constraints have to ensure that the points that build a face are in one plane. For a line parameterisation constraints have to be applied to ensure the intersection of the lines and constraints are needed to ensure the lines are in their planes. The plane parameterisation does not need any constraints as (non-parallel) planes always intersect in the lines and points of the topology (as long as not more than three planes intersect in one point otherwise an object constraint is involved, see section 5.2). So the number of parameters and the number of constraints depends on the choice of parameterisation. In Table 4 these numbers are listed for two example objects.

Parameterisation by	Tetrahedron # parameters	Tetrahedron # constraints	Hexahedron # parameters	Hexahedron # constraints
Points (3 par.)	12	non	24	6
Lines (4 par.)	24	12	48	30
Planes (3 par.)	12	non	18	non

Table 4: Number of parameters and constraints of a tetrahedron and a hexahedron

Because there is no need for constraints in case of a plane parameterisation it seems attractive but there are two major drawbacks. First the plane parameterisation can only be applied to describe the geometry of solids. A single or several connected planes in space cannot be parameterised with only the parameters of the plane(s) as they are not bounded. The second drawback is the fact that the plane parameters can only be related to the line (and point) observations in the images through the lines in space being the intersections of the planes. This could lead to the conclusion that the line parameterisation is to be preferred as e.g. in Ref.13, 19 and 20. But the number of parameters and constraints involved is a disadvantage in this case. The point parameterisation is a compromise from the point of

view of the number of parameters and constraints and in terms of establishing the relations between observations and parameters.

Independent of the parameterisation chosen the mathematical model consists of condition equations with observations and parameters. In addition constraints have to be imposed. This model can be written as follows (after linearisation):[18, 22]

$$\mathbf{B}^{\mathrm{T}} E\{\mathbf{y}\} = \mathbf{A}\mathbf{x}\ ,\ \mathbf{C}^{\mathrm{T}} E\{\mathbf{y}\} = \mathbf{0}\ ,\ \mathbf{D}^{\mathrm{T}}\mathbf{x} = \mathbf{0}\ ;\ \mathbf{Q}_{\mathbf{y}} \tag{1}$$

with:

$E\{\}$	mathematical expectation
$\mathbf{y}$	vector of observations (image lines and points)
$\mathbf{x}$	vector of parameters (object parameter and exterior orientation parameters)
$\mathbf{A}$, $\mathbf{B}$	design matrices
$\mathbf{C}^{\mathrm{T}} E\{\mathbf{y}\} = \mathbf{0}$	constraints on the observations (see Table 2)
$\mathbf{D}^{\mathrm{T}}\mathbf{x} = \mathbf{0}$	constraints on the object parameters
$\mathbf{Q}_{\mathbf{y}}$	covariance matrix of the observations

It can be advantageous to regard the constraints on the object parameters as observations as in Ref. 1 and 21 but then the adjusted object parameters do not fully satisfy the constraints. Although the resulting model might be more realistic because of differences between the as-built and the designed geometry, often the user is not interested in these discrepancies.

We will avoid this rather complex model (1) by rewriting the condition equations and converting the constraints on the object parameters to constraints on the observations. In this way the object parameters can be eliminated from the mathematical model but the exterior orientation parameters remain. Without object parameters in the adjustment they have to be computed in a separate step in the so-called object reconstruction (see section 7). In the object reconstruction step adjusted observations (image lines and points) are used to compute parameters of the object points.

To avoid the object parameters, conditions have to be imposed on the observations to ensure that:

- Object points are on lines that are related to image points (collinearity condition)
- Object lines are in the planes that relate to image lines (image-object coplanarity condition)
- Object lines are in their related object planes (object-object coplanarity condition)

These conditions can be called topology constraints because they result from the image-object topology as well as the topology of the object itself. Geometric object constraints like parallelism and perpendicularity of lines or planes is a second type of constraints sometimes called internal constraints.[1, 17] These constraints can be introduced in the same way as the topology constraints. Many of these constraints are discussed in detail in the next section. The (linearised) model that we are looking at now is a model with only condition equations (in (2) $\mathbf{A}$, $\mathbf{B}$ and $\mathbf{x}$ are different from (1)):

$$\mathbf{B}^{\mathrm{T}} E\{\mathbf{y}\} = \mathbf{A}\mathbf{x}\ ;\ \mathbf{Q}_{\mathbf{y}} \tag{2}$$

On the right hand side only the exterior orientation parameters appear in the vector of parameters. This formulation has several advantages. If the exterior orientation parameters are known beforehand, they can be eliminated from the model (2), which then reduces to a model with condition equations with only observations (in (3) $\mathbf{B}$ is different from (2)):

$$\mathbf{B}^{\mathrm{T}} E\{\mathbf{y}\} = \mathbf{0}\ \ ;\ \mathbf{Q}_{\mathbf{y}} \tag{3}$$

Another way to simplify the model (2) is to regard the exterior orientation parameters as observations as well. The estimates of the exterior orientation parameters obtained with the method described in the next section are introduced as observations in the model. In this approach the stochastic model needs special attention as correlation between image observations and exterior orientation parameters cannot be neglected.

An advantage of the model (3) compared to (1) is the absence of object parameters and therefore there is no need for approximate values of these parameters. A second major advantage of the model (3) is the possibility of a sequential adjustment of this model (see section 6). Constraints can be introduced sequentially in the model (1) but then all the parameters involved have to be estimable. During interactive modelling this is not guaranteed for all the parameters. Sequential adjustment allows a separate evaluation of each condition and is especially important in a semi-automatic measurement system. The misclosure of each condition can be tested as soon as the condition is introduced and the observations involved are available. And maybe even more important, the independency of a newly introduced condition in relation to conditions introduced previously can be verified (see section 6). This eliminates one of the main drawbacks of the condition equation approach, namely the need for independent conditions. A remaining drawback is the effort that has to be put in the formulation of the condition equation i.e. the formulation of the constraints as a function of the observations. This is the subject of section 5.

4.3 Approximate values

There are quite a few alternatives to obtain approximate values for the exterior orientation parameter of the images. A lot of research has concentrated on the so-called perspective three and four point problem.[14, 15] Often space coordinates of object points are assumed to be available. We want to make use of the rectangularity of object features because rectangular shapes appear frequently in man-made objects like buildings. An efficient and direct solution has been derived for which only a parallelogram (or rectangle) in object space is needed.[16] So only information on parallelism is used and exterior orientation parameters can be derived in an arbitrary object coordinate system. If a specific object coordinate system is to be used a similarity transformation has to be applied. With estimates of the exterior orientation parameters these parameters can be eliminated from (2) by regarding them as observations. Then the model (3) can be used if the covariance matrix of the exterior orientation *observations* is available.

5 Formulation of condition equations

The condition equations involve only observations and are the result of two types of geometric constraints. This distinction is used by Weik[17] as well. One type of constraints results from (image-object) topological information such as two lines intersecting in one point or three planes intersecting in one line. This type is called topology constraints. The second type results from constraints between object features such as two planes that have to be perpendicular and is called object constraints. Both types are discussed in this section.

Two problems in the formulation of condition equations can arise. The first one is the possibility of dependency between the various constraints. It will not always be possible to avoid the introduction of dependent constraints during modelling. Constraints depending on (combinations of) previously established constraints have to be eliminated from the mathematical model. This can be done by numerically testing the independency of a candidate constraint. This is part of the sequential adjustment that is the subject of section 6. The second problem is the choice for a particular formulation of a condition equation. There can be many alternatives in the choice of the observations that are used to specify a

constraint. The constraint should be formulated in such a way that the condition of the system of normal equations is optimised.

First the topology constraints are presented in section 5.1. The object constraints are discussed in section 5.2.

5.1 Topology constraints

The topology constraints are constraints that result from the image-object topology. For instance all the lines in the images that are related to one line of the object define planes that have to intersect at the object line. During the interactive modelling process this type of constraints can be set up automatically based on the topology available. Depending on the observations available the geometrical parameters of the object features can be computed. Whether sufficient observations are present can be continuously verified by the system. Topology constraints can be divided into (object) point, line and plane constraints.

Point constraints. An object point can be related to image points and to image lines. The object point constraint for image points has the form (Figure 4):

$$\left[\mathbf{R}^i\mathbf{d}^i, \mathbf{R}^j\mathbf{d}^j, l^i_{\mathbf{r}}\mathbf{r}^i - l^j_{\mathbf{r}}\mathbf{r}^j\right] = 0 \qquad (4)$$

with:

[ ]	determinant
$\mathbf{R}^i, \mathbf{r}^i, l^i_{\mathbf{r}}$	exterior orientation parameters of image i (Table 3)
$\mathbf{d}^i$	observation vector of the object point in image i

This coplanarity condition is used for many other constraints as well. The number of independent constraints per object point of this type is 2 ·(#images for the object point) – 3, with two or more images per point. If there are more than two images per point two independent constraints have to be built for each image except two, using the observations of two other images.

In the sequel the rotation matrix of the exterior orientation will be left out for clarity. Observation vectors are assumed to be rotated into a common coordinate system.

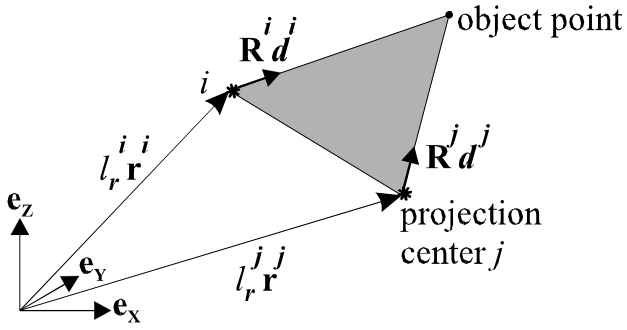

Figure 4: Object point constraint

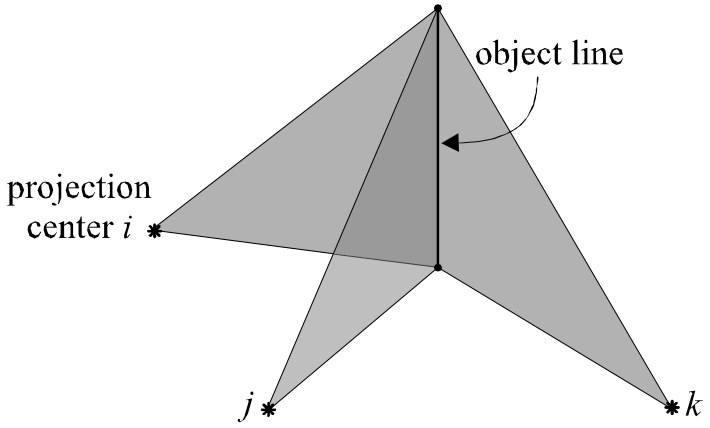

Figure 5: Object line constraint

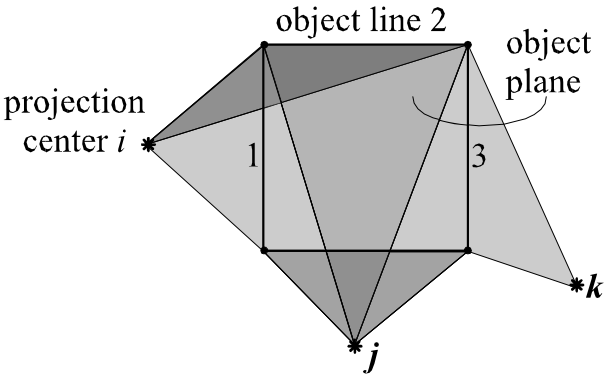

Figure 6: Object plane constraint

The object point constraint for image lines has the same form as the constraint for image points if at least two lines related to an object point are available in each image. Then $\mathbf{d}^i$ is replaced by $\mathbf{n}_1^i \times \mathbf{n}_2^i$ in (4), i.e. the direction of the intersection of the two planes in image i. If there are more than two lines in an image related to one object point additional constraints are needed to ensure the intersection of the image lines in one point in the image:

$$\left[\mathbf{n}_1^i, \mathbf{n}_2^i, \mathbf{n}_3^i\right] = 0 \tag{5}$$

Where $\mathbf{n}_1^i$ is the normal vector to the plane associated with line 1 in image i. The number of independent constraints per object point of this type is (#image lines for the point) – 2.

Line constraints. For object lines we have to distinguish between direction and position constraints. The direction constraint is a coplanarity constraint on the normal vectors to the planes associated with image lines and has the following form (Figure 5):

$$\left[\mathbf{n}_1^i, \mathbf{n}_1^j, \mathbf{n}_1^k\right] = 0 \tag{6}$$

Molenaar[23] also used this constraint for the formation of image triplets. The number of independent constraints per object line of this type is (#images for the object line) – 2.
The position constraints for object lines have the following form:

$$\frac{\left|\mathbf{n}^i \times \mathbf{n}^{ij}\right|}{\left|\mathbf{n}^i \times \mathbf{n}^j\right|^2} = \frac{\left|\mathbf{n}^k \times \mathbf{n}^{jk}\right|}{\left|\mathbf{n}^k \times \mathbf{n}^j\right|^2} \tag{7}$$

Here $\mathbf{n}^{ij} = (l_{\mathbf{r}}^{i}\mathbf{r}^{i} - l_{\mathbf{r}}^{j}\mathbf{r}^{j}) \times (\mathbf{n}^{i} \times \mathbf{n}^{j})$ is the normal to the plane through the projection centres i and j. This plane is parallel to the object line. The number of independent constraints per object line of this type is (#images for the object line) – 2.

Plane constraints. The plane constraints ensure that all object lines that border an object plane are parallel to that plane. These object lines are intersecting due to the object point constraints described above and therefore they will not only be parallel to, but in this plane as well. The object plane constraints for direction have the following form (Figure 6):

$$\left[\mathbf{n}_{12}^{ij}, \mathbf{n}_{3}^{i}, \mathbf{n}_{3}^{j}\right] = 0 \qquad (8)$$

Where $\mathbf{n}_{12}^{ij} = (\mathbf{n}_{1}^{i} \times \mathbf{n}_{1}^{j}) \times (\mathbf{n}_{2}^{i} \times \mathbf{n}_{2}^{j})$ the normal to the object plane constructed from the lines 1 and 2 in images i and j. Other combinations of images can be used to set up the constraint as well. The number of independent constraints per object plane is (#object lines for the plane) – 2, where only object lines observed in at least two images should be counted.

The need for the plane constraint for position arises for lines in an object plane that are not part of its boundary because then the position of the lines in the plane is not warranted by the point constraint. This is a special case from the geometric modelling point of view. We will not consider this type of constraint here.

5.2 Object Constraints

The topology constraints on the observations presented in the previous section ensure that planes associated with image lines intersect at the points, lines and planes of the object. Object constraints are constraints that hold between object features. We distinguish between constraints on the position of the object features and constraints on the orientation of the features. An overview of the object constraints is given in Table 5.

Feature	Point	Line	Plane
Point (position)	distance	(shortest) distance	(shortest) distance
Line (position)		(shortest) distance	distance (in case of parallelism)
Plane (position)			distance (in case of parallelism)
Line (orientation)	non	angle	angle
Plane (orientation)	non		angle

Table 5: Overview of object constraints

The symmetry constraints form a separate category of object constraints. These constraints relate three or four object features instead of two. Replacing “distance” by “distance ratio” and “angle” by “angle ratio” in Table 5 results in an overview of this type of constraints. We will not discuss the object symmetry constraints in more detail but present the angle constraint between two lines as an example.

The angle (α) between two object lines can be written as a function of the image line observations:

$$\cos(\alpha) = \frac{(\mathbf{n}_{1}^{i} \times \mathbf{n}_{1}^{j}) \cdot (\mathbf{n}_{2}^{i} \times \mathbf{n}_{2}^{j})}{\left\|\mathbf{n}_{1}^{i} \times \mathbf{n}_{1}^{j}\right\| \left\|\mathbf{n}_{2}^{i} \times \mathbf{n}_{2}^{j}\right\|} \qquad (9)$$

Where $\mathbf{n}_1^i$ is the normal to the plane through the observed line 1 in image i. Both lines have to be observed in at least two images. This constraint can be specified for each pair of object lines. Of course dependency of the constraints could arise. Perpendicularity ($\cos(\alpha) = 0$) and parallelism ($\cos(\alpha) = 1$) are two special cases of this constraint. Parallelism leads to additional coplanarity constraints of the form:

$$[\mathbf{n}_1^i, \mathbf{n}_2^j, \mathbf{n}_3^k] = 0 \tag{10}$$

In this formulation the constraint involves three object lines observed in three different images. In fact the constraint can be specified for any combination of three line observations of object lines that are parallel. This includes line observations in the same image. In that case the direction in space of the object line is found by the intersection of the planes associated with the image line observations. The image lines then intersect in the so-called vanishing point and constraint (10) is identical to (5).

The number of independent constraints of this type is (#line observations of parallel object lines) – 2. But these constraints are fully dependent on the constraints (9). Note the dependency on the line constraints (6) involving a single object line.

To derive the constraints of Table 5 in terms of the point and line observation vectors generally leads to a formulation that is more complex than the formulation in terms of object parameters. The complexity of the object constraints in terms of observations is a disadvantage of the mathematical model with only condition equations with observations.

6 Sequential adjustment

The objective of a sequential adjustment is an adjustment in steps where in each step condition equation(s) and observations can be added to the mathematical model. The condition equation model (3) can be partitioned in two parts in the following way:

$$\begin{pmatrix} \mathbf{B}_1{}^{\mathrm{T}} \\ \mathbf{B}_2{}^{\mathrm{T}} \end{pmatrix} E\{\mathbf{y}\} = \begin{pmatrix} \mathbf{0} \\ \mathbf{0} \end{pmatrix} \;;\; \mathbf{Q}_{\mathbf{y}} \tag{11}$$

The first part of the model ($\mathbf{B}_1{}^{\mathrm{T}} E\{\mathbf{y}\} = \mathbf{0}$) represents the condition equations processed previously. The second part ($\mathbf{B}_2{}^{\mathrm{T}} E\{\mathbf{y}\} = \mathbf{0}$) consists of only one condition equation namely the condition that is to be investigated before being added to the system. The solution of the first part of (11) is:[18]

$$\hat{\mathbf{y}}_1 = \mathbf{P}_{\mathbf{B}1}^{\perp}\mathbf{y} \;,\; \mathbf{Q}_{\hat{\mathbf{y}}_1} = \mathbf{P}_{\mathbf{B}1}^{\perp}\mathbf{Q}_{\mathbf{y}} \tag{12}$$

with:
$$\mathbf{P}_{\mathbf{B}1}^{\perp} = \mathbf{I} - \mathbf{Q}_{\mathbf{y}}\mathbf{B}_1(\mathbf{B}_1^{\mathrm{T}}\mathbf{Q}_{\mathbf{y}}\mathbf{B}_1)^{-1}\mathbf{B}_1^{\mathrm{T}} \tag{13}$$

Then the new condition equation is added:

$$\mathbf{B}_2^{\mathrm{T}} E\{\hat{\mathbf{y}}_1\} = 0 \;,\; \mathbf{Q}_{\hat{\mathbf{y}}_1} \tag{14}$$

The solution is found in the same way as for the first part of the model but now the adjusted observations are used with their (propagated) covariance matrix $\mathbf{Q}_{\hat{\mathbf{y}}_1}$:

$$\hat{\mathbf{y}} \;= \hat{\mathbf{y}}_{2,1} = \mathbf{P}_{\mathbf{B}2,1}^{\perp}\hat{\mathbf{y}}_1 \;,\; \mathbf{Q}_{\hat{\mathbf{y}}} = \mathbf{Q}_{\hat{\mathbf{y}}_{2,1}} = \mathbf{P}_{\mathbf{B}2,1}^{\perp}\mathbf{Q}_{\hat{\mathbf{y}}_1} \tag{15}$$

with:
$$\mathbf{P}_{\mathbf{B}2,1}^{\perp} = \mathbf{I} - \mathbf{Q}_{\hat{\mathbf{y}}_1}\mathbf{B}_2(\mathbf{B}_2^{\mathrm{T}}\mathbf{Q}_{\hat{\mathbf{y}}_1}\mathbf{B}_2)^{-1}\mathbf{B}_2^{\mathrm{T}} \tag{16}$$

Several remarks to this approach have to be made:

- In principle the full covariance matrix of the observations has to be stored and processed. In practice the covariance matrix will retain a certain degree of sparsity because each constraint involves only a small number of observations. With the amount of memory available in nowadays computers storage is not a serious disadvantage of the sequential adjustment.
- There is no matrix inversion needed for a new condition equation, as the matrix $(\mathbf{B}_2^T\mathbf{Q}_{\hat{y}_1}\mathbf{B}_2)$ is identical to a scalar.
- If $(\mathbf{B}_2^T\mathbf{Q}_{\hat{y}_1}\mathbf{B}_2)$ approaches zero the new condition depends on constraints previously included in the model. In case of dependency the new condition is already satisfied and should (can) not be included in the model.
- For each constraint the misclosure can be computed and statistically tested. In this way possible errors can be detected and corrected during interactive modelling.

7 Object reconstruction

The adjusted observations i.e. the image lines and points are input to the object reconstruction process depicted in Figure 7. After adjustment the observations are consistent in the sense that the image points and lines correspond to lines and planes in space that intersect in the points, lines and planes of the object. Furthermore the constraints on the object features like parallelism are satisfied.

Before reconstruction the observations are transformed into the object coordinate system using the exterior orientation parameters of the images. Two types of reconstruction operations are needed. These are the intersection and the construction operation. The first one can be split up in line-line, plane-plane and line-plane intersection. These operations are discussed next. To assess the precision of object features the covariance matrix of the adjusted observations has to be propagated to the covariance matrix of the object parameters.

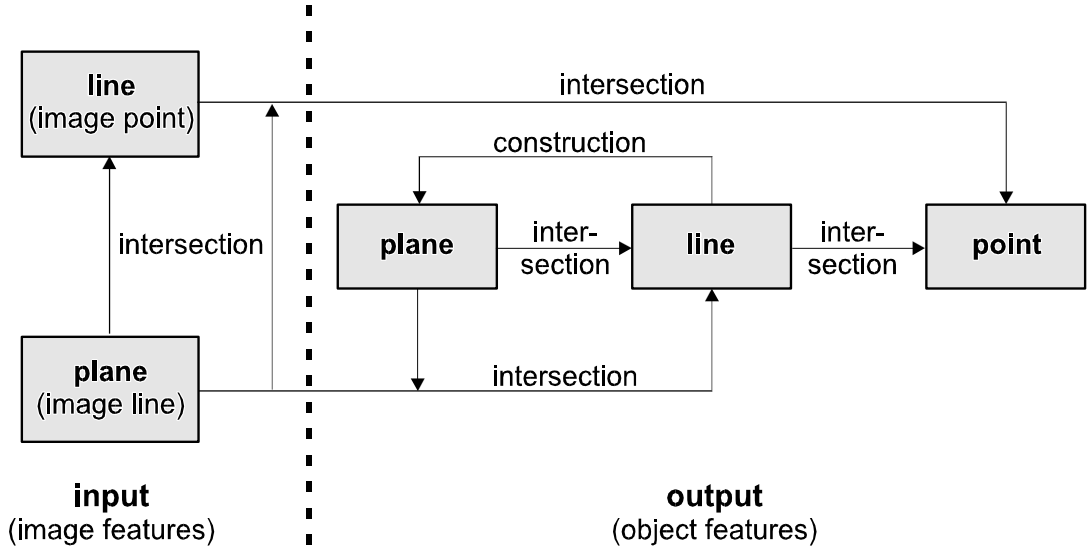

Figure 7: Object reconstruction flow chart

Line-line intersection. The direction to the point that results from the intersection of lines 1 and 2 follows from:

$$\mathbf{x} = \frac{(\mathbf{p}_1 \times \mathbf{d}_1) \times (\mathbf{p}_2 \times \mathbf{d}_2)}{\left|(\mathbf{p}_1 \times \mathbf{d}_1) \times (\mathbf{p}_2 \times \mathbf{d}_2)\right|} \tag{17}$$

The length of the vector to the object point results from the projection of the position vector of the lines:

$$l_x = \frac{l_{p1}}{(\mathbf{x} \cdot \mathbf{p}_1)} = \frac{l_{p2}}{(\mathbf{x} \cdot \mathbf{p}_2)} \tag{18}$$

A special case arises if $\left|(\mathbf{p}_1 \times \mathbf{d}_1) \times (\mathbf{p}_2 \times \mathbf{d}_2)\right|$ approaches zero in other words if the four vectors defining the two lines are in or near to one plane. Then the line resulting from the intersection of the planes defined by the line position vectors $l_{p1}\mathbf{p}_1$ and $l_{p2}\mathbf{p}_2$ has to be intersected with one of the two original lines. This involves a plane-plane intersection described next.

Plane-plane intersection. The direction of the line that results from the intersection of planes 1 and 2 follows from:

$$\mathbf{d} = \frac{(\mathbf{n}_1 \times \mathbf{n}_2)}{\left|\mathbf{n}_1 \times \mathbf{n}_2\right|} \tag{19}$$

If $\left|\mathbf{n}_1 \times \mathbf{n}_2\right|$ approaches zero the two planes are (nearly) parallel and an intersection cannot be computed. If this is not the case the position vector results from:

$$l_p\mathbf{p} = \frac{l_{n1}(\mathbf{n_2} \times \mathbf{d})}{\mathbf{n}_1 \cdot (\mathbf{n_2} \times \mathbf{d})} + \frac{l_{n2}(\mathbf{n}_1 \times \mathbf{d})}{\mathbf{n}_2 \cdot (\mathbf{n}_1 \times \mathbf{d})} = \frac{l_{n1}(\mathbf{n_2} \times (\mathbf{n}_1 \times \mathbf{n}_2)) - l_{n2}(\mathbf{n}_1 \times (\mathbf{n}_1 \times \mathbf{n}_2))}{\left|\mathbf{n}_1 \times \mathbf{n}_2\right|^2} \tag{20}$$

From which l_p and $\mathbf{p}$ can be derived.

Line-plane intersection. The intersection of a line and a plane can be performed by a plane-plane intersection followed by a line-line intersection. The plane-plane intersection uses the original plane and the position vector of the line as a plane definition. In the second step the original line is intersected with the line resulting from the plane-plane intersection. In this way there is no need for an explicit formulation of the line-plane intersection.

Construction of a plane from intersecting lines. The normal vector of the plane defined by intersecting lines 1 and 2 is found from:

$$\mathbf{n} = \frac{(\mathbf{d}_1 \times \mathbf{d}_2)}{\left|\mathbf{d}_1 \times \mathbf{d}_2\right|} \tag{21}$$

If $\left|\mathbf{d}_1 \times \mathbf{d}_2\right|$ approaches zero the two lines are (nearly) parallel and the plane remains undefined. If this is not the case the distance of the plane to the origin results from the projection of the position vector of one of the lines:

$$l_n = l_{p1}(\mathbf{p}_1 \cdot \mathbf{n}) = l_{p2}(\mathbf{p}_2 \cdot \mathbf{n}) \tag{22}$$

Object constraints can aid in object reconstruction. These constraints are satisfied because they have been applied to the observations (see section 5.2). But parts of the object model might not be computable without them, that is with image observations only. This could occur if redundancy is low (or absent) and many object constraints are included in the model. The latter is true if polyhedral primitives are used for CSG (see section 3). In that case the object reconstruction is split up in two parts. First the shape parameters of the

primitives and their position and orientation are determined from the observations through the intersection and construction operations described above. The (relative) positions and orientations of the primitives satisfy the constraints imposed on them. In the second part of the reconstruction the CSG-tree grown in the modelling process is evaluated and the primitives are combined using CSG-operations resulting in the final model of the object or building.

8 Conclusions and future work

A novel formulation of a line-photogrammetric mathematical model was presented. The proposed model is based on condition equations with observations only. Image pose parameters and object parameters are removed from the model. Estimates of the image pose parameters are determined using only information on parallelism in object space. Knowing the pose parameters they can be eliminated from the mathematical model. Constraints on the object parameters are transformed to constraints on the observations. The advantage of this approach is the absence of parameters in the mathematical model and therefore there is no need for approximate values of these parameters. Furthermore the model facilitates sequential adjustment so possible errors can be detected during interactive modelling. Disadvantages are the additional processing step i.e. the separate object reconstruction and the complexity of the formulation of the geometric object constraints as a function of the observations. This type of constraints is especially frequent in CSG-primitives as these shapes are defined by only a few parameters. In the approach presented here primitives have to be represented by a combination of topology and constraints. Modelling with CSG will improve efficiency considerably as with each primitive the topology and constraints of many object features are provided.

The research will continue with a final choice of an integrated data structure for image observations and object parameters. The choice of a mathematical model, the CA(A)D environment to be used and the solid modelling kernel will be the starting-point for the implementation. Then the research will be directed towards a knowledge-based approach to image analysis.

References

[1] Streilein, A., Hirschberg, U., “Integration of digital photogrammetry and CAAD: constraint-based modelling and semi-automatic measurement”, *CAAD Futures '95 International Conference*, Singapore, 1995

[2] Lang, F., Förstner, W., “Surface reconstruction of man-made objects using polymorphic mid-level features and generic scene knowledge”, *International Archives of Photogrammetry and Remote Sensing*, Vol.31, Part B3, pp.415-420, Vienna, 1996

[3] Mason, S., “3D Building Reconstruction using Composites of Surface Primitives: Concept”, *International Archives of Photogrammetry and Remote Sensing*, Vol.31, Part B3, pp.517-522, Vienna, 1996

[4] Hsieh, Y., “SiteCity: A semi-automated site modelling system”, *IEEE conference on Computer Vision and Pattern Recognition*, pp.499-506, San Francisco, 1996

[5] Förstner, W., “A Framework for Low Level Feature Extraction”, *Computer Vision - ECCV '94*, Vol. II, pp.383-394, Ed.: J. O. Eklundh, LNCS 802, Springer, 1994

[6] Burns, J.B., Hanson, A.R., Riseman, E.M., “Extracting Straight Lines”, *IEEE Transactions on Pattern Analysis and Machine Intelligence*, Vol. PAMI-8, No.4, pp.425-455, 1986

[7] Lang, F., Förstner, W., “3D-city modelling with a digital one-eye stereo system”, *International Archives of Photogrammetry and Remote Sensing*, Vol.31, Part B4, pp.261-265, Vienna, 1996

[8] Sinning-Meister, M., Grün, A., Dan, H., “3D City models for CAAD-supported analysis and design of urban areas”, *ISPRS Journal,* nr.51, pp.196-208, 1996

[9] Debevec, P.E., Taylor, C.J., Malik, J., “Modelling and rendering architecture from photographs: a hybrid geometry- and image-based approach”, *Computer Graphics proceedings, Annual Conference Series*, pp.11-20, New Orleans, 1996

[10] Mortenson, M.E., *Geometric modelling*, John Wiley & Sons, Inc., ISBN 0-471-12957-7, New York, 1997

[11] Molenaar, M. “A topology for 3D vector maps”, *ITC Journal* nr.1, pp.25-33, 1992

[12] Kanatani, K., *Statistical optimization for geometric computation: theory and practice*, Machine Intelligence and Pattern Recognition Series, Vol.18, Elsevier Science B.V., Amsterdam, 1996

[13] Patias, P., Petsa, E., Streilein, A., *Digital Line Photogrammetry*, IGP Bericht nr. 252, Eidg. Technische Hochschule, ISBN 3-906513-73-4, Zürich, 1995

[14] Horaud, R., Conio, B., Leboullieux, O., “An analytic solution for the perspective 4-point problem*”, Computer Vision, Graphics, and Image Processing* 47, pp.33-44, 1989

[15] Haralick, R.M., Lee, C.-N., Ottenberg, Noelle, M., “Review and analysis of solutions of the three point perspective pose estimation problem”, *Int. Journal of Computer Vision,* Vol.13, No.3, pp.331-356, 1994

[16] Heuvel, F.A. van den, “Exterior Orientation using Coplanar Parallel Lines”, *10th Scandinavian Conference on Image Analysis*, (in press), Lappeenranta (Finland), 1997

[17] Weik, S., Grau, O., “Recovering 3-D object geometry using a generic constraint description”, *International Archives of Photogrammetry and Remote Sensing*, Vol.31, Part B3, pp.593-598, Vienna, 1996

[18] Teunissen, P.J.G., *Adjustment Theory*, Lecture notes Faculty of Geodetic Engineering, Delft University of Technology, Delft, 1994

[19] Zielinski, H., *Object reconstruction with digital line photogrammetry*, Doctoral thesis Department of Geodesy and Photogrammetry, Royal Institute of Technology, Stockholm, 1993

[20] Gülch, E., “Line photogrammetry: a tool for precise localization of 3D points and lines in automated object reconstruction”, *Integrating Photogrammetric Techniques with Scene Analysis and Machine Vision II*, SPIE Vol. 2486, pp.2-12, Orlando, 1995

[21] McGlone, J.C., “Bundle adjustment with object space geometric constraints for site modelling”, *Integrating Photogrammetric Techniques with Scene Analysis and Machine Vision II*, SPIE Vol. 2486, pp.25-36, Orlando, 1995

[22] Mikhail, E.M., *Observations and Least Squares*, IEP-A Dun-Donnelley Publisher, New York, 1976

[23] Molenaar, M., “Some aspects of sequential processing of photogrammetric bundle blocks”, *ITC Journal* nr.4, pp.398-411, 1982

2.3

Vanishing point detection for architectural photogrammetry[1]

[1] Reference: Heuvel, F.A. van den, 1998. **Vanishing point detection for architectural photogrammetry**. International archives of photogrammetry and remote sensing (Hakodate, Japan), H. Chikatsu & E. Shimizu (eds.), Vol. 32, part 5, pp. 652-659.

Vanishing point detection for architectural photogrammetry

Frank A. van den Heuvel

Delft University of Technology
Faculty of Civil Engineering and Geosciences
Thijsseweg 11, 2629 JA Delft, The Netherlands

Commission V, Working Group 5

ABSTRACT

A priori object information like parallelism and perpendicularity can be very useful for 3D-reconstruction, especially in architectural photogrammetry. With digital close-range imagery parallelism of object lines can be exploited by applying automatic vanishing point detection. This image analysis technique allows the detection of parallel object lines and leads to their spatial orientation in the camera system. The latter can be used for 3D-reconstruction as well as for the determination of the exterior orientation parameters of the image involved. A priori object information in the form of angles between object lines (like perpendicularity) can improve vanishing point detection considerably.

The paper gives a short overview of research in vanishing point detection that has a long history in the computer vision community. A new method for vanishing point detection that is based on rigorous statistical testing and perpendicularity constraints is presented. First results of the application of this method to imagery of buildings are discussed.

Keywords: vanishing point, image analysis, geometric constraints, adjustment, architecture

1 Introduction

Lines in an image that are projections of parallel lines in object space intersect in one point in the image plane, the so-called vanishing point. This holds under the assumption of a perfect pinhole camera model. The vanishing point is found as the intersection of the interpretation planes associated with the image lines and the image plane (figure 1). In case of parallelism of image plane and object lines the vanishing point is at infinity. To avoid this singularity, the vanishing point can be defined as the intersection of the interpretation planes and the Gaussian sphere (Shufelt, 1996). In other words: the vanishing point is related to an orientation in object space represented by a point on the Gaussian sphere. In the sequel the contradictory term "vanishing point orientation" is used to denote this spatial orientation.

With the detection of a vanishing point the orientation of the object lines is known in the camera system. With the detection of several vanishing points the resulting orientations can be used for object reconstruction and for exterior orientation (van den Heuvel, 1997). In all applications where parallel object lines are present, vanishing point detection can be a valuable tool for the automation of these major tasks of vision systems.

Vanishing point detection is traditionally applied for the navigation of autonomous vehicles or robots in indoor or outdoor man-made environments (Pla et al.,1997; Straforini et al., 1992). This paper concentrates on the application of vanishing point detection to terrestrial close-range imagery of buildings. An example of this application can be found in (Collins,

1993). An application to building reconstruction from aerial imagery is investigated in (Shufelt, 1996). The main difference between applications for navigation and for object reconstruction is the fact that navigation applications demand fast algorithms because of their real-time nature. In applications for object reconstruction this limiting condition can be dropped, as full automation is generally not possible and thus operator interaction will be the bottleneck for the processing time.

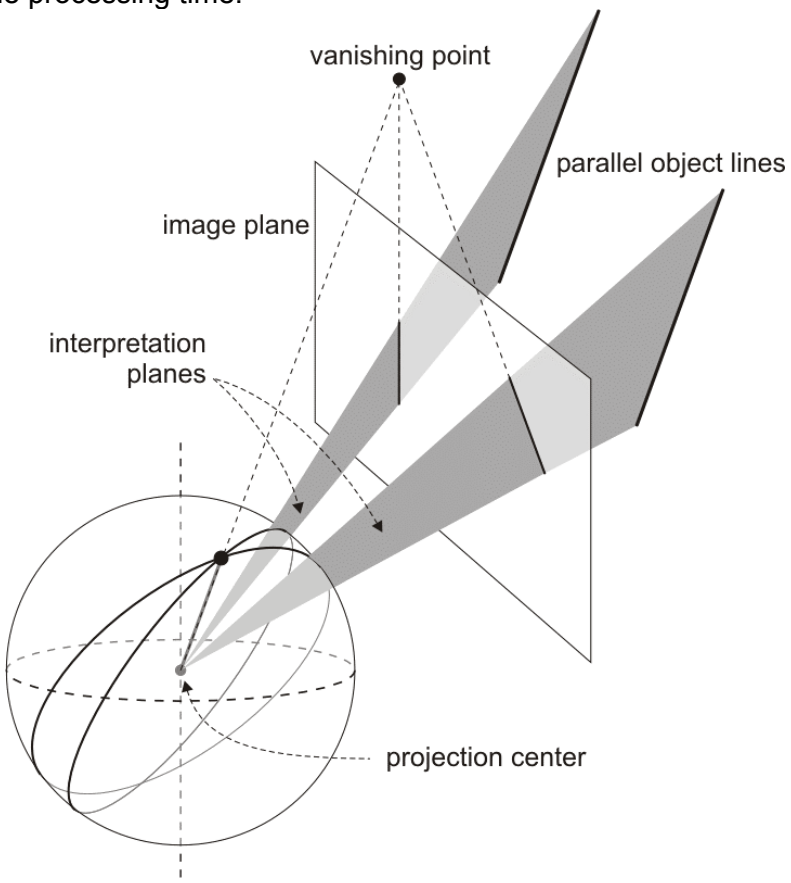

Figure 1: Vanishing point on image plane and Gaussian sphere after (Shufelt, 1996)

After a discussion of the characteristics of existing vanishing point detection techniques in section 2, a new technique is presented in section 3. This technique is more computationally expensive than existing techniques, but it is rigorous from a statistical point of view. In section 4 some examples of applications of the proposed technique are presented.

2 Vanishing point detection techniques

Straight line features have to be extracted from the image prior to the vanishing point detection. This preprocessing step will not be discussed here as it has been thoroughly investigated (Burns et al., 1986; Förstner, 1988). In this section only the major characteristics of previous research in vanishing point detection are emphasized.

Vanishing point detection can be regarded as the search for a set of lines that intersect at one point in the image plane. It is assumed that the largest sets of lines correspond to vanishing points. As a vanishing point can be outside the image boundaries and even at infinity, the search area is unbounded. In order to bound the search domain, most vanishing point detection techniques apply a specific representation of the image lines.

In Straforini (1993) a representation in a bounded and partitioned polar space is used. Each line is represented by a point in polar space and grouped with lines that are located in the same partition. In this approach there are restrictions to the relative position of camera and object. Other shortcomings are the dependency of the partitioning of the polar space on the orientation of the camera relative to the object and the fact that the precision of the line parameters is not taken into account.

Most of the vanishing point detection techniques use a Hough transform approach in which the parameter space is located on a so-called Gaussian sphere, see for instance (Lutton et al., 1994). In these approaches interpretation planes associated with image lines are intersected with a (unit) sphere with its centre positioned at the projection centre. Then these intersections are great circles and vanishing points are found as intersections of great circles (figure 1). In order to detect a vanishing point a quantisation of the sphere is performed and the number of great circles running through each bucket (or pixel) of the grid on the sphere is counted. Then maxima are detected and assumed to correspond to vanishing points. In this approach there are no restrictions on the orientation of the camera and the search space is limited. A disadvantage is the choice for the quantisation of the sphere to be made.

In Shufelt (1996) several alternatives for Gaussian sphere-based vanishing point detection are investigated, including two complementary methods. The first method integrates a priori knowledge on camera orientation and knowledge on the geometry of the imaged objects. The second method applies edge error modelling in order to account for the precision (and length) of the lines. These and existing methods are combined resulting in 24 experimental options that are tested on aerial imagery.

In the next section a new method for vanishing point detection is presented that applies geometric object information, but does not use the Hough transform and thereby eliminates its disadvantages. This method is tested on close-range imagery of buildings.

3 A new method for vanishing point detection

The principal goal of the new method for vanishing point detection is the robust detection of image lines that intersect at the three main vanishing points, under the assumption of perpendicularity between the three corresponding orientations in object space. The image line feature extraction is not part of the procedure but considered as a pre-processing step. The principles of the method can be used for the detection of an arbitrary number of vanishing points with or without a priori information on object geometry.

3.1 Overview

The method proposed here is based on the statistical testing of the intersection hypotheses of combinations of 3 image lines or rather the intersection of the 3 interpretation planes associated with these lines. This test is discussed in the next section. The major steps of the procedure are the following (the procedure is discussed in detail in section 3.3):

- Compute statistical test values of all combinations of 3 interpretation planes (i.e. image lines)
- Detection of groups of lines that intersect in a vanishing point by clustering based on these test values (section 3.4)
- For the largest clusters: statistical testing of line error hypotheses using all condition equations and iterative elimination of rejected lines
- Final selection of largest cluster as the vanishing point cluster

- Restart of the procedure for the next vanishing point with the use of information on perpendicularity to previously detected vanishing point(s)
- After detection of the 3 vanishing points: statistical testing of all condition equations (for intersection and perpendicularity)

3.2 The statistical test of the intersection constraint

The intersection constraint introduced in the previous section is formulated with the normals to the interpretation planes of the 3 lines involved. The image lines are represented by the image coordinates of the end points (figure 2). The image coordinates are assumed to be corrected for lens and image plane distortions. Then a point in the image corresponds to a direction in object space (in the coordinate system of the camera):

$$\mathbf{x} = (x, y, -c)\,, \quad c\text{: camera constant} \qquad (1)$$

The normal to the interpretation plane of the image line i with end points *1* and *2* is found with:

$$\mathbf{n}^i = \mathbf{x}_1 \times \mathbf{x}_2 \qquad (2)$$

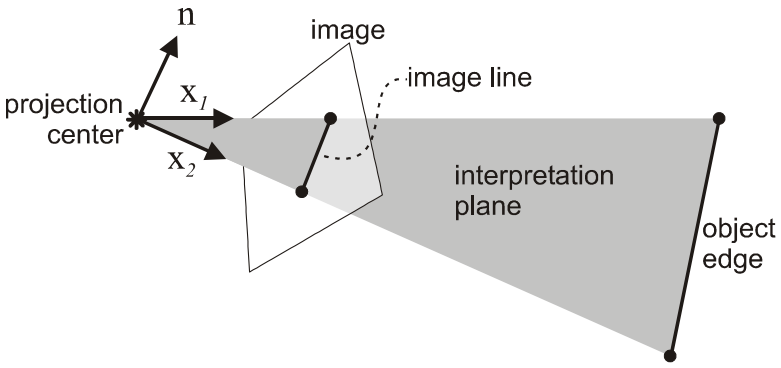

Figure 2: The interpretation plane

The intersection constraint can be written as the determinant of the matrix build from the 3 normal vectors i, j and k (van den Heuvel and Vosselman, 1997):

$$\left[\mathbf{n}^i, \mathbf{n}^j, \mathbf{n}^k\right] = \det\left(\mathbf{n}^i, \mathbf{n}^j, \mathbf{n}^k\right) = 0 \qquad (3)$$

In case the lines do not (perfectly) intersect this constraint will result in a misclosure (m):

$$\left[\mathbf{n}^i, \mathbf{n}^j, \mathbf{n}^k\right] = m \qquad (4)$$

The hypothesis of interpretation plane intersection is tested with the normalised misclosure relative to a critical value (cv):

$$\left|\frac{m}{\sigma_m}\right| < cv \qquad (5)$$

The standard deviation of the misclosure (σ_m) is computed from the covariance matrix of the image coordinates ($\mathbf{Q}$):

$$\sigma_m{}^2 = \mathbf{b}^{\mathrm{T}}\mathbf{Q}\mathbf{b} \qquad (6)$$

with $\mathbf{b}$ the vector of partial derivatives. The part of $\mathbf{b}$ for image point *a* can be written as:

$$\mathbf{b}^a = \frac{\partial m}{\partial \mathbf{n}^i} \frac{\partial \mathbf{n}^i}{\partial \mathbf{x}^a} \qquad (7)$$

The camera constant is assumed to be error free. For the image points covariance matrix several options are available for the stochastic model:

- If lines are extracted using an edge detection approach, the variances of the coordinates of the end points are assumed to decrease linearly with the length of the line in pixels.
- For lines that are extracted manually by measurement of their end points, a constant variance is assumed for all end point coordinates.

Precision information available from the feature extraction procedure could be used for the stochastic model, but then the model does not account for imperfections of the camera model or for possible deformations of the object. Line orientation does not play a role in the stochastic model as only precision information perpendicular to the line affects the precision of the interpretation plane normals.

3.3 The procedure

In this section the procedure for vanishing point detection is discussed in detail. Although the method consists of the steps in section 3.1 there are differences between the parts of the procedure for each vanishing point. The differences relate to the use of perpendicularity assumptions.

3.3.1 The first vanishing point

The intersection constraint introduced in section 3.2 involves 3 lines. If a statistical test is computed for each combination of 3 lines, we have to deal with an O(n^3) problem (n is the number of image lines). Although computing efficiency is not a design goal, the order is reduced to n^2 by selecting a line of the first vanishing point, the so-called start-line. The longest line is chosen as the start-line and in many cases this line belongs to one of the 3 vanishing points to be detected. If this is not the case the start-line can be chosen manually. The procedure for the first vanishing point runs as follows:

- The test value of (n-1)(n-2)/2 combinations of the start-line and two other image lines is computed according to (5).
- Lines are clustered using the results of the testing (section 3.4).
- For the largest clusters an adjustment is set up, based on all (independent) constraints in the cluster and a line error hypothesis is tested for each line.
- Rejected lines are removed from the cluster and the adjustment is repeated until all lines are accepted.
- The largest cluster is selected as the vanishing point cluster.

From the adjustment the adjusted 3D orientation of the first vanishing point results. This orientation is input to the detection procedure of the next vanishing point.

3.3.2 The second vanishing point

Because the orientation of the second vanishing point is assumed to be perpendicular to the orientation of the first, the normal to the interpretation plane of the start-line can be replaced by the orientation of the first vanishing point ($\mathbf{v}_1$) in the procedure for the first vanishing point. $\mathbf{v}_1$ results from the normals of two interpretation planes i and j of the first vanishing point:

$$\mathbf{v}_1 = \mathbf{n}_1{}^i \times \mathbf{n}_1{}^j \qquad (8)$$

The normals are computed with adjusted observations from (2). The constraint (3) is rewritten as:

$$\left[\mathbf{n}^i, \mathbf{n}^j, \mathbf{v}_1\right] = 0 \qquad (9)$$

Again the computation of the statistical test values is of order n^2. The perpendicularity between the second and third vanishing point orientation is used to detect both vanishing points in one go. Therefore a second statistical test is introduced to test the hypothesis of perpendicularity of the two vanishing points of lines i and j. The related constraint is:

$$\left(\mathbf{n}^i \times \mathbf{v}_1\right) \cdot \left(\mathbf{n}^j \times \mathbf{v}_1\right) = 0 \qquad (10)$$

Now two sets of test values are available for the clustering. First the clustering is performed using the smallest of the two values. This results in a (largest) combination cluster of lines of the second and third vanishing point. Then the clustering is repeated using only the lines of the combination cluster and test values from the parallelism test (5). In this way the second vanishing point is detected as a subset of the combination cluster, thereby increasing the chances of a correct detection.

3.3.3 The third vanishing point

For the detection of the third vanishing point the remaining lines of the combination cluster could be used. But in order to use the information contained in the detection of the second (and first) vanishing point, all lines are used for an intersection test that is based on the orientations of the first two vanishing points computed from (8). Now (9) is rewritten as:

$$\left[\mathbf{n}^i, \mathbf{v}_2, \mathbf{v}_1\right] = 0 \qquad (11)$$

The computation of the statistical test values reduces to order n because in fact the third vanishing point is already known with the detection of the first two. This is due to the perpendicularity assumption:

$$\mathbf{v}_3 = \mathbf{v}_1 \times \mathbf{v}_2 \qquad (12)$$

By allowing all lines to be candidate for the detection of each vanishing point – even lines that are in a cluster of a previously detected vanishing point – the lines can be detected that are on (or close to) a so-called horizon line, the line that connects two vanishing points in the image plane (Williamson and Brill, 1989). It is important to detect these lines because an ambiguity in their spatial orientation remains.

3.4 Clustering

The acceptance of statistical test (5) is evidence for the intersection of 3 lines in a point in the image plane. A clustering is applied to the test results that aims at the detection of groups of lines that intersect in one image point. The clustering procedure for the first two vanishing points includes the following steps:

- For each accepted test it is checked whether one of the two lines is present in an existing cluster (the third line is the so-called start-line or a vanishing point orientation). If this is not the case, a new cluster is established.
- If a line of an accepted test is present in an existing cluster, the other line becomes a candidate for the cluster.
- The candidate line becomes a member of the cluster if all the tests of lines already in the cluster and the candidate line are accepted. If this is not the case, a new cluster is established.

This procedure is repeated as long as new clusters are created. In the last iteration all tests are evaluated in the presence of all clusters. The result is that lines can appear in more than one cluster and overlap between clusters can be close to 100%. The major advantage is the reduced sensitivity of the clustering result to the order in which the lines are processed. The largest clusters are analysed in more detail in order to decide which lines belong to the

vanishing point (see the next section). The size of a cluster is defined by the number of lines it contains, or optionally by the sum of the lengths of all lines in the cluster. In the latter case clusters with longer lines are preferred.

In the clustering procedure two critical values are used for evaluation of the statistical tests. One critical value for the candidate test (first step of the procedure) and another value for the membership test (last step of the procedure). Because type I errors (rejection of the intersection hypothesis although it is true) have to be avoided in the clustering phase, for the level of significance (α) the value 0.1% is chosen for the candidate test. For the membership test a lower value for the level of significance is chosen (e.g. 0.01%) in order to avoid the creation of many overlapping clusters.

For the detection of the third vanishing point the clustering procedure can be simplified due to the perpendicularity to the orientations of the first two vanishing points detected previously. For the third vanishing point only one cluster is built from all lines for which the statistical test (5) is accepted.

3.5 Adjustment and testing

The clustering procedure described in the previous section results in groups of lines that are candidates for a vanishing point. For a preset number (e.g. 3) of the largest clusters an adjustment is set up. The functional model contains a complete set of *n*-2 independent condition equations (*n* is the number of image lines). These equations have the form of (3), (9) or (11) for respectively the first, second and third vanishing point. After linearisation this model can be written as:

$$\mathbf{B}^{\mathrm{T}} E\{\mathbf{y}\} = \mathbf{0} \;;\; \mathbf{Q}_{\mathbf{y}} \qquad (13)$$

with:

$E\{\}$ mathematical expectation
$\mathbf{y}$ vector of observations (image coordinates)
$\mathbf{B}$ design matrix (partial derivatives, see (7))
$\mathbf{Q}_{\mathbf{y}}$ covariance matrix of the observations

The solution to this model is presented in (van den Heuvel and Vosselman, 1997).

Two different types of statistical tests are applied. First an overall test or Fisher test is applied by computing the estimated variance of unit weight:

$$(\hat{\sigma}^2 =) \frac{\mathbf{m}^{\mathrm{T}} (\mathbf{B}^{\mathrm{T}} \mathbf{Q}_{\mathbf{y}} \mathbf{B})^{-1} \mathbf{m}}{(n-2)} < cv\sigma_0^{\,2} \qquad (14)$$

The vector of misclosures ($\mathbf{m}$) is computed from the non-linearised condition equations. The critical value (cv) of this test is derived from the Fisher distribution (degrees of freedom *n*-2, ∞; α=1%) multiplied with a factor 2 in order to avoid type I errors in this stage of the procedure. The second test is a line error test, examining the alternative hypothesis of an error in a single line. This is a so-called non-conventional alternative hypothesis (Baarda, 1968) and will not be discussed in detail here. The level of significance for this test is chosen in the same way as for the overall test. If a line test is rejected, the line is removed from the cluster and the model is built again. This iterative testing procedure stops if all line tests are accepted. The largest cluster of which the overall test and all line tests are accepted is assumed to be the cluster with the lines intersecting at the vanishing point.

After the detection of the three vanishing points a final adjustment is performed. Then the three sets of condition equations used for each vanishing point are combined in one adjustment with the three perpendicularity conditions of the form:

$$(\mathbf{n}_1^i \times \mathbf{n}_1^j) \cdot (\mathbf{n}_2^i \times \mathbf{n}_2^j) = 0 \qquad (15)$$

This is the condition equation for perpendicularity between the orientations of the first two vanishing points (1 and 2), derived from the normals of two interpretation planes (i and j for each vanishing point). As an option, the inclusion of the perpendicularity constraints can be dependent on the outcome of the statistical test of the perpendicularity hypothesis.
For the final adjustment only lines that are uniquely clustered to one of the vanishing points are used, so horizon lines are excluded. The level of significance for the overall test and line error tests is set to 1%.

Figure 3: Delft image: lines of first, second and third vanishing point (from left to right)

Figure 4: Delft image: rest of the lines, adjusted lines and non-adjusted lines (from left to right)

4 Examples

In this section two applications of the new method for vanishing point detection are discussed. Both images are taken with a calibrated Kodak DCS420 digital camera with a 20mm lens. The CCD sensor of this camera contains approximately 1500x1000 pixels with a pixel spacing of 9μm. The images are taken from about 1.5m above the ground and as a result they contain a horizon line (the connecting line between the two vanishing points of the horizontal lines, see section 3.3). Before the extraction of straight lines, the images are corrected for lens distortion. Without correction long lines tend to break up in smaller parts due to line curvature. Straight lines were extracted using a line-growing algorithm (Förstner, 1988).

4.1 Example 1: image of a historic building

The first image is taken in the historic centre of Delft (figure 5). The number of extracted lines varies with the parameter settings for the line-growing algorithm. The settings used resulted in 397 lines with a minimum line length of 50 pixels. The standard deviation of the coordinates of the end points of the lines is modelled as follows:

$$\sigma = \frac{0.1}{\sqrt{l}} \text{ mm} \qquad (16)$$

Where *l* is the line length in pixels. Then the largest standard deviation is 1.3 pixel. For the longest line (517 pixels) the standard deviation drops below 0.5 pixel. These values are chosen relatively high because of deformations present in this old building. Assuming a better precision, lines in some parts of the building would be excluded from their vanishing points.

Figure 5: Test image of a historic building in Delft

The result of the vanishing point detection is visualized in figure 3. In figure 4 on the left lines are shown that were not accepted as a member of one of the vanishing point clusters. Some lines obviously do not have a vanishing point orientation, for other lines – like the ones above and below the door – deformations of the building are suspected. The picture in the centre of figure 4 shows lines that are adjusted for parallelism and perpendicularity constraints. In this example the maximum deviation from perpendicularity is 1.4 degree and the statistical test of the perpendicularity hypothesis was rejected. Lines that intersect with the first and third vanishing point (left and right in figure 3) are not adjusted because no choice for one of the vanishing points could be made. In figure 6 a part of the image is enlarged. The adjusted lines are shown in the upper half, the original lines extracted by line growing in the lower half of the figure. The angle between the adjusted lines and the original lines (1.2 degree) is due to deformations of the building in combination with the use of perpendicularity constraints. Without perpendicularity constraints the angle reduces to 0.7 degree.

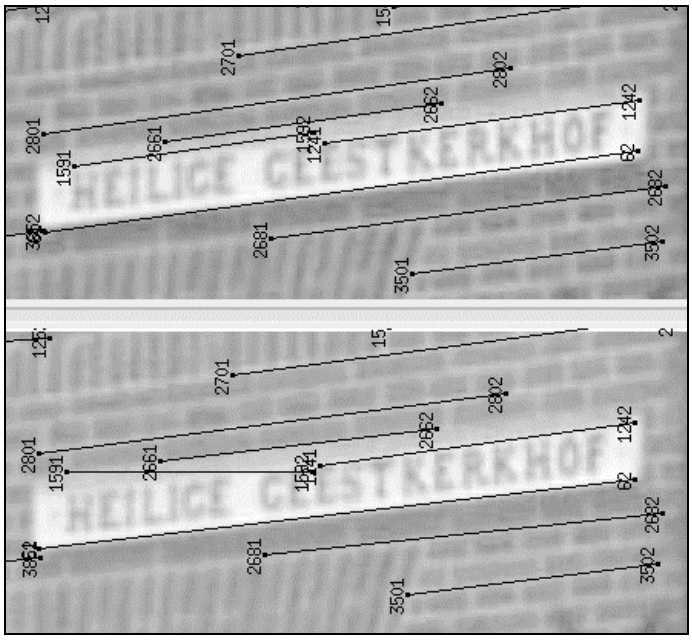

Figure 6: Enlargement showing adjusted (top) and original lines

In figure 4 on the right all the lines are pictured that are not adjusted. These are the lines that could not be (uniquely) grouped to one of the vanishing points. 30 of them are horizon lines. In table 1 results of clustering and statistical testing are summarised for both examples.

Vanishing point	Example 1		Example 2	
	# lines (rejected)	$\frac{\hat{\sigma}^2}{\sigma_0^2}$	# lines (rejected)	$\frac{\hat{\sigma}^2}{\sigma_0^2}$
1	175 (1)	2.08	61(0)	0.32
2	130 (3)	1.67	160 (9)	1.26
3	104 (0)	1.25	20 (0)	2.49
All	349 (0)	1.49	202 (0)	1.05

Table 1: Results of the clustering and testing

4.2 Example 2: image of the faculty building

The second test image is an image of our faculty building (figure 7). Settings that were used for the line-growing algorithm resulted in 250 lines with a minimum line length of 30 pixels. The standard deviation of the coordinates of the end points is a factor 2 smaller than in the previous example, but depends on the line length in the same way (equation 16). The largest standard deviation is close to 1 pixel. For the longest line (1062 pixels) the standard deviation drops to 0.17 pixel. The result of the vanishing point detection is visualized in figure 8. The order of the pictures is as in the previous example. From top left the first three images show the lines of the three vanishing points. The fourth image shows the lines that were not accepted as a member of one of the vanishing point clusters. It was concluded from visual inspection that none of these lines is expected to intersect at a vanishing point. Because the image is taken almost perpendicular to the façade, there are not many lines detected for the third vanishing point. In fact there is only one line of the third vanishing point visible (and detected) that has the spatial orientation of the third vanishing point (this is the line on top of the right tower of the building). The other 19 lines are all identified as horizon lines and thus excluded from the final adjustment (see bottom row of figure 8 with adjusted lines on the left and non-adjusted lines on the right). The adjustment only contains one perpendicularity condition between lines of the first and second vanishing point. The deviation from perpendicularity before adjustment was 0.065 degree and the statistical test of the perpendicularity hypothesis was accepted. Clustering and testing results are summarized in table 1.

Figure 7: Test image of the faculty building

5 Conclusions

A new method for vanishing point detection has been presented. This method is based on rigorous statistical testing and exploits the assumption of perpendicularity between the three major spatial orientations of the object lines. This assumption as well as the assumption of parallelism of object lines – the basic assumption for vanishing point detection – frequently holds for man-made objects like buildings.

The characteristics of the method can be summarized as follows:

- The method involves only a small number of parameters. Two types of parameters can be distinguished: parameters for the stochastic model of the observations and parameters for the statistical testing (i.e. the levels of significance).
- After detection of the first vanishing point the detection of second and third vanishing point is facilitated by the use of perpendicularity information. In the example of section 4.2 even a single line with the spatial orientation associated with the third vanishing point, was detected.
- The detection of lines on (or close to) the horizon line is part of the procedure.
- The adjusted spatial orientations of the lines that have been uniquely identified to intersect at a vanishing point, result as a by-product.
- The method is not designed for real-time applications because it is computationally expensive.

Although the new method has not been extensively tested and compared to existing techniques for vanishing point detection, the results of the presented tests show its suitability for architectural applications.

References

Baarda, W., 1968. A testing procedure for use in geodetic networks. Netherlands Geodetic Commission, New Series, Vol. 2 (5), Delft.

Burns, J.B., Hanson, A.R., Riseman, E.M., 1986. Extracting straight lines. IEEE transactions on pattern analysis and machine intelligence, Vol. 8 (4), pp. 425-455.

Collins, R.T., 1993. Model Acquisition using Stochastic Projective Geometry. dissertation, Department of Computer Science, University of Massachusetts, Amherst.

Förstner, W., 1988. Model Based Detection and Location of Houses as Topographic Control Points in Digital Images. International Archives of Photogrammetry and Remote Sensing, Kyoto, Vol. 27 (B11-III), pp.505-517.

Heuvel, F.A. van den, 1997. Exterior Orientation using Coplanar Parallel Lines, 10th Scandinavian Conference on Image Analysis, Lappeenranta, pp. 71-78.

Heuvel, F.A. van den, and G. Vosselman, 1997. Efficient 3D-modeling of buildings using a priori geometric object information. Videometrics V, Sabry F. El-Hakim (ed.), SPIE Vol. 3174, pp. 38-49.

Lutton, E., Maitre, H., Lopez-Krahe, J., 1994. Contribution to the Determination of Vanishing Points Using Hough Transform. IEEE transactions on pattern analysis and machine intelligence, Vol. 16 (4), pp. 430-438.

Pla, F., Sanchiz, J.M., Marchant, J.A., Brivot, R., 1997. Building perspective models to guide a row crop navigation vehicle. Image & Vision Computing, Vol. 15 (6), pp. 465-473.

Shufelt, J.A., 1996. Performance Evaluation and Analysis of Vanishing Point Detection Techniques, ARPA Image Understanding Workshop, Morgan Kaufmann Publishers, Palm Springs, pp. 1113-1132.

Straforini, M., Coelho, C., Campani, M., 1993. Extraction of vanishing points from images of indoor and outdoor scenes. Image and Vision Computing, Vol. 11 (2), pp. 91-99.

Williamson, J.R., Brill, M.H., 1989. Dominant Geometry Combinations of Two- and Three-Point Perspective in Close-Range Applications. Photogrammetric Engineering and Remote Sensing, Vol. 55 (2), pp. 223-230.

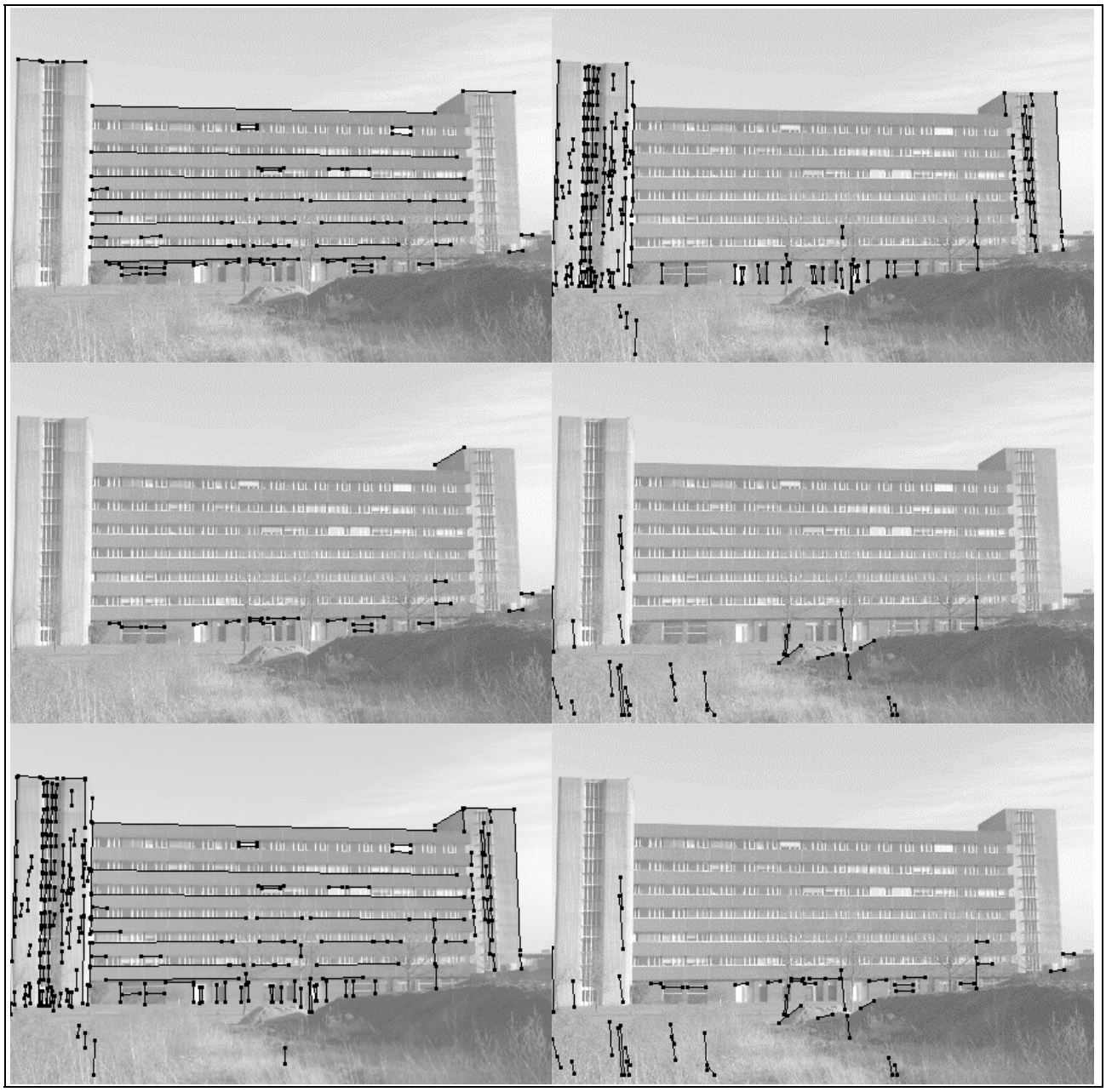

Figure 8: Vanishing point detection results for the image of the faculty building. From top left to bottom right: the lines of the three vanishing points, the rest of the lines, adjusted lines and non-adjusted lines

2.4

3D reconstruction from a single image using geometric constraints[1]

[1] Reference: Heuvel, F.A. van den, 1998. **3D reconstruction from a single image using geometric constraints.** ISPRS Journal of Photogrammetry and Remote Sensing, Vol.53, No.6, Elsevier, Amsterdam, pp. 354-368.

3D reconstruction from a single image using geometric constraints

Frank A. van den Heuvel

Delft University of Technology
Faculty of Civil Engineering and Geosciences
Thijsseweg 11, 2629JA Delft, The Netherlands

Abstract

Photogrammetry has many advantages as a technique for the acquisition of three-dimensional models for virtual reality. But the traditional photogrammetric process to extract 3D geometry from multiple images is often considered too labour-intensive. In this paper a method is presented with which a polyhedral object model can be efficiently derived from measurements in a single image combined with geometric knowledge on the object. Especially man-made objects can often be described by a polyhedral model and usually many geometric constraints are valid. These constraints are inferred during image interpretation or may even be extracted automatically. In this paper different types of geometric constraints and their use for object reconstruction are discussed. Applying more constraints than needed for reconstruction will lead to redundancy and thereby to the need for an adjustment. The redundancy is the basis for reliability that is introduced by testing for possible measurement errors. The adjusted observations are used for object reconstruction in a separate step. The model that is obtained from a single image will often not be complete, for instance due to occlusion. An arbitrary number of models can be combined using similarity transformations based on the coordinates of common points. The information gathered allows for a bundle adjustment if highest accuracy is strived for. In virtual reality applications this is generally not the case, as quality is mainly determined by visual perception. A visual aspect of major importance is the photo-realistic texture mapped to the faces of the object. This texture is extracted from the same (single) image.
In this paper the measurement process, the different types of constraints, their adjustment and the object model reconstruction are treated. A practical application of the proposed method is discussed in which a texture mapped model of a historic building is constructed and the repeatability of the method is assessed. The application shows the feasibility of the method and the potential of photogrammetry as an efficient tool for the production of 3D models for virtual reality applications.

Keywords: architecture, line photogrammetry, geometric constraints, adjustment, object reconstruction, virtual reality

1 Introduction

Many applications of virtual reality do not pose the highest accuracy demands. Because of this and the fact that photogrammetry is a specialised discipline that can be labour-intensive, other methods like tacheometric survey are sometimes chosen for the acquisition of 3D models of existing structures. Then photographs are taken only to obtain photo-realistic textures.

The goal of the research presented here is the development of an efficient method for the acquisition of 3D models that are suitable for virtual reality applications. In these applications aspects that relate to visual perception are often more important than the precision of the coordinates as such. Two major aspects of visual perception are:

- The sensitivity of the eye to certain geometric properties of the model like parallelism, perpendicularity and symmetries.
- The amount of detail of the model. Without increasing the amount of geometric detail, a model is considerably enhanced by adding detail in a radiometric way in the form of photo-realistic textures on the surface of the object model.

The need for efficiency improvement of photogrammetric model acquisition has stimulated research efforts directed towards automation (e.g. Hsieh, 1996; Streilein and Hirschberg, 1995; Lang and Förstner, 1996). But it has become clear that – at least for many years to come – we will not be able to reach full automation. Interpretation by an operator cannot be eliminated entirely. Research aims at a reduction of operator interaction by automation of parts of the photogrammetric process. Another opportunity for efficiency improvement lies in the reduction of the number of images to be manually processed. This approach for efficiency improvement is chosen here.

The method that is discussed in this paper is directed towards the application and user requirements listed above. It is a line-photogrammetric method (i.e. image lines are the basic measurements, see section 2) suitable for objects that can be described by a polyhedral object model and for which a certain number of geometric constraints like parallelism of object lines hold. The number of constraints needed depends on the topology of the model and is discussed in section 3. An application field in which these constraints are abundant is architecture. For most buildings a redundant number of constraints can be specified and therefore an adjustment can be applied (section 4). Adjustment in combination with statistical testing and the elimination of erroneous measurements or constraints leads to a reliable object model even when only one image is used. Redundant constraints result in condition equations for the observations. In an adjustment based on only condition equations and no parameters, there is no need for approximate values. Another advantage is the absence of an object coordinate system and the related rank deficiency. From the adjusted image observations and the object information available, the 3D coordinates of the object model are computed (section 5). The result of the proposed method is a boundary representation of the object with texture extracted from the image mapped to each face (section 6).

In figure 1 a flow chart of the photogrammetric process for object modelling from a single image is depicted. The interpretation of a single image by an operator results in photogrammetric measurements, the topology of the object model and geometric constraints. This information is processed in two steps: adjustment of redundant constraints followed by 3D reconstruction using adjusted observations.

Of course, only a part of the three-dimensional object can be modelled from a single image. If a complete object model is desired, additional images have to be taken and processed in the same way as the first image. With the identification of corresponding object points in overlapping parts of the models, the parameters of a 3D similarity transformation can be computed. In this way the relative position and orientation of the partial models is computed and thereby the relative orientation of the images associated with these models. In this way the partial models can be transferred to a common coordinate system. The number of images needed to generate a complete object model mainly depends on the geometric complexity of the object involved. For some objects (e.g. a cube) only two images are needed for a full model.

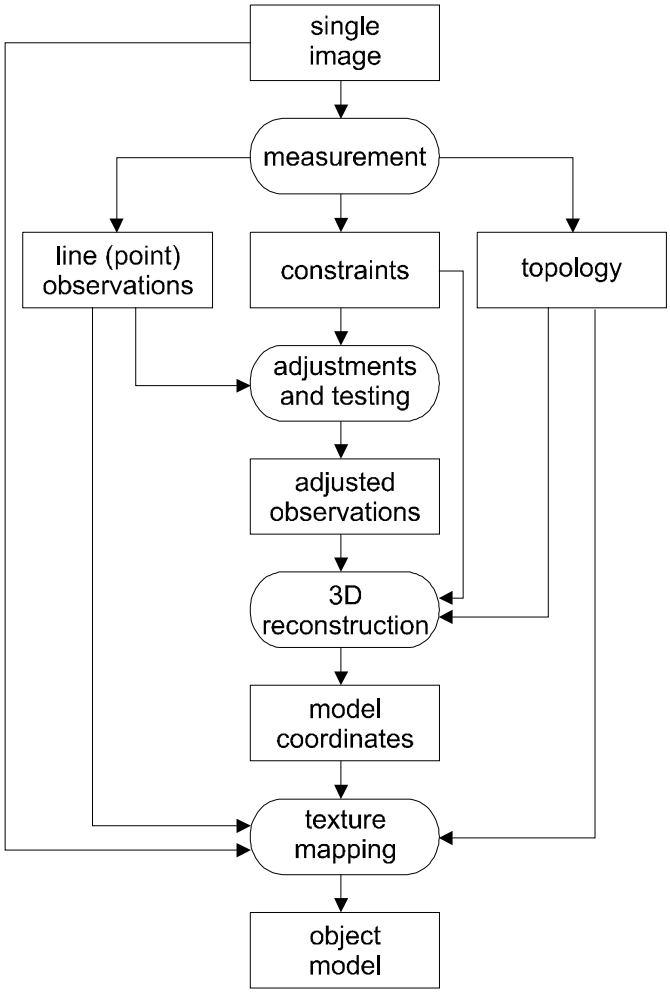

Figure 1: The photogrammetric process for object modelling from a single image

The approach outlined above is not only suitable for virtual reality applications, but as well for the reconstruction of demolished historic buildings of which only a few (single) images are available. If parameters of the camera model like the focal length are unknown, it is possible to estimate them with the use of geometric object information (van den Heuvel, 1997; Kraus et al., 1996; Williamson and Brill, 1989). The method described in this paper assumes the camera to be calibrated, i.e. the interior orientation parameters are known.

The proposed method of object reconstruction from a single image is demonstrated in an example application in which a texture-mapped model of a historic building is obtained (section 7).

2 The measurement process

The measurement process is the process of gathering all information that is needed for the 3D reconstruction from a single image. Two types of information are distinguished: measured image lines and object information. In section 2.1 the photogrammetric observations are introduced i.e. the position and orientation of image lines or image points being the intersections of the lines. Together with the measurement of image lines the topology of the object is specified. In section 2.2 the gathering of different types of additional, mainly geometric object information is discussed.

2.1 The image lines and object topology

In this research a line-photogrammetric approach is chosen. The advantages of this approach over conventional (point-based) photogrammetry can be found in (Patias et al., 1995). The main advantages are the improved possibilities for automatic feature extraction and the fact that only a part of a line needs to be visible in the image. The advantages apply especially to applications where many linear features are present like in architectural photogrammetry.

The image line observations can be derived by manual measurement or by semi-automatic line extraction. Automatic (straight) line extraction has been extensively studied (e.g. Burns et al., 1986). Even in the case that lines are extracted automatically, operator interaction cannot be avoided. First the line segments corresponding to relevant edges of the object have to be selected from the extracted straight lines. Possibly some lines that were not extracted automatically have to be measured manually. Secondly topological relations between the lines have to be specified by the operator i.e. line segments are connected to closed polylines that border a face of the object. An example of the result of this process is depicted in figure 11.

Independent of the way in which the image lines are derived each line is defined by the image coordinates (x, y) of its end points. In the mathematical model however the normal vector $(\mathbf{n})$ to the interpretation plane is introduced as observation vector instead of the coordinates of the end points i and j (see figure 2):

$$\mathbf{n} = \frac{\mathbf{x}^i \times \mathbf{x}^j}{\left| \mathbf{x}^i \times \mathbf{x}^j \right|} \qquad (1)$$

with:

$$\mathbf{x} = \frac{(x, y, -c)}{\left| x, y, -c \right|}$$

and: c: camera constant

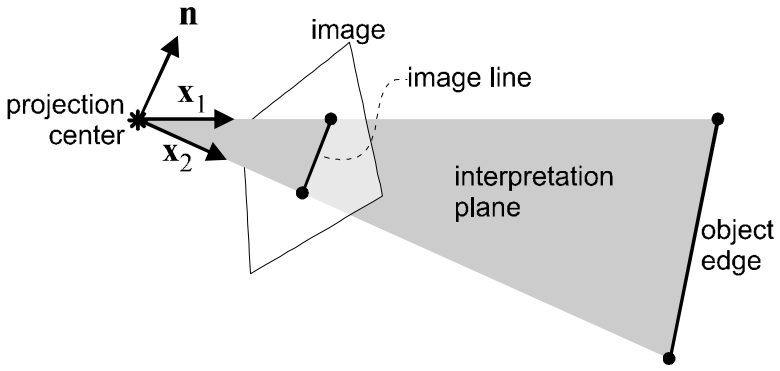

Figure 2: The interpretation plane relates image line and object edge

Interior orientation parameters have to be known to compute directions in object space (x) from points in the image. In the sequel image coordinates are assumed to be corrected for deviations from the pinhole camera model.

2.2 The additional object information

The object reconstruction from image lines of a single image in combination with the object topology is only possible when additional information is available. The additional information consists of object information in the form of topological and geometric constraints.

In (van den Heuvel and Vosselman, 1997) an overview of different types of constraints is given. The most common constraints are:

- Coplanarity
- Parallelism
- Perpendicularity
- Symmetry
- Distance (ratio)

Below the specification of these constraints during the measurement process is treated. The subject of the next section is the mathematical formulation of the constraints and their contribution to the object reconstruction.

- The specification of **coplanarity** constraints is performed in one step with the line measurement and topology specification. Image lines are measured as a part of a closed polyline. In object space the polyline is assumed to surround a planar face of the object so all the individual lines of the polyline are coplanar. Furthermore, different polylines (i.e. faces) can be specified to be coplanar. Coplanarity is the only constraint of topological nature.
- Each edge of the object model is assigned a code for its presumed orientation in object space. **Parallelism** is assumed to be present between lines that have the same code. The three major object orientations are distinguished from other orientations.
- **Perpendicularity** can be assigned to any combination of orientations in object space. This constraint is applied to combinations of the major object orientations by default.
- **Symmetry** can be assigned to an edge of a polyline. The symmetry applies to the angles between this edge and the two connected edges (see figure 3). Of course many more types of symmetry constraints could be defined, for instance if a door has to be centred within a façade. This and other symmetry constraints might also be incorporated in the form of distance ratio constraints.

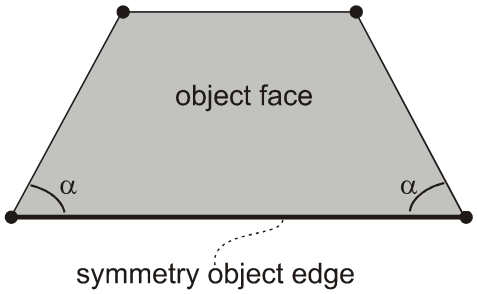

Figure 3: Symmetry constraint: equal angles α

- Geometry from a single image lacks scale information. Scale can be supplied with the length of an edge of the object model. In virtual reality applications scale plays a minor role as the model can generally be viewed at any scale. **Distance ratios** are more important because they allow determining the relative scale between objects in the scene. This is especially important for unconnected objects where relative scale cannot be determined. This is illustrated in figure 4 where relative scale (and therefore relative position) can only be determined when a distance ratio between two edges is supplied, or

when a coplanarity constraint is used stating that the two quadrangles are in one plane. The distance ratio constraint is not implemented.

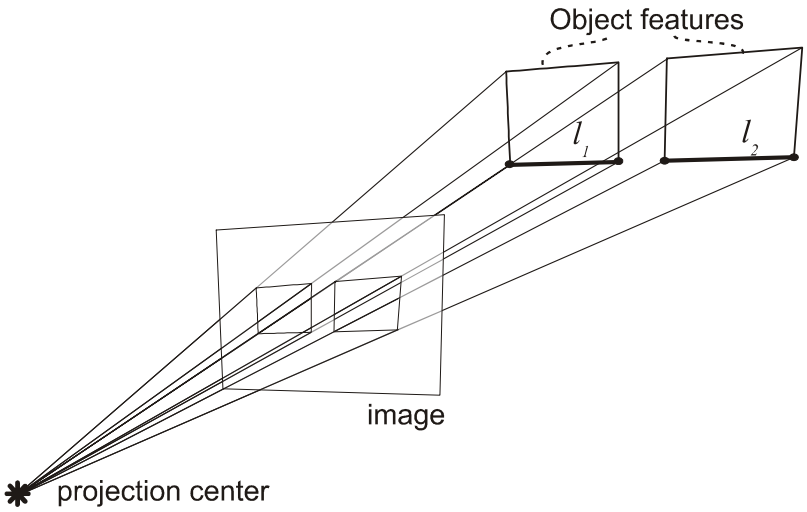

Figure 4: The distance ratio $l_1 : l_2$ determines the relative scale and position of the two quadrangles

For an efficient handling of geometric constraints a dedicated user-interface is a must. This user-interface should facilitate image line measurement in combination with the specification of geometric constraints. So far such a user-interface has only been partly implemented.

3 Mathematical formulation of geometric constraints

In this section two aspects of the geometric constraints will be dealt with. The first aspect is the way in which the constraint can be applied in the object reconstruction. The second aspect is the formulation of the constraint in the form of a condition equation in case of redundancy. This formulation is needed for the mathematical model of the adjustment discussed in section 4. Combinations of different types of constraints will frequently result in redundancy and thereby in the formulation of condition equations. The condition equations resulting from parallelism and perpendicularity constraints have been implemented and will be discussed in detail.

The geometric constraints can be split in two groups. The first group are the constraints that result from topological relations between image and object features and constraints resulting from the object topology itself. These constraints are called the topology constraints (van den Heuvel and Vosselman, 1997). The second group of constraints contains additional information on the geometry of the object and therefore they are called geometric object constraints or internal constraints.

3.1 Topology constraints

The topology constraints ensure a valid boundary representation and a valid image-object topology. The topology constraints are all of the coplanarity type. Three types of topology constraints can be distinguished: object point, line and plane constraints.

3.1.1 Object point constraint

The intersection of two object lines i and j results in an object point. The two interpretation planes associated with the projections of the two lines in the image have to intersect at a line through the object point (see figure 5). This is the object point constraint and the way it is used for object reconstruction. In formula:

$$\mathbf{x} = \frac{\mathbf{n}^i \times \mathbf{n}^j}{\left| \mathbf{n}^i \times \mathbf{n}^j \right|} \qquad (2)$$

Redundancy arises when more than two lines intersect at an object point. The condition equation involved is the coplanarity of the normals to the interpretation planes:

$$\det(\mathbf{n}^i, \mathbf{n}^j, \mathbf{n}^k) = \left[\mathbf{n}^i, \mathbf{n}^j, \mathbf{n}^k\right] = 0 \qquad (3)$$

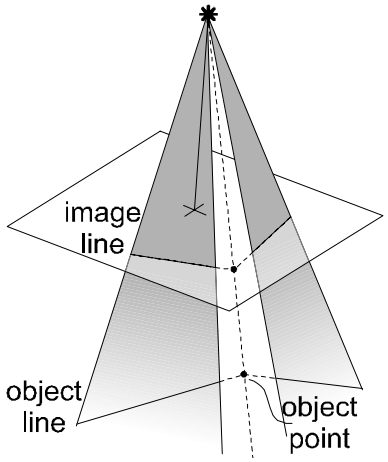

Figure 5: The intersection of two interpretation planes

In other words, the image lines associated with the same object point have to intersect in a single point in the image. This constraint is superfluous if image lines are specified by their end points. Then a single point is stored as the end point of several lines.

3.1.2 Object line constraint

An object line has to be in the interpretation plane associated with an image line, i.e. the object line i (direction vector $\mathbf{d}$) and the interpretation plane j have to be coplanar. This is the object line constraint that can be written as:

$$\mathbf{d}^i \cdot \mathbf{n}^j = 0 \qquad (4)$$

For a single image no condition equation can arise from this constraint alone, as there exists a one-to-one relation between an image line and an object line.

3.1.3 Object plane constraint or coplanarity

A polyline measured in the image specifies the relation between a set of image lines being the projection of object edges bordering a single planar face of the object. The object plane constraint states that all the object lines have to be in one plane and therefore the intersections of these lines (i.e. the object points) have to be in the same plane. For object reconstruction this means that all the object lines can be determined by intersection of interpretation planes and object plane (figure 5, figure 6 and section 5). Of course the object plane then has to be known.

The combination of the coplanarity constraint with other types of constraints can lead to redundancy. The general form of the condition equations is very similar to (4) where the normal to the interpretation plane has to be replaced by the normal to the object plane. The condition equation resulting from the combination of coplanarity and parallelism is presented in the next section.

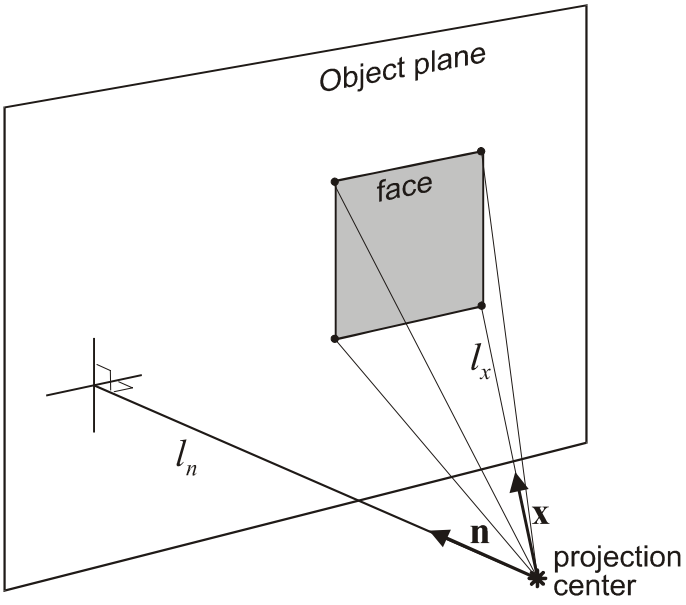

Figure 6: Reconstruction of an object face

3.2 Object constraints

The object constraints apply to the geometry of the object. They represent (a priori) geometric object information of object lines or planes. Three types of object constraints are discussed: parallelism, perpendicularity and symmetry. Coplanarity of lines of a single object face was treated in the previous section. Coplanarity between different object faces is not implemented.

3.2.1 Parallelism

Parallelism of object lines is one of the major geometric object constraints. First because it is used as the basis for object reconstruction and second because man-made objects often show many parallel edges. For most buildings the assumption of parallelism is easily inferred during the interpretation process because of our knowledge of the way in which they are constructed. Parallelism of object lines can be detected in a semi-automatic way by so-called vanishing point detection (van den Heuvel, 1998).

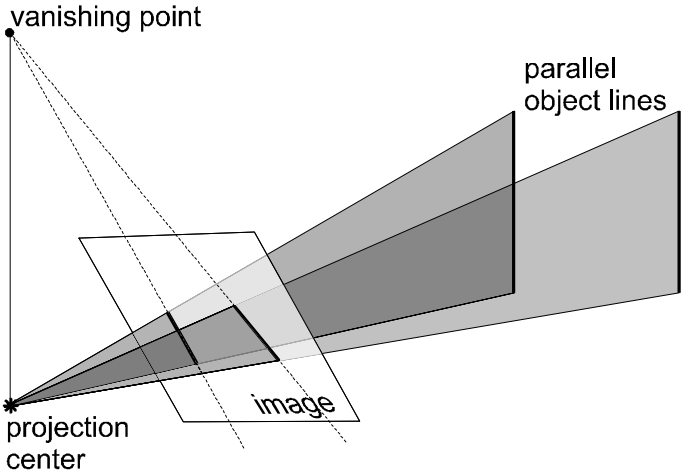

Figure 7: Vanishing point from parallel object lines

Parallelism is a powerful constraint for object reconstruction due to the fact that the orientation of the parallel lines in object space can be derived from the intersection of the interpretation planes related to these lines (figure 7). The object space direction $\mathbf{d}$ is computed in the same way as the direction to an object point (equation (2)) from the normals to the interpretation planes i and j as follows:

$$\mathbf{d} = \frac{\mathbf{n}^i \times \mathbf{n}^j}{\left| \mathbf{n}^i \times \mathbf{n}^j \right|} \qquad (5)$$

If there are more than two parallel object lines present in the image, a condition equation independent of previous ones can be established for each additional line.

This condition equation is identical to the object point condition equation (3) which is not surprising knowing that all image lines of parallel object lines have to intersect at a point in the image plane: the vanishing point.

Parallelism in combination with other object constraints gives rise to other types of condition equations. As an example the condition equation from the combination of three parallelism constraints on pairs of coplanar object lines with three different directions $\mathbf{d}$ can be written as:

$$\left[\mathbf{d}^i, \mathbf{d}^j, \mathbf{d}^k\right] = \left[\mathbf{n}^{i1} \times \mathbf{n}^{i2}, \mathbf{n}^{j1} \times \mathbf{n}^{j2}, \mathbf{n}^{k1} \times \mathbf{n}^{k2}\right] = 0 \qquad (6)$$

This condition suffices if the lines border one face due to the object point constraints (section 3.1.1). An additional condition equation is needed for coplanarity between object lines in different faces.

3.2.2 Perpendicularity

As many objects are constructed along three perpendicular axes, perpendicularity is an important constraint. For object reconstruction this constraint is used to construct the third direction $\mathbf{d}^k$ from two available object directions ($\mathbf{d}^i, \mathbf{d}^j$). The needed object directions can be computed using parallelism constraints using (5):

$$\mathbf{d}^k = \mathbf{d}^i \times \mathbf{d}^j \qquad (7)$$

Redundancy due to perpendicularity constraints will usually originate from combinations with other types of constraints. Independent of the way in which the object orientations are derived, the condition equation for perpendicularity can be written as:

$$\mathbf{d}^i \cdot \mathbf{d}^j = 0 \qquad (8)$$

If the three major object orientations are assumed to be perpendicular, "only" three independent condition equations of this type can be formulated when parallelism conditions are applied to all lines of each object orientation.

3.2.3 Symmetry

The symmetry constraint is defined in section 2.2 (figure 3). To be able to apply this constraint the object coordinates of the end points of the symmetry edge have to be known. The procedure for object reconstruction using the symmetry constraint is explained in section 5.2.

Redundancy can arise from combinations of symmetry constraints and other constraints. The resulting condition equations have not been implemented. A combination of two symmetry constraints that leads to redundancy occurs for instance for the type of roof of the house visualised in figure 8.

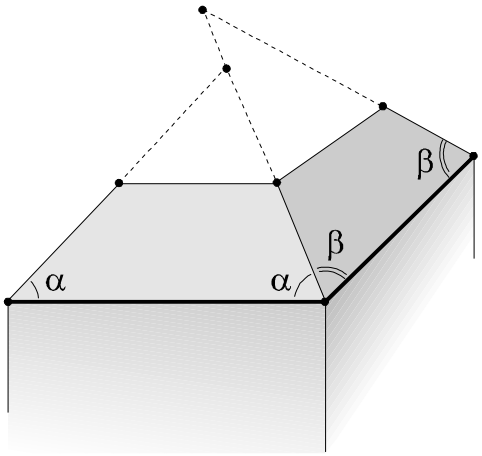

Figure 8: Two redundant symmetry constraints for a house roof

4 Adjustment and testing

A redundant number of geometric constraints leads to condition equations that build the functional model for a least-squares adjustment. In contrast to the mathematical model adopted by Zielinski (Zielinski, 1993), this model contains no parameters and therefore requires no approximate values. Zielinski solves for the parameters of the object lines while in this approach the object parameters are derived in a separate step (see section 5). After linearisation this model can be written as:

$$\mathbf{B}^{\mathrm{T}} E\{\mathbf{y}\} = \mathbf{0} \;;\; \mathbf{Q}_{\mathrm{y}} \qquad (9)$$

with:

$E\{\}$	mathematical expectation
$\mathbf{y}$	vector of observations (image lines)
$\mathbf{B}$	design matrix (partial derivatives)
$\mathbf{Q}_{\mathrm{y}}$	covariance matrix of the observations

The conditions can be processed in a sequential manner (van den Heuvel and Vosselman, 1997). This has advantages for an interactive measurement system because a condition can be tested as soon as it is specified by the operator. Rejection of such a statistical test forces the operator to a re-evaluation of the constraints or the measurements involved.

Condition equations resulting from combinations of parallelism and perpendicularity constraints have been implemented. Although dependency between condition equations can be detected numerically, it can be avoided by automatic selection of independent constraints. Independency of parallelism equations is guaranteed by the selection of *n*-2 condition equations, if *n* lines have been specified to be parallel. Each condition equation involves three lines (see section 3.2). After application of parallelism constraints perpendicularity constraints can be applied to combinations of orientations in object space. Each perpendicularity condition involves two pairs of lines. Each pair of two parallel lines can be used to compute an orientation in object space. In the current system the three major object orientations (X, Y and Z) can be made to be perpendicular by applying three perpendicularity constraints (combinations X-Y, Y-Z and Z-X). These constraints are adjusted in a sequential manner as well.

The adjusted observations that are input to the 3D reconstruction are computed as follows (Teunissen, 1994):

$$\hat{\mathbf{y}} = \mathbf{P}_{\mathbf{B}}^{\perp}\ \mathbf{y} \qquad (10)$$

with:

$$\mathbf{P}_{\mathbf{B}}^{\perp} = \mathbf{I} - \mathbf{Q}_{\mathbf{y}}\mathbf{B}\ (\mathbf{B}^{\mathrm{T}}\mathbf{Q}_{\mathbf{y}}\mathbf{B}\ )^{-1}\mathbf{B}^{\mathrm{T}}$$

Apart from the adjusted observations the covariance matrix of adjusted observations is also needed for the 3D reconstruction in order to perform error propagation and assess the precision of the resulting coordinates. The covariance matrix of the adjusted observations is computed with:

$$\mathbf{Q}_{\hat{\mathbf{y}}} = \mathbf{P}_{\mathbf{B}}^{\perp}\mathbf{Q}_{\mathbf{y}} \qquad (11)$$

The major types of condition equations - parallelism and perpendicularity - have been implemented. A few condition equations that result from combinations with other types of constraints are missing. As a consequence the model computed in the 3D reconstruction will not fulfil all constraints and minor discrepancies show up during object reconstruction.

5 3D reconstruction

The 3D reconstruction is the step of the photogrammetric process in which the object coordinates are computed. As no object coordinate system is introduced it is appropriate to name the 3D coordinates of the object *model coordinates*, especially because a seven parameter similarity transformation is needed to arrive at coordinates in a world coordinate system. This transformation is called *absolute orientation* of a model in stereo photogrammetry. Absolute orientation can be performed if the world coordinates of at least three (suitable) object points are available. To avoid confusion the 3D coordinates computed during reconstruction are named *object coordinates*, although the coordinate system is related to the system of the camera.

The approach for object reconstruction presented here is similar to the one presented in (Braun, 1994). The procedure of Braun is an iterative one in which object information is added in each iteration step until the (visible part of the) object is fully reconstructed. Another difference with the procedure adopted here is the fact that the adjustment step is performed after the object reconstruction, while in our approach the adjustment is executed first and does not involve object parameters.

5.1 The procedure for reconstruction

In the object reconstruction first the orientations of the lines and planes in object space are determined followed by the calculation of the positions of the object features.
The object coordinate computation is performed in 4 steps:

1. Orientation of the object lines
2. Orientation of the object planes
3. Positioning of the object planes
4. Computation of the coordinates of object points

Step 1: orientation of the object lines. The spatial orientation of the object lines is computed as the intersection of two interpretation planes of lines known to be parallel in object space (equation (5))

Step 2: orientation of the object planes. The orientation (**n**) of each plane of the object is derived from two non-parallel lines in the plane. The orientation of these lines ($\mathbf{d}^i, \mathbf{d}^j$) is known from step 1.

$$\mathbf{n} = \frac{\mathbf{d}^i \times \mathbf{d}^j}{\left| \mathbf{d}^i \times \mathbf{d}^j \right|} \qquad (12)$$

Note that more than one face of the object can be located in an object plane due to coplanarity constraints.

Step 3: positioning of the object planes. The position of the plane in space is derived from the known position of an object point in the plane. The position of a plane is specified with the distance to the projection centre along its normal (l_n), see figure 6. The position of the plane is computed as a projection of the distance from the point to the projection centre (l_x):

$$l_n = (\mathbf{n} \cdot \mathbf{x})\, l_x \qquad (13)$$

If there is no known point available in the plane (which is the case for the first plane to be computed) the distance to the projection centre is set to 1. Thereby the choice for the scale of the model is made.

Step 4: computation of the coordinates of object points. The positions of all object lines in the plane are determined by the intersection of the interpretation plane of the line and the object plane. The intersection of the object lines leads to the coordinates of the object points. In practice image points are computed from the intersections of image lines and rays corresponding to image points are intersected with the object plane to find the coplanar object points. The inverse of (13) is used to compute the distance to the object point from the distance to the plane.

The planes are processed in an order in which they are connected by common points. This implies that the topology of the object model has to be such that all faces are connected. However, the connection can be obtained from object constraints in the form of distance ratios between unconnected parts of the model or by coplanarity between different object faces (figure 4).

5.2 Use of perpendicularity and symmetry

The 3D reconstruction described uses parallelism and coplanarity. Perpendicularity is only used for reconstruction of an object orientation that is specified to be perpendicular to two orientations known from parallelism constraints. Due to the adjustment of perpendicularity conditions the object orientations reconstructed using adjusted observations are perpendicular.

In case of symmetry the first step of the procedure described in the previous section has to be replaced. The directions of the two edges connected to the so-called symmetry edge are computed from the symmetry constraint (see figure 3). The procedure continues with the steps 2 to 4 described in the previous section.

In figure 9 the object reconstruction from the symmetry constraint is depicted. A direction resulting from the intersection of interpretation planes is intersected with a plane of symmetry instead of a plane of the object itself. The following steps result in the object directions of the two lines connected to the symmetry edge:

1. The plane of symmetry is constructed from the position vectors of the end points of the symmetry edge.

2. The direction from the projection centre to the intersection point is derived from the intersection of the two interpretation planes.
3. The intersection of this direction with the plane of symmetry results in the object coordinates of the intersection of the lines and thereby to the directions of the two lines.

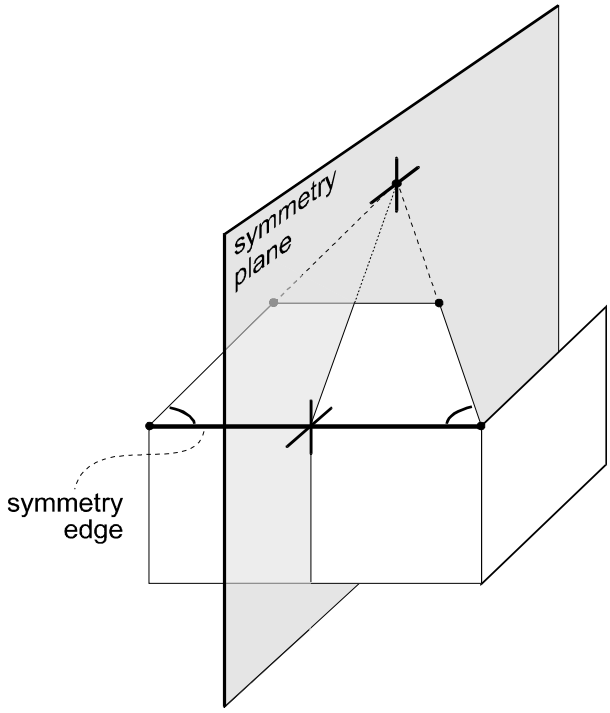

Figure 9: Object reconstruction with the symmetry constraint

The symmetry constraint can be used for object reconstruction if the projection centre is neither near the plane of symmetry nor near the plane to be reconstructed because then the intersection of the three planes involved is not well defined.

5.3 Combining models from different images

A single image will usually show only a part of a three-dimensional object. If a complete model of an object is desired, the method described here has to be applied to several partly overlapping images. This does not mean we are back at a traditional multi-image approach because the number of images needed here is reduced considerably by the use of geometric constraints for object reconstruction. In fact the images are treated sequentially and do only have to have a minimum of three points in common. These object points should not be on (or near to) one line, as the 7 parameters of a 3D similarity transformation have to be computed from their coordinates. These parameters can then be applied in the transformation of the coordinates of one model to the coordinate system of the other model.

Although this procedure of combining overlapping models is quite effective, there are some drawbacks. A complete set of condition equations has to be applied in order to guarantee a unique solution for the object coordinates. To ensure unique coordinates when combining two models, condition equations have to be formulated that involve observations of both images. Without these condition equations the two models are not identical with respect to their shape. Because the applied constraints are all directional constraints like parallelism and perpendicularity, the major type of conditions to be applied are conditions that guarantee that distance ratios in the two models are identical.
These types of condition equations that involve observations of more than one image are not implemented.

The approach of combining models by transformation is very suitable for determining approximate values for the relative orientation of two images or the exterior orientation of an image when coordinates of control points are available. This approach for exterior orientation is described in detail in (van den Heuvel, 1997). The derived approximate values can be used for a rigorous multi-image bundle adjustment. This adjustment will eliminate the discrepancies mentioned above. However, the geometric constraints have to be applied in this adjustment in order not to loose this information, i.e. in order to ensure parallelism of object lines, perpendicularity and other constraints.

5.4 Image acquisition

It is important to carefully select the images to be used because in the approach chosen here a minimum number of images is processed. Furthermore, the usefulness for reconstruction of some constraints depends on the orientation of the image relative to the object. Some rules of thumb for image acquisition for reconstruction from a single image are listed here:

- What is not visible in the image cannot appear in the model constructed from it. This is an obvious rule and a clear limitation of the procedure. However it can be overcome by combining several models (section 5.3) and some occluded object points can be reconstructed with the assumption of intersection of object lines.
- The more pixels the projection of a face occupies, the better the precision of the orientation of the plane of the face derived from parallelism constraints applied to its edges. Besides, the subsequent texture mapping is improved.
- For a complete model of an object an angle between the optical axis and the three major object orientations of 45 degree is optimal. Then faces with different orientation can be reconstructed facilitating the connection with overlapping models.
- For a model of a (planar) face the optical axis has to be as perpendicular to the face as possible. But in that case the symmetry constraint cannot be applied.
- To apply the symmetry constraint the optical axis has to have an angle as close as possible to 45 degree with the plane of symmetry and with the plane to be reconstructed (see section 5.2).
- For a visualisation as realistic as possible the textures should be free of shadows. This is the reason why images should preferably be taken not with direct point-like light sources like the sun but with a clouded sky.

6 Texture mapping and visualisation

To visualise the derived model the photogrammetric data is converted to VRML (Virtual Reality Modelling Language). VRML is a format for 3D data with features like hierarchical transformations, light sources, viewpoints, geometry, animation, fog, material properties and texture mapping (Carey and Bell, 1997). VRML is an open format that has become popular because of its suitability for publishing 3D data on the World Wide Web. For this reason there is a lot of software available that can handle VRML. This software allows a user-friendly interactive examination and visualisation of the data.

The conversion to VRML is fully automatic and consists of two parts: geometry conversion and texture mapping (see figure 1). In the geometric part the object coordinates and the topology information are converted. The texture mapping is performed with an 8 parameter image rectification for each face of the object. When there are more than 4 points bordering a face the 8 parameters are determined through a least-squares adjustment. For only three points in a face the projective transformation is approximated by a 6 parameter affine transformation.

For the image plane to object plane rectification no exterior orientation data is needed because the rectification implies a direct transformation from image to object plane. Exterior orientation data has to be available for the method used in (Debevec et al., 1996), which is based on a projection of image data onto the surface of the object. The advantage of their approach is that faces that are partly visible can be handled.

Image rectification involves resampling. The size of a pixel of the texture (in units of the object coordinate system) can be freely selected. The resampling allows a choice of three interpolation methods for resampling: nearest neighbour, bilinear and cubic convolution. Besides, a number of image enhancement options are available in order to obtain texture images that are homogeneous with respect to brightness and contrast. The texture of each face is written to a separate file in JPEG format. The selected JPEG quality factor determines the compression ratio. In VRML the texture file name is stored, the object face it belongs to and the positions in the texture image of the corner points of the face.

7 Application example

Two images of a historic building in Delft are used to test the method and assess the precision that can be obtained (figure 10). The images are taken on a clouded day with a digital camera Kodak DCS420 with a 20 mm lens. The camera had been calibrated beforehand. No artificial targets, control points or scale bars are used.

Figure 10: Original images

The lines are measured manually (figure 11). Together with the line measurement the object topology is specified and thereby the coplanarity of the lines bordering a face. Parallelism of object lines is manually registered in a separate file with a code for each line. The code corresponds to the orientation of the line in object space. For the three major object orientations a total of 107 and 96 condition equations (first, respectively second image) resulting from parallelism are sequentially adjusted. Three perpendicularity constraints are used to ensure perpendicularity between the three major object orientations. For the lines of the oblique roof edges no parallelism constraints are applied because the orientation computed from parallelism would not be accurate due to the small distance between the parallel edges. Instead, the plane of the roof edges is kept parallel to the façades underneath it.

In the first image 38 faces and 94 points are measured. In the second image four of these faces are not visible and the number of points reduces to 82. The topology of the models that result from the two images is identical, apart from one face that is only partly visible in

the second image. The two models have 56 points in common. The rest of the object points are not identical due to occlusion.

Figure 11: Line and topology measurements (faces are not indicated)

If point measurements in the two images would have been used for coordinate computation by forward intersection, the redundancy is equal to the number of object points. In the single image example presented here the redundancy is higher. Important for the visual perception of the model is the fact that with this approach faces are perfectly planar and parallel or perpendicular as defined during the measurement process, if a complete set of condition equations is applied. In the models of this experiment some minor discrepancies remain because only the condition equations related to parallelism and perpendicularity have been implemented.

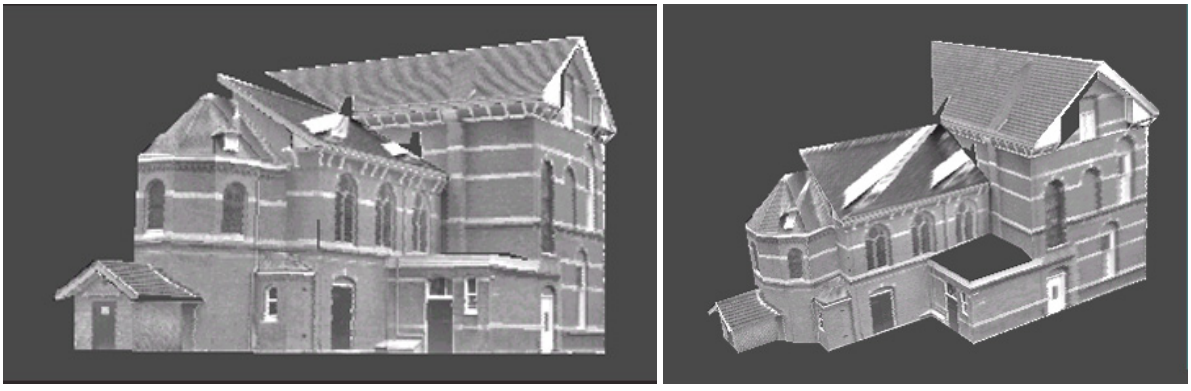

Figure 12: Two views of the model reconstructed from the first image (the model can be accessed at www.geo.tudelft.nl/frs/architec/single.html)

The result of the two reconstructions is converted to VRML for visualisation. Two views from different angles are pictured in figures 12 and 13 (the models can be accessed at www.geo.tudelft.nl/frs/architec/single.html). These models directly result from the measurements and are not edited in any way. The first view in figures 12 and 13 is taken from the same position as the original image is taken from (compare to figure 10). The quality of the texture mapping decreases rapidly when the angle between the optical axis and the object face is getting smaller. This is visible in some of the faces of the roofs. It has to be stressed that the two images were processed fully independently. They only share the

same topology information. The quality of the textures can be improved by using more favourable images for texture mapping. In this way the disturbing effects in the textures due to unordered parts could be minimised as well. This is clearly illustrated by the comparison of the two models with respect to the effects of the unordered ornaments on the roof. If only one image is used for texture mapping, the model is viewed best from a position close to where the image was taken.

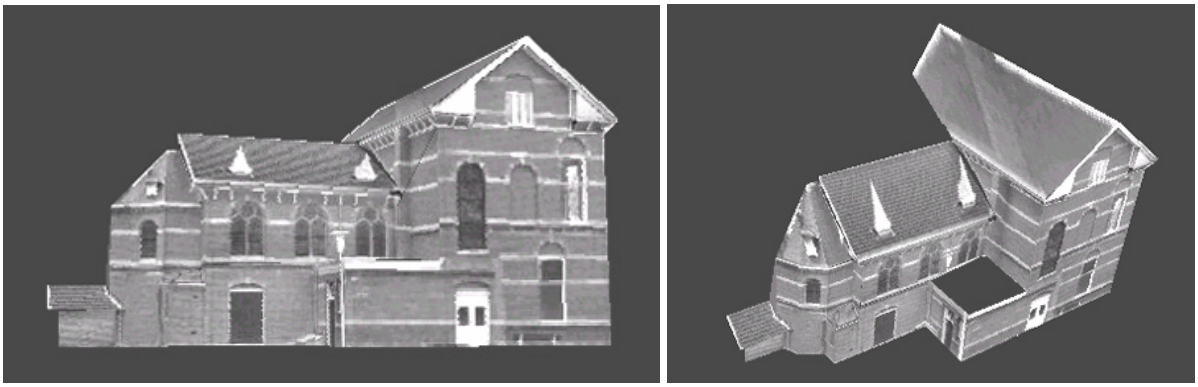

Figure 13: Two views of the model reconstructed from the second image

The two sets of coordinates allow for a repeatability test to assess the geometric quality of the models assuming the geometric constraints are valid. The coordinates of one of the models are transformed with a 7-parameter similarity transformation to the coordinate system of the other model in order to compare the two sets of coordinates. The results are summarised in table 1. All numbers in the table are relative to the longest distance between two points of the model. The Y-axis is roughly in vertical direction. The depth direction is in the X-Z plane and the differences between the two sets are 2 to 2.5 times larger in this plane. For a rigorous assessment of the precision that can be obtained with the presented method a comparison with reference data of a higher order of precision has to be undertaken.

Fraction $\times 10^{-3}$	X	Y	Z
RMSE	7.7	4.3	10.6
Minimum	-20.6	-9.9	-24.1
Maximum	17.7	7.8	14.8

Table 1: Difference between the two sets of coordinates (fraction of object size)

8 Conclusions

A method is presented that aims at making photogrammetry a more efficient tool for the acquisition of models of man-made objects meeting the demands of many virtual reality applications. The method is based on a combination of line-photogrammetric measurement of a single image and geometric object information that is derived through image interpretation. The object information needed for reconstruction are constraints such as parallelism of object lines, perpendicularity or symmetries. In man-made objects such as buildings these constraints appear frequently. An adjustment using a mathematical model of condition equations is applied in case of redundancy due to combinations of parallelism and perpendicularity constraints. This redundancy allows for the statistical testing of the constraints and the observations involved. The adjusted observations are input to the object

reconstruction procedure by which object coordinates are computed from image measurements and geometric constraints.

The proposed method is applied for modelling a part of a historic building. This example application showed the feasibility of the proposed method for object reconstruction from measurements in a single image. Comparison with the results of the reconstruction of the same part of the building from a second image resulted in an assessment of the repeatability. After similarity transformation the RMS of the coordinate differences was 1% of the object size and less.

Visual inspection of the acquired models led to the conclusion that the models show a high degree of realism in which texture mapping plays a major role. Texture mapping can be improved if images taken from different angles are available. Then disturbing effects in the textures due to unmodelled object features can be minimised. Missing parts of the model can be added by using additional images. Even for a complete model a considerable reduction of the number of images to be processed is achieved in comparison to conventional photogrammetric techniques. In combination with semi-automatic line extraction and generation of constraint hypotheses there is a great potential for efficiency improvement.

References

Braun, C., 1994. Interpretation von Einzelbildern zur Gebäuderekonstruktion, Dissertation Bonn University, Druckerei Schwarzbold, Germany.

Burns, J.B., Hanson, A.R., Riseman, E.M., 1986. Extracting Straight Lines, IEEE Transactions on Pattern Analysis and Machine Intelligence, Vol. PAMI-8, No.4, pp.425-455.

Carey, R., Bell, G., 1997. The Annotated VRML 2.0 Reference Manual, Addison-Wesley Developers press, ISBN 0-201-41974-2.

Debevec, D.E., Taylor, C.J., Malik, J., 1996. Modeling and rendering architecture from photographs: a hybrid geometry- and image-based approach, Computer Graphics proceedings, New Orleans, Annual Conference Series, pp.11-20.

Heuvel, F.A. van den, 1997. Exterior Orientation using Coplanar Parallel Lines, 10th Scandinavian Conference on Image Analysis, Lappeenranta (Finland), ISBN 951-764-145-1, pp.71-78.

Heuvel, F.A. van den, 1998. Vanishing point detection for architectural photogrammetry, proceedings of ISPRS commission V symposium, International archives of photogrammetry and remote sensing, Vol. 32 part 5, pp. 652-659.

Heuvel, F.A. van den, Vosselman, G., 1997. Efficient 3D modeling of buildings using a priori geometric object information, Videometrics V, Sabry El-Hakim (ed.), Vol.3174, pp.38-49.

Hsieh, Y., 1996. SiteCity: A semi-automated site modelling system, IEEE conference on Computer Vision and Pattern Recognition, San Francisco, pp. 499-506.

Kraus, K., Jansa, J., Kager, H., 1996. Photogrammetrie, Band 2: Verfeinerte Methoden und Anwendungen, Dümmler Verlag, Bonn, pp. 115-119.

Lang, F., Förstner, W., 1996. Surface reconstruction of man-made objects using polymorphic mid-level features and generic scene knowledge, Zeitschrift für Photogrammetrie und Fernerkundung, Vol. 64, No. 6, pp. 193-201.

Patias, P., Petsa, E. Streilein, A., 1995. Digital Line Photogrammetry, IGP Bericht nr. 252, Eidg. Technische Hochschule, Zürich, ISBN 3-906513-73-4.

Streilein, A., Hirschberg, U., 1995. Integration of digital photogrammetry and CAAD: constraint-based modelling and semi-automatic measurement, CAAD Futures '95 International Conference, Singapore, 14 p.

Teunissen, P.J.G., 1994. Adjustment Theory, Lecture notes Faculty of Geodetic Engineering, Delft University of Technology, Delft.

Williamson, J.R., Brill, M.H., 1989. Dominant Geometry Combinations of Two- and Three-Point Perspective in Close-Range Applications. Photogrammetric Engineering and Remote Sensing, Vol. 55, No. 2, pp. 223-230.

Zielinski, H., 1993. Object reconstruction with digital line photogrammetry, Doctoral thesis Department of Geodesy and Photogrammetry, Royal Institute of Technology, Stockholm.

2.5

A Line-photogrammetric mathematical model for the reconstruction of polyhedral objects[1]

[1] Reference: Heuvel, F.A. van den, 1999. **A Line-photogrammetric mathematical model for the reconstruction of polyhedral objects.** in Videometrics VI (San Jose), Sabry F. El-Hakim (ed.), Proceedings of SPIE Vol. 3641, ISBN 0-8194-3112-5, pp. 60-71.

A line-photogrammetric mathematical model for the reconstruction of polyhedral objects

Frank A. van den Heuvel[2]

Delft University of Technology
Faculty of Civil Engineering and Geosciences
Thijsseweg 11, 2629 JA Delft, The Netherlands

Abstract

Man-made objects often have a polyhedral shape. For polyhedral objects it is advantageous to use a line-photogrammetric approach, i.e. lines are observed in the images instead of points. A novel line-photogrammetric mathematical model is presented. This model is built from condition equations with image line observations and object parameters in the form of the coordinates of object points and the parameters of object planes. The use of plane parameters significantly simplifies the formulation of geometric constraints. Object line parameters are not included in the model. The duality of the point and plane representation in space is exploited and leads to linear equations for the computation of approximate values. Constraints on the parameters are used to eliminate the rank deficiency and to enforce geometric object constraints. The exterior orientation of the images is assumed to be approximately known. The rotation matrix is parameterised by a unit quaternion.
The main advantages of the presented mathematical model are the use of image lines as observations and the way in which it facilitates the incorporation of all types of geometric object constraints. Furthermore, the model is free of singularities through a combination of over-parameterisation and constraints. The least squares adjustment allows a rigorous assessment of the precision of the computed parameters and allows for statistical testing to detect possible errors in the observations and the constraints. Examples demonstrate the advantages of the proposed mathematical model and show the effects of the introduction of geometric constraints.

Keywords: close-range photogrammetry, computer vision, line photogrammetry, geometric constraints, mathematical model, least squares adjustment, polyhedral object reconstruction

1 Introduction

Many man-made objects are constructed using predefined rules that result in regularity of the shape of the object. Planar faces appear frequently, as do symmetries such as parallel and perpendicular object lines and planes. This is definitely the case in the application field of architectural photogrammetry for which the novel mathematical model is primarily designed.

The goal of the research is the adjustment of image line observations and geometric object constraints, in combination with the construction of a polyhedral object description. Advantages of using image lines over points as the basic photogrammetric observations can be found in e.g. [1], [2] and [3]. The image lines are assumed to result from the projection of edges of the object and can be extracted manually or automatically. In both cases the topological relations between image lines and object features are specified manually. The same holds for the object topology. Other premises are the use of a calibrated camera (i.e.

[2] E-mail: F.A.vandenHeuvel@geo.tudelft.nl

the interior orientation including lens distortions is known) and the availability of approximate values for the exterior orientation or pose of each image.

In [4] a solution to this problem was presented that consists of two steps. The first step is the adjustment of the image line observations and the second step is the object reconstruction. The adjustment of image lines does not involve object parameters. The main advantage of this approach is that there is no need for a choice of the parameterisation of the object, nor for approximate values of the object parameters. This makes the approach especially suitable for (sequential) adjustment and statistical testing of observations during interactive modelling when object parameters are not estimable throughout the modelling process. However, a disadvantage is that some geometric object constraints are difficult to formulate; this holds in particular for distance constraints. Another disadvantage lies in the separate step needed for the object reconstruction.

The approach presented in this paper fully eliminates the disadvantages of the former approach. The drawback is that the new model is less suitable for adjustment during interactive modelling. This is due to the introduction of object point and plane parameters and the need for approximate values of these parameters because of the non-linearity of the model. The plane parameters are introduced to facilitate object constraints like coplanarity of the points, perpendicularity between faces of the object, and distance constraints between parallel planes. The use of object parameters implies a choice for the representation of an object. This is the subject of section 2.

The mathematical model itself including the geometric constraints is discussed in detail in section 3. Approximate values of the point and plane parameters are computed from a possibly redundant set of linear equations (section 4). In section 5 three examples are presented where the mathematical model is applied for the adjustment and reconstruction of parts of a building. The examples differ in the amount of a priori object information that is used.

2 Geometric object modelling

In many present-day CAD systems there are two approaches to geometric modelling. The first one is the surface or boundary representation (B-rep) of the object and the second one is a solid representation. In the latter case the model is built from a combination of primitives (simple solid shapes like boxes) using Constructive Solid Geometry (CSG). In architectural photogrammetry a surface representation has advantages because very often only parts of a building, like façades, are modelled and a volumetric description with solids is not useful. Furthermore, occlusions of (small) parts of a building prohibit the construction of a solid description without considerable generalization. In our research the object is described by a boundary representation to which geometric object constraints are added. As a first step towards a volumetric description inside and outside of object faces are defined, based on the assumption that the object is viewed from the outside.

The research is restricted to polyhedral objects. Points, lines and planes and their topological relations make up a boundary representation of a polyhedral object. It is most common to only store the 3D coordinates of the points in order to describe the geometry. However, in the case of an object face with a contour that consists of more than three edges (or points) the parameterisation by coordinates is redundant. In such a case constraints are needed to ensure a valid boundary representation. In the object parameterisation adopted here plane parameters are introduced in order to facilitate the formulation of this coplanarity constraint. This constraint then involves the parameters of one point and one plane; while with only point parameters this constraint would involve the parameters of four points. Another reason to introduce plane parameters is the simplification of object constraints, like

parallelism, perpendicularity or a distance constraint between parallel planes. These constraints are discussed in section 3.4. Line parameters are not used, mainly because they would imply a considerable burden (see section 4.2 of [4]), although they could simplify the formulation of constraints between lines. If desired, line parameters can be derived from the coordinates of points on the lines. Although no line parameters are included in the model, the presented mathematical model is called a *line-photogrammetric* model because the observations solely consist of image lines. In most of the research on line photogrammetry four or six parameters are used for the object lines ([1], [2], [3], [4], [6], [7]). In [8] parameters for the planes are used, but no coordinates of object points. In [9] the object is described by a combination of polyhedral blocks of which the shape parameters are stored. This approach has many advantages such as the reduction in the number of parameters to recover. However, the constraints used to reduce the number of parameters are absolute (or "hard constraints", see section 4) and cannot be relaxed as in the approach presented in this paper.

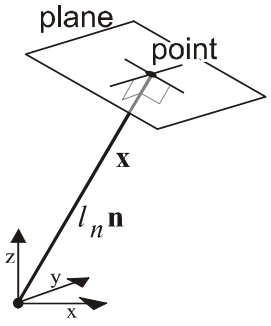

Figure 1: Duality of the point and plane representation

The object parameterisation adopted in the research described here consists of point and plane parameters. Three coordinates of a vector define the position of a point in space. Due to the duality between point and plane representation, a vector can parameterise a plane as well, where the orientation of this vector is normal to the plane. The disadvantage of this parameterisation lies in the singularity that occurs when the origin of the coordinate system lies in the plane, because then the orientation of the plane is undefined due to the zero length of the plane vector. To avoid this singularity for each plane an additional parameter is introduced that specifies the distance of the plane to the origin. This over-parameterisation is compensated by a constraint on the length of the normal vector. The object parameters of the mathematical model are summarized in Table 1 and visualised in Figure 1.

Entity	Orientation	Position	Constraints
Point		$\mathbf{x} = (x, y, z)$	
Plane	$\mathbf{n} = (x, y, z)_{\mathbf{n}}$	$l_{\mathbf{n}}$	$\lvert\mathbf{n}\rvert = 1$

Table 1: Object parameterisation by points and planes

3 The mathematical model

In this section the novel line-photogrammetric mathematical model is presented. First the observations in the form of image lines are discussed in section 3.1, followed by the parameters in section 3.2. The parameters consist of object parameters (section 2) and exterior orientation parameters. Then the relations between observations and parameters are treated in section 3.3. In section 3.4 the incorporation of geometric object constraints in

the model is discussed and in section 3.5 the least squares solution to the model is presented.

3.1 The observations

The mathematical model supports the adjustment of automatically extracted or manually measured straight lines in the image. Assuming a pinhole camera model, an image point observation relates to a spatial direction vector $\mathbf{d}$ (Figure 2):

$$\mathbf{d} = (x, y, -f) \tag{1}$$

Where (x, y) is the location of the point in the camera system (corrected for deformations in the image plane and lens distortions) and the focal length *f*. The straight line features in the image all have a begin and an end point, possibly on the border of the image. But these points do not have to represent projections of the vertices of the object. This is even unlikely if the lines result from automatic feature extraction. This is the reason why each line feature is represented in the model only through the normal vector $\mathbf{n}_{ij}$ of the plane. This is the so-called interpretation plane, through line *j* and the projection centre of image i. The normal vector can be computed from the direction vectors of begin and end point through their cross product and is rotated to the object coordinate system by multiplication with the rotation matrix of exterior orientation $\mathbf{R}_i$ (Figure 2):

$$\mathbf{n}_{ij} = \mathbf{R}_i \, (\mathbf{d}_1 \times \mathbf{d}_2)_j \tag{2}$$

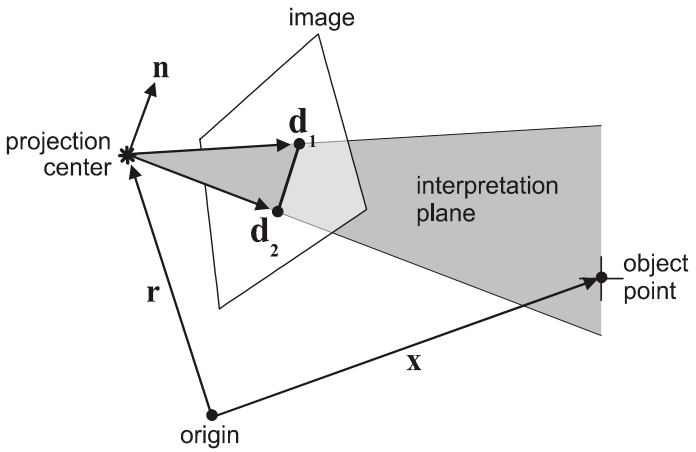

Figure 2: Object point in interpretation plane

The mathematical model is formulated in such a way that the length of the normal vector $\mathbf{n}$ does not play a role. Only the image coordinates (*x*,*y*) are treated as observations. The focal length is treated as a constant.

3.2 The parameters

Two types of parameters are distinguished. First the model contains object parameters as discussed in section 2. The second type refers to parameters for exterior orientation of the images.

The object parameters consist of three parameters for each object point and four parameters for a plane. A constraint is needed for each plane as a result of the over-parameterisation (Table 1). The exterior orientation parameters consist of three parameters for the location of the projection centre (vector $\mathbf{r}_i$ for image i) and four parameters of a quaternion $\mathbf{q}$ that defines a rotation matrix $\mathbf{R}_i$. These parameters are also called the Euler-Rodrigues

symmetric parameters [10]. The major advantage of this parameterisation of the rotation matrix is the absence of singularities (i.e. critical conditions [11]). However, a normalization constraint has to be applied, like with the over-parameterisation used for the planes:

$$\left|\mathbf{q}\right| = \sqrt{\mathbf{q}_1^{\,2} + \mathbf{q}_2^{\,2} + \mathbf{q}_3^{\,2} + \mathbf{q}_4^{\,2}} = 1 \tag{3}$$

3.3 The relations between the observations and the parameters

The main relation used for the mathematical model can be simply stated as *a point is located in the planes to which it relates.* There is only one relation between the observations and the parameters, namely: an *object point is located in the interpretation planes to which it relates* (Figure 2). A similar relation is applied to the object features: a*n object point is located in the object planes to which it relates.* The latter relation will be discussed in the next section. The relations between the observations and the parameters (image i, image line j, and object point k) can be written as:

$$\mathbf{n}_{ij} \cdot \mathbf{x}_k - \mathbf{n}_{ij} \cdot \mathbf{r}_i = 0 \tag{4}$$

It is important to note that in this formulation the length of the normal vector to the interpretation plane $\left|\mathbf{n}_{ij}\right|$ does not play a role and thus the over-parameterisation of the orientation of the interpretation plane does not play a role.

3.4 The geometric object constraints

The main advantage of the approach presented here is the way in which it facilitates the incorporation of geometric object constraints, also called internal constraints. The constraints are directly imposed on the object parameters, in contrast to the approach in [4], where the object constraints are formulated in terms of the observations (i.e. the normals to the interpretation planes). Two types of geometric constraints can be distinguished. First, the constraints needed for a valid polyhedral object description, i.e. the constraints that force the object points to be in the object plane(s) they belong to. Second, the constraints that result from a priori knowledge on the geometry of the object. These are constraints that affect the shape of the resulting polyhedral object model like parallelism or perpendicularity of object planes. Constraints that affect the definition of the coordinate system, like horizontal or vertical lines or planes, are not dealt with here, but are treated separately in section 3.5.

Point-point constraint. There is only one constraint between two points *i* and *j*, i.e. the distance between them is known:

$$\left|\mathbf{x}_i - \mathbf{x}_j\right| = d_{ij} \tag{5}$$

d_{ij} : distance between points i and j.

Line-line constraints. Apart from a (shortest) distance constraint between two lines, the angle constraint is a constraint with more practical significance. It involves the parameters of four points defining two lines i and j:

$$\frac{(\mathbf{x}_{i1} - \mathbf{x}_{i2}) \cdot (\mathbf{x}_{j1} - \mathbf{x}_{j2})}{\left|\mathbf{x}_{i1} - \mathbf{x}_{i2}\right|\left|\mathbf{x}_{j1} - \mathbf{x}_{j2}\right|} = \cos(a_{ij}) \tag{6}$$

a_{ij} : angle between the lines i and j.

Plane-plane constraints. The major constraint of this type is the angle constraint between two planes *i* and *j*:

$$\mathbf{n}_i \cdot \mathbf{n}_j = \cos(a_{ij}) \tag{7}$$

a_{ij} : angle between the plane i and j.

Thanks to the (over-)parameterisation chosen for the planes (see Table 1) the distance between two parallel planes *i* and *j* is simply constrained by:

$$\left| l_{\mathbf{n}_i} - l_{\mathbf{n}_j} \right| = d_{ij} \tag{8}$$

d_{ij} : distance between planes i and j.

It has to be noted that the sign of *l* is to be reversed if the normals have an opposite direction. This constraint is linear in contrast to a distance constraint between two points of the object model.

Point-line constraint. The only constraint of this type is the shortest distance between a point *i* and a line defined by the points *j* and *k*:

$$\frac{\left|(\mathbf{x}_i - \mathbf{x}_j) \times (\mathbf{x}_k - \mathbf{x}_j)\right|}{\left|\mathbf{x}_k - \mathbf{x}_j\right|} = d_{ijk} \tag{9}$$

d_{ijk} : distance between point i and line j-k.

Point-plane constraint. This constraint is of the same type as the point-line constraint:

$$\left|\mathbf{x}_i \cdot \mathbf{n}_j - l_{\mathbf{n}_j}\right| = d_{ij} \tag{10}$$

d_{ij} : distance between point i and plane j.

This constraint is slightly modified to be used as the constraint that forces an object point into the planes it relates to:

$$\mathbf{x}_i \cdot \mathbf{n}_j - l_{\mathbf{n}_j} = 0 \tag{11}$$

It has to be noted that the plane parameter $l_{\boldsymbol{n}}$ carries a sign that depends on the sign of the normal vector $\mathbf{n}$.

Line-plane constraints. A distance constraint can be formulated in case of parallelism of line and plane. The angle constraint between a line and a plane is of the form:

$$\frac{(\mathbf{x}_{i1} - \mathbf{x}_{i2}) \cdot \mathbf{n}_j}{\left|\mathbf{x}_{i1} - \mathbf{x}_{i2}\right|} = \sin(a_{ij}) \tag{12}$$

a_{ij} : angle between the line *i* and plane *j*.

Special cases of some of the geometric constraints need further investigation. These cases occur if the right hand side equals one (equations (6) and (7)) or zero (equations (9) and (12)). Then two equations are needed instead of one.

At the time of writing only the point-plane constraint (10) and the plane-plane angle constraint (7) have been implemented. These constraints are applied in the examples of section 6.

3.5 The definition of the coordinate system

The geometric object constraints do not eliminate the rank deficiency of the design matrix that results from the introduction of a coordinate system in combination with parameters for all object points and planes and all exterior orientation parameters. Additional constraints are needed to fix the coordinate system and thereby eliminate the rank deficiency. For this purpose constraints are introduced for a minimum of seven suitable coordinates of object points, although other (combinations of) parameters like the position and/or orientation information of the images could also be used. Over-constraining occurs if more than seven coordinates are available. There are various ways to introduce these constraints in the mathematical model. This is the subject of the next section. There it is explained why all the constraints are introduced as observation equations. For the coordinate constraints these observation equations have the following form:

$$E\{\mathbf{x}_0\} = \mathbf{I}\,\mathbf{x};\ \mathbf{Q}_{\mathbf{x}_0} \tag{13}$$

with:

$E\{\}$	mathematical expectation
$\mathbf{x}_0$	vector of observations (known coordinates of control points)
$\mathbf{x}$	vector of parameters (coordinates of control points)
$\mathbf{I}$	unit matrix
$\mathbf{Q}_{\mathbf{x}_0}$	covariance matrix of observations (implemented as a diagonal)

Other constraints that are useful for fixing the coordinate system are the so-called “partial absolute” constraints [12], like horizontal or vertical lines or planes. A vertical line or a horizontal plane constraint fixes two of the seven degrees of freedom of the coordinate system. A horizontal line or a vertical plane fixes one degree of freedom. These constraints on the orientation of the coordinate system involve coordinates of two points (for a line constraint) or the orientation parameters of a plane. If the same partial absolute constraint is enforced on more than one line or plane, the constraints on all but one line or plane can be replaced by parallelism constraints (section 3.4).

4 Least squares adjustment

In the previous section the observations of the mathematical model, the parameters and their relations have been presented. In this section a least squares solutions to the mathematical model is discussed. The way in which the various types of constraints are enforced in the adjustment leaves room for discussion.
The mathematical model consists of condition equations with observations and parameters. In addition constraints have to be imposed on the parameters. This model can be written as follows (after linearisation, see [13] and [14]):

$$\mathbf{B}^{\mathrm{T}} E\{\mathbf{y}\} = \mathbf{A}\,\mathbf{x};\ \mathbf{0} = \mathbf{C}^{\mathrm{T}}\mathbf{x};\ \mathbf{Q}_{\mathrm{y}} \tag{14}$$

with:

$\mathbf{B}^{\mathrm{T}} E\{\mathbf{y}\} = \mathbf{A}\mathbf{x}$	condition equations
$\mathbf{0} = \mathbf{C}^{\mathrm{T}}\mathbf{x}$	constraints on the object parameters
$\mathbf{y}$	vector of (corrections to) the observations (i.e. image line observations)

$\mathbf{x}$	vector of (corrections to) the parameters (i.e. object parameters and exterior orientation parameters)
$\mathbf{A}, \mathbf{B}, \mathbf{C}$	design matrices (partial derivatives)
$\mathbf{Q}_y$	covariance matrix of the observations (implemented as a diagonal matrix)

The condition equations result from linearisation of equation (4) in section 3.3. The constraint equations on the parameters can be of various types; namely the geometric constraints described in section 3.4 or constraints needed for the elimination of rank deficiencies. These rank deficiencies result from over-parameterisation of the object planes (section 2, Table 1) and the rotation matrix (section 3.2, (3)) or result from the use of coordinates (section 3.5, (13)). It is not possible to solve the part of the model with the condition equations first and apply the constraints on the object parameters in a second step. This is caused by the rank deficiency of the system built from the condition equations only ($\mathbf{A}$ has a rank defect). This is the main reason to transform the model (14) to a model with observation equations only. In [1], [16] and [14] this is called the unified approach. In our approach not all approximate values are treated as observations.

$$E\left\{\begin{matrix}\mathbf{z}_1\\ \mathbf{z}_2\end{matrix}\right\} = \begin{pmatrix}\mathbf{A}\\ \mathbf{C}^{\mathrm{T}}\end{pmatrix}\mathbf{x};\ \mathbf{Q}_{\mathbf{z}_1};\ \mathbf{Q}_{\mathbf{z}_2} \quad \text{or} \quad E\{\mathbf{z}\} = (\mathbf{A}_{\mathbf{C}})\,\mathbf{x};\ \mathbf{Q}_{\mathbf{z}} \tag{15}$$

with:

$\mathbf{z}_1 = \mathbf{B}^{\mathrm{T}}\mathbf{y}$	vector of (corrections to) the derived observations
$\mathbf{Q}_{\mathbf{z}_1} = \mathbf{B}^{\mathrm{T}}\mathbf{Q}_{\mathrm{y}}\mathbf{B}$	covariance matrix of the derived observations
$\mathbf{z}_2 = \mathbf{0}$	vector of (corrections to) pseudo or constraint observations
$\mathbf{Q}_{\mathbf{z}_2}$	covariance matrix of the pseudo observations (diagonal)

The model consists of two parts that are solved simultaneously. Due to the transformation of constraints into pseudo observations the complete system ($\mathbf{A}_{\mathbf{C}}$) is of full rank. In the first part the condition equations lead to observation equations with derived observations ($\mathbf{z}_1$) of which the (full) covariance matrix ($\mathbf{Q}_{\mathbf{z}_1}$) is derived by propagation. In the second part pseudo observations are introduced of which the variances are chosen to be very small compared to the variances of the original and derived observations. This holds for the variances of the "constraint observations" that are used to eliminate the rank deficiency resulting from the over-parameterisation. For other constraints, like the constraints for the coordinates of control points, a realistic value for the variance of the pseudo observations can be chosen. The same applies to the geometric object constraints. The variance adopted for the pseudo observation reflects the uncertainty in the constraint. In practice, it is difficult to find realistic values for these variances because they will differ considerably from one application to the other. The variance determines the weight of the constraint in the adjustment. A very large weight will result in an object model that fully complies with the constraint, a realistic weight will allow discrepancies between adjusted model and constraint. These different weightings are sometimes referred to as hard and soft constraints ("weak forms" in [12]).

The least squares solution to the model (15) is well known:

$$\hat{\mathbf{x}} = (\mathbf{A}_{\mathbf{C}}^{\mathrm{T}}\,\mathbf{Q}_{\mathbf{z}}^{-1}\,\mathbf{A}_{\mathbf{C}})^{-1}\,\mathbf{A}_{\mathbf{C}}^{\mathrm{T}}\,\mathbf{Q}_{\mathbf{z}}^{-1}\,\mathbf{z} \tag{16}$$

The residuals of the derived and pseudo observations are computed as follows:

$$\hat{\mathbf{e}}_{\mathbf{z}} = \mathbf{z} - \mathbf{A}_{\mathbf{C}}\hat{\mathbf{x}} \tag{17}$$

The residuals of the original image line observations are computed from the first part of the model (15):

$$\hat{\mathbf{e}}_y = \mathbf{Q}_y \mathbf{B} \mathbf{Q}_{z_1}^{-1} (\mathbf{z}_1 - \mathbf{A} \hat{\mathbf{x}}) \quad (18)$$

It has to be noted that $\mathbf{B}^T$ has to be of full rank for an invertible $\mathbf{Q}_{z1}$ (and $\mathbf{Q}_z$). This can only be the case if no more than two condition equations per image line are used. Therefore, it is not possible to relate more than two object points to one interpretation plane. Object constraints have to be used to force more than two points onto an object line.

Because we deal with a non-linear model in both the parameters and the observations, a so-called mixed model [13], the solution is computed in an iterative procedure in which parameters and observations are updated. This implies that equation (18) is evaluated in each step of the iteration process. This is not the case in a conventional (non-mixed) non-linear model with observation equations.

5 Approximate Values

Initial values are needed for all parameters in the model because the equations presented in the previous section are non-linear. Two types of parameters have to be distinguished. These are the object parameters and the parameters of exterior orientation or pose parameters of the images. The computation of approximate values for exterior orientation is discussed first.

There are several ways to obtain approximate values for the exterior orientation parameter of the images. Direct methods for space resection based on a priori information on object coordinates are available [17]. In [18] a method is proposed that makes use of the parallelism of coplanar object lines. A direct solution has been derived for which only the projection of (parts of) the edges of a parallelogram (or rectangle) in object space is needed. If the same parallelogram is visible in two images, relative orientation between them can be determined. If a specific object coordinate system is to be used a similarity transformation has to be applied.

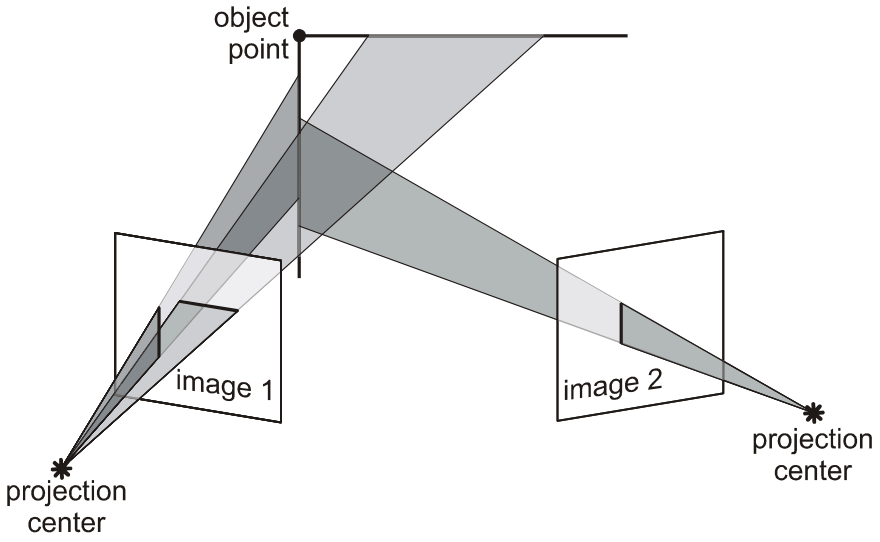

Figure 3: Minimum configuration

With the exterior orientation parameters (approximately) known, the object point parameters are computed using equation (4). This equation is linear if exterior orientation parameters ($\mathbf{R}$ and $\mathbf{r}$) and observations (represented by the normal vector to the interpretation plane $\mathbf{n}$) are treated as constants. Equations of this type are gathered and a least squares adjustment is performed to compute the coordinates of the object point ($\mathbf{x}$). This adjustment per object

point allows for an assessment of the estimability of the coordinates of the point. In case of an over-determined system of equations, statistical testing can be applied to detect errors in the observations or errors in the approximate values for the exterior orientation parameters. A minimum configuration of three interpretation planes for an object point is depicted in Figure 3. Poor intersection angles between interpretation planes are detected in the approximate value computation of each object point.

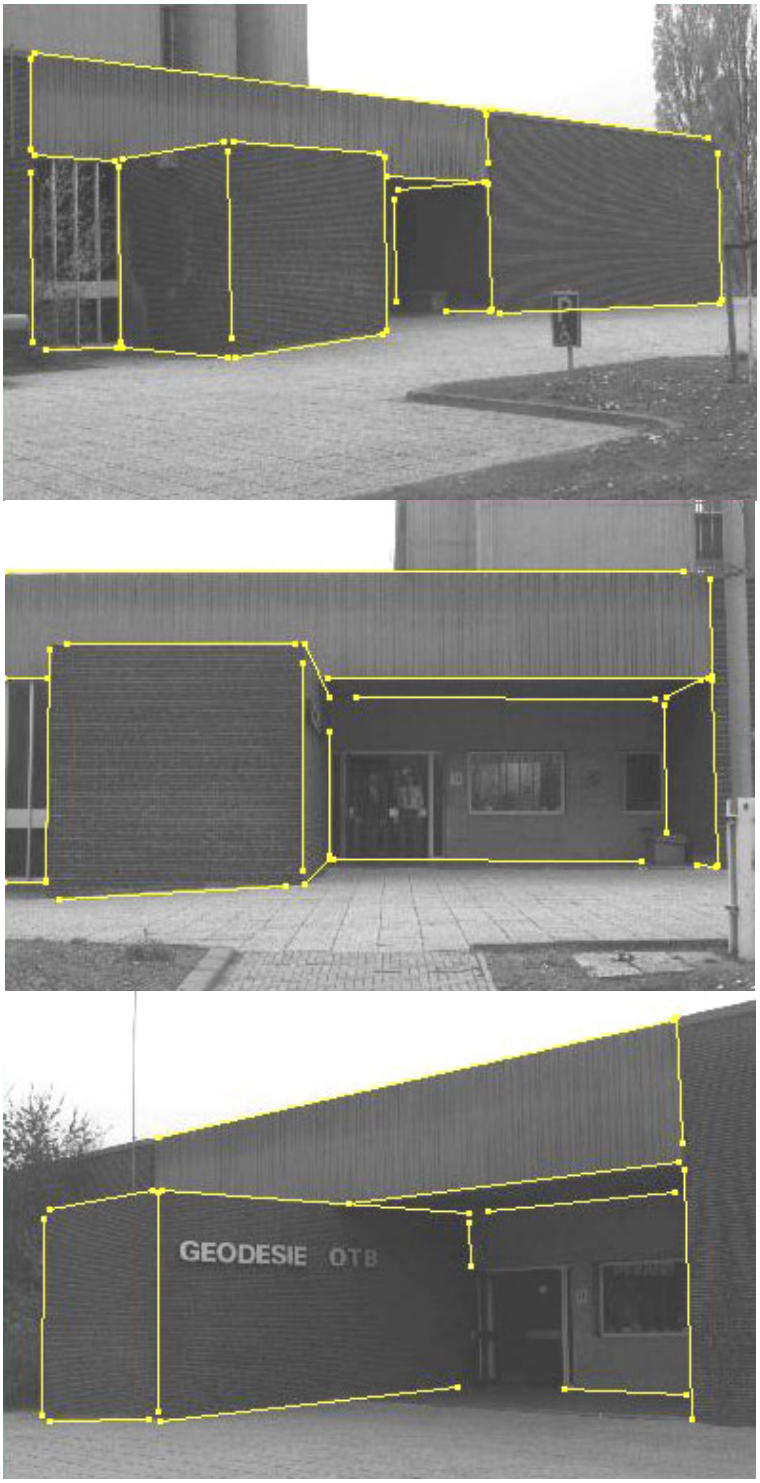

Figure 4: Image line measurements

The plane parameters are computed after the computation of object point coordinates. Now equation (11) is applied with $\mathbf{x}$ and $l_{\mathbf{n}}$ as constants. Then these equations are gathered for each plane and the three parameters of $\mathbf{n}$ are solved with $l_{\mathbf{n}}$ set to one. Normalization of $\mathbf{n}$ results in $l_{\mathbf{n}}$ being the length of the original vector $\mathbf{n}$. Equation (11) is also linear and, in fact, identical to the rewritten equation (4) used for the point coordinate computation. Points and planes are treated in the same way in the approximate value computation, making use of the point-plane duality discussed in section 87. It has to be noted that the computation of approximate plane parameters is not singularity-free.

With the availability of the plane parameters, additional equations are available for the computation of the coordinates of the points that are specified to be in that plane. Point and plane parameters are computed in an alternating way until no new point or plane parameters are computed. With this approach it is possible to compute approximate values for object points that are visible in only one image, or not in any image, if there are at least three object planes intersecting at that point. The parameters of these planes then have to be previously computed from the coordinates at least three other points in the plane. The result is that, due to the point-plane constraints (section 3.4), it can occur that parts of the model visible in less than two images can be reconstructed. This is demonstrated by the examples described in the next section.

6 Examples

The mathematical model presented in this paper is applied for modelling the entrance part of our department building. Three images were taken with a digital camera (Kodak DCS420 with a 20 mm lens) of which the interior orientation (including lens distortion) is known. Lines were measured manually by measuring a start and end point of each straight line. These points were chosen in such a way that the line in the image is as long as possible and the edge showed good contrast. The three images and the image line observations are visualised in Figure 4. Note that there is no correspondence between points in different images. The standard deviation of the observations was chosen to be constant at 1 pixel for all tests. When lines are extracted automatically the stochastic model can be chosen in accordance with the precision estimation from the line extraction method. A stochastic model in which the variance of the coordinates of the end points depends on the length of the measured line is presented in [19].

Advantages of line-photogrammetric measurement over point measurement are illustrated by the details in Figure 5. In the top left picture three object points at the corners of three faces are visible (in the centre of the three clusters of end points) while in the top right picture only one of the three points could have been measured had point measurements been used. The other two corner points are not visible because one point is off image and the other point is occluded. With line measurements a part of the edge between the two missing points can be measured and in this case that line is crucial for the reconstruction. In the two pictures at the bottom of Figure 5 occlusion of a corner point by a box that is not modelled does not prohibit the reconstruction of the object point because a sufficient number of image lines relating to this point can be measured.

Apart from the image line measurements the object topology was specified i.e. the faces, the edges and the vertices of the object and their relations were defined. Furthermore, each image line was related to two vertices of the object. This is the specification of what is called the image-object topology. Approximate values for exterior orientation parameters were obtained with the use of parallelism information on edges of the object [18]. Seven approximate object coordinates were fixed to define the coordinate system of the model (section 3.5).

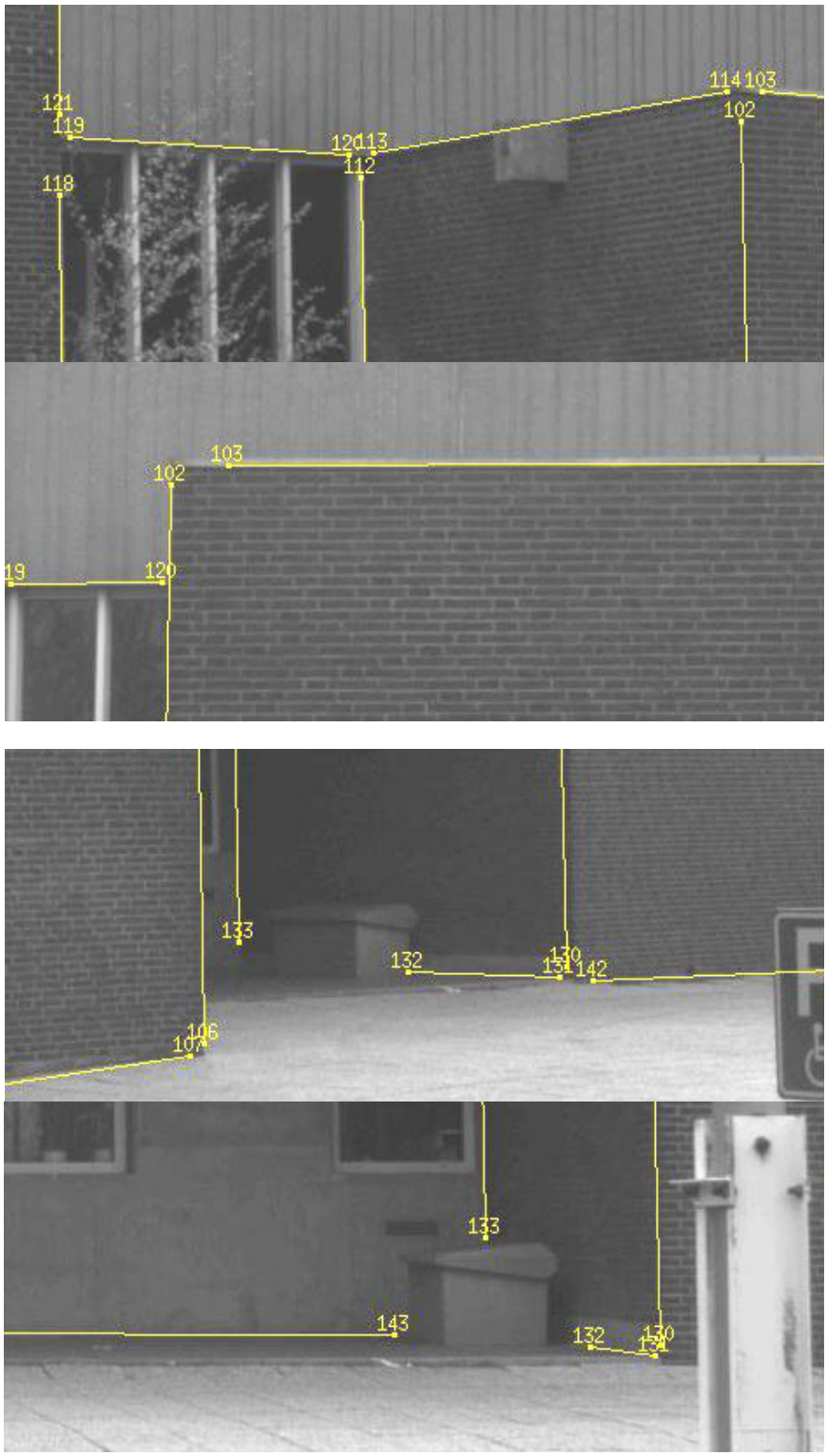

Figure 5: Details of left and middle image

Three adjustments have been performed, all with the same set of line measurements and the same stochastic model. The adjustments only differ in the amount of object information supplied. The main characteristics of the adjustments are summarized in Table 2. The three resulting texture-mapped models can be accessed through the Internet at www.geo.tudelft.nl/frs/architec/triple.html.

In the first adjustment all faces are treated independently, i.e. there are no object constraints apart of the constraints that force a corner point into the plane of a face. The resulting model is pictured in Figure 6.

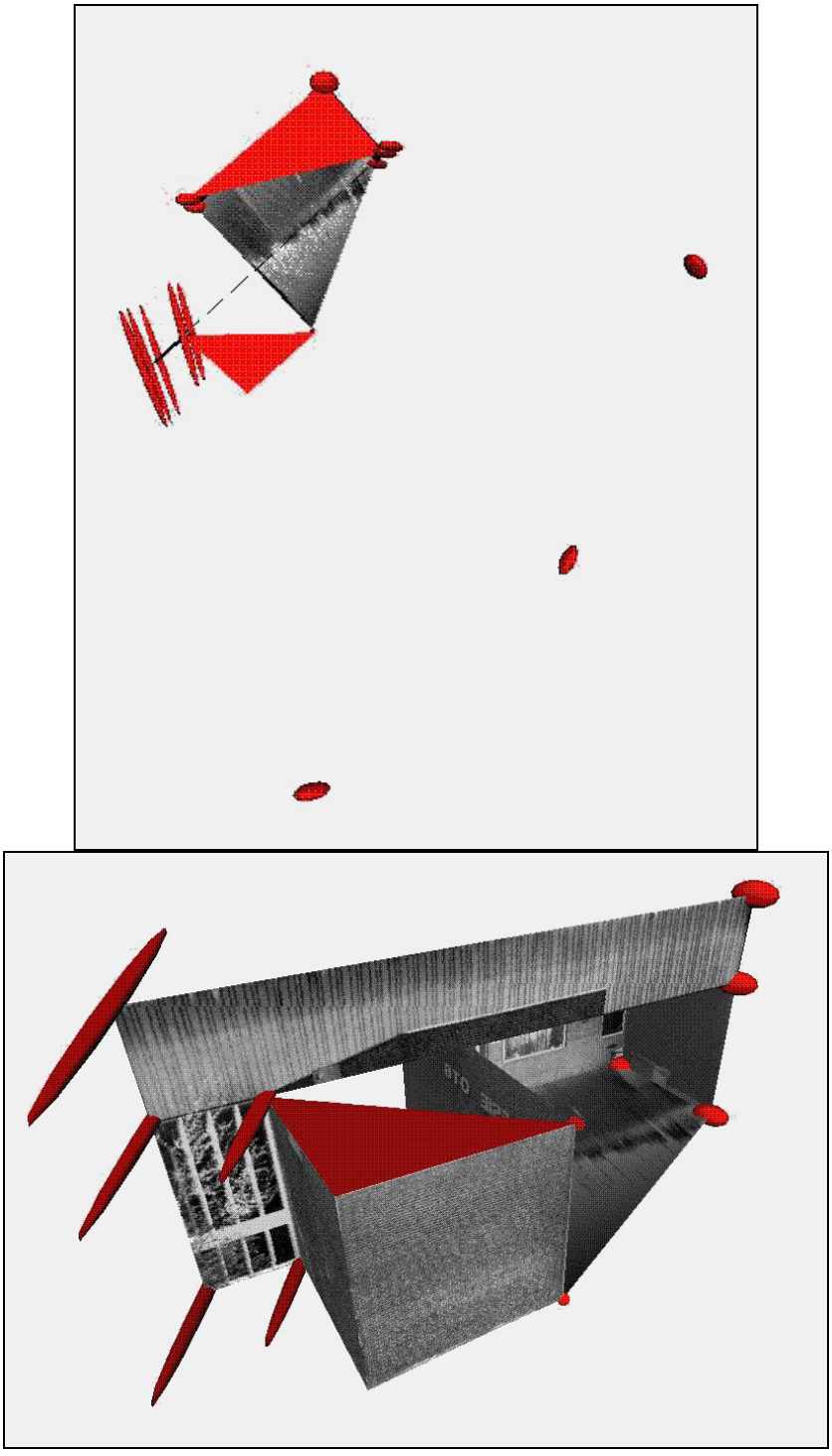

Figure 6: Top and oblique view of the first model (see www.geo.tudelft.nl/frs/architec/triple.html)

In each point of the model an ellipsoid is positioned in order to visualize the precision of the coordinates. The scale of all ellipsoids is a factor 10 larger than the scale of the model. Furthermore, the ellipsoids of the position of the three projection centres is visible in the top views. The precision of the coordinates is dependent on the choice for the definition of the coordinate system. Here, the three coordinates of the two points on the left of the brick wall

in the front are fixed using equation (13) with (very) large weights. The seventh coordinate that is fixed in this way is located at the top right of the same wall. The size and shape of the ellipsoids depend on this choice, but it does not affect the precision of the shape of the model. For instance, the precision of distances computed from the coordinates is not affected by the choice of the coordinate system.

Two auxiliary triangular horizontal faces have been defined. They do not play a role in the first adjustment. Note the five elongated ellipsoids on the left side of the model. This is due to small intersection angles between interpretation planes associated with approximately horizontal lines in the images. For better intersection angles the images should have been taken from different height levels. These five ellipsoids point towards the projection centre of the leftmost image because only this image contains two line measurements for each of these points (see Figure 4). Information on the precision is summarized in Table 3. The number of iterations is determined by the criterion for the maximum correction to the parameters (set to 10^{-6}).

Adjustment	Points	Planes (faces)	Parameters	Equations ($\mathbf{A_C}$)	Equations ($\mathbf{B}^T$)	Redundancy
1	16	8 (10)	101	149	98	48
2	18	8 (11)	107	160	102	53
3	18	8 (11)	107	171	102	64

Table 2: Number of parameters and redundancy

In the second adjustment additional object information is incorporated in the form of coplanarity constraints. Three vertical faces are assumed to be in one plane and the same holds for the two triangular horizontal roof faces. As a result, the number of plane parameters reduces by eight (two planes less, but one additional face). Because of these additional constraints the coordinates of a new face become estimable. Furthermore, the precision of the coordinates improves, which is reflected by smaller ellipsoids (see Figure 7 and Table 3). The number of planes is the same for all three adjustments (Table 2) because in the first adjustment there are no plane parameters introduced for two horizontal triangular faces. There is no need for those parameters because these planes do not involve constraints. In the second adjustment there is one set of plane parameters for these two faces and one set of parameters for the three faces that make up the front of the building.

Adjustment	Iterations	Estimated standard deviation (pixel)	Largest standard deviation of object coordinate (percentage of object size)
1	4	0.67	1.7%
2	4	0.74	0.41%
3	5	1.37	0.28%

Table 3: Results of the adjustments

In the third adjustment a new type of geometric object constraint is introduced. This is the angle constraint between two planes. In total eleven perpendicularity constraints were applied. All vertical planes were set perpendicular to the horizontal roof plane (six constraints) and each vertical plane was set perpendicular to its neighbouring vertical plane (five constraints). From Figure 8 and Table 3 it is clear that the formal precision is improved by the additional object information. However, the estimated standard deviation increases considerably. This raises the question whether there are model errors present. Is the stochastic model too optimistic, is the camera model correct (interior orientation), and are all the object constraints valid in their absolute form? Statistical testing of individual constraints and image line observations can provide an answer, but is not implemented yet.

Furthermore, realistic weighting of the constraints and its effect on precision is to be investigated. The same holds for the reliability aspects of the presented mathematical model.

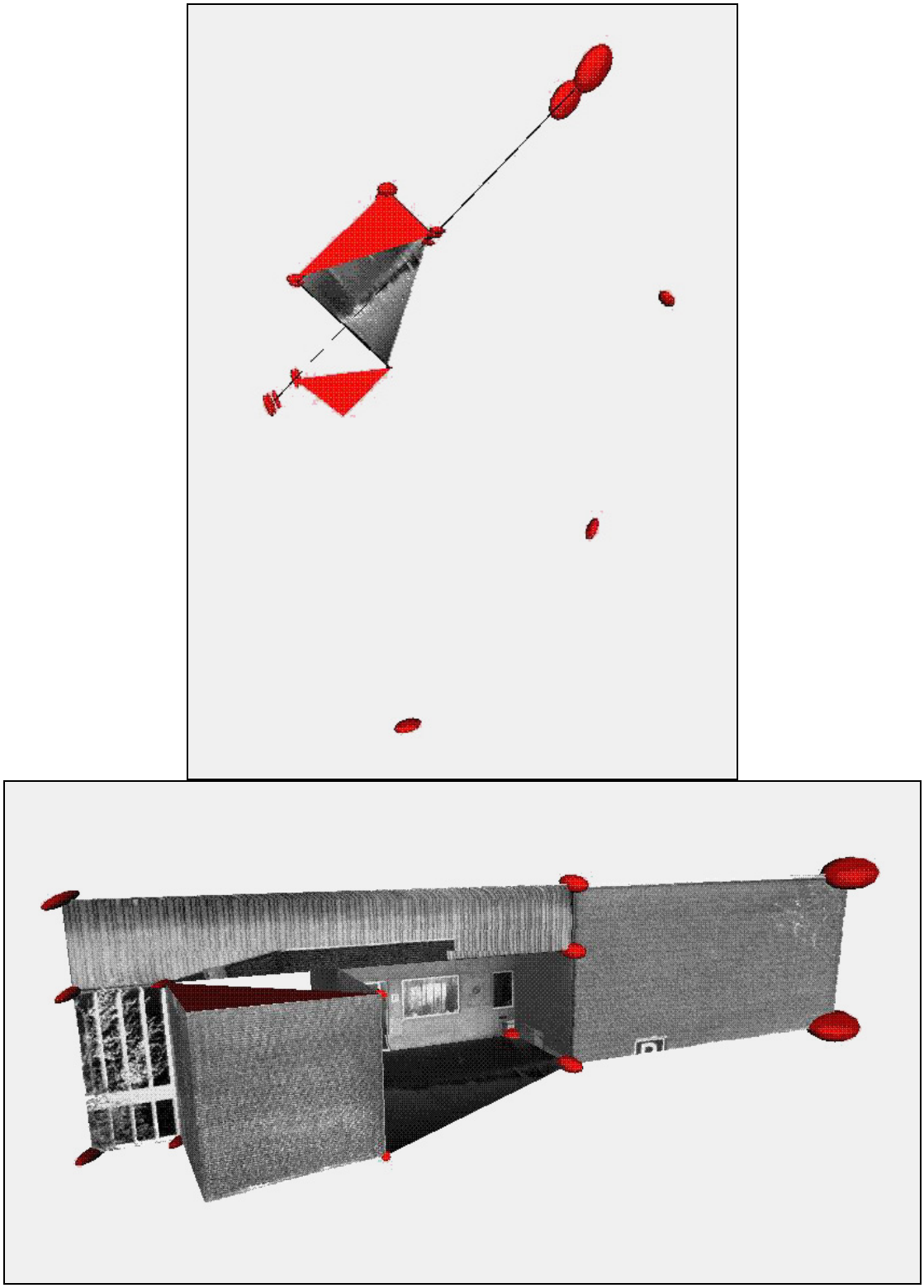

Figure 7: Top and oblique view of second model

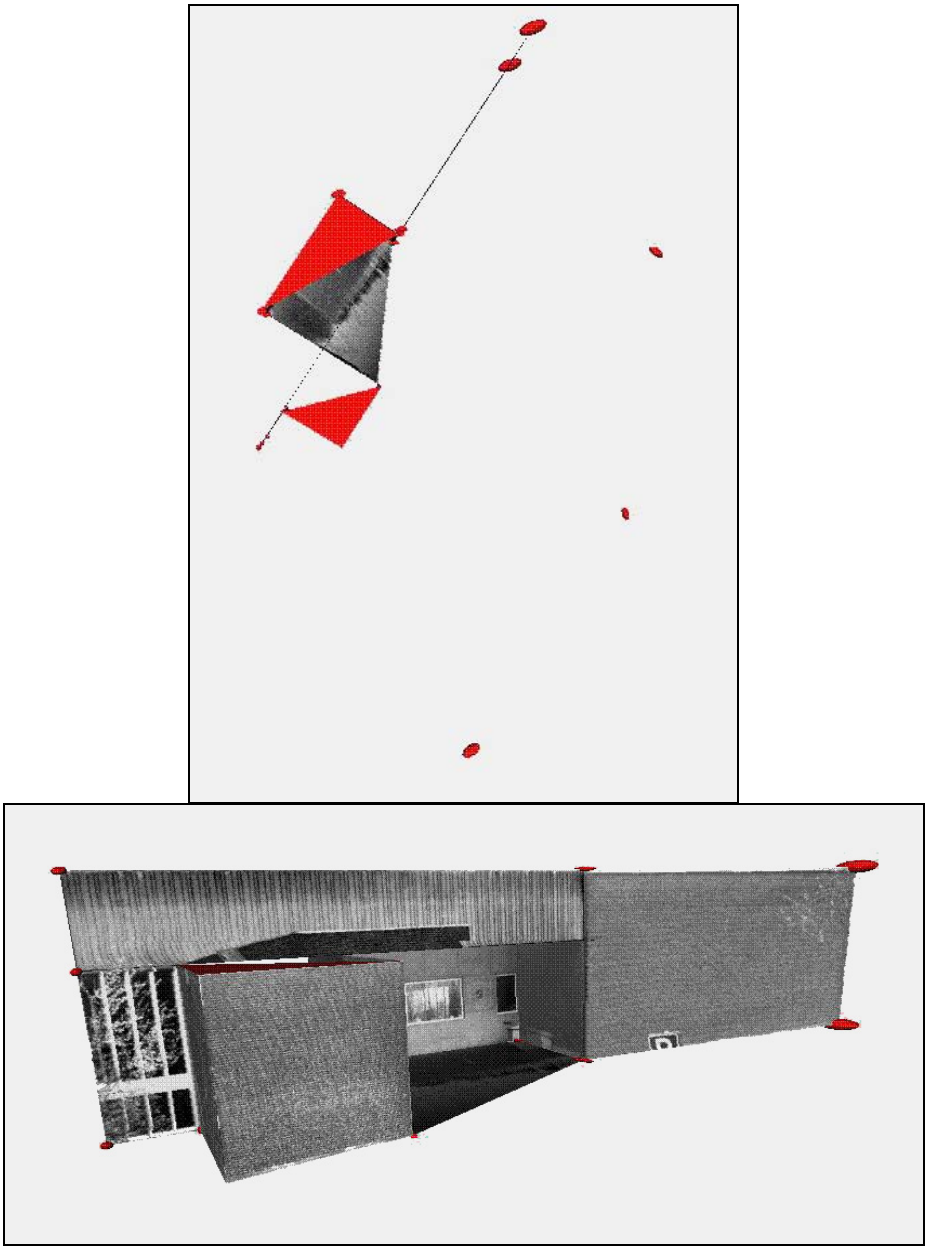

Figure 8: Top and oblique view of third model

7 Conclusions

A new mathematical model for the reconstruction of polyhedral objects using line photogrammetry is presented. The main difference from existing models is the use of condition equations with observations and parameters. Apart from parameters for the exterior orientation of the images, parameters for object points and planes are incorporated in the model. The plane parameters facilitate the formulation of geometric object constraints, such as coplanarity, and angle or distance constraints between planes of the object. Over-parameterisation in combination with constraints for the rotation matrix and the planes result in a mathematical model free of singularities. Approximate values of all object parameters are computed from, possibly redundant, sets of linear equations.

The examples demonstrate the advantages of the approach. Due to the use of line photogrammetry occluded object points can be reconstructed. Parts of the building visible in

only one image can be modelled due to the introduction of coplanarity constraints. Furthermore, the formal precision improves significantly with the introduction of constraints like perpendicularity between object planes. The validation of the object constraints in combination with their weighting is to be investigated.

References

1. Zielinski, H., Object reconstruction with digital line photogrammetry, Doctoral thesis Department of Geodesy and Photogrammetry, Royal Institute of Technology, Stockholm, 1993
2. Patias, P., Petsa, E., Streilein, A., Digital Line Photogrammetry, IGP Bericht nr. 252, Eidg. Technische Hochschule, ISBN 3-906513-73-4, Zürich, 1995
3. Mikhail, E.M., Weerawong, K., "Exploitation of linear features in surveying and photogrammetry", Journal of Surveying Engineering, Vol. 123, No. 1, pp. 32-47, 1997
4. Heuvel, F.A. van den, Vosselman, G., "Efficient 3D-modelling of buildings using a priori geometric object information", Videometrics V, Sabry F. El-Hakim (ed.), SPIE Vol. 3174, pp.38-49
5. Gülch, E., "Line photogrammetry: a tool for precise localization of 3D points and lines in automated object reconstruction", Integrating Photogrammetric Techniques with Scene Analysis and Machine Vision II, SPIE Vol. 2486, pp.2-12, Orlando, 1995
6. Mulawa, D., Estimation and photogrammetric treatment of linear features, Doctoral thesis, Purdue University, 1989
7. Schwermann, R., Geradengestützte Bildorientierung in der Nahbereichsphotogrammetrie, Doctoral thesis, Geodätischen Instituts der Rheinisch-Westfälische Technischen Hochschule Aachen, ISSN 0515-0574, Aachen, 1995
8. Weik, S., Grau, O., "Recovering 3-D object geometry using a generic constraint description", International Archives of Photogrammetry and Remote Sensing, Vol.31, Part B3, pp.593-598, Vienna, 1996
9. Debevec, P.E., Taylor, C.J., Malik, J., "Modelling and rendering architecture from photographs: a hybrid geometry- and image-based approach", Computer Graphics proceedings, Annual Conference Series, pp.11-20, New Orleans, 1996
10. Shuster, M.D., "A Survey of Attitude Representations", Journal of the Astronautical Sciences, Vol. 41, No. 4, pp. 439-517, 1993
11. Shih, T.-Y., "The Duality and Critical Condition in the Formulation and Decomposition of a Rotation Matrix, Photogrammetric Engineering and Remote Sensing, Vol. 56, No. 8, pp. 1173-1179, 1990
12. Barakat, H.F., Weerawong, K., Mikhail, E.M., "Feature-based Photogrammetric and Invariance Techniques for Object Reconstruction", International Archives of Photogrammetry and Remote Sensing, Vol.31, Part B3, pp. 535-541, Vienna, 1996
13. Teunissen, P.J.G., Adjustment Theory, Lecture notes Faculty of Geodetic Engineering, Delft University of Technology, Delft, 1994
14. Mikhail, E.M., Observations and Least Squares, IEP-A Dun-Donnelley Publisher, New York, 1976
15. Streilein, A., Hirschberg, U., "Integration of digital photogrammetry and CAAD: constraint-based modelling and semi-automatic measurement", CAAD Futures '95 International Conference, Singapore, 1995
16. McGlone, "Bundle adjustment with geometric constraints for hypothesis evaluation", International Archives of Photogrammetry and Remote Sensing, Vol.31, Part B3, pp. 529-534, Vienna, 1996
17. Haralick, R.M., Lee, C.-N., Ottenberg, K., Noelle, M., "Review and analysis of solutions of the three point perspective pose estimation problem", Int. Journal of Computer Vision, Vol. 13, No. 3, pp.331-356, 1994
18. Heuvel, F.A. van den, "Exterior Orientation using Coplanar Parallel Lines", 10th Scandinavian Conference on Image Analysis, Lappeenranta (Finland), pp.71-78, 1997
19. Heuvel, F.A. van den, "Vanishing Point Detection for Architectural Photogrammetry", International Archives of Photogrammetry and Remote Sensing, Vol.32, Part 5, pp. 652-659, Hakodate, 1998

2.6

Estimation of interior orientation parameters from constraints on line measurements in a single image[1]

[1] Reference: Heuvel, F.A. van den, 1999. **Estimation of interior orientation parameters from constraints on line measurements in a single image.** International Archives of Photogrammetry and Remote Sensing (Thessaloniki, Greece), Vol. 32, part 5W11, pp. 81-88.

Estimation of interior orientation parameters from constraints on line measurements in a single image

Frank A. van den Heuvel

Delft University of Technology
Faculty of Civil Engineering and Geosciences
Thijsseweg 11, 2629JA Delft, The Netherlands

Commission V, Working Group 5

ABSTRACT

In this paper a method is presented for the estimation of interior orientation parameters and lens distortion using measurements of lines in a single image and constraints derived from a priori information on the orientation of the related object lines. The interior orientation parameters consist of the location of the principle point and the focal length. Radial lens distortion is modelled with one parameter. The straight image lines are extracted automatically using a line-growing algorithm. The constraints on the orientation of the object lines are parallelism and perpendicularity constraints. These constraints are specified automatically using a vanishing point detection algorithm. The two-step procedure starts with the least-squares estimation of the lens distortion using only parallelism constraints. In this step, the image line observations are checked for blunders and their precision is assessed. In the second step, the principal point and the focal length are estimated using adjusted observations from the first step and constraints for perpendicularity in addition to the parallelism constraints. The formal precision of the parameters results from propagation of variances. The precision turned out to be in the order of 0.1 mm for the tests performed with wide-angle imagery (focal length 9.2 mm, sensor size 8.6x6.9 mm^2).
The procedure is applied to several images of a building and the results of the parameter estimation are evaluated. The quality of the estimated interior orientation parameters depends strongly on the orientation of the image relative to the object and the focal length of the camera. Furthermore, the availability and distribution of object lines and constraints plays an important role.
This automatic procedure for the estimation of lens distortion and interior orientation parameters is well suited to application to historic imagery taken with an unknown camera, or for imagery taken with a camera with an unstable interior orientation. This holds true for wide-angle, three-point perspective (i.e. no object edges are parallel to the image plane) imagery of objects showing straight lines that can be assumed parallel and perpendicular.

Keywords: interior orientation, lens distortion, camera calibration, single image, line-photogrammetry, geometric constraints, adjustment, architecture

1 Introduction

It is common practice in photogrammetry to estimate the interior orientation parameters of a camera from multiple images of a point field (Fryer, 1996). The camera is assumed stable during a longer period. When self-calibration is applied, the camera is assumed stable during image acquisition only, and coordinates of the points need not be known a priori. These standard procedures cannot be used for a camera with unstable interior orientation or when geometric information is to be extracted from (single) images taken with a camera of which the interior orientation is unknown. The method presented here uses constraints on

lines in the image that result from a priori information on the geometry of the related lines in object space. The major advantage of this line-photogrammetric method over the use of point measurements is the possible application of automatic line-extraction procedures. Furthermore, the constraints are inferred automatically by a vanishing point detection procedure. No other information on the position or orientation of the object lines is required.

A method that uses geometric object constraints for camera calibration (including exterior orientation) from point measurements in multiple images is presented in (Youcai and Haralick, 1999). Graphical and analytical methods for the estimation of interior orientation parameters from vanishing points in a single image can be found in (Williamson and Brill, 1990).

2 Estimation of interior orientation parameters

The procedure for estimation of the interior orientation using a single image consists of three steps:

1. Extraction of straight lines from the image.
2. Specification of parallelism and perpendicularity between the corresponding lines in object space.
3. Estimation of the interior orientation parameters and lens distortion using these constraints.

2.1 Straight line extraction

Due to lens distortion, straight lines in object space appear as slightly curved lines in the image. Straight lines are extracted using a line-growing algorithm. Any algorithm for straight-line extraction will break up long curved image lines into smaller sections. The object edges that relate to these sections are parallel and, without lens distortion, the image lines would intersect in a single point, the so-called vanishing point. Therefore, lens distortion is to be removed for vanishing point detection. In this paper, the estimation of the lens distortion is discussed, using the same vanishing point intersection constraint (van den Heuvel, 1998a).

2.2 The geometric constraints

Two types of constraints are applied, namely parallelism and perpendicularity constraints. The constraints can be specified manually or automatically using a vanishing point detection algorithm (van den Heuvel, 1998a). In principle, all known angles between (groups of parallel) lines of the object can be used, but only parallelism and perpendicularity, as the most common angles in man-made objects, are implemented.

Both constraints are formulated using the normals to the interpretation planes of the image lines involved. The image lines are represented by the image coordinates of the end points (figure 1). The image coordinates (x, y) are related to a direction vector in object space ($\mathbf{d}$ in the coordinate system of the camera) (Fryer, 1996):

$$\mathbf{d} = \begin{pmatrix} x - x_o - k_1(x - x_o)r^2 \\ y - y_o - k_1(y - y_o)r^2 \\ -f \end{pmatrix} \qquad (1)$$

with:
f : effective focal length
x_o , y_o : coordinates of the principle point

k_1 : radial lens distortion parameter, $r^2 = (x - x_o)^2 + (y - y_o)^2$
Lens distortion is often modelled more extensively. Although the model presented here can be extended, applying parameter k_1 only eliminates the major part of the lens distortion.

The normal to the interpretation plane of the image line i, with end points 1 and 2 is found using:

$$\mathbf{n}^i = \mathbf{d}_1 \times \mathbf{d}_2 \qquad (2)$$

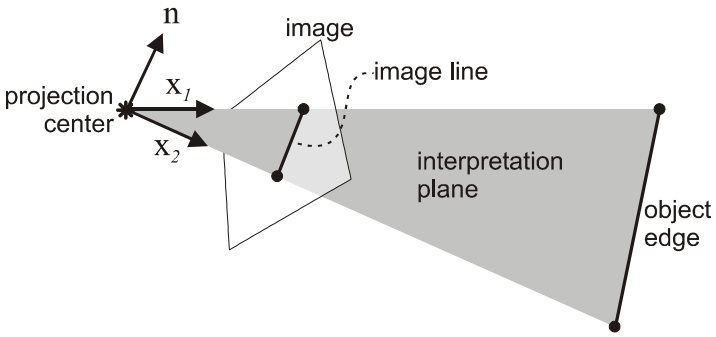

Figure 1: The interpretation plane

2.2.1 The parallelism constraint

The parallelism constraint can be written as the determinant of the matrix built from the normal vectors to the three interpretation planes of lines i, j and k (van den Heuvel and Vosselman, 1997):

$$\left[\mathbf{n}^i, \mathbf{n}^j, \mathbf{n}^k\right] = \det(\mathbf{n}^i, \mathbf{n}^j, \mathbf{n}^k) = 0 \qquad (3)$$

As can be seen from equations (1) and (2), equation (3) contains parameters (x_o, y_o, f, k_1) and observations (image coordinates x, y). In order to set up a least-squares adjustment this equation is linearised with respect to both the parameters and the observations. This leads to a so-called mixed model (Teunissen, 1994):

$$\mathbf{B}^{\mathrm{T}} E\{\mathbf{y}\} = \mathbf{A}\,\mathbf{x} \;;\; \mathbf{Q}_{\mathrm{y}} \qquad (4)$$

with:

$\mathbf{y}$	vector of (corrections to) the observations
$\mathbf{x}$	vector of (corrections to) the parameters
$\mathbf{A}, \mathbf{B}$	design matrices (partial derivatives)
$\mathbf{Q}_{\mathrm{y}}$	covariance matrix of the observations

The covariance matrix $\mathbf{Q}_{\mathrm{y}}$ of the image points is implemented as a diagonal matrix. Several options are available for the stochastic model:

- If lines are extracted using an edge detection approach, the variances of the coordinates of the end points are assumed to decrease linearly with the length of the line, in pixels.
- For lines that are extracted manually by measurement of their end points, a constant variance is assumed for all end point coordinates.

Line orientation does not play a role in the stochastic model as only precision information perpendicular to the line affects the precision of the interpretation plane normals.

2.2.2 The perpendicularity constraint

The perpendicularity constraint involves the interpretation plane normals of four lines, consisting of two perpendicular sets (1 and 2) of two lines that are parallel in object space. This constraint can be written as:

$$\left(\mathbf{n}_1^i \times \mathbf{n}_1^j\right) \cdot \left(\mathbf{n}_2^k \times \mathbf{n}_2^l\right) = 0 \qquad (5)$$

In this equation, the vector that results from the cross product has the same spatial orientation as the related object edges. The result of the dot product relates to the angle between orientations 1 and 2.

Like the parallelism constraint, this constraint is linearised with respect to the parameters of interior orientation and the observations. The system of condition equations (4) is extended with linearised perpendicularity constraints.

2.2.3 Selection of constraints

The least-squares solution to the system (4) is discussed in section 2.3. In order to be able to compute the solution, all constraints have to be independent. This is achieved in the following way. First, for each object orientation the two image lines are selected that best define the object orientation (the longest vector that results from a cross product in equation 5). Let us call these two lines the *base* lines. Then for each of the *n*-2 remaining lines of that orientation, parallelism constraints are set up (*n* is the number of lines in a cluster of parallel lines). Each constraint involves three lines, two of which are the base lines. In this way, *n*-2 independent constraints are defined for each object orientation.

Second, a maximum of three perpendicularity constraints is set up for the three major object orientations (*X, Y, Z*). These constraints are formulated using the base lines of each object orientation that have been used for the parallelism constraints as well. The three independent constraints define perpendicularity between three combinations of two object axes (*XY, YZ,* and *ZX*).

The selection of parallelism and perpendicularity constraints presented here, leads to an independent set of condition equations. Other selections of independent constraints are possible and will lead to the same results, in principle. However, numerically unfavourable selections have to be avoided.

In this paper, we concentrate on estimation of interior orientation parameters from a single image. However, if several images taken with the same camera are available, the lines and constraints of all images can be used to build the system of condition equations (4). Of course, the interior orientation of the camera is assumed identical for all the images.

2.3 Parameter estimation

The system of condition equations (4) is transformed into a standard system of observations equations by the introduction of the so-called derived observations ($\mathbf{z}$):

$$E\{\mathbf{z}\} = \mathbf{A}\,\mathbf{x}\,;\ \mathbf{Q}_\mathbf{z} \qquad (6)$$

with:

$\mathbf{z} = \mathbf{B}^\mathrm{T}\mathbf{y}$ vector of (corrections to) the derived observations

$\mathbf{Q}_\mathbf{z} = \mathbf{B}^\mathrm{T}\mathbf{Q}_\mathbf{y}\mathbf{B}$ covariance matrix of the derived observations

The covariance matrix $\mathbf{Q}_\mathbf{z}$ (treated as a full matrix) of the derived observations results from propagation of the diagonal covariance matrix of the observations $\mathbf{Q}_\mathbf{y}$. The least-squares solution to this system is well known:

$$\hat{\mathbf{x}} = (\mathbf{A}^T \mathbf{Q}_z^{-1} \mathbf{A})^{-1} \mathbf{A}^T \mathbf{Q}_z^{-1} \mathbf{z} \qquad (7)$$

The computation of the residuals of the original observations is explained in (van den Heuvel, 1999).

Since the mathematical model is non-linear in both the parameters and the observations, the iteration process needs special attention. In principle, convergence has to be obtained by iterating in the parameters only. After that, iteration in both the parameters and the observations leads to a set of parameters and observations that perfectly fit the model. For this iteration in parameters and observations, only one iteration step was needed.

Experiments showed that no convergence of the iteration in the parameters could be obtained when the interior orientation parameters were estimated. Convergence was only obtained when the lens distortion parameter was estimated, and the principal point and focal length were not. The reason for the absence of convergence in the parameter iteration lies in the sensitivity of the solution to the coefficients in the design matrix ($\mathbf{A}$). These coefficients depend on the observations and are imperfect due to noise in the observations (and possibly blunders). Using adjusted observations, the iteration in the parameters converges well.

3 Estimation in two steps

In this section, separating the estimation of the parameters in two steps extends the procedure described in the previous section:
1. Estimation of radial lens distortion.
2. Estimation of interior orientation.

This separation in two steps is also made in (van den Eelaart and Hendriks, 1999). Furthermore, the first step of the procedure can be classified as an “on-the-job plumb-line calibration” (Fryer, 1996).

The mathematical model is identical to the one described in section 2. However, in the first step of the procedure only parallelism constraints are applied. In the second step, both types of constraints are used to estimate the parameters using adjusted observations from the first step. In other words, the (adjusted) image lines used in the second step all intersect at their vanishing points. In principle, only the perpendicularity constraints are needed in the second step. The parallelism constraints are added for the assessment of the formal precision of the parameters. The solution is identical to the one without parallelism constraints, and identical to the direct solution from three perpendicular sets of two parallel lines (called *base* lines in the previous section) published in (Kraus, 1996).

A few remarks to the two-step procedure:
- The solution of the first step does not depend on the focal length, so an arbitrary initial value can be selected.
- However, the solution of the first step depends on the initial location of the principle point. In the examples described in the next section, the centre of the image format is chosen as the point of symmetry. Iteration in the initial position of the principle point is possible, but was not examined.
- The residuals of the observations are not affected in the second step. The reason lies in the one-to-one relation between the location of the three (adjusted) vanishing points resulting from the first step, and the three parameters of interior orientation. This relation is established by the three independent constraints for perpendicularity. Therefore,

statistical testing of the observations is performed in the first step of the procedure, and not in the second step.

4 Examples

The method for estimation of interior orientation parameters from a single image is applied to the calibration of an Olympus C1400 digital camera. The imaging sensor contains 1280 by 1024 pixels (pixel size 6.7 μm). The camera has a zoom lens of which the two extreme settings were used, i.e. 9.2 mm and 28 mm nominal focal length. In the following, these two settings are called the wide-angle and narrow-angle settings, respectively. The lens system was focussed at infinity. At both settings, three images of a Delft University building were taken from street level. The camera settings were identical for the three images. The first image was taken roughly perpendicular to the façade. The second one is an oblique image of the same façade and the third image is the only one that contains all three major object orientations.

4.1 Wide-angle imagery

The first wide-angle image (9.2 mm lens), overlaid with the automatically extracted image lines, is shown in figure 2. The number of extracted lines varies with the parameter settings for the line-growing algorithm. The settings used resulted in 230 lines. The vanishing point detection resulted in two sets of lines, 55 vertical and 145 horizontal lines. It has to be noted that the nominal values for the interior orientation have been used for the vanishing point detection. This implies that the principle point is located at the centre of the image format and the focal length is set to its nominal value (9.2 mm). If this information is not available, a minimum number of lines (three perpendicular sets of two parallel lines) has to be measured manually. The a priori standard deviation used for the vanishing point detection was chosen to be relatively high to ensure that the lens distortion did not hinder the clustering:

$$\sigma_o = \frac{0.1\,\text{mm}}{\sqrt{\text{line length (pixel)}}}$$

In all the tests for the estimation of the interior orientation parameters, the a priori standard deviation of the end point coordinates (σ_o) is fixed at 5 μm or 0.75 pixel. The estimation of the lens distortion parameter using the original observations (the first step of the procedure) showed this value to be realistic for most experiments (see the test values ($\frac{\hat{\sigma}^2}{\sigma_0^2}$) in Table 1).

Maximum residuals of end point coordinates are sometimes large (around 4 times the a priori standard deviation). This can be due to the limited model for the lens distortion, or imperfections in the line clustering of the vanishing point detection procedure.

In the first step of the procedure, the parameter for radial lens distortion was estimated using only parallelism constraints. The results are summarized in Table 1. Figure 2 shows the image corrected for radial lens distortion.

Figure 2: First wide-angle image with extracted lines (top) and corrected for radial lens distortion (bottom).

In the second step, the interior orientation parameters could not be estimated. The location of the principle point cannot be estimated because only two object orientations are available. The focal length cannot be estimated because the image is taken perpendicular to the façade, and therefore the angle between the two orientations in object space (reconstructed from the image line observations) is not affected by the focal length.

Figure 3: Oblique wide-angle imagery with extracted lines; façade (top) and three-point perspective

The second and the third image were taken with the same camera settings as the first (Figure 3). The second image is an oblique one of a single façade, and does not allow estimation of the principle point. However, the focal length can be estimated if the principle point is assumed to be in the centre of the image. The third image has a so-called three-point perspective (i.e. no object edges parallel to the image plane) and thus all interior orientation parameters can be estimated (Williamson and Brill, 1990). Note that due to the lack of windows in one of the façades, the number of lines and their distribution over the image is not optimal. The results of the parameter estimation are summarized in Table 1.

Wide-angle	Number of constraints par. + per.	k_1 (10^{-3} mm^{-2})	x_o (mm)	y_o (mm)	f (mm)	$\frac{\hat{\sigma}^2}{\sigma_0^2}$	Maximum residual (μm)
1. Perpendicular	198 (+1)	-1.627 (0.061)	-	-	-	0.68	21.5
2. Oblique façade	163 + 1	-1.823 (0.078)	-	-	9.212 (0.115)	1.33	20.2
3. Oblique	69 + 3	-1.685 (0.135)	-0.162 (0.165)	-0.154 (0.045)	9.250 (0.044)	0.87	8.8

Table 1 : Parameter estimation results for the wide-angle images (standard deviation between brackets).

Narrow-angle	Number of constraints par. + per.	k_1 (10^{-3} mm^{-2})	x_o (mm)	y_o (mm)	f (mm)	$\frac{\hat{\sigma}^2}{\sigma_0^2}$	Maximum residual (μm)
1. Perpendicular	247 (+1)	0.953 (0.059)	-	-	-	0.38	9.9
2. Oblique façade	326 + 1	1.127 (0.081)	-	-	26.984 (2.93)	2.08	31.1
3. Oblique	194 + 3	1.261 (0.145)	2.59 (1.17)	0.868 (0.502)	26.388 (0.561)	0.82	24.8

Table 2 : Parameter estimation results for the narrow-angle images (standard deviation between brackets).

4.2 Narrow-angle imagery

The three narrow-angle images (28 mm nominal focal length) show the same perspective as the three wide-angle images. However, the narrow-angle images have two related disadvantages in comparison to the wide-angle images. First, the longer focal length leads to a degradation of the precision of the location of the vanishing points, due to a more unfavourable intersection of image lines. Second, the longer focal length is also the reason that the images are taken almost parallel to the vertical object orientation. For the third image, the perspective is very close to a two-point perspective (i.e. one object orientation is parallel to the image plane), for which the principle point cannot be estimated (Williamson and Brill, 1990). This explains why the precision of x_o is significantly lower than the precision of y_o for both the wide-angle (close to a two-point perspective) and the narrow-angle image.

Due to the two disadvantages mentioned, the method presented in this paper is not suited for the estimation of the interior orientation parameters of narrow-angle images. As can be concluded from Table 2, this holds especially for the estimation of the principle point (in *y*-direction the standard deviation amounts 0.5 mm or 75 pixels). However, for reconstruction purposes with this type of imagery, errors in the location of the principle point will have only minor effects on the results of the reconstruction. Therefore, the centre of the image format can usually be taken to represent the principle point with sufficient precision.

The estimation of the lens distortion does not depend on the focal length. It can be estimated for both wide- and narrow-angle images with similar precision.

Figure 4: The narrow-angle images (28 mm lens).

5 Conclusions

A method for the estimation of lens distortion and interior orientation parameters from a single image, using constraints on line measurements, has been presented. The constraints on the image line observations are derived from geometric constraints on the related lines in object space. The object line constraints are parallelism and perpendicularity between the three major orientations of the object edges. These assumptions are valid for many man-made objects and they occur very frequently in buildings. Therefore, this method is suitable for historic images of buildings, taken with an unknown camera. However, the orientation of the image relative to the object is crucial for the estimation of the interior orientation parameters. For the estimation of lens distortion the image orientation does not play a role.

The characteristics of the method can be summarized as follows:

- Least-squares estimation of lens distortion and interior orientation parameters using line measurements in a single image.
- The only object information required is the parallelism and perpendicularity of object edges.
- The precision of the parameters is assessed by rigorous error propagation.
- When an approximate value for the focal length is available, the method is fully automatic, using a straight-line extraction and a vanishing point detection algorithm. If this is not the case, a few manual measurements are required.
- The method is only applicable to images of objects with parallel and perpendicular edges.
- For the estimation of the interior orientation parameters, the orientation of the image relative to the object plays a crucial role. A so-called three-point perspective is required.
- The precision of the estimated interior orientation parameters is generally higher when the focal length is shorter.

Camera calibration is not a goal in itself. Calibration is a necessity for accurate 3D measurement. The application of the presented calibration procedure has not been tested in combination with 3D reconstruction, possibly from the same (single) image using the same constraints (van den Heuvel, 1998b). The use of the object constraints in the 3D reconstruction will reduce the effects of errors in the parameters of the camera model. However, it will not eliminate them. The use of the calibration procedure in combination with 3D reconstruction is a topic for future work.

References

Eelaart, I. van den, and Hendriks, E.A., 1999. “A Flexible Camera Calibration System that uses Straight Lines in a 3D Scene to Calculate the Lens Distortion”. Proceedings ASCI’99, 5th annual conference of the Advanced School for Computing and Imaging (Heijen, The Netherlands, June 1999), ASCI, Delft.

Fryer, J.G., 1996. “Camera calibration”. In: Close-range photogrammetry and machine vision, K.B. Atkinson (ed.), Whittles Publishing, ISBN 1-870325-46-X, pp. 156-179.

Heuvel, F.A. van den, and Vosselman, G., 1997. “Efficient 3D-modeling of buildings using a priori geometric object information”. In: Videometrics V, Sabry F. El-Hakim (ed.), SPIE Vol. 3174, pp. 38-49.

Heuvel, F.A. van den, 1998a. “Vanishing point detection for architectural photogrammetry”. International archives of photogrammetry and remote sensing, Vol. 32, part 5, ISSN 0256-1840, pp. 652-659.

Heuvel, F.A. van den, 1998b. “3D reconstruction from a single image using geometric constraints”. ISPRS Journal of Photogrammetry & Remote Sensing, Vol. 53, pp. 354-368.

Heuvel, F.A. van den, 1999. “A Line-photogrammetric mathematical model for the reconstruction of polyhedral objects”. In: Videometrics VI, Sabry F. El-Hakim (ed.), Proceedings of SPIE Vol. 3641, pp. 60-71.

Kraus, K., 1996. “Photogrammetrie – Band 2: Verfeinerte Methoden und Anwendungen”. Ferd. Dümmlers Verlag, Bonn, pp. 115-120.

Mikhail, E.M., 1976. “Observations and Least Squares”. IEP-A Dun-Donnelley Publisher, New York.

Teunissen, P.J.G., 1994. “Adjustment Theory”. Lecture notes Faculty of Geodetic Engineering, Delft University of Technology, Delft.

Williamson, J.R. and Brill, M.H., 1990. “Dimensional Analysis through Perspective – A Reference Manual”. American Society for Photogrammetry and Remote Sensing, ISBN 0-8403-5673-0.

Youcai, H., and Haralick, M., 1999. “Testing Camera Calibration with Constraints”. Photogrammetric Engineering & Remote Sensing, Vol. 65, No. 3, pp. 249-258.

2.7

Line-photogrammetry and its application for reconstruction from a single image[1]

[1] Reference: Heuvel, F.A. van den, 2000**. Line-photogrammetry and its application for reconstruction from a single image.** 19. Jahrestagung der DGPF (Essen), Publikationen der Deutschen Gesellschaft fuer Photogrammetrie und Fernerkundung, Vol.8, pp.255-263.

Line-photogrammetry and its application for reconstruction from a single image

Frank A. van den Heuvel

Delft University of Technology
'Faculty of Civil Engineering and Geosciences
Thijsseweg 11, 2629 JA Delft, The Netherlands

Abstract

For many applications of photogrammetry the use of image line observations has advantages over the use of points. This is true for photogrammetric modelling of man-made objects that can be described with a polyhedral model. Architectural photogrammetry is such an application. Line-photogrammetry focuses on the use of image line observations for accurate object modelling. In the paper an overview is presented of two line-photogrammetric adjustment approaches. One approach is for the estimation of object parameters from line observations of multiple images, and one for the adjustment of line observations of a single image. In the latter case object reconstruction is performed in a separate step. The use of point and plane parameters in the first approach simplifies the formulation of geometric object constraints. In the single image approach the object constraints are reformulated into condition equations with only observations. The pros and cons of both approaches are discussed in the paper.

Zusammenfassung

In vielen Anwendungen der Photogrammetrie weist die Messung von Linien Vorteile auf gegenüber dem Gebrauch von Punkten. Dies gilt insbesondere für die Modellierung von künstlichen Objekten, zum Beispiel in der Architekturphotogrammetrie. Die Publikation diskutiert die Vorteile von Linien gegenüber Punkten und zeigt mathematische Modelle für die Ausgleichung von Linienbeobachtungen sowohl in Mehrbildverbänden wie in Einzelbildern. In der Bündelblockausgleichung für Linienbeobachtungen kann a-priori Objektinformation wie z.B. Parallelität, Koplanarität und Orthogonalität in Form von zusätzlichen Bedingungsgleichungen verarbeitet werden; ausreichende a-priori Information dieser Art ist selbstverständlich essentiell für die 3-D Rekonstruktion aus Einzelbildern. Beide Modelle können um zusätzliche Kameraparameter erweitert werden, wodurch Selbstkalibrierung ermöglicht wird. Die Vorzüge beider Modelle und der Linienphotogrammetrie im Allgemeinen liegen neben der (semi-)automatischen Messung und der besseren Eignung für die Modellierung beispielsweise auch in der Rekonstruktion verdeckter Objektpunkte oder in nur einem Bild sichtbarer Objektteile.

1 Introduction

Image lines are more and more used in photogrammetry. This is most apparent in application fields where edges or contours of the object to be modelled are visible in the images. Examples are modelling of piping installations (Ermes et al., 1999), or the reconstruction of buildings (Streilein, 1998). The approaches for the adjustment of line observations and object reconstruction outlined in this paper aim at the latter application field, i.e. architectural photogrammetry.

In the last years, different line-photogrammetric measurement systems using parameterised object models have been developed (Debevec et al., 1996; Ermes et al., 1999; Lang & Förstner, 1996). The first extensive treatment of linear features from a photogrammetric standpoint is by Mulawa & Mikhail (1988). Like in many line-photogrammetric approaches, a parameterisation of 3D lines in object space is chosen, and the parameters of the object lines are related to image points on the projection of the lines in the images (Zielinski, 1993; Gülch, 1995). In some approaches a parameterisation of the line in the image is chosen, and related to the parameters of the object line (Schwermann, 1995; Patias et al., 1995). Streilein (1998) intersects lines in image space, and processes the resulting image points in a conventional bundle adjustment. The approaches in this paper use a polyhedral boundary representation of which point and plane parameters appear in the line-photogrammetric bundle adjustment.

In the literature many advantages of using line observations instead of points can be found. The most prominent advantage is the better automation potential for extraction and measurement of lines in digital imagery (Burns, 1986). To obtain a structured object model, interpretation of the imagery by an operator is usually required. This leads to a manual or semi-automatic line measurement (Stylianidis & Patias, 1999). From the geometrical point of view lines have the advantage that they only have to be partly visible in the image, and this does not have to be the same part for different images (Fig. 1). Therefore, in case of manual or semi-automatic measurements, the endpoints of the image lines can be measured at locations where the edge is well visible in the image. This increased flexibility of correspondence leads to another advantage; in this approach an object point is defined as the intersection of object lines. This means that occluded object points, or object points that are not well defined, can be accurately reconstructed if sufficient measurements of related lines are available.

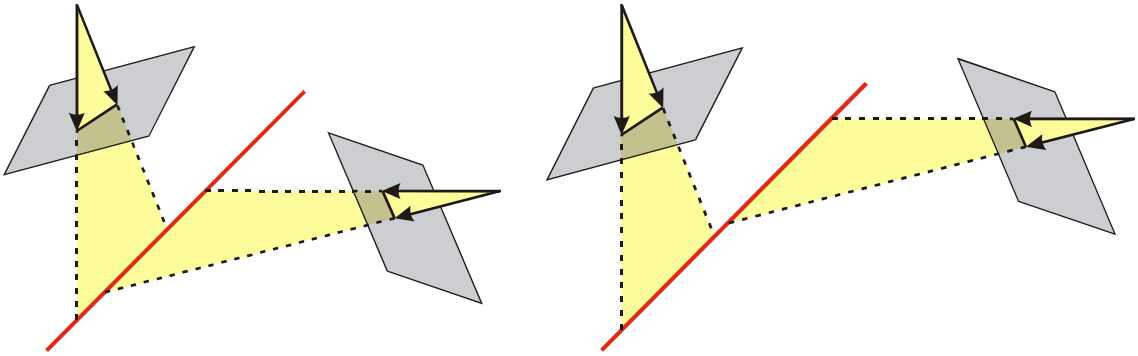

Fig. 1: Flexibility of line correspondence between two images

In the two line-photogrammetric approaches presented in this paper the straight image lines are represented by their endpoints, but only the normal vector to the plane spanned by the two direction vectors related to the endpoints is used in the formulation of the mathematical models (section 2). The first approach can be regarded as the line-photogrammetric counterpart of the conventional bundle adjustment (section 3). The use of object parameters for points and planes leads to condition equations of a simple form, and greatly facilitates the implementation of geometric object constraints. The parameterisation is free of singularities. It is to be stressed that there is no explicit parameterisation of object lines used.

The second approach is designed for object reconstruction from a single image, and thus fully depends on a priori object information (section 4). In this approach the adjustment of redundant constraints does not involve object parameters. Object reconstruction is performed with adjusted image line observations in a separate step. The adjustment does not require approximate values, and can be executed even when the object reconstruction

cannot be completed due to a lack of observations or object constraints. Compared to the first approach, the error propagation needed for assessing the quality of the reconstruction is more complicated due to the separate step for object reconstruction.

2 Image line observations

The main difference of the line-photogrammetric approaches presented in this paper with conventional (point-) photogrammetry is found in the type of observations used. In section 2.1 the representation of a straight line in the image and the role of the interpretation plane is discussed. In section 2.2 the camera model and the possibilities for self-calibration are reviewed.

2.1 The interpretation plane

A straight line in the image can be parameterised in several ways. Although two parameters suffice for the representation of an image line, the four image co-ordinates (*x*, *y*) of the end points are used here. This guarantees a singularity-free representation, and simplifies the formulation of the stochastic model. The image co-ordinates are uncorrelated and thus the precision of the line is independent of its orientation.

Like a point in the image is associated with a ray in space, a line in the image is associated with a plane in space. This plane is called the interpretation plane (Fig. 2).

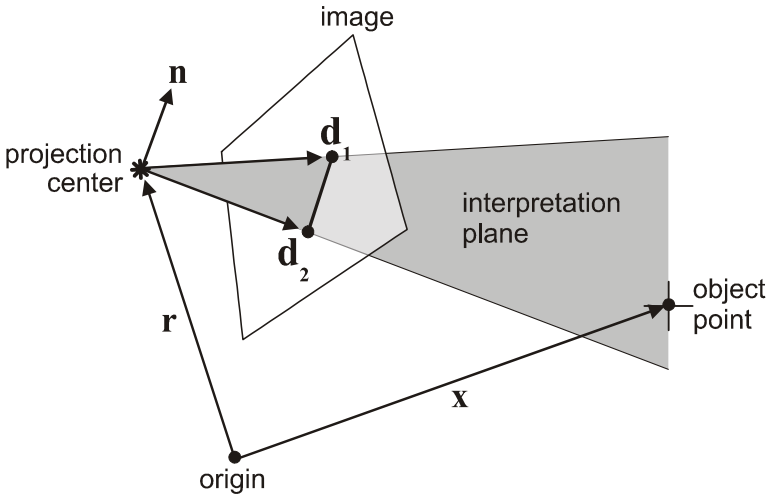

Fig. 2: A line in the image and its associated interpretation plane

Assuming a perfect central projection with focal distance f, the orientation of the interpretation plane is defined by its normal vector that is constructed from the vectors from the projection centre to the endpoints of the line:

$$\mathbf{n} = \mathbf{R}\ (\mathbf{d}_1 \times \mathbf{d}_2), \text{ with: } \mathbf{d} = (x, y, -f) \tag{1}$$

The normal vector to the interpretation plane is rotated into the object co-ordinate system by applying the rotation matrix of exterior orientation ($\mathbf{R}$). In the line-photogrammetric models presented in this paper only the normal vectors to the interpretation planes are used to formulate the relations with the observations.

2.2 Camera calibration

Equation (1) is to be applied after correction of the image co-ordinates for deviations from the perfect central projection, such as deformations in the image plane or lens distortions. If these distortions are unknown, camera calibration parameters can be introduced in (1):

$$\mathbf{d} = \begin{pmatrix} x - x_o - k_1(x - x_o)\,r^2 \\ y - y_o - k_1(y - y_o)\,r^2 \\ -f \end{pmatrix} \tag{2}$$

with:
f, x_o, y_o : effective focal length, coordinates of the principle point
k_1 : radial lens distortion parameter, $r^2 = (x - x_o)^2 + (y - y_o)^2$

If required, this camera model can be extended (Fryer, 1996). However, whether it is possible to estimate the parameters introduced, strongly depends on the information available, i.e. image configuration, number and distribution of image line observations, and availability of object constraints. The camera model (2) is implemented in the single-image approach (section 4), but not yet available for the multi-image bundle adjustment described in the next section.

3 Line-photogrammetric bundle adjustment

The line-photogrammetric bundle adjustment aims at the estimation of parameters that represent the geometry of the object from the image line observations of multiple images. The basic relation of the line-photogrammetric bundle adjustment is the point-in-plane constraint (section 3.1). The relations that build the mathematical model are non-linear in the parameters and non-linear in the observations. The least-squares solution to this uncommon model is discussed in section 3.2. More details on the line-photogrammetric bundle adjustment can be found in (van den Heuvel, 1999a). An example with line measurements in three images is available on the web at “www.geo.tudelft.nl/frs/architec/triple.html”.

3.1 Mathematical model

The primary type of object parameters are the 3D co-ordinates of the object points, like in a conventional bundle adjustment. The main part of the mathematical model is build with condition equations that force object points in related interpretation planes (Fig. 2):

$$\mathbf{n} \cdot \mathbf{x} - \mathbf{n} \cdot \mathbf{r} = 0 \tag{3}$$

In (3) **n** denotes the normal vector to the interpretation plane in the object co-ordinate system, and **x** and **r** the position vectors of the object point and the projection centre, respectively. This equation relates the image line observations and the co-ordinates of the object points.
Next to object point co-ordinates the parameters of the object planes are introduced in order to facilitate the formulation of object constraints. The object plane parameters enter the mathematical model through the object point-in-plane constraint similar to (3):

$$\mathbf{n}_p \cdot \mathbf{x} - l_p = 0 \tag{4}$$

In (4) $\mathbf{n}_p$ is the normal vector to the object plane (forced to unit length by an additional constraint), and parameter l_p represents the distance of the plane to the origin. This representation of a plane in space is free of singularities. With condition equations (3) and (4) the object point and plane parameters ($\mathbf{x}$ respectively $\mathbf{n}_p$, l_p), and the exterior orientation

parameters (**r**, **R**) can be estimated from the image line observations (**d**, in (1)). Due to the coplanarity equations (4) the faces of the reconstructed object will be planar.
Only two geometric object constraints are presented here to demonstrate the way in which the plane parameters facilitate their formulation. A complete set of constraints can be found in (van den Heuvel, 1999a). The angle (a_{ij}) constraint between two planes *i* and *j*:

$$\mathbf{n}_i \cdot \mathbf{n}_j = \cos(a_{ij}) \tag{5}$$

The distance (d_{ij}) between two parallel planes i and j is constrained by:

$$\left| l_{p_i} - l_{p_j} \right| = d_{ij} \tag{6}$$

With only point parameters, these constraints would involve 12 to 18 parameters (4 to 6 points).

3.2 Adjustment

Approximate values of all parameters have to be available for the formulation of the condition equations. An approximate value computation has been implemented that only requires approximations for the parameters of exterior orientation

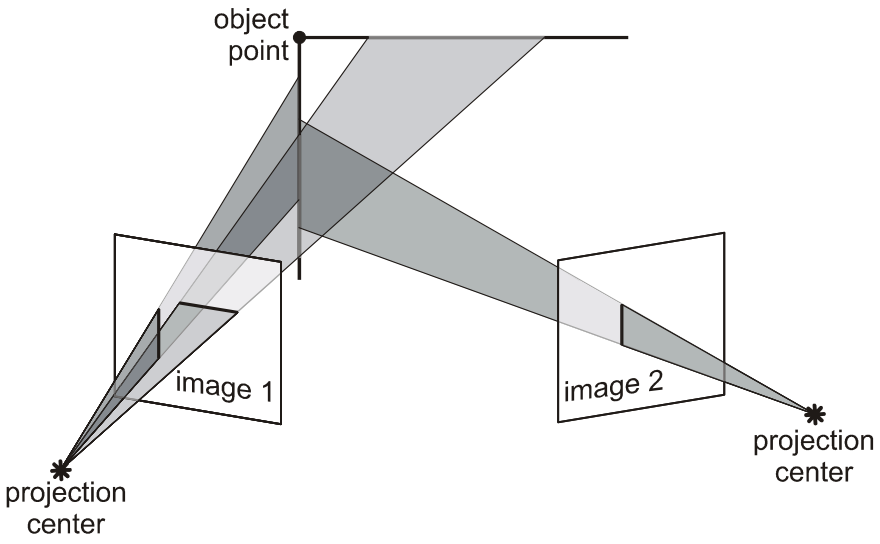

Fig. 3: Forward intersection of interpretation planes (minimum configuration)

Object points are derived from intersection of interpretation planes (Fig. 3). Plane parameters are computed from object point co-ordinates in a similar way exploiting the duality of the point and plane representation.

The mathematical model consists of condition equations with observations and parameters. In addition constraints are imposed on the parameters. Both types of equations are implemented as observation equations. The model consists of two parts that are solved simultaneously. Due to the inclusion of constraints for at least seven object co-ordinates, the complete system is of full rank. Because the model is non-linear in both the parameters and the observations, the solution is computed in an iterative procedure in which parameters and observations are updated. In order to avoid biases in the solution due to imperfections in approximate values, observations should only be updated after convergence on the parameters is reached.

4 Single image adjustment and reconstruction

Object reconstruction from measurements in a single image and a priori object information has been investigated many times before (Williamson & Brill, 1990; Braun, 1994; Bräuer-Burchardt & Voss, 1999). This technique is e.g. applied for deriving metric information of destroyed buildings of which only one or a few photographs are available (Karras & Petsa, 1999). However, also in aerial photogrammetry a priori object information is applied to support the object reconstruction, possibly from a single image (Lang & Förstner, 1996; Shufelt, 1999). In the approach presented here, the adjustment of observations is performed in a separate step and does not involve object parameters. Therefore, the adjustment does not depend on the choice for a parameterisation of the object, or on the availability of approximate values. This is the main difference with the line-photogrammetric approach of section 3, and many other approaches.

The incorporation of knowledge on the geometry of the object, like coplanarity or parallelism, makes it possible to reconstruct parts of the object that are visible in one image. Object reconstruction from a single image relies primarily on these two types of object constraints. A variety of object constraints can be used for the reconstruction, but it can be difficult to detect redundant constraints, and formulate corresponding condition equations for the observations. Other disadvantages compared to a multiple image approach are the separate step needed for the reconstruction, and the error propagation within this step. Furthermore, it is obvious that an object can never be modelled completely from a single image.

Although the adjustment described here does not involve parameters, the model was extended with parameters for interior orientation and lens distortion (section 2.2). Whether these parameters can be estimated strongly depends on the availability of image lines and constraints, and on the orientation of the image relative to the building (van den Heuvel, 1999b).

The geometric object constraints and their formulation as condition equations on the observations are discussed in section 4.1. The least-squares adjustment that results in adjusted image lines is briefly discussed in section 4.2. Object reconstruction from the adjusted lines is performed in a separate step (section 4.3). More details on the approach can be found in (van den Heuvel, 1998b). An example of a single image reconstruction can be found on the web at “www.geo.tudelft.nl/frs/architec/single.html”.

4.1 Mathematical model

Two types of constraints are to be distinguished. First, constraints that result from the topology of the object, such as edges intersecting in an object point. The topology is derived from image interpretation. When more than two edges intersect, a condition equation on the related image lines can be formulated:

$$\left[\mathbf{n}^i, \mathbf{n}^j, \mathbf{n}^k\right] \;=\; \det\left(\mathbf{n}^i, \mathbf{n}^j, \mathbf{n}^k\right) \;=\; 0 \qquad (7)$$

The three vectors $\mathbf{n}$ are the normals to the interpretation planes in the camera co-ordinate system ($\mathbf{R} = \mathbf{I}$ in (1)). Other constraints that are inherent in the polyhedral object description, such as coplanarity of object points and lines of a face, only lead to condition equations in combination with the second type of constraints. These are the geometric object constraints. The main object constraint for reconstruction is parallelism of object edges. The projections of parallel object edges intersect at a vanishing point in the image plane. Therefore, the condition equation is of the same form as the one for intersection at an object point (7). The number of independent equations equals the number of lines minus two.

Redundancy can arise from combinations of different types of constraints. For a unique object reconstruction from adjusted observations a complete set of independent condition equations is to be formulated. Not all the possible combinations of constraints were studied. Apart from condition equation (7), condition equations for combinations of perpendicularity and parallelism, as well as coplanarity and parallelism were implemented.

4.2 Adjustment

The condition equations form the non-linear functional model for the least-squares adjustment. This model contains no parameters and therefore there are no approximate values needed. The conditions can be processed in a sequential manner. This has advantages for an interactive measurement system because a condition can be tested as soon as the operator specifies it. The adjustment results in adjusted observations that are input to the object reconstruction.

4.3 Object reconstruction

The 3D reconstruction is performed in the camera system at arbitrary scale. If control points are available, an absolute orientation can be used to transform the model into a world co-ordinate system. In the object reconstruction first orientations of lines and planes in object space are determined followed by the calculation of positions of object features. This approach is similar to the one proposed by Braun (1994). The object reconstruction is performed in four steps:

1. Orientation of the object lines
2. Orientation of the object planes
3. Positioning of the object planes
4. Computation of the co-ordinates of object points

The orientation of the parallel lines in object space results from the intersection of the interpretation planes related to these lines (Fig. 4). The object space orientation (**o**) is computed from the normals to the interpretation planes *i* and *j* as follows:

$$\mathbf{o} = \mathbf{n}^i \times \mathbf{n}^j \tag{8}$$

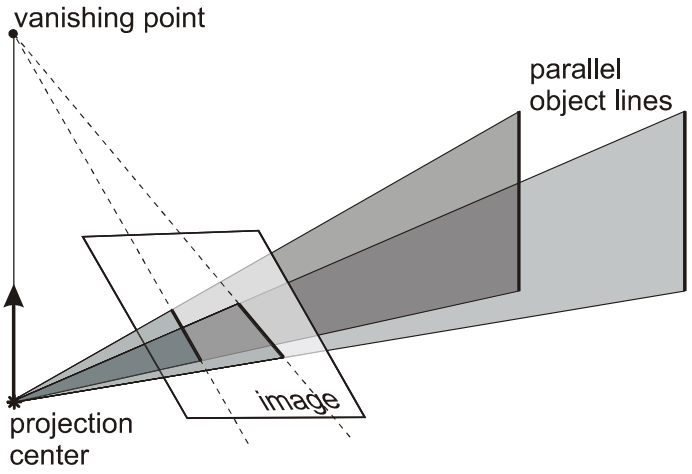

Fig. 4: The orientation of object lines from the intersection of interpretation planes

The orientation of each plane of the object is derived from two non-parallel lines in the plane. The orientation of these lines is known from the first step. The position of the plane in space is derived from the known position of an object point in the plane. If there is no known point

available (which is the case for the first plane to be computed) the distance to the projection centre is set to 1, thus defining the scale of the model. Image points are computed from the intersections of image lines. Rays corresponding to image points are intersected with the object plane to find the coplanar object points. The planes have to be processed in an order that allows the computation of the position of a plane from previously computed point positions.

5 Conclusions

Image line measurements have advantages over points for applications of photogrammetry where the objects show edges or contours, such as architectural photogrammetry. Mathematical models for the adjustment of image line observations for both a multi-image approach and a single image approach are presented. The parameterisation of the polyhedral object model chosen for the line-photogrammetric bundle adjustment is free of singularities, and facilitates the incorporation of a priori object information. The adjustment and the reconstruction from line measurements in a single image fully rely on this type of information. In this case the adjustment does not involve object parameters. Therefore, the adjustment can be performed even when there is insufficient information for a reconstruction. However, the quality of the object model is more difficult to assess due to the additional step for the object reconstruction. Camera parameters can be added to both models, allowing self-calibration.

Future work will be directed towards an integration of the two approaches. The single image approach is suitable for statistical testing of geometric constraints and line observations during interactive modelling, and for approximate value computation. The line-photogrammetric bundle adjustment is then applied as a final step in which all available information is processed; line observations and constraints are tested, and the precision of the object model is assessed.

References

Braun, C., (1994): Interpretation and correction of single line drawings for the reconstruction of objects in space. ISPRS Commission III, Munich, Vol. 2357, pp. 85-90

Bräuer-Burchardt, C., Voss, K., (1999): Monocular 3D-reconstruktion of buildings. In: Girod B, Niemann H and Seidel HP (edts.): VMV '99, Infix, 1999, pp. 109-116

Burns, J.B., Hanson, A.R., Riseman, E.M., (1986): Extracting Straight Lines. IEEE Transactions on Pattern Analysis and Machine Intelligence, Vol. 8 (4), pp. 425-455

Debevec, P.E., Taylor, C.J., Malik, J., (1996): Modeling and rendering architecture from photographs: a hybrid geometry- and image-based approach. SIGGRAPH'96, Annual Conference Series New Orleans, pp. 11-20

Ermes, P., Heuvel, F.A. van den, Vosselman, G., (1999): A Photogrammetric Measurement Method using CSG Models. International Archives of Photogrammetry and Remote Sensing, Vol. 32 (5W11), pp. 36-42

Lang, F., Förstner, W., (1996): 3D-city modeling with a digital one-eye stereo system. International Archives of Photogrammetry and Remote Sensing, Vol. 31 (B4), pp. 261-265

Fryer, J.G., 1996. “Camera calibration”. In: Close-range photogrammetry and machine vision, K.B. Atkinson (ed.), Whittles Publishing, ISBN 1-870325-46-X, pp. 156-179

Gülch, E., (1995): Line photogrammetry: a tool for precise localization of 3D points and lines in automated object reconstruction. Integrating Photogrammetric Techniques with Scene Analysis and Machine Vision II, Orlando, Vol. 2486 pp. 2-12

Heuvel, F.A. van den, (1998a): Vanishing point detection for architectural photogrammetry. International archives of photogrammetry and remote sensing, Vol. 32 part 5 pp. 652-659

Heuvel, F.A. van den, (1998b): 3D reconstruction from a single image using geometric constraints. ISPRS Journal of Photogrammetry and Remote Sensing, Vol.53, No.6, pp. 354-368

Heuvel, F.A. van den, (1999a): A Line-photogrammetric mathematical model for the reconstruction of polyhedral objects. Videometrics VI, 28-29 Jan. 99, San Jose, Proceedings of SPIE, Vol. 3641 pp. 60-71

Heuvel, F.A. van den, (1999b): Estimation of interior orientation parameters from constraints on line measurements in a single image. International archives of photogrammetry and remote sensing, Vol. 32 (5W11), pp. 81-88

Karras, G.E., Petsa, E., (1999): Metric information from uncalibrated single images. Proceedings XVII CIPA Symposium October 99, IAPRS Vol. ?, Recife/Olinda, Brazil

Mulawa, D.C., Mikhail, E.M., (1988): Photogrammetric treatment of linear features. IAPRS, Vol. 27 (Part B10), pp. 383-393

Patias, P., Petsa, E., Streilein, A., (1995): Digital Line Photogrammetry. IGP Bericht 252, ETH Zürich

Schwermann, R., (1995): Geradengestuetzte Bildorientierung in der Nahbereichs-photogrammetrie. Veroeffentlichung des Geodetischen Institutes der RWTH Aachen, Vol. 52

Shufelt, J.A., (1999): Performance evaluation and analysis of monocular building extraction from aerial imagery. IEEE transactions on pattern analysis and machine intelligence, Vol. 21 (4), pp. 311-326

Streilein, A. (1998): Digitale Photogrammetrie und CAAD. Dissertation Nr. 12897, ETH Zuerich, 160p.

Stylianidis, E., Patias, P., (1999): Semi-automatic "interest line" extraction in close-range images. International Archives of Photogrammetry and Remote Sensing, Vol. 32 (5W11), pp. 237-242

Williamson, J.R., Brill, M.H., (1990): Dimensional analysis through perspective - a reference manual. ASPRS, ISBN 0-8403-5673

Zielinski, H., (1993): Object Reconstruction with Digital Line Photogrammetry. Dissertation Royal Institute of Technology, Sweden

2.8

Object reconstruction from a single architectural image taken with an uncalibrated camera[1]

[1] Reference: Heuvel, F.A. van den, 2001. **Object reconstruction from a single architectural image taken with an uncalibrated camera**. Photogrammetrie Fernerkundung Geoinformation, J. Albertz (ed.), No. 4, DGPF / E.Schweizerbart'sche Verlagsbuchhandlung, Stuttgart, pp. 247-260.

Object reconstruction from a single architectural image taken with an uncalibrated camera

Frank A. van den Heuvel

Delft University of Technology
'Faculty of Civil Engineering and Geosciences
Thijsseweg 11, 2629 JA Delft, The Netherlands

Abstract

This paper reports on a line-photogrammetric approach for modelling architectural objects using a single image. For the estimation of the object model parameters a least-squares bundle adjustment is developed. In addition to the manually derived image line observations several constraints on the object parameters are incorporated in the adjustment. Coplanarity, parallelism, and perpendicularity are examples of these constraints. The constraints improve the quality of the estimated object parameters and reduce the number of image line observations required. This paper concentrates on the extreme case where the number of images required for reconstruction is reduced to one.
The interior orientation parameters of the single image are determined in a separate least-squares adjustment. The mathematical model of this adjustment is based on parallelism and perpendicularity constraints on image line observations that are extracted using a line-growing algorithm. These constraints result from a vanishing point detection procedure. With successful vanishing point detection the determination of the parameters of the interior orientation does not require manual interaction.
As an example, the approach is applied for the reconstruction of part of a demolished building using a single image from the Meydenbauer archives. The interior orientation of the image was unknown. It is concluded that the approach is very suitable for this type of imagery and results in a partial reconstruction of which the precision is assessed.

1 Introduction

The research reported in this paper concentrates on object modelling in architectural photogrammetry. The main goal is to exploit the characteristics of this application in order to allow object modelling from a minimum number of images, and assess the quality of the resulting object model. The latter is especially important when redundancy is low which is even more likely to occur when only a single image is used. However, in architectural photogrammetry sufficient object information can generally be inferred from the image for an estimation of the object model parameters with considerable redundancy. This holds true, even for reconstruction from a single image, as is illustrated by the example presented in section 4.

The main characteristic of the application is the availability of object information that results from knowledge or assumptions on the construction of the building. The object information applied in the approach presented in this paper is split into three groups:

1. Object edges are straight. When lens distortion is absent, straight object edges result in straight line features in the image. Especially in architectural photogrammetry line features show advantages over point features for measurement (Streilein, 1998; van den Heuvel, 2000). Therefore, only line features are used as photogrammetric observations.
2. Object faces are planar. In fact, this type of object information relates to the previous type as the intersection of two planar faces leads to a straight edge. This object

information implies that a polyhedral boundary representation or B-rep is a suitable type of representation for the object at hand. In this representation the object edges and faces intersect in the object points. To ensure a valid B-rep, object constraints are used that force the points into the planes.

3. Object shape constraints. The main constraints used are:
   - Parallelism of object edges and faces
   - Perpendicularity of object edges and faces
   - Coplanarity of object points and faces
   - Symmetry of object edges

Control points, i.e. object points with known co-ordinates, are not required, other than a minimum set for defining a co-ordinate system. It is possible to include known distances between two points or between two parallel planes.

The use of a priori object information as outlined above distinguishes this approach from other ones. Here, the term line-photogrammetry is applied because the line features in the images are the observations. However, there is no explicit parameterisation for the edges in object space as in many other line-photogrammetric approaches (Mulawa & Mikhail, 1988; Zielinski, 1993; Patias et al., 1995; Schwermann, 1995). The main reasons for not using object line parameters are the large number of object constraints required for a valid B-rep, in combination with the complexity of the formulation of these and other object constraints.

Assumptions on the shape of the building are applied in the reconstruction in the form of weighted constraints. The need for object constraints also results from the use of a polyhedral B-rep for model representation. The so-called point-in-plane constraint (section 4.1) ensures planar faces. Other methods refrain from the use of shape constraints and therefore these methods require multiple images (Streilein, 1998) or an image sequence (Pollefeys et al., 2000).

Object reconstruction from measurements in a single image is frequently investigated by researchers from the computer vision community (Bräuer-Burchardt & Voss, 1999; Guillou et al., 2000; Jelinek & Taylor, 1999; Liebowitz et al., 1999; Sturm & Maybank, 1999), and less in the photogrammetric community (Williamson & Brill, 1990; Braun, 1994; Karras & Petsa, 1999). The International Committee for Architectural Photogrammetry (CIPA) established a task group on the topic (CIPA-TG2, 2001). All methods use at least parallelism and perpendicularity information of edges in object space. Sometimes edge detectors are used to extract the line features in the image. However, manual interaction is often required, especially for the extraction of edges needed for object reconstruction. It is beyond the scope of this paper to discuss the differences between the various approaches. The main difference of the approach presented in this paper and approaches found in the literature is the application of a rigorous least-squares adjustment for the parameter estimation for the camera calibration as well as for the object reconstruction. This adjustment facilitates error propagation and simplifies the assessment of the quality of the results.

The line-photogrammetric bundle adjustment for multiple images was developed a few years ago (van den Heuvel, 1999a). The application of this bundle adjustment to line observations in a single image is new. For single image bundle adjustment the approximate value computation for the object parameters needs special attention (section 4.2). The main reason is that the parameters cannot be approximated by forward intersection with two or more images. Furthermore, new object shape constraints are implemented.

Previous research on single image object reconstruction concentrated on the adjustment of condition equations that contain no object parameters (van den Heuvel, 1998b). Object reconstruction (i.e. the computation of the parameters of the object model) was done in a

separate step using the adjusted image line observations and object constraints. This approach does not result in a unique solution for the object model in all cases. Another disadvantage is that error propagation is cumbersome due to the separate object reconstruction step. Therefore, the quality of the object model cannot be assessed as with a weighted bundle adjustment with parameters. Furthermore, the object constraints in the form of condition equations on the line observations are complex for many types of constraints. However, its advantage is that approximate values for object parameters are not required.

The rest of this paper is structured as follows. Section 2 gives an overview of the method. The camera calibration from a single image is presented in section 3, and the object reconstruction in section 4. The method is applied to a scanned reproduction from the Meydenbauer archives. The results are discussed in sections 0 and 4.3. Conclusions are drawn in section 5.

2 Overview of the method

The developed method for object reconstruction from a single image with unknown interior orientation consists of two main steps (Figure 1). The first step is a highly automated procedure for the least-squares estimation of the interior orientation parameters including lens distortion.

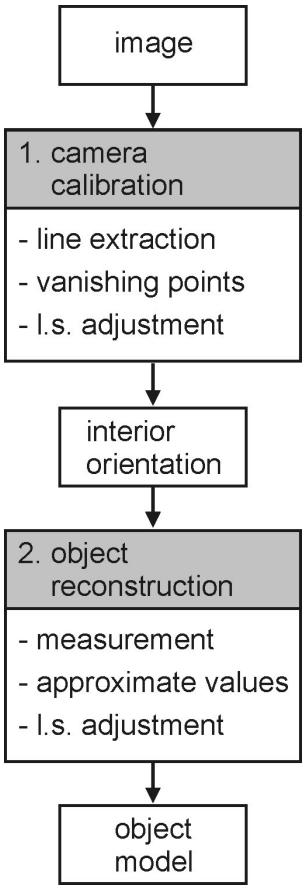

Figure 1: Overview of the procedure for single image object reconstruction

The mathematical model is built from parallelism and perpendicularity object constraints on straight edges in the image. The edges are extracted using a line-growing algorithm. The

constraints result from a vanishing point detection procedure that also does not require manual interaction.

In the second step manual measurements are required to extract edges in the image that correspond to object edges. Furthermore, object information such as topology and shape constraints is to be inferred from the image. After computation of approximate values, a bundle adjustment is used to adjust the line observations and estimate the parameters of the object model, and the exterior orientation. Interior orientation parameters from the first step are not estimated in the latter adjustment because high correlations with the exterior orientation parameters would deteriorate the solution, and is even likely to prohibit convergence of the iterative procedure. Furthermore, it is not expected that the precision of the interior orientation parameters can be improved in the second step, assuming a correct constraint specification by the vanishing point detection procedure. The types of object constraints used in the first step are also used in the second step, supplemented with other types of object constraints such as symmetry constraints. However, the image line observations are different in both steps.

3 Camera calibration

In the first step of the procedure the interior orientation parameters of the single image are determined from edges extracted using image processing. Section 3.1 deals with the edge extraction and the representation of an edge in the mathematical model. In section 3.2 the vanishing point detection method is discussed. This can be regarded as a procedure for grouping edges that have the same orientation in space. This information is used for the formulation of condition equations that build the mathematical model. The estimation of the interior orientation parameters using this model is discussed in section 3.3.

3.1 From edge extraction to observations

In the approach presented here, lines in the image plane serve as observations in the mathematical models, and not points as in conventional photogrammetry. The method for line extraction is briefly discussed in the next section. The parameterisation of the image lines and the options for the stochastic model are presented in the sections thereafter.

3.1.1 Edge extraction by line-growing

Edges are automatically extracted by applying a line-growing algorithm that is summarised as follows. The line-growing process starts at seed points in the image where the gradient is above a pre-set threshold. The algorithm searches in the direction indicated by the gradient for pixels that sufficiently match the seed point pixel in gradient strength and orientation. The neighbouring pixels that match the criteria are added to the pixels of the line. A line is fitted to the gathered pixels and the growing process is continued. When no more pixels can be added to the line, the resulting fitted line - specified by its endpoints - is checked against a pre-set minimum line length. The number and length of extracted straight image lines depends on the parameters such as the minimum gradient strength and the minimum line length.

For the estimation of the interior orientation parameters only lines extracted with this line-growing algorithm are used. No manual measurements are required.

3.1.2 The interpretation plane

A straight line in the image can be parameterised in several ways. Although two parameters suffice for the representation of an image line, the four image co-ordinates (x, y) of the end

points are used here. This guarantees a singularity-free representation, and simplifies the formulation of the stochastic model.

Like a point in the image is associated with a ray in space, a line in the image is associated with a plane in space. This plane is called the interpretation plane (Figure 2).

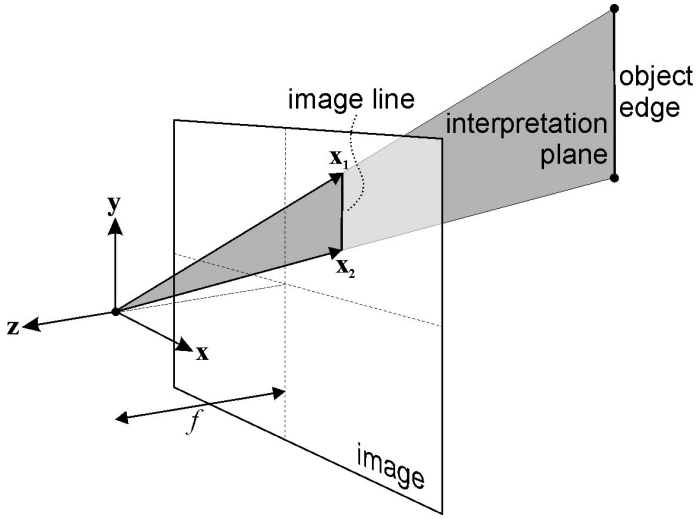

Figure 2: A line in the image and its associated interpretation plane

Assume a perfect central projection with the principal point in the centre of the image, and focal distance f. The orientation of the interpretation plane is defined by its normal vector ($\mathbf{n}$) that is constructed from the two vectors from the projection centre to the endpoints of the line ($\mathbf{x}$):

$$\mathbf{n} = \mathbf{x}_1 \times \mathbf{x}_2, \text{ with: } \mathbf{x} = (x, y, -f) \tag{1}$$

The calibration procedure is started with a rough approximation for the focal length.

3.1.3 The stochastic model

The stochastic model plays an important role in the quality assessment of the parameters estimated by a weighted least-squares adjustment. To set up the covariance matrix ($\mathbf{Q}$) of the observations two options have been implemented:

The variances of the co-ordinates of the endpoints decrease linearly with the length of the line in pixels.

The variance is constant for all endpoint co-ordinates.
The first model is designed for lines extracted using an edge detection approach. The second model is used for lines that are extracted manually by measurement of their endpoints. For the tests described in this paper only the latter model is applied.

3.1.4 Example

Figure 3 shows the image that is used to illustrate the methods presented in this paper. It is a low-resolution scan (1200 $\times$ 865 pixels) of a reproduction of a photograph by Albrecht Meydenbauer taken in the year 1911. It depicts a building in the historical centre of Berlin called “Kommandantur”. This building no longer exists like many other buildings in the historical centre. There is a need for reconstruction using the photographs from the Meydenbauer archives such as this one (Wiedeman et al., 2000). In Figure 3 (right) the lines extracted using the line-growing algorithm presented in section 3.1.1 are overlayed with the

image. The extraction was limited to the part of the image that contains the building. 223 lines were extracted with the minimum line length set to 40 pixels.

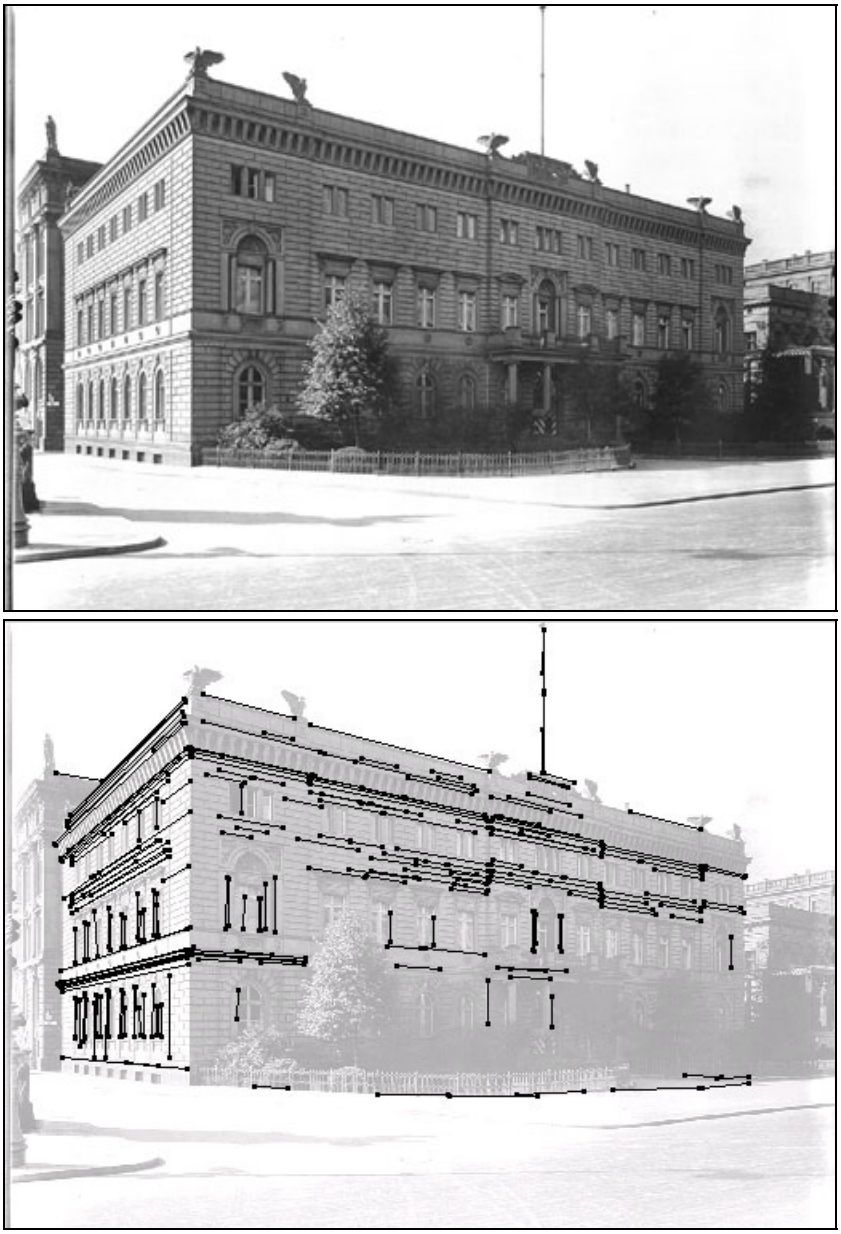

Figure 3: The Meydenbauer image (left) and the automatically extracted image lines (right).

3.2 Vanishing point detection

When straight image lines have been extracted the parameters of interior orientation are determined by applying two types of object constraints. First, parallelism assumptions of object edges are applied. Second, perpendicularity is used of the three major object orientations defined by three groups of parallel edges. When lens distortion is absent, the projections of object edges that are parallel intersect in a point in the image called the vanishing point (Figure 4). With the detection of a vanishing point the parallelism of the related object edges is assumed.

The method for vanishing point detection was designed to make use of the assumption of perpendicularity between the three main object orientations (van den Heuvel, 1998a). However, when principal point and effective focal length are unknown only parallelism assumptions can be used in the vanishing point detection procedure. Projections of parallel object edges intersect in a vanishing point independent of the location of the principal point or the focal length. The perpendicularity assumption is introduced to allow the estimation of the interior orientation parameters (section 3.3).

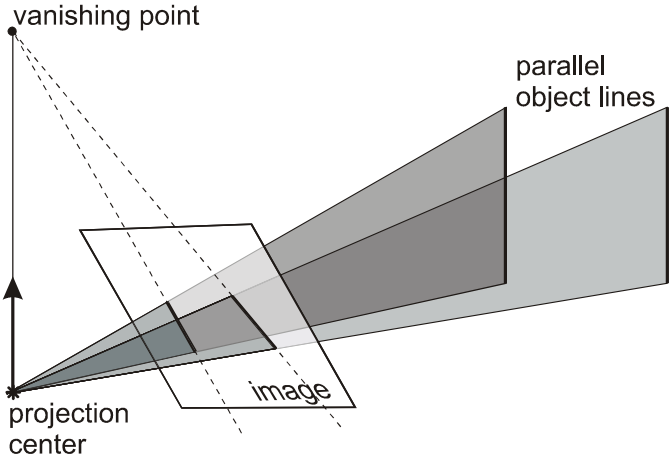

Figure 4: Vanishing point as the intersection of the projections of parallel lines in object space

3.2.1 Intersection of three interpretation planes

The method for vanishing point detection is based on the statistical testing of the intersection hypotheses of combinations of three image lines, or rather the intersection of the three interpretation planes associated with these lines. The intersection constraint can be written as the determinant of the matrix built from the three normal vectors ($\mathbf{n}$) of the interpretation planes $i, j,$ and k:

$$\left[\mathbf{n}^i, \mathbf{n}^j, \mathbf{n}^k\right] = \det\left(\mathbf{n}^i, \mathbf{n}^j, \mathbf{n}^k\right) = 0 \tag{2}$$

In case the lines do not (perfectly) intersect this constraint will result in a misclosure (m):

$$\left[\mathbf{n}^i, \mathbf{n}^j, \mathbf{n}^k\right] = m \tag{3}$$

The hypothesis of interpretation plane intersection is tested with the normalised misclosure relative to a critical value (cv):

$$\left|\frac{m}{\sigma_m}\right| < cv \tag{4}$$

The standard deviation of the misclosure (σ_m) is computed from the covariance matrix of the image co-ordinates ($\mathbf{Q}$) (section 3.1.3):

$$\sigma_m{}^2 = \mathbf{b}^{\mathrm{T}}\mathbf{Q}\,\mathbf{b} \tag{5}$$

with $\mathbf{b}$ the vector of partial derivatives. The part of $\mathbf{b}$ for image point a can be written as:

$$\mathbf{b}^a = \frac{\partial m}{\partial \mathbf{n}^i}\frac{\partial \mathbf{n}^i}{\partial \mathbf{x}^a} \tag{6}$$

3.2.2 The procedure for vanishing point detection

The procedure for the detection of the vanishing points is summarised as follows:

- The longest of all available image lines is chosen as the first line of the vanishing point.
- The test values of all combinations of this longest line and two other image lines are computed according to (4).
- Lines are clustered using the results of the testing. This usually results in several clusters that often have a large number of lines in common.
- For the largest clusters an adjustment is set up, based on all (independent) constraints in the cluster and a line error hypothesis is tested for each line.
- Rejected lines are removed from the clusters and the adjustment is repeated until all remaining lines are accepted.
- The cluster with the largest number of lines is selected as the first vanishing point cluster.

The procedure is repeated with the remaining (non-clustered) lines to detect the other two vanishing points. More details on this procedure are found in (van den Heuvel, 1998a).

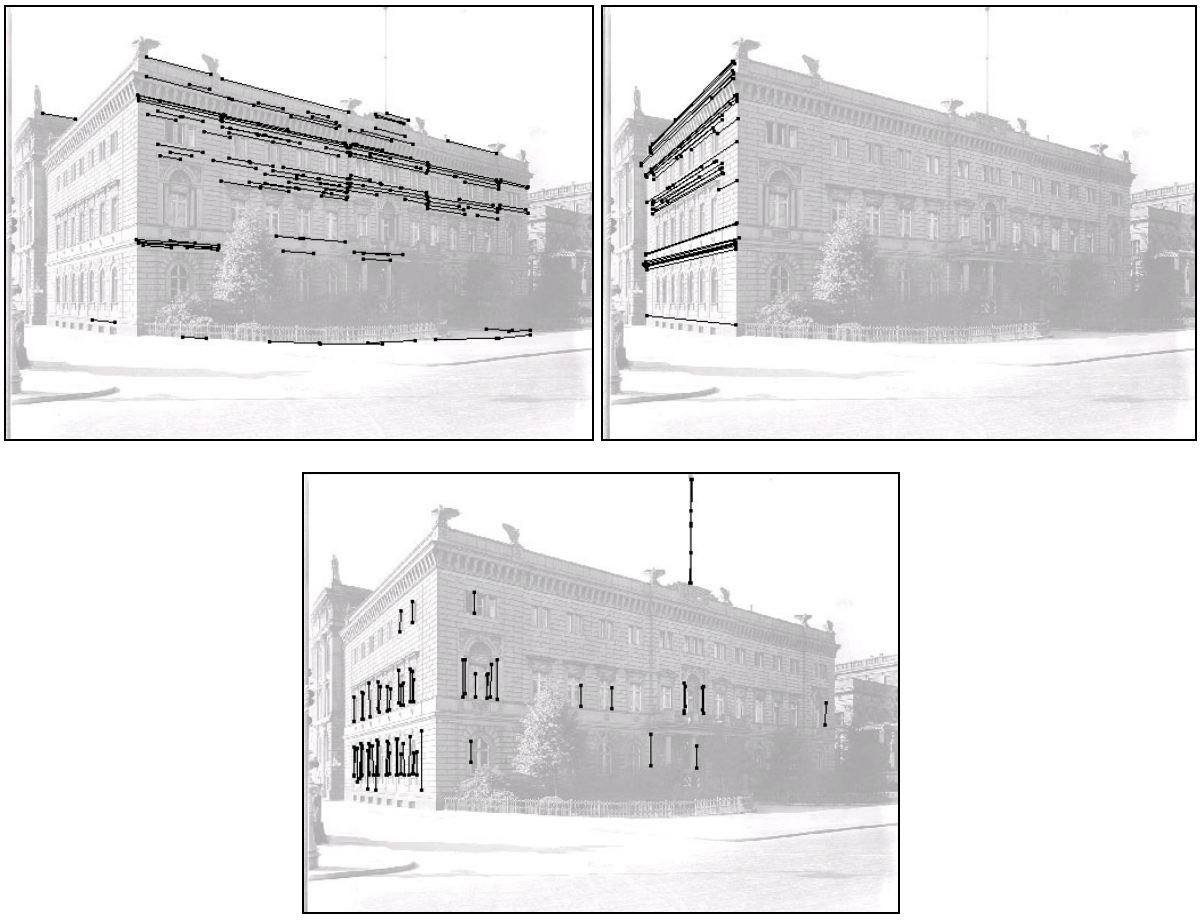

Figure 5: Result of detection of three vanishing points.

3.2.3 Example

The result of the vanishing point detection procedure applied to the extracted lines of the Meydenbauer image is shown in Figure 5. The left most image corresponds to the first vanishing point and contains the longest line (264 pixels). A few lines of this vanishing point

do not correspond to object edges with the same orientation, but were not removed. All extracted lines were assigned to one of the three vanishing points. The number of lines of the first, second, and third vanishing point is respectively 117, 42, and 64. Note that the third vanishing point is at infinity in the image plane. In other words, the image is in a two-point perspective (Williamson & Brill, 1990). In the current implementation, the interior orientation parameters are input to the procedure. It has been verified that the vanishing point detection is not affected by a change in these parameters. With an a priori standard deviation of 1 pixel (constant value for the endpoint co-ordinates of an image line) the estimated variance factor of the adjustment of all parallelism constraints is 0.576.

3.3 Interior orientation parameter estimation

3.3.1 The mathematical model with parameters

To build the mathematical model for the least-squares parameter estimation two types of constraints are applied, i.e. parallelism and perpendicularity constraints. The constraints are specified automatically using the vanishing point detection algorithm described in the previous section. There, only the parallelism constraint is used and the mathematical model does not contain parameters. Now the model is extended with the interior orientation parameters and (1) becomes:

$$\mathbf{x} = \begin{pmatrix} x - x_o - k_1(x - x_o)r^2 \\ y - y_o - k_1(y - y_o)r^2 \\ -f \end{pmatrix} \tag{7}$$

with:
f : effective focal length
x_o , y_o : co-ordinates of the principal point
k_1 : radial lens distortion parameter

$$r^2 = (x - x_o)^2 + (y - y_o)^2$$

If required, lens distortion can be modelled more extensively.
The perpendicularity constraints involve the interpretation plane normals of four lines, consisting of two perpendicular sets (1 and 2) of two lines that are parallel in object space. This constraint can be written as:

$$\left(\mathbf{n}_1^i \times \mathbf{n}_1^j\right) \cdot \left(\mathbf{n}_2^k \times \mathbf{n}_2^l\right) = 0 \tag{8}$$

In order to set up a least-squares adjustment, equations (2) and (8) are linearised with respect to both the parameters and the observations. This leads to a so-called mixed model (Teunissen, 1999):

$$\mathbf{B}^{\mathrm{T}}\, E\{\mathbf{y}\} = \mathbf{A}\,\mathbf{x} \;;\; \mathbf{Q}_{\mathrm{y}} \tag{9}$$

with:

$E\{.\}$	expectation operator
$\mathbf{y}$	vector of the observations (observed – computed)
$\mathbf{x}$	vector of corrections to the parameters
$\mathbf{A}, \mathbf{B}$	design matrices (partial derivatives)
$\mathbf{Q}_{\mathrm{y}}$	covariance matrix of the observations (section 3.1.3)

The constraints used for the model (9) have to be independent in order to compute the solution as described in the next section. This is achieved in the following way. First, for each object orientation the two image lines are selected that best define the object orientation. Let us call these two lines the *base* lines. Then for each of the *n*-2 remaining

lines of that orientation, parallelism constraints are set up according to (2) (*n* is the number of lines in a cluster of parallel lines). Each constraint involves three lines, two of which are the base lines. In this way, *n*-2 independent constraints are defined for each object orientation. Second, only three perpendicularity constraints are set up according to (8). These constraints are formulated using the base lines of each object orientation that have been used for the parallelism constraints as well. The three independent constraints define perpendicularity between three combinations of two object axes (*XY, YZ,* and *ZX*).

3.3.2 Parameter estimation

The system of equations (9) is transformed into a standard system of observations equations by the introduction of the so-called derived observations ($\mathbf{z}$):

$$E\{\mathbf{z}\} = \mathbf{A}\,\mathbf{x}\,;\ \mathbf{Q}_{\mathbf{z}} \tag{10}$$

with:

$$E\{\mathbf{z}\} = \mathbf{B}^{\mathrm{T}}\,E\{\mathbf{y}\}\,;\quad \mathbf{Q}_{\mathbf{z}} = \mathbf{B}^{\mathrm{T}}\mathbf{Q}_{\mathbf{y}}\mathbf{B}$$

The full covariance matrix $\mathbf{Q}_{\mathbf{z}}$ of the derived observations results from propagation of the diagonal covariance matrix of the observations $\mathbf{Q}_{\mathbf{y}}$. The least-squares solution to the system (10) is well known:

$$\hat{\mathbf{x}} = (\mathbf{A}^{\mathrm{T}}\,\mathbf{Q}_{\mathbf{z}}^{-1}\,\mathbf{A}\,)^{-1}\,\mathbf{A}^{\mathrm{T}}\,\mathbf{Q}_{\mathbf{z}}^{-1}\,\mathbf{z} \tag{11}$$

The computation of the residuals of the original observations is explained in (van den Heuvel, 1999a).

Since the mathematical model is non-linear in both the parameters and the observations, the iteration process needs special attention. Convergence has to be obtained by iterating in the parameters first to avoid a solution that is biased by the approximate values of the parameters. After that, iteration in both the parameters and the observations leads to a set of parameters and observations that fit the model.

In the presence of considerable lens distortion the solution is to be computed in two steps (van den Heuvel, 1999b). In the first step the lens distortion is estimated. In the second step the interior orientation parameters are estimated using the results of the first step.

Interior orientation (pixels)	Original observations		Adjusted observations	
	Parameter	St. deviation	Parameter	St. deviation
Principal point *y*	586	12.3	601	12.8
Focal length	1131	10.7	1152	9.4

Table 1. Estimated interior orientation parameters (in pixels).

3.3.3 Example

The procedure for estimation of interior orientation parameters is applied to the Meydenbauer image, using the results of the vanishing point detection for the specification of the parallelism and the three perpendicularity constraints. Trying to estimate the three interior orientation parameters using the adjusted observations from the vanishing point detection, a correlation of close to a 100% between the focal length and the principal point *x* co-ordinate appears. This is due to the two-point perspective (section 3.2.3). Fixing the principal point in the middle of the image in column direction, the estimation of the two remaining parameters converged in five iteration steps. Convergence is not sensitive to the approximate values. For both parameters starting values were more than 150 pixels different from the solution presented in Table 1. Formal standard deviations are based on the a priori

standard deviation of 1 pixel for the endpoints of the image lines. Using the original line observations the estimated variance factor is 0.588 (218 degrees of freedom), close to the value of the vanishing point adjustment (section 3.2.3). Estimation of the radial lens distortion parameter k_1 results in a value of 0.30×10^{-3}, only 2.5 times its standard deviation.

4 Object reconstruction

The line-photogrammetric bundle adjustment was developed for the estimation of the parameters of a boundary representation from the image line observations of multiple images (van den Heuvel, 1999a). In this section, first an overview of the line-photogrammetric bundle adjustment is presented (section 4.1). Approximate values for the parameters are required because of the non-linearity of the model. Especially in the case of single image processing, approximate value computation needs special attention (section 4.2). The application of the presented bundle adjustment procedure on the Meydenbauer image is discussed in section 4.3.

4.1 Overview of the line-photogrammetric bundle adjustment

The mathematical model of the line-photogrammetric bundle adjustment relates the image line observations (section 3.1) to the parameters of the object model. Although usually only the co-ordinates of the points represent the geometry of a B-rep, in this approach also the parameters of the object planes are incorporated in the model. The reason is the simplicity of the formulation of geometric object constraints. Two groups of parameters can be distinguished:

1. Object model parameters (points and planes)
2. Exterior orientation parameters

Interior orientation parameters are not estimated and have to be determined beforehand (section 3).

Over-parameterisation is applied in combination with constraints to avoid singularities inherent in some parameter choices. Four parameters are used for each object plane, i.e. the normal vector of the plane and a position parameter. The position is the perpendicular distance of the plane to the origin. A constraint is used to force the normal vector length to 1. The rotation matrix of exterior orientation is parameterised by four parameters of a quaternion. The length of the vector of the quaternion elements is constrained to 1.

The basic relation of the line-photogrammetric bundle adjustment is the point-in-plane constraint. First, there is an *object point in interpretation plane* constraint (Figure 6). Second, the *object point in object plane* constraint is formulated that is very similar to the first one.

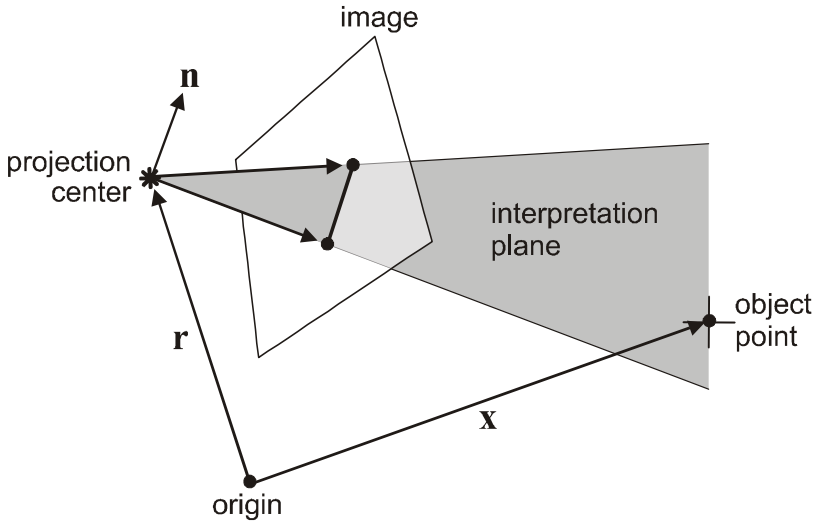

Figure 6: Object point in interpretation plane.

For the object point in interpretation plane constraint the normal vector to the interpretation plane is rotated into the object co-ordinate system by applying the rotation matrix of exterior orientation ($\mathbf{R}$), and (1) becomes for line i:

$$\mathbf{n}_i = \mathbf{R} \quad (\mathbf{x}_1 \times \mathbf{x}_2) \tag{12}$$

With the vector to the projection centre ($\mathbf{r}$) and the vector to the object point ($\mathbf{x}$), the object point in interpretation plane constraint for image line i is written as:

$$\mathbf{n}_i \cdot \mathbf{x} \; - \; \mathbf{n}_i \cdot \mathbf{r} \; = 0 \tag{13}$$

With the (signed) plane position parameter l_i the object point in object plane constraint becomes:

$$\mathbf{n}_i \cdot \mathbf{x} \; - \; l_i = 0 \tag{14}$$

Equation (13) relates the observations to the object point parameters, while (14) relates the object point parameters to the object plane parameters. With more than three points in a plane, the latter constraint enforces coplanarity of object points. It is important to note that object faces that are coplanar share the same plane parameters.

A number of object shape constraints have been implemented that will not be discussed in detail here. In (Hrabacek & van den Heuvel, 2000) the formulation of most of them is presented:

- Points: coplanarity (14), distance between two points, and co-ordinates of control points.
- Lines: parallelogram, symmetry constraint (section 4.2).
- Planes: angle, parallelism, and distance between two planes.

All constraints have been implemented as weighted observation equations. This has the advantage that realistic weights can be used for instance for the shape constraints, and thus uncertainty in the constraints is taken into account. Furthermore, constraints do not have to be independent. The relations that build the mathematical model are non-linear in the parameters and non-linear in the observations. The least-squares solution to this model is discussed in section 3.3.

4.2 Measurement and approximate value computation

Only a few of the lines extracted using the line-growing algorithm described in section 3.1.1 are suitable for object modelling and correspond to the edges of the building façades. Many other edges show poor contrast in the image. Therefore, manual interaction is required. Not only for line measurement, but also for the specification of the topology of the B-rep, and object shape constraints.

Approximate values of all parameters have to be available to set up the linearised observation equations. With the image line measurements, object topology, and shape constraints available, the approximate values are computed in the following order:

1. Exterior orientation parameters
2. Object point parameters
3. Object plane parameters

The last two steps are then repeated until no new parameters are computed.

In the first step the direct solution that is presented in (van den Heuvel, 1997) is used to compute the exterior orientation parameters based on the measurement of 4 points (or lines) that correspond to a rectangle in object space. For the second step all available linear equations that contain the object co-ordinates are gathered. These equations relate to the following constraints:

- *Point in interpretation plane.* The exterior orientation parameters as well as the interpretation plane normals are regarded as constants and thus equation (13) becomes linear in the object point co-ordinates.
- *Point in object plane.* When step 2 is repeated, object plane parameters are available from step 3. Regarding them as constants, also (14) becomes linear in the co-ordinates.
- *Control point co-ordinates.* These linear equations are of the form $\mathbf{x} - \mathbf{x}_c = 0$, where $\mathbf{x}_c$ is the vector of control point co-ordinates.
- *Parallelogram equations.* These equations relate the four corner points of a parallelogram in object space, and have the simple linear form $(\mathbf{x}_1 - \mathbf{x}_2) - (\mathbf{x}_3 - \mathbf{x}_4) = 0$.

Apart from the control point constraint, all these constraints are independent of the choice of the co-ordinate system. This is not the case for the symmetry constraint. This constraint has the same form as the parallelogram constraint, apart from the fact that the vector $(\mathbf{x}_3 - \mathbf{x}_4)$ is mirrored with respect to the XY, YZ, or XZ plane. In the current implementation this constraint is only used for object reconstruction.

The computation of approximate plane parameters is based on (14) only. Then the point co-ordinates from step 2 are treated as constants, and (14) is linear in the plane parameters. Plane parameters can be computed when the co-ordinates of at least three points are available. Similarly, object point co-ordinates can be computed when three or more planes are available. These planes can be interpretation planes as well as object planes.

4.3 Example

In Figure 7 the manual measurements are overlayed on the Meydenbauer image. Closed polygons are measured through their corner points of which the image co-ordinates are stored. Each corner point is an endpoint of at least two individual image lines and relates to one point in object space. Each closed polygon is associated with an object face and each image line with an interpretation plane (Figure 2). In this way the topology of the polyhedral B-rep is specified together with the relations between image measurements and object points.

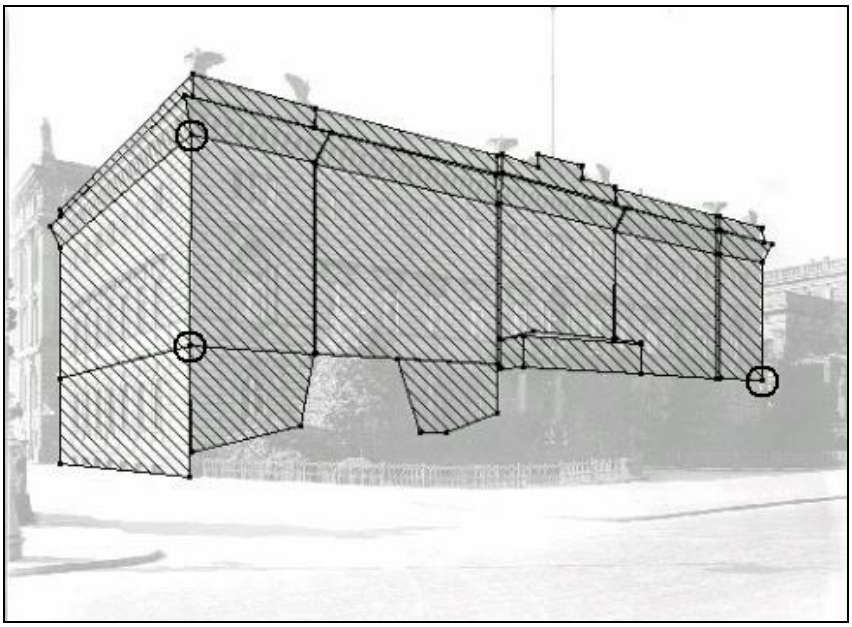

Figure 7: Manually measured points, lines, and faces.

In this approach only object parts (parts of building faces) that are visible in the image are reconstructed. As in the multiple image example described in (van den Heuvel, 1999a), some occluded object parts can be reconstructed with only one image also, but this has not been investigated here.

	Number	Parameters	Equations	Precision (σ)
Image lines	100	-	152	$\mathbf{Q}_z$ (10)
Distance	1	-	1 (control)	0.1m
Object points	76	228	6 (control)	0.001m
Object planes	12	48	12	10^{-6}
Image orientation	1	7	1	10^{-6}
Point-in-plane	-	-	123	0.01m
Plane angles	11	-	11	0.1deg
Parallelogram	15	-	45	0.01m
Symmetry	6	-	18	0.01m
Totals		283	369	

Table 2. Parameters and equations in the adjustment.

In Table 2 the number of image and object features and the related number of parameters and equations are listed. This table also contains an overview of the object constraints that were inferred from the image and the precision that was assigned to them. Although 29 faces were specified, for only 12 planes there are parameters in the model. In this way coplanarity of several faces is enforced.
In Figure 7 three control points are indicated by circles. Six co-ordinates of these points have been fixed. The distance between the two points on the front of the building was derived from a cadastral map (41.39m), and processed as a distance constraint. In this way the co-ordinate system is fixed with minimum control. The estimated variance factor is 0.535 with an a priori standard deviation for the endpoints of the lines of 1 pixel (86 degrees of freedom). The formal standard deviations of the object co-ordinates (excluding control points) are summarised in Table 3. Note that the standard deviations depend on the control point choice, and the applied shape constraints and their weights. The largest residual to an endpoint co-ordinate is 2.0 pixel. Reliability parameters are not computed. However, it is noted that for some observations there is no redundancy and thus reliability is absent.

Standard deviation (m)	X	Y	Z
Average	0.080	0.095	0.055
Minimum	0.013	0.008	0.022
Maximum	0.135	0.384	0.127

Table 3. Precision of the object points (σ in meter).

The estimated exterior orientation parameters show that the photograph was taken at a distance of 34.5m (σ 0.17m) from the corner of the building at a height of 1.78m (σ 0.08m) above the lowest (ground) points of the object model.

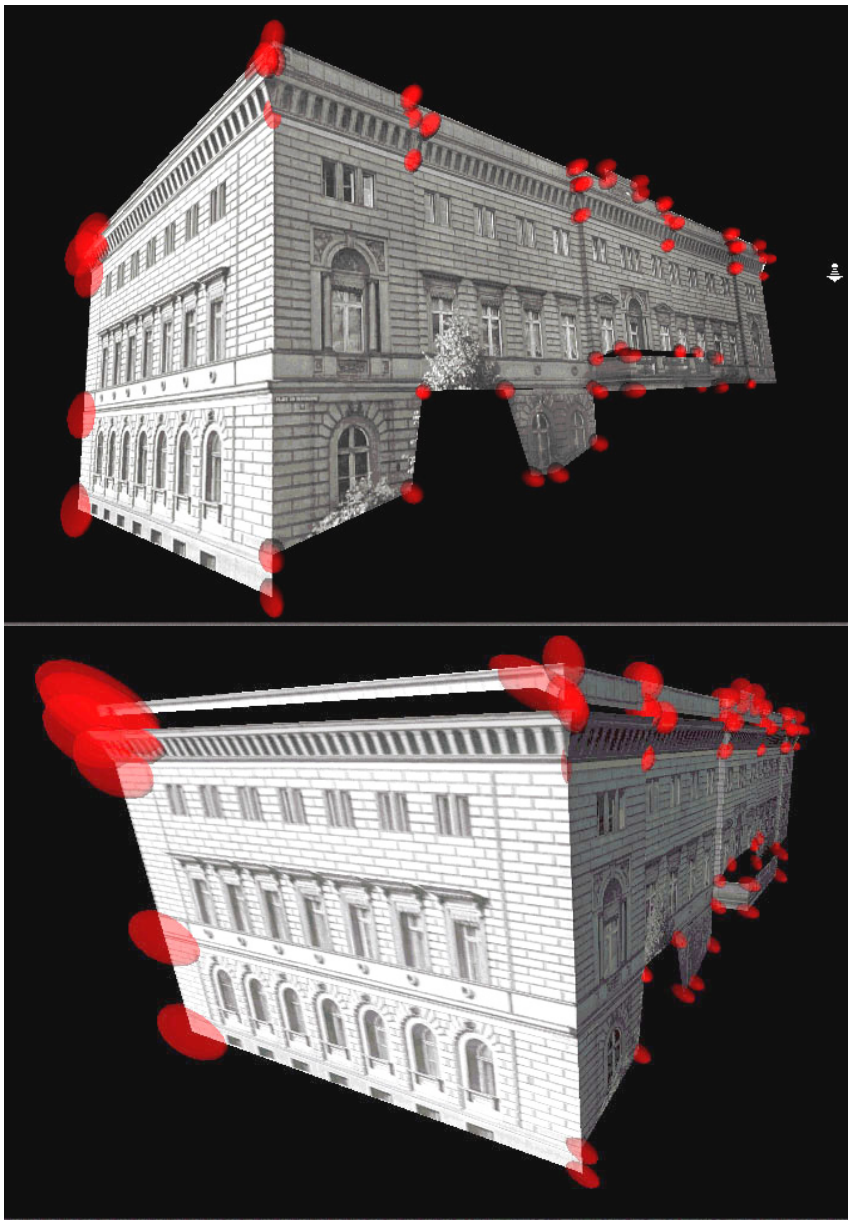

Figure 8: Two views on the texture mapped model (error ellipsoids enlarged with a factor 10).

The determined boundary representation is converted to VRML-format with textures derived from the image by a rectification for each face. Two views of the resulting object model are shown in Figure 8. The error ellipsoids are enlarged with a factor 10 relative to the model

and visualise the covariance matrices of the object points. The model is available on the Internet (Meydenbauer, 2001).

5 Conclusions

Methods are presented for camera calibration and object reconstruction from line measurements in a single image. No manual measurements are required for the procedure for camera calibration when vanishing point detection is successful. The parameters of interior orientation are estimated in a least-squares adjustment from image lines extracted by line-growing. The mathematical model is built with independent constraint equations that are non-linear in the parameters as well as in the observations. A vanishing point detection algorithm infers the constraints. Applying the calibration procedure to a historical image of a building, the position of the principal point could not be estimated in column direction due to the two-point perspective. Estimation in row direction showed the principal point is more than 150 pixels below the centre of the image. The formal precision of the principal point is 12 pixels (1σ). The precision of the focal length is 11 pixels.

In the procedure for object reconstruction the point and plane parameters of a B-rep are estimated together with the parameters of exterior orientation using a line-photogrammetric bundle adjustment. The adjustment model is built from point-in-plane constraint equations that relate the image line measurements to the object co-ordinates, and the co-ordinates to the plane parameters. Furthermore, the topology of the B-rep and several object shape constraints are incorporated in the least-squares adjustment through weighted observation equations. Adjustment of 100 image lines (standard deviation of endpoints set to 1 pixel) and 32 shape constraints resulted in the 3D co-ordinates of 76 points with an average precision between 5 and 10 cm.

The paper demonstrates the potential of a single image with unknown interior and exterior orientations for partial reconstruction of architectural objects. All parameters involved are estimated using a least-squares adjustment that facilitates the assessment of their precision. If available, more images with possibly different interior orientations can be included in the adjustment. A more complete reconstruction of higher quality will be the result.

References

IAPRS - International Archives of Photogrammetry and Remote Sensing

Braun, C., 1994: Interpretation and correction of single line drawings for the reconstruction of objects in space. ISPRS Commission III, Munich, Vol. 2357, 85-90.

Bräuer-Burchardt, Ch., Voss, K., 1999: Monocular 3D-reconstruction of buildings. In: Girod B, Niemann H and Seidel HP (edts.): VMV '99, Infix, 109-116.

CIPA-TG2, 2001: http://info.uibk.ac.at/sci-org/cipa/tg2_1.html, accessed May 14, 2001.

Guillou, E., Meneveaux, D., Maisel, E., Bouatouch, K., 2000: Using vanishing points for camera calibration and coarse 3D reconstruction from a single image. The visual computer, Springer, Vol. 16, 396-410.

Heuvel, F.A. van den, 1997: Exterior Orientation using Coplanar Parallel Lines. 10th Scandinavian Conference on Image Analysis, Lappeenranta, 71-78.

Heuvel, F.A. van den, 1998a: Vanishing point detection for architectural photogrammetry. IAPRS, Hakodate, Vol. 32 part 5, 652-659.

Heuvel, F.A. van den, 1998b: 3D reconstruction from a single image using geometric constraints. ISPRS Journal of Photogrammetry and Remote Sensing, Vol.53, No.6, 354-368.

Heuvel, F.A. van den, 1999a: A Line-photogrammetric mathematical model for the reconstruction of polyhedral objects. Videometrics VI, 28-29 Jan. 99, San Jose, Proceedings of SPIE, Vol. 3641, 60-71.

Heuvel, F.A. van den, 1999b: Estimation of interior orientation parameters from constraints on line measurements in a single image. IAPRS, Thessaloniki, Vol. 32 (5W11), 81-88.
Heuvel, F.A. van den, 2000: Line-photogrammetry and its application for reconstruction from a single image. 19. Jahrestagung der DGPF, Essen, Publikationen der Deutschen Gesellschaft für Photogrammetrie und Fernerkundung, Vol. 8, 255-263.
Hrabacek, J., Heuvel, F.A. van den, 2000: Weighted geometric object constraints integrated in a line-photogrammetric bundle adjustment. IAPRS, Amsterdam, Vol. 33, Part B5, 380-387.
Jelinek, D., Taylor, C.J., 1999: Reconstruction of linearly parameterized models from single images with a camera of unknown focal length. CVPR'99, Fort Collins, Vol. 2, 346-352.
Karras, G.E., Petsa, E., 1999: Metric information from uncalibrated single images. Proceedings XVII CIPA Symposium October 99, Recife/Olinda, Brazil.
Liebowitz, D., Criminisi, A., Zisserman, A., 1999: Creating architectural models from images. Eurographics'99, Vol. 18, 3, 39-50.
Meydenbauer, 2001: http://www.geo.tudelft.nl/frs/architec/Meydenbauer/, accessed May 14, 2001.
Mulawa, D.C., Mikhail, E.M., 1988: Photogrammetric treatment of linear features. IAPRS, Vol. 27, part B10, 383-393.
Patias, P., Petsa, E., Streilein, A., 1995: Digital Line Photogrammetry. IGP Bericht 252, ETH Zürich.
Pollefeys, M., Koch, R., Vergauwen, M., Gool, L. van, 2000: Automated reconstruction of 3D scenes from sequences of images. ISPRS Journal of Photogrammetry & Remote Sensing, Elsevier, Vol. 55, 4, 251-267.
Schwermann, R., 1995: Geradengestuetzte Bildorientierung in der Nahbereichs-photogrammetrie. Veröffentlichung des Geodetischen Institutes der RWTH Aachen, Vol. 52.
Streilein, A., 1998: Digitale Photogrammetrie und CAAD. Dissertation Nr. 12897, ETH Zuerich.
Sturm, P.F., Maybank, S.J., 1999: A method for interactive 3D reconstruction of piecewise planar objects from single images. BMVC 10th British Machine Vision Conference, Nottingham, England, 265-274.
Teunissen, P.J.G., 1999: Adjustment Theory – an Introduction. Delft University Press, Delft, ISBN 90-407-1974-8.
Wiedemann, A., Hemmleb, M., Albertz, J., 2000: Reconstruction of historical buildings based on images from the Meydenbauer archives. IAPRS, Amsterdam, Vol. 33, part B5, 887-893.
Williamson, J.R., Brill, M.H., 1990: Dimensional analysis through perspective - a reference manual. ASPRS, ISBN 0-8403-5673.
Zielinski, H., 1993: Object Reconstruction with Digital Line Photogrammetry. Dissertation Royal Institute of Technology, Sweden.

2.9

Towards automatic relative orientation for architectural photogrammetry[1]

[1] Reference: Heuvel, F.A. van den, 2002. **Towards automatic relative orientation in architectural photogrammetry.** International archives of photogrammetry and remote sensing (Corfu, Greece), Vol. 34, Part 5, pp 227 – 232.

Towards automatic relative orientation for architectural photogrammetry

Frank A. van den Heuvel

Delft University of Technology
Department of Geodesy
Thijsseweg 11, 2629 JA Delft, The Netherlands

Commission V, WG V/2

ABSTRACT

A major challenge in close-range photogrammetry and computer vision is the automation of model acquisition from imagery. Determining the relative position and orientation of close-range imagery is usually the first step in a procedure for modelling, assuming that the camera has been calibrated beforehand. An essential part of an orientation procedure based on image content is the establishment of correspondence between the images. The problem at hand is to find correspondence between two convergent images and their relative orientation simultaneously and automatically. In computer vision this is called the wide-baseline stereo problem. For the approach presented in this paper, a new feature-based matching procedure is designed that exploits the characteristics of the application by applying generic knowledge of the construction of the building. The procedure relies on rigorous statistical testing of constraints on the observations. The outline of the procedure is presented, as well as the results of experiments. Relative orientation was successfully detected for two images with an angle of 65 degree between the optical axes. It is shown that the procedure is robust with respect to unfavourable characteristics of the application, such as occlusions and repetitive structures in the building facades.

Keywords: relative orientation, wide-baseline stereo, vanishing point detection, feature-based matching, architecture

1 Introduction

Determination of the relative orientation of images is a prerequisite for object modelling. Although relative orientation of two images includes relative position, it however excludes the distance between the images and thus the scale of the model remains undetermined. Camera calibration, i.e. the determination of interior orientation (intrinsic) parameters, is also essential, however, in photogrammetry cameras are usually pre-calibrated. In this paper, the camera is assumed to be calibrated, although imagery of unknown interior orientation can be handled by applying a method for the estimation of interior orientation parameters from vanishing points (van den Heuvel, 1999).

Without using external measurement methods, such as the Global Positioning System (GPS), relative orientation of two images is based on corresponding features in the images. With only two images, we have to rely on point features because there is no information on relative orientation in corresponding image lines. With at least seven corresponding points available, the five parameters of relative orientation (in computer vision; the parameters of the *essential matrix*) can be determined by a direct solution (Förstner, 2000). Automatic relative orientation, therefore, is equivalent to solving the correspondence problem

automatically. This topic has been extensively studied in photogrammetry, especially aerial photogrammetry (Heipke, 1997), and in computer vision (Pritchett and Zisserman, 1998), (Matas et al., 2001).

Our goal is the automatic relative orientation of two widely separated views, i.e. (strongly) convergent imagery. In computer vision this problem is known as *wide-baseline stereo*. Generic knowledge of the architectural application field is applied in the method and this facilitates a robust solution of the correspondence problem. For the method proposed here, prerequisites for the image acquisition are limited to:

- No major image rotation around the optical axis (κ less than 45 degree).
- Image tilt (rotation around x-axis, ω) less than 45 degree.
- Overlap between the two images.

The automatic procedure consists of three main steps (Figure 1). In each step different types of a priori object knowledge, i.e. knowledge on the construction of the building, are applied. Firstly, straight lines are extracted from the two images. This implies that the majority of building edges be assumed straight, and that lens distortion is limited or removed in advanced by resampling the image. Secondly, vanishing points are detected for each image. The building is assumed to be built along three orthogonal axes. The detection of at least two vanishing points related to these object orientations, results in an ambiguous orientation of the image relative to the building, and a set of edges of which the object orientation is known. In the third and last step, edges are intersected to points in image space, and finally point correspondence and relative orientation are detected simultaneously. The paper concentrates on this last step that relies on the assumption of planar facades, in which the object points recede.

The remainder of the paper is structured as follows. After discussing related research in the next section, the developed procedure for automatic relative orientation is described in section 3. In section 4, results from several experiments are analysed. Conclusions are drawn in section 5.

2 Related research

In aerial photogrammetry the automatic relative orientation (as a part of automatic triangulation) is commonly available in digital photogrammetric workstations (Heipke, 1997). More and more, external measurement devices – usually an integration of GPS and INS – are used. For a range of aerial applications they make triangulation even superfluous. External measurement of image orientation is also used in close-range photogrammetry (Teller, 2001). For finding correspondence from the image itself, usually a feature-based matching technique is applied at different levels of the image pyramid. Wang (Wang, 1998) presents a structural matching method that requires an image pyramid. The method is applied to aerial images, as well as to terrestrial images of a building. In (Habib and Kelley, 2001) a robust feature-based method is described that does not require an image pyramid. This method is based on a Hough transform and relaxes the required quality of orientation angles to the order of 10 degrees. The method presented in this paper is feature-based, but differs from the approaches of Habib & Kelly and Wang in the more extensive use of generic object knowledge. Choices for parameterisation required by the Hough transform are avoided by the use of rigorous statistical testing of constraints on the observations. Furthermore, the proposed method does not rely on image segmentation required by structural matching.

In the use of image sequences without external measurement of camera orientation, approximate orientation values of an image are derived from the determined values of

previous images in the sequence. In these *short-baseline* applications area-based matching is a commonly used technique to establish image correspondence at sub-pixel level (Pollefeys et al., 2000). With increasing baseline length, feature-based matching techniques are expected to be more successful, especially in applications where occlusions are frequent. The general approach of a feature-based matching procedure is described by Matas (Matas et al., 2001) and can be summarised as follows:

- Features that have viewpoint invariant characteristics are extracted in both images.
- Based on their characteristics, the features of two images are compared and a list of possible matches is established.
- A geometrically consistent set of matches is searched for. In this step the RANSAC algorithm is often applied (Fischler and Bolles, 1981).

Examples of this general approach are found in (Pritchett and Zisserman, 1998), (Tuytelaars and Van Gool, 2000), and (Baumberg, 2000). The method presented in this paper differs in the following aspects:

- Object information, as described in the previous section, is exploited at several stages. This makes the method robust, but limits its applicability to images of buildings or man-made structures with similar characteristics.
- The features are straight image lines – projections of the building edges – and not (invariant) image regions as in the approaches above. The intersection of two straight lines and a number of viewpoint invariant characteristics are used in the matching.
- Vanishing point detection is applied for the initial estimation of the orientation of the images relative to the object. Apart from a remaining ambiguity in the rotation matrix of each image, the vanishing point detection reduces the relative orientation problem to a relative position problem.
- The emphasis is on the use of geometric constraints for the selection of the set of correct matches, and not on photometric information. In the current application the photometric content in a region around for instance the corner of a window strongly depends on the viewpoint of the image as a result of discontinuities in the facade of the building. Furthermore, buildings often show repetitive patterns, such as identical windows. As a result, photometry is not a strong clue for detecting correct matches.
- Clustering is based on the results of statistical testing of geometric constraints. All possible combinations of tentative matches are tested. The number of tests is of the order m^2 (with m the number of tentative matches). This is in contrast to the RANSAC procedure in which the selection of the final solution is based on a randomly chosen subset of possible matches. In the method presented here the computational burden is reduced to an acceptable level by keeping the number of possible matches low.

3 Procedure for relative orientation

As stated in the introduction, the procedure consists of three steps. An overview is depicted in Figure 1. If an uncalibrated camera is used, an additional step that follows the vanishing point detection is required (van den Heuvel, 1999). The detection of the three main vanishing points is more reliable in case of a calibrated camera. Then, after the detection of the first vanishing point, the search space for the other two is reduced considerably (van den Heuvel, 1998). In order not to complicate the description of the procedure, use of a calibrated camera is assumed.

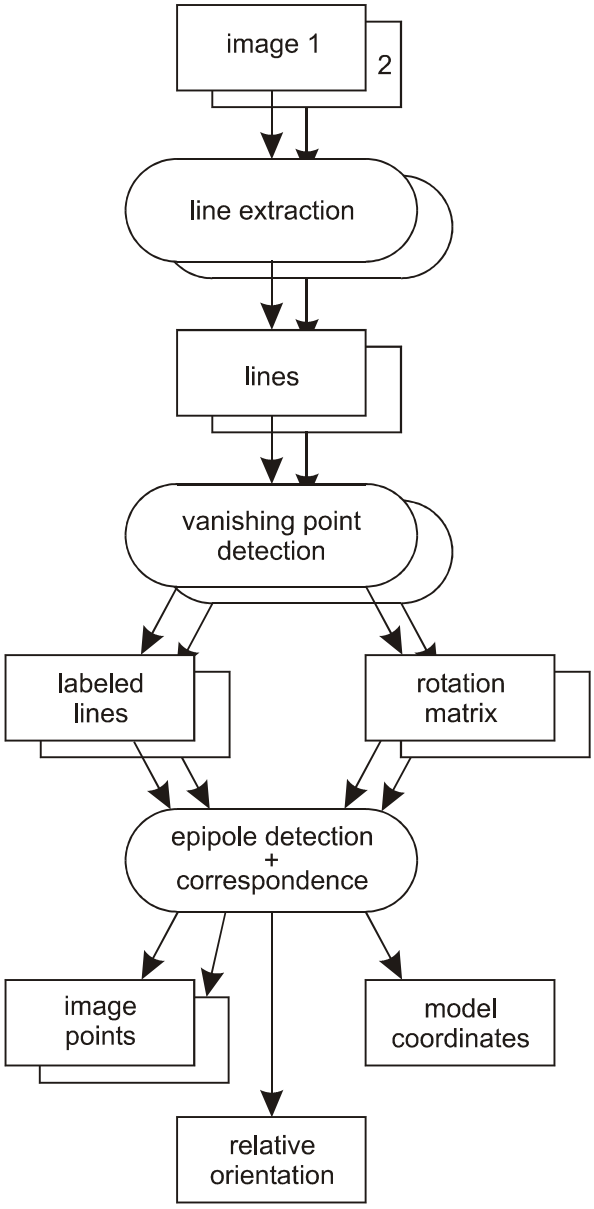

Figure 1. Overview of the procedure

3.1 Line feature extraction

Edges are automatically extracted by applying a line-growing algorithm (van den Heuvel, 2001). The coordinates of the endpoints represent the image lines. The interpretation plane is the plane in which both the image line and object edge recede (Figure 2). The image coordinates (x,y) are assumed to be corrected for lens and image plane distortions. Then the spatial vector ($\mathbf{x}$) related to an endpoint can be written as:

$$\mathbf{x} = (x, y, -f)\,, \quad f\text{: focal length} \tag{1}$$

The normal to an interpretation plane ($\mathbf{n}$) is computed from the rays ($\mathbf{x}$) to the endpoints of the line:

$$\mathbf{n} = \mathbf{x}_1 \times \mathbf{x}_2 \tag{2}$$

This normal vector plays a major role in the vanishing point detection procedure that is summarised in the next section.

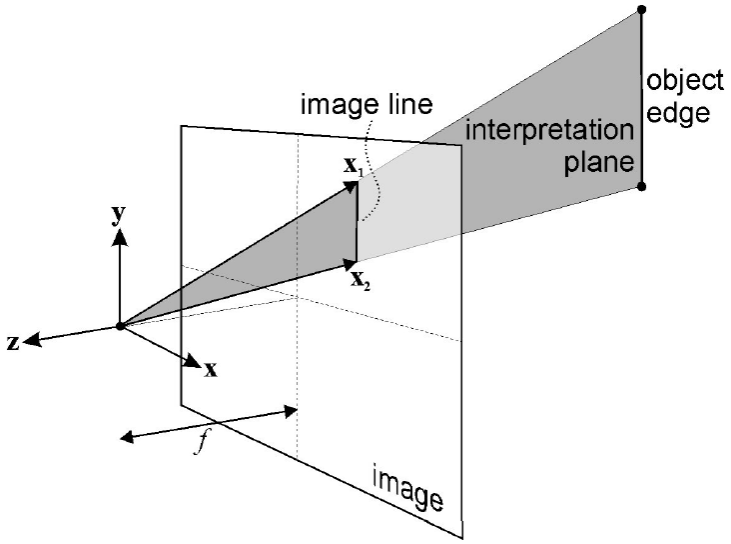

Figure 2: The interpretation plane

3.2 Vanishing point detection and image orientation

The extracted straight lines are input to a vanishing point detection procedure. This procedure starts with the selection of the longest extracted line that is assumed to intersect with other image lines in one of the three main vanishing points. In fact, the procedure is based on the analysis of intersection constraints on interpretation planes and thus does not require the lines to actually intersect in image space. Image lines are grouped, based on accepted statistical tests on the intersection constraint of three interpretation planes:

$$0 = (\mathbf{n}_1 \times \mathbf{n}_2) \cdot \mathbf{n}_3 \tag{3}$$

A complete set of independent constraints is adjusted. The object orientations (**v**) that relates to the vanishing points are computed from the adjusted observations:

$$\mathbf{v} = \mathbf{n}_1 \times \mathbf{n}_2 \tag{4}$$

Here we concentrate on the results, as the procedure has been described in detail in (van den Heuvel, 1998).

As a by-product of the vanishing point detection, the orientation of the image relative to the object is found. The rotation matrix can be constructed when at least two of the three vanishing points – associated with orthogonal object orientations – have been detected (Förstner and Gülch, 1999):

$$\mathbf{R} = (\mathbf{v}_1, \mathbf{v}_2, \mathbf{v}_3) \tag{5}$$

However, this rotation matrix is ambiguous because there is no unique relation between the object orientations (**v**) from the vanishing points and the object coordinate system. To reduce the ambiguity in this rotation matrix it is assumed that the object orientation that is closest to the y-axis of the camera system corresponds to the Z-axis of the object system. Now four options for the rotation matrix remain, corresponding to four 90-degree rotations of the object system around the Z-axis. Note that – up to this ambiguity – the orientation of the images is found by the vanishing point detection, and thus only relative position remains to be determined in order to complete the relative orientation.

In the sequel of the procedure only those image lines are used that have been uniquely grouped to one vanishing point. Especially lines on or near the connecting line between two

vanishing points (a so-called horizon) cannot be uniquely grouped and therefore these lines are not used for the final and main step of the procedure for automatic relative orientation described in the next section.

3.3 Correspondence and relative position

With the orientation of the images relative to the building known, the relative position and correspondence problem shows many similarities with the vanishing point detection problem. The line in space that connects the two projection centres intersects the images in a point that is called the epipole (Figure 3). The spatial orientation associated with a vanishing point is found as the intersection of interpretation planes, while the relative position vector is found as the intersection of epipolar planes. An interpretation plane is constructed from the two endpoints of an image line. An epipolar plane also needs two (corresponding) image points, one from each image. Because of these similarities the procedures for the detection of the epipole is also similar to the one for the vanishing point detection. However, there are some important differences. First, correspondence between the two images is unknown, while in the vanishing point detection an image line links the two endpoints. On the other hand there exist only one epipole (per image), while an image of a building usually shows two or more vanishing points.

Like for the vanishing point detection, statistical tests on the intersection of planes (now epipolar instead of interpretation planes) can be grouped for detecting correspondences that support the same epipole. However, the number of possible correspondences, and consequently the number of statistical tests to evaluate would explode without the use of additional object knowledge. With n points per image, there are n^2 correspondence hypotheses, and thus n^2 possible epipolar planes. As an intersection constraint involves three planes, the number of tests is of the order n^6.

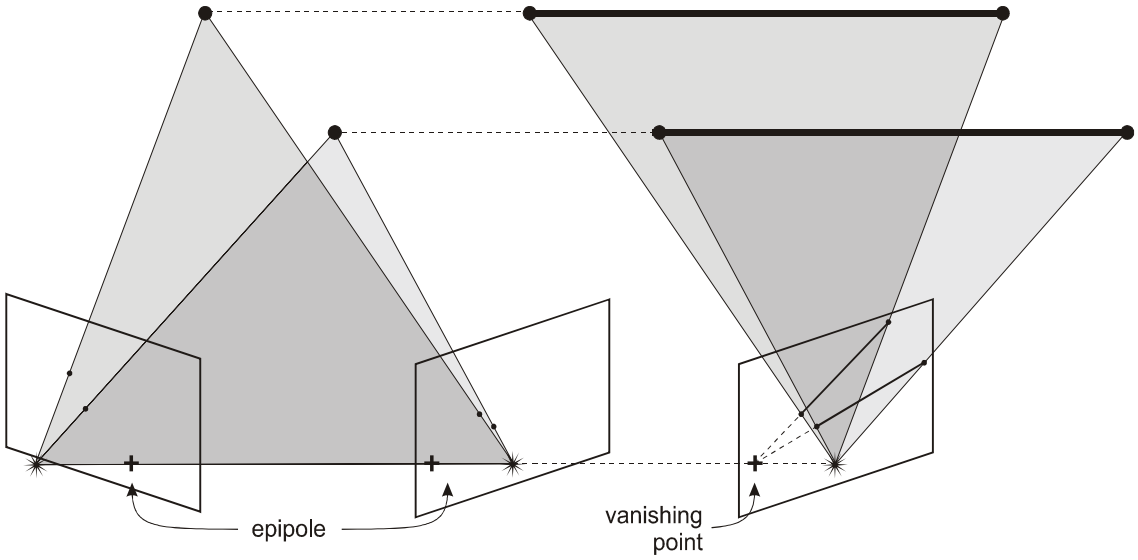

Figure 3 : Two epipolar planes and the epipoles (left), two interpretation planes and the vanishing point (right)

Introducing a new constraint reduces the number of tests to investigate. This constraint on the coplanarity of two object points involves two instead of three correspondences, reducing the order of the number of tests to n^4. Further significant reduction of the number of tests is achieved by computing a number of attributes for each constructed image point. A correspondence hypothesis is only set up when the attributes of the two points match to a sufficient degree.

The procedure for deriving relative position, *epipole detection* in short, consists of the following five steps:

1 Compute points in each image through line intersection.
2 Establish correspondence hypotheses between the computed points.
3 Compute statistical tests for coplanarity of all combinations of two correspondences.
4 Grouping of correspondences based on the test results and epipolar plane intersection constraints.
5 Refinement of grouped correspondences by overall adjustment and testing.

Each step is repeated for each of the four possible permutations of the rotation matrix of the second image. The exterior orientation of the first image determines the object co-ordinate system.

3.3.1 From lines to points

Points are created in each image as intersection of two image lines being projections of edges with a different (perpendicular) orientation in object space. This orientation is determined by the vanishing point detection procedure. Two lines are intersected when an endpoint of a line is within a preset distance (commonly set to 5 pixels) from the other line. Furthermore, the following attributes are computed and registered for each point:

- The orientation of the plane passing through the object point (perpendicular to the orientations of the two intersected lines)
- The type of junction (T-junction or L-junction)
- The orientation of the junction (4 options: Figure 4)
- The ratio of the lengths of the two edges

These attributes are all evaluated in object space, i.e. after projecting the lines onto a plane of which the orientation is known, again through the vanishing point detection.

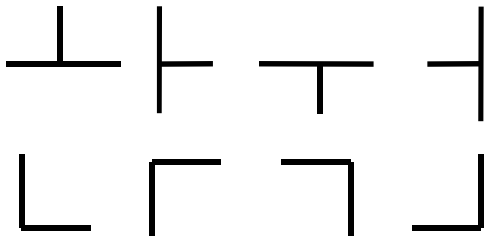

Figure 4: Four T-junctions (top) and four L-junctions

3.3.2 The correspondence hypotheses

In the next step of the procedure a list of possible corresponding image points is set up. A correspondence is added to the list only when the attributes of points have been compared. Both points have to have the same (plane) orientation, the same junction type, and the same junction orientation. The ratio of the line lengths should be similar for both points with a typical maximum difference of 50%. The correspondence search turned out not to be sensitive to this criterion.

The creation of image points, their attributes, and consequently the correspondence hypotheses depend on the current permutation of the rotation matrix of the second image. With each permutation the vanishing point (i.e. object orientation) line labels for X and Y are exchanged.

3.3.3 Statistical testing of coplanarity

With the image orientations known, the epipole is defined by a minimum of only two correspondences (the intersection of the two related epipolar planes; Figure 3).

Furthermore, because each image point is constructed from the intersection of two lines of which the spatial orientation is known from the vanishing point detection, the orientation of the object plane in that point is known. With the epipole derived from the two correspondences, the location of the two object points in model space can be computed by forward intersection, and thus the position of the two parallel planes through those points and the distance between the planes is known. The coplanarity constraint requires this distance to be zero.

For the formulation of the coplanarity constraint the ray of an image point is rotated to the object co-ordinate system. After replacement of equation (1) by

$$\mathbf{x}^i = \mathbf{R}^i (x, y, -f) \tag{6}$$

in which i refers to one of the two images, equations (2) and (4) are used to compute the orientation vector of the epipole ($\mathbf{v}$) from two correspondences. Knowing the epipole, forward intersection results in the distance (d) from the projection centre to an object point. This distance is projected onto the normal $\mathbf{n}_\mathrm{p}$ of the object plane. For image i and correspondence j:

$$\bar{d}^i_j = d^i_j \frac{\mathbf{x}^i \cdot \mathbf{n}_p}{\left| \mathbf{x}^i \right|} \tag{7}$$

Normal $\mathbf{n}_\mathrm{p}$ is a unit vector in the object X or Y direction, dependent on the orientation of the façade. For the formulation of the coplanarity constraints the first image is used (in principle, using the second image would yield identical results). The constraint for coplanarity of the two object points can now be written as:

$$0 = \bar{d}^1_1 - \bar{d}^1_2 \tag{8}$$

The statistical testing of the hypothesis is explained in (van den Heuvel, 1998). The coefficients of the linearised form of equation (8) are derived numerically.

3.3.4 Clustering of correspondences

For all combinations of two possible correspondences the statistical test based on constraint (8) is evaluated. Each test links two correspondences that define an epipole. The clustering procedure aims at grouping of correspondences of which the inter-correspondence tests are accepted, and at the same time support the same epipole. In order to verify the latter, a statistical test is used that is based on the intersection of epipolar planes. This constraint is identical to the intersection of interpretation planes constraint (3).

The clustering procedure includes the following steps:

- For each accepted test (8) it is checked whether one of the two correspondences is present in an existing cluster. If this is not the case, a new cluster is established.
- If a correspondence of an accepted test is present in an existing cluster, the other correspondence becomes a candidate for that cluster.
- The candidate correspondence becomes a member of the cluster if all tests of constraints (3) are accepted. These tests involve three correspondences: the candidate and two correspondences already in the cluster.

This procedure is repeated as long as new clusters are created. The result is that overlap between clusters can be considerable. Many of these clusters contain a set of correct correspondences with minor differences. The clusters that contain more than a minimum number of correspondences are analysed in more detail by applying an integrated adjustment of all constraints.

3.3.5 Overall adjustment and testing

The clustering procedure results in groups of correspondences that support the same relative orientation, while the related object points are expected to recede in the same object plane. An overall adjustment is set up for all clusters with more than a minimum number of correspondences. The functional model contains n-1 condition equations for coplanarity (equation (8), n is the number of correspondences), and n-2 condition equations for intersection of epipolar planes (equation (3)). A set of independent equations results. The adjusted epipole is computed from adjusted observations. Two different types of statistical tests are applied. First an overall test or Fisher test is applied. The second test examines the alternative hypothesis of an error in a single correspondence. If such a test is rejected, the correspondence is removed from the cluster and the model is built again. This iterative testing procedure stops if all correspondence tests are accepted. The cluster with the largest number of correspondences of which no correspondence tests are rejected is selected. This cluster is expected to contain corresponding image points of which the related object points are in (or near to) a plane. More details on the statistical testing can be found in (van den Heuvel, 1998).

3.3.6 Towards automatic reconstruction

Apart from the primary cluster detected as described above, other clusters can also contain correct correspondences of which the related object points are in a different plane. In order to detect such clusters, all clusters that meet the following two requirements are incorporated in the overall adjustment:

1. The cluster does not have a correspondence (nor an image point) in common with the primary cluster.
2. The correspondences of the cluster confirm the epipole of the primary cluster.

For all correspondences – those of the primary as well as those of the clusters selected by the criteria above – the epipolar plane intersection constraints are set up. Of course, the coplanarity constraints are only applied to correspondences of the same cluster.
With the integrated adjustment of more than only the primary cluster, there is not only additional evidence gathered for the epipole, but at the same time different object planes are being detected. Preliminary faces can be created by a bounding box around the object points of a cluster. Object planes are then to be intersected to find the edges of the building. The detection of object planes is a by-product of the proposed procedure for automatic relative orientation, but also a first step towards automatic reconstruction. The experiments described in the next section aim at the detection of the primary object plane only.

4 Experimental results

In this section an experiment is discussed in which the procedure for automatic relative orientation is applied to three images of a historic building. The images are taken from ground level with a handheld calibrated digital camera (1536x1024 pixels). They were taken from the south-south-west (SSW), south-east (SE), and east (E) approximately (Figure 5). The number of extracted straight lines can be found in Table 1.

Figure 5: The three images (labelled SSW, SE, and E)

The a priori precision of the endpoints of the lines was set to 1 pixel standard deviation in the vanishing point and the epipole detection. The "vanishing lines" are the lines that were uniquely grouped to one of the three vanishing points. These lines are displayed in Figure 6. Especially near the horizon line of image SE a considerable number of lines is lost because the vanishing point detection cannot distinguish between the left and right façade. As a result, for this image most of the intersection points are created in the upper part of the facades. Some statistics of the epipole detection are listed in Table 2.

	SSW	SE	E
# lines	339	457	202
# vanishing lines	286	276	143
# intersection points	164	78	30

Table 1: Numbers of extracted lines and points

	SSW - SE	SE – E
# correspondence hypotheses	1109	144
# coplanarity tests # accepted tests	182899 15825	3308 1102
# clusters max. # points in a cluster	5638 16	424 9
# clusters accepted max. # points in a cluster	97 15	85 7
Fisher-test / critical value	4.4	1.0
Deviation manually measured	1.7 deg	1.6 deg

Table 2: Statistics of the epipole detection

The detected correspondences are displayed in Figure 7. Note that for the first image pair only those corresponding points are detected that are on the central part of the façade because this part is in a different plane from the rest of the façade. In fact, all possible correspondences are detected. However, looking at the location of the image points in detail, two corresponding points are often not at exactly the same location on the building. The reason is that many edges border occlusions. When there are several points created close together – which often is the case in the corners of the windows – the statistical testing cannot distinguish between different possible correspondences. Indeed, many of the accepted clusters are very similar in the correspondences they contain and their Fisher-test. Furthermore, as a result of a large number of "imperfect" correspondences (the image points are not projections of exactly the same point on the building), the overall Fisher-test is often rejected, while all tests of individual correspondences are accepted. The lack of "perfect" correspondences reduces the precision that can be reached. To check this precision, relative orientation of both pairs was determined through least-squares adjustment of 20 manually measured points. The deviations in the orientation of the detected epipole are below 2 degree (Table 2). As expected the computational burden of the

proposed method is considerable. For the first pair computational time is in the order of 10 minutes on a modern PC.

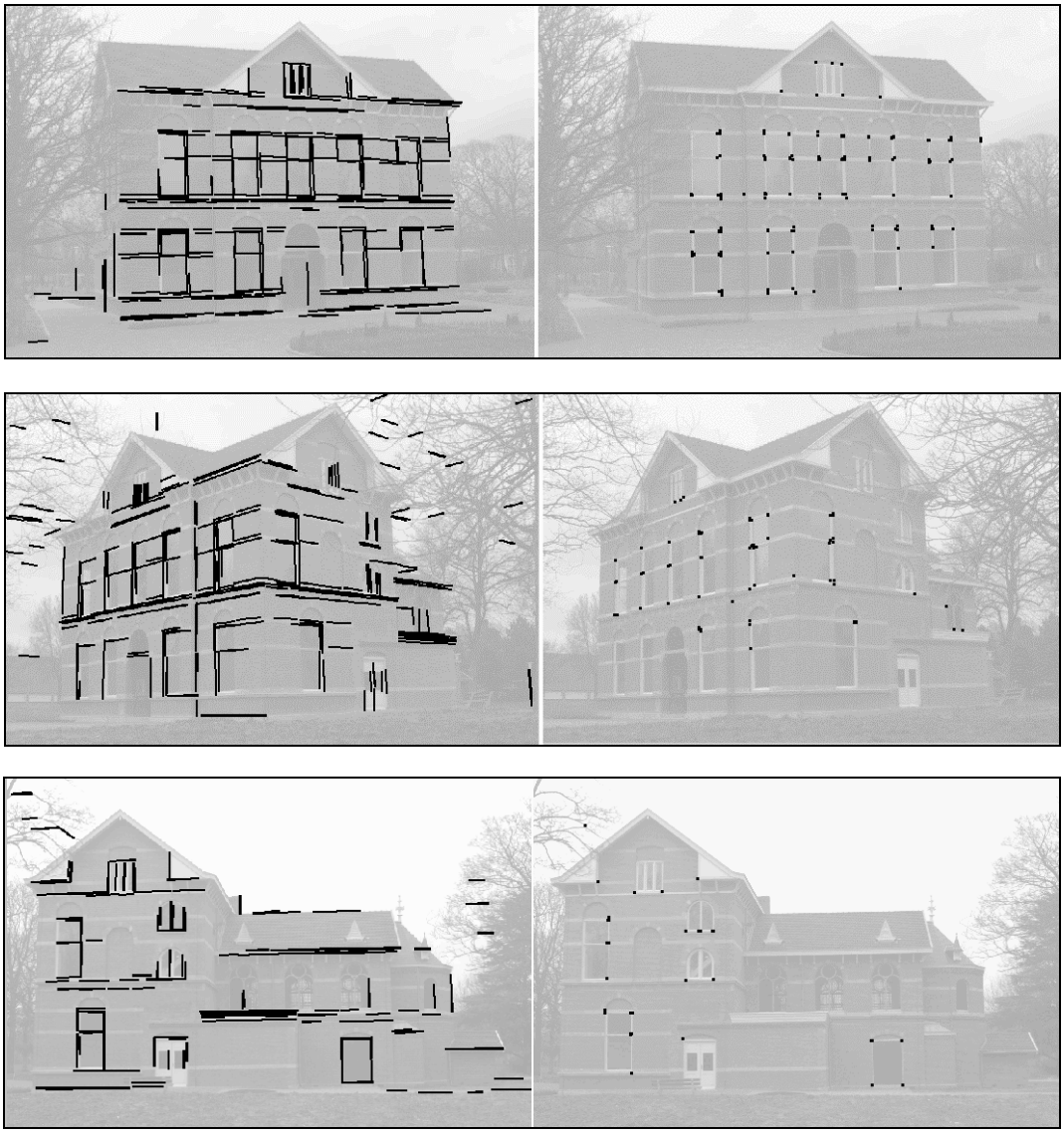

Figure 6: The lines grouped to vanishing points (left) and created points (right).

5 Conclusions

A new method for automatic relative orientation has been presented. It relies on the extraction of straight image lines and their vanishing point labelling. Vanishing point detection is a crucial step in the procedure that results in an ambiguous orientation of the images relative to the building. The epipole detection shows many similarities with the vanishing point detection. Both are based on clustering of rigorous statistical tests and adjustment of constraints on the observations.

Experiments show that relative orientation can be detected successfully between two images with an angle of 65 degree between the optical axes (see section 4, first image pair), while the difference in orientation with a manually determined relative position vector was less than 2 degree.

The proposed method can be regarded as a first step towards automated reconstruction because the model coordinates of the corresponding points and the parameters of the plane in which they recede become available as a by-product.

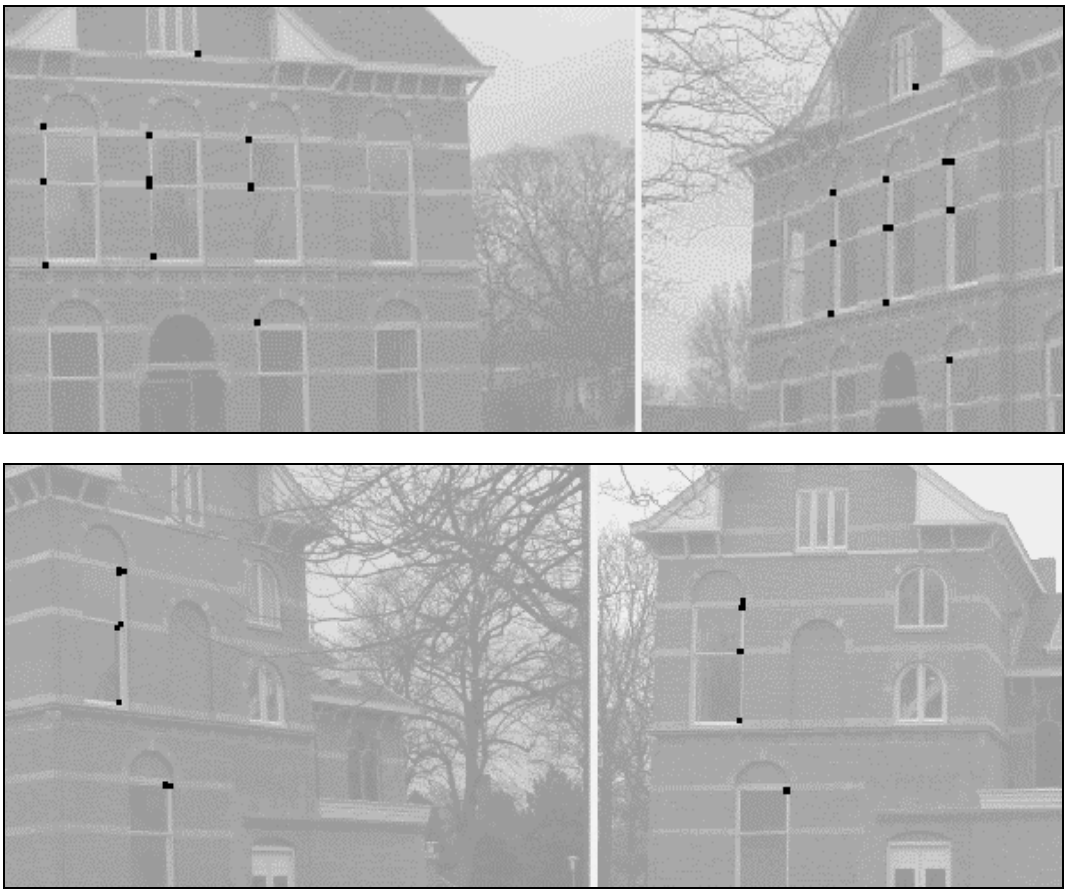

Figure 7: The detected correspondences of both pairs.

References

Baumberg, A., 2000. Reliable feature matching across widely separated views, Computer Vision & Pattern Recognition (CVPR) 2000, pp. 774-781.

Fischler, M.A. and Bolles, R.C., 1981. Random sample consensus: a paradigm for model fitting with applications to image analysis and automated cartography. Communications of the ACM, Vol. 24(6), pp. 381-395.

Förstner, W., 2000. New orientation procedures. International Archives of Photogrammetry and Remote Sensing, Vol. 33 part 3, pp. 297-304.

Förstner, W. and Gülch, E., 1999. Automatic orientation and recognition in highly structured scenes. J. of Photo-grammetry and Remote Sensing, Vol. 54, pp. 23-34.

Habib, A. and Kelley, D., 2001. Automatic relative orientation of large scale imager over urban areas using modified iterated Hough transform. J. of Photogrammetry and Remote Sensing, Vol. 56, pp. 29-41.

Heipke, C., 1997. Automation of interior, relative, and absolute orientation. ISPRS J. of Photogrammetry and Remote Sensing, Vol. 52, pp. 1-19.

Heuvel, F.A. van den, 1998. Vanishing point detection for architectural photogrammetry. In: H. Chikatsu and E. Shimizu (Editors). International Archives of Photogrammetry and Remote Sensing, Vol. 32 part 5, pp. 652-659.

Heuvel, F.A. van den, 1999. Estimation of interior orientation parameters from constraints on line measurements in a single image. In: P. Patias (Editor). International Archives of Photogrammetry and Remote Sensing, Vol. 32 part 5W11, pp. 81-88.

Heuvel, F.A. van den, 2001. Object reconstruction from a single architectural image taken with an uncalibrated camera. Photogrammetrie, Fernerkundung, Geoinformation, Vol. 2001(4), pp. 247-260.

Matas, J., Urban, M. and Pajdla, T., 2001. Unifying view for wide-baseline stereo matching. In: B. Likar (Editor), Computer Vision Winter Workshop. Slovenian Pattern Recorgnition Society, pp. 214-222.

Pollefeys, M., Koch, R., Vergauwen, M. and Van Gool, L., 2000. Automated reconstruction of 3D scenes from sequences of images. ISPRS J. of Photogrammetry and Remote Sensing, Vol. 55(4), pp. 251-267.

Pritchett, P. and Zisserman, A., 1998. Wide baseline stereo matching, Sixth International Conference on Computer Vision, pp. 754 -760.

Teller, S., 2001. Scalable, controlled imagery capture in urban environments. Report 825, MIT Laboratory for Computer Science.

Tuytelaars, T. and Van Gool, L., 2000. Wide Baseline Stereo Matching based on Local, Affinely Invariant Regions, British Machine Vision Conference BMVC'2000, pp. 412-425.

Wang, Y., 1998. Principles and applications of structural image matching. ISPRS J. of Photogrammetry and Remote Sensing, Vol. 53, pp. 154-165.

3 Experiments using imagery of the CIPA reference data set

3.1 Introduction

The goal of this chapter is to demonstrate the applicability of the designed methods by applying them to a subset of the images of the CIPA reference data set. This data set was set up by CIPA (*The ICOMOS & ISPRS Committee on Documentation of Cultural Heritage*, the former *International Committee of Architectural Photogrammetry*) in 1999 and consists of images of a historic building, the old city hall of Zurich (Streilein et al., 1999). By processing a selection of images of this data set insight is provided in the applicability of the developed procedures for the three main tasks in architectural photogrammetry: camera calibration, image orientation, and object reconstruction.

The CIPA reference data set consists of two sets of images taken with two different digital cameras. Here, only a subset of the images taken with the Olympus C1400 is used. Due to the manual interaction required for the reconstruction of a structured object model, one of the goals of the research is to use only a minimum number of images in order to make the modelling more efficient. Therefore, only four images taken from the corners of the building are used for reconstruction. For camera calibration five images were used in total (Figure 3). The results were compared with the camera parameters provided in the CIPA reference data set.

In the next section the automatic procedure for camera calibration is presented. This procedure is based on vanishing point detection. In section 3.3 a semi-automatic procedure for image orientation that also relies on vanishing point detection is discussed, as well as a manual procedure. The manual procedure applies single image object reconstruction techniques. The limits of a fully automatic procedure for orientation become apparent in its application to the CIPA data set. Depending on the image configuration, a few image points have to be measured for the successful orientation of more than two images. The procedure for image orientation results in a partial reconstruction of the building. For a full reconstruction manual line measurements are needed. Section 3.4 elaborates on the line-photogrammetric bundle adjustment applied for the reconstruction of the Zurich city hall from line measurements in four images.

Figure 3: The subset of used images. Images 8, 9, 10 (top row), 11, 6, 3, and 16 (bottom). Five images have been used for calibration (images 8, 9, 10, 11, and 6). The images in the bottom row are used for reconstruction.

3.2 Camera calibration

3.2.1 The procedure for camera calibration

The automatic procedure for camera calibration is summarised in the following three steps (Heuvel, 1999a):

1. Extraction of straight image lines
2. Detection of the object orientation of the image lines through vanishing point detection
3. Estimation of camera parameters from parallelism and perpendicularity constraints on image lines

The quality of the estimated parameters is dependent on a correct vanishing point labelling of image lines performed in step 2. With the camera parameters unknown, the automatic detection of the three vanishing points that correspond with edges of the three orthogonal object space orientations is critical. Two factors play a role. They are the unknown lens distortions and missing a priori information for the location of the second and third vanishing point after detection of the previous ones. Lens distortion results in curved projections of straight object edges, and thus hinders the (straight) line detection and prohibits the detected lines intersecting in one point in image space. Unknown focal length and principle point make it impossible to limit the search space after detection of one or two vanishing points. As a result each vanishing point is detected independent of previously detected vanishing points. In conclusion, the chance that the procedure detects the main object orientations decreases when camera parameters are unknown.

A solution could be to manually select one image line for each vanishing point as a start line for the vanishing point detection. The start line is an image line that belongs to the vanishing point to be detected and initiates the search. The chances of correct vanishing point detection would greatly improve, but this will also reduces the level of automation. In order to avoid image interpretation by an operator the procedure below is applied to the CIPA data set. The lens distortion is determined first, followed by the other parameters of the camera model (focal length and principle point). Rough initial values are required for all camera parameters.

1. *Start with vanishing point detection for those images that contain only one façade of the building*. For these images only two vanishing points are to be detected, one for the vertical object orientation, and one for the horizontal object edges. These images are usually close to a so-called one-point perspective (image perpendicular to the façade). The separation of the lines of the two orthogonal horizontal object orientations, that is often problematic, is avoided. This separation is difficult for those lines that are close to the horizon line (line connecting two vanishing points) present in two- or three-point perspective imagery (e.g. images of a corner of a building).
2. If only images with two (presumably orthogonal) façades are available, *only the vanishing point that corresponds to the vertical object orientation is detected* and its lines used for estimation of the lens distortion. This approach assumes limited camera tilt and rotation around the optical axis. A threshold is set with which the angle of the normal of the interpretation plane of the start line, as well as the angle of the detected object orientation with the vertical direction is checked. With the mentioned limitations on the image orientation relative to the building, the image lines of the "vertical" vanishing point can be reliably detected, as the image does not usually contain a part of the lines that connect the "vertical" vanishing point with the two horizontal ones.
3. *Estimate lens distortion* using the detected and labelled lines of at least one but preferably more images. In case 1 two vanishing points are used, in case 2 the

vanishing point of the vertical object orientation is used. In the next steps the estimated lens distortion is applied, i.e. lens distortion is eliminated from the observations.

4. *Detection of three vanishing points*. When this vanishing point detection is not successful, manual interaction is required for the measurement (or selection) of at least two lines for each of the three vanishing points. In principle, the labelling of the detected lines could be performed automatically using the vanishing points known from the manual measurements. This has not been implemented. Three-point perspective imagery is required for the estimation of the focal length and the principle point. An image of the corner of a building is in three-point perspective when camera tilt is present. However, the optical axis is often nearly horizontal and thus a one-point or two-point perspective remains. With near two-point perspective imagery the principle point location in horizontal direction (camera x-axis) cannot be estimated, or only with very low precision.
5. *Estimate focal length and principle point* using the detected and labelled lines of at least one but preferably more images.
6. All images with a correct vanishing point detection and thus line labelling are combined to set up *one least-squares adjustment for the estimation of all camera parameters*.

3.2.2 Camera calibration using the CIPA data set

Image lines are extracted for all the selected images of the CIPA data set. For the line-growing algorithm used for straight line extraction two parameters were set. First the parameter for the minimum gradient strength was selected in such a way that most of the characteristic features of the building – especially the windows – were extracted. The second parameter is the minimum length in pixels of an extracted image line. This parameter was fixed to 30 pixels for all the images used for camera calibration.

Lens distortion

Detection of two vanishing points was performed on two images (numbers 8 and 9) that show only one face of the building. This is step 1 of the procedure described in section 3.2.1. The result is shown in Figure 4. In this and following figures the image lines are colour-coded using the line labelling results of the vanishing point detection:

- Red no (unique) labelling
- Yellow first vanishing point (near camera y-axis)
- Green second vanishing point (near camera x-axis)
- Blue third vanishing point (near optical axis)

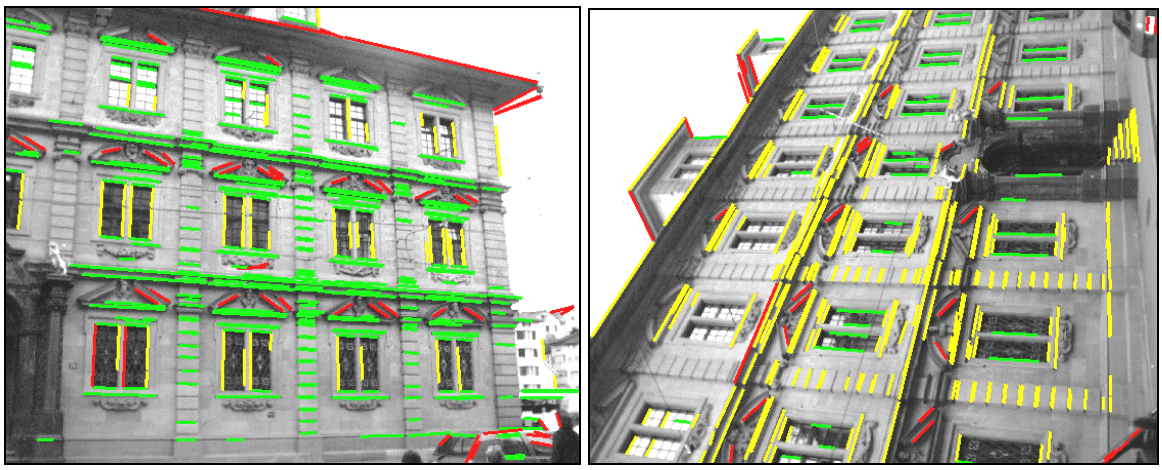

Figure 4 : color-coded image lines of the vanishing point detection for image 8 (left) and 9 (right).

For the vanishing point detection the precision of the co-ordinates of the endpoints of the lines was set to 1 pixel standard deviation. A more sophisticated stochastic model, in which the precision of the endpoint co-ordinates varies with the length of the line, is implemented but not extensively tested. This model gives better results only when the length of the extracted lines varies considerably (in the order of a factor of 10). Due to the characteristics of the building and the presence of lens distortion the length of the extracted lines is relatively homogeneous for the CIPA data set. Although generally the precision of extracted straight lines can be expected to be better than 1 pixel standard deviation, this value is chosen because of two reasons. First, lines that contain systematic errors in their location as a result of lens distortion are to be labelled to a vanishing point. Second, due to a relatively low threshold on the image gradients for edge detection, the extracted lines sometimes show small deviations from the vertical or horizontal structures of the building.

The results of the estimation of the lens distortion parameter $k1$ using only parallelism condition equations are listed in Table 1. Here the a priori standard deviation was also set to 1 pixel (= 0.006445 mm). The a posteriori standard deviation is 0.56 and 0.68 pixel ($\sqrt{0.314}$ and $\sqrt{0.469}$ respectively). Combining image 8 and 9 the estimated parameter is 7.0 times its estimated standard deviation and thus significant. Parameter $k1$ was fixed to the value in the last column of Table 1 for the estimation of focal length and principle point described in the next section.

	Image 8	Image 9	**Image 8 & 9**
Variance factor	0.314	0.469	**0.383**
Critical value (1%)	1.02	1.11	**1.00**
Degrees of freedom	363	293	**656**
Maximum residual (mm / pixel)	0.0111 / 1.7	0.0148 / 2.3	**0.0148 / 2.3**
$k1$	-0.548×10^{-3}	-0.596×10^{-3}	$\mathbf{-0.570} \times 10^{-3}$
Formal σ	0.176×10^{-3}	0.191×10^{-3}	$\mathbf{0.131} \times 10^{-3}$

Table 1 : Results of the lens distortion parameter estimation

Focal length and principle point

Lines of three vanishing points are required for the focal length and principle point estimation. The grouping of image lines that results in the automated vanishing point detection (only using the lens distortion parameter as described in the previous section, so no orthogonality constraints) is shown in Figure 5. Image 16 was not used because of an unfavourable image scale. The estimated parameters for these three images were not consistent (Table 2). Especially the difference in the estimated focal length was considerable (varying 1.75 mm, 20 times its standard deviation of 0.086 mm).

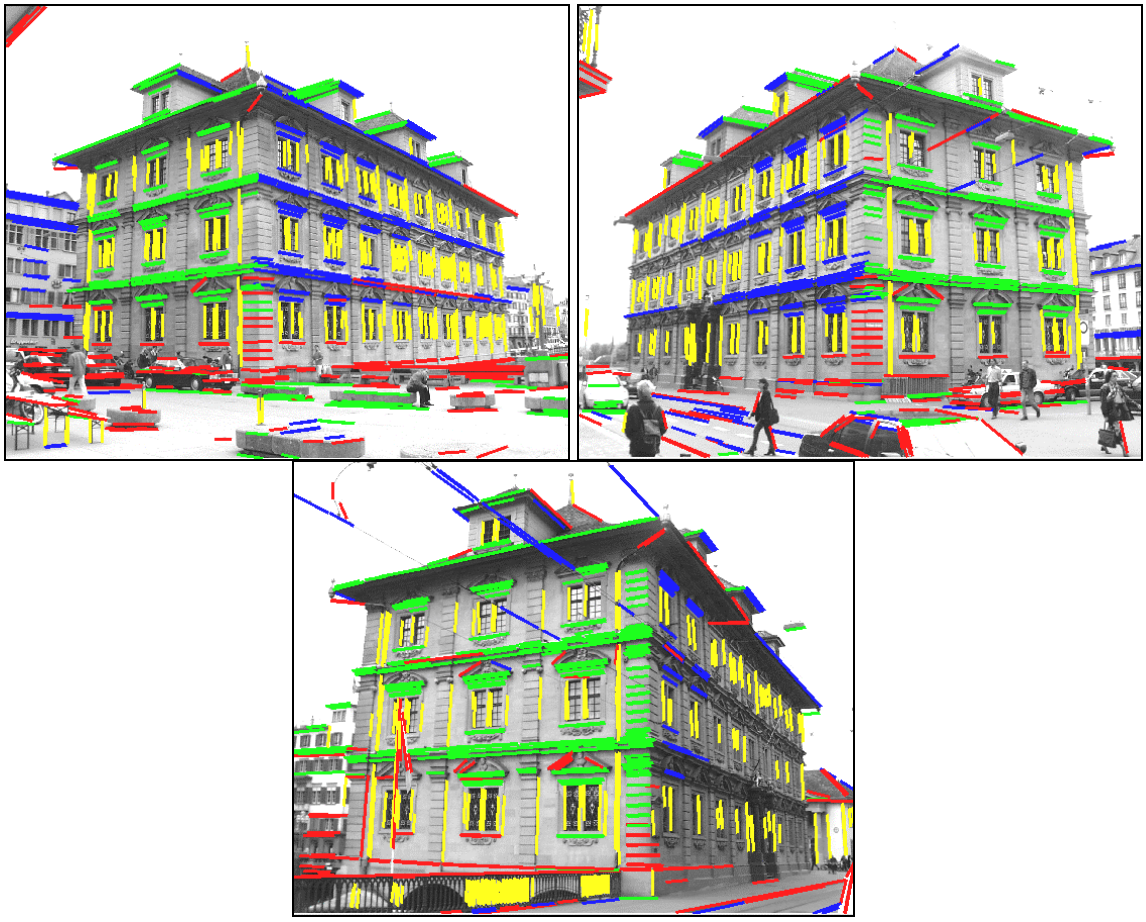

Figure 5: Vanishing point detection results for images 3, 6, and 11.

	Image 3	Image 6	Image 11	Image 3 (Manual)	Image 6 (Manual)	Image 11 (Manual)
Variance factor	1.027	0.903	0.665	1.152	0.132	2.320
d.o.f.	487	454	476	7	7	7
Max. residual (mm / pixel)	0.018 / 2.8	0.018 / 2.8	0.017 / 2.6	0.010 / 1.6	0.003 / 0.4	0.011 / 1.8
Focal length (mm)	8.668	9.663	10.420	8.514	10.092	10.032
(σ)	(0.052)	(0.079)	(0.068)	(0.046)	(0.058)	(0.049)
Principle point y (mm)	-0.200	-0.053	0.112	-0.085	0.376	0.176
(σ)	(0.057)	(0.067)	(0.076)	(0.066)	(0.076)	(0.067)

Table 2 : Results of camera parameters estimation of three images using automatically and manually extracted and labeled image lines.

The location of the principle point could not be estimated in x-direction due to the near two-point perspective of the imagery. In order to verify the results, four image lines for each object orientation were manually measured in each image (Figure 6), and the camera parameter estimation was repeated. The manual measurements confirmed the significant difference between the focal length of image 3 and those estimated with images 6 and 11 (Table 2). The differences between the automated and manual focal length determination are between 2.2 and 4.6 times their standard deviation. The precision of the parameters estimated from manual measurements is better, especially for the focal length. Therefore, hereafter only the manually extracted lines are used for the camera calibration. This choice is also to be preferred because it limits the assumptions of parallelism and perpendicularity to the measured edges of the building.

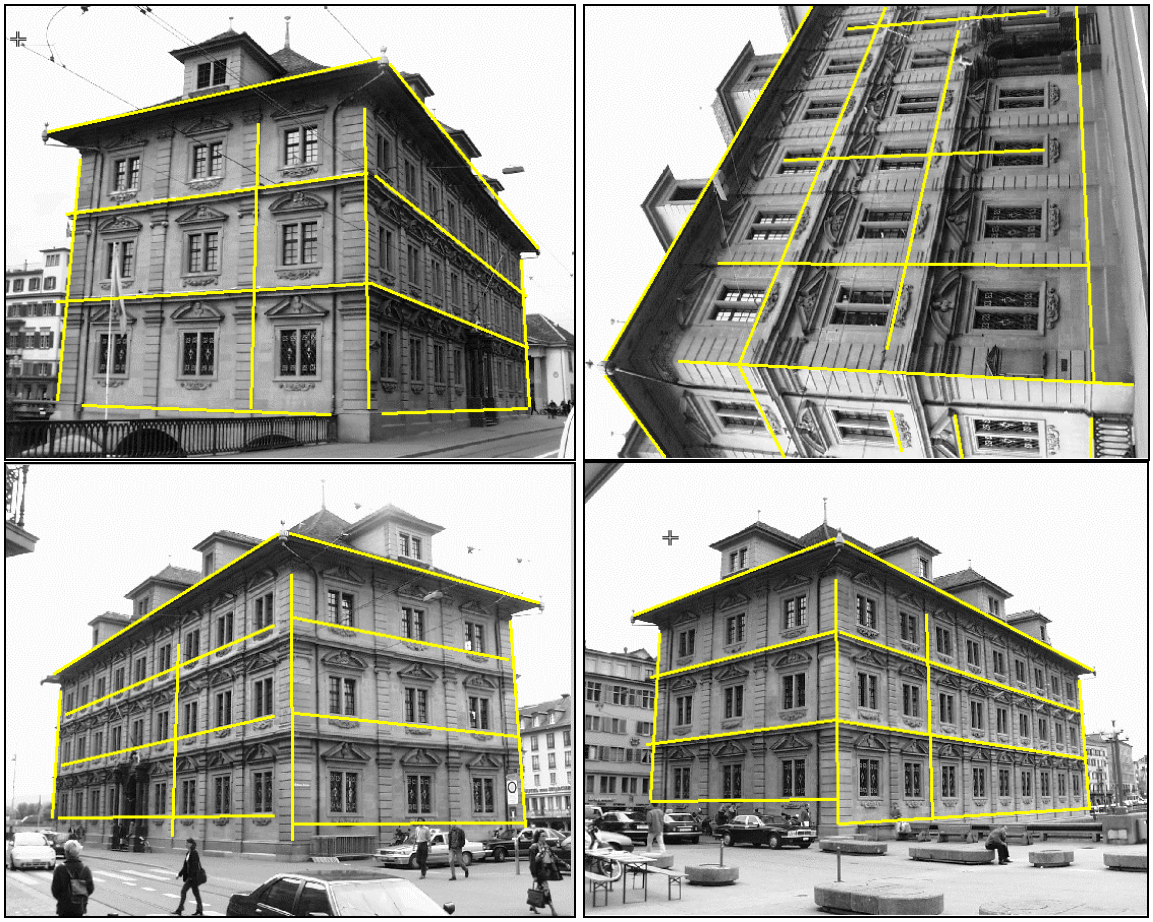

Figure 6: Manual line measurements for camera calibration (from top left to bottom right: images 11, 10, 6, 3)

The source of the inconsistency was traced by estimating the camera parameters using the manual measurements of all combinations of two images. The results are shown in Table 3. Only the fit of the combination in which image 3 is missing is of good quality, the overall test is accepted (critical value 1.93).

	Image 3, 6	Image 3, 11	Image 6, 11
Variance factor	31.01	31.63	1.435
d.o.f.	16	16	16
Max. residual (mm / pixel)	0.058 / 8.8	0.052 / 8.1	0.012 / 1.8
Focal length (mm)	9.124	9.234	10.056
(σ)	(0.035)	(0.032)	(0.037)
Principle point y (mm)	0.158	0.028	0.267
(σ)	(0.048)	(0.046)	(0.050)

Table 3: Camera parameter estimation using the manual measurement of combinations of images

Image 10 was now added in the estimation in order to verify the results. In Table 4 adjustment results using the manual measurements of three images are presented, with and without estimation of the x-co-ordinate of the principle point. As the critical value is 1.8 (5% significance level) both adjustments are accepted. Due to the 90 degree rotation around the optical axis of image 10 the principle point x co-ordinate can also be estimated. The fit improves significantly. Note that the manual line measurements are not suitable for estimation of lens distortion. The results in the last column of Table 4 are considered to be the final estimates of the camera parameters.

	Image 6, 10, 11	**Image 6, 10, 11 Final**
Variance factor	1.553	**1.211**
d.o.f.	26	**25**
Max. residual (mm / pixel)	0.0131 / 2.0	**0.0100 / 1.6**
Focal length	10.103	**10.116**
(σ)	(0.029)	**(0.030)**
Principle point x (mm)	-	**-0.146**
(σ)		**(0.041)**
Principle point y (mm)	0.222	**0.220**
(σ)	(0.047)	**(0.046)**

Table 4: Camera parameter estimation using the final combination of three images

The CIPA data set was also analysed by others (Streilein et al., 2000), (Rottensteiner et al., 2001). In the paper by Rottensteiner the images taken with the Olympus camera are split in two groups, one with a focal length of 8.598 mm and the other with a focal length of 10.132 mm (balanced lens distortion). Obviously, the setting of the zoom lens is different for the two sets of images. Hereafter, the camera parameter values from (Rottensteiner et al., 2001) derived with bundle adjustment software Orpheus, are used as a reference. Comparison with camera parameters provided in this set showed a good match. The lens distortion parameter is not compared because the number and definition of distortion parameters differs in the set determined with Orpheus. The difference in the focal length is 3.0 times its standard deviation. Differences in the principle point location are smaller than 2.0 times the standard deviation. Table 5 summarises the comparison of the estimated parameters with the reference values. Table 6 contains the camera parameters used for the second zoom setting applicable to images 3 and 16. These values are used for the orientation and reconstruction steps described in the next sections.

	Estimated (Table 4)	Estimated (Balanced)	Reference (Balanced)	Estimated - Reference
Focal length (mm)	10.116	10.024	10.132	0.108 (3.0 σ)
(σ)	(0.030)		(0.020)	(0.036)
Principle point x (mm)	-0.146		-0.202	0.044 (0.9 σ)
(σ)	(0.041)		(0.030)	(0.051)
Principle point y (mm)	0.220		0.202	0.112 (2.0 σ)
(σ)	(0.047)		(0.031)	(0.056)

Table 5 : Comparison of estimated and reference values of camera parameters.

	Reference (Unbalanced)	Reference (Balanced)
Focal length (mm)	8.676	8.598
(σ)	(0.019)	(0.019)
Principle point x (mm)	-0.101	-0.101
(σ)	(0.029)	(0.029)
Principle point y (mm)	0.198	0.198
(σ)	(0.029)	(0.029)

Table 6 : Reference values of camera parameters for images 3 and 16.

3.3 Image orientation

3.3.1 Procedures for image orientation

Three different procedures for image orientation will be presented. The main goal of these methods is to find approximate values for image orientation in an efficient way using a priori object information. They all involve (partial) reconstruction of an object model that can be regarded as a by-product. The first two methods are similar in the sense that they are based on partial object reconstruction using a single image. These methods require manual line measurement and object knowledge in the form of coplanarity, parallelism, and orthogonality of object edges. The third method makes use of the same assumptions on the object geometry, but aims at automated relative orientation of two or more images. This method is shown to work in many cases; however, successful orientation depends on the image configuration and the structure of the building. In cases of failure between one and three corresponding points have to be measured manually, turning the method into a semi-automatic one.

The first method is described in (Heuvel, 1997). It requires the measurement through points or lines of the same rectangle in object space in two (or more) images. Model coordinates of the corner points are then computed with a direct method. These coordinates are defined in the camera system. A direct method for the 3D similarity transformation between two corresponding sets of model points results in the relative orientation of the two images.

The second method can be regarded as an extension of the first one. The idea is to reconstruct a larger part (more than one rectangle) of the building from manual line measurements of a single image (Heuvel, 1998). These line measurements are identical to the ones needed for the multi-image reconstruction of the building. The relative orientation obtained is expected to be of better quality than the one obtained with the first method because of the increased number of points used and the possibility of adjustment of redundant observations. The first method involved only one condition that results from the orthogonality of the rectangle.
The third method differs considerably from the first two because it aims at full automation. It is described in (Heuvel, 2002). The method relies on automated straight line extraction and vanishing point detection, and results in a model coordinate system that is aligned with the building. Successful orientation can require a few manual measurements to allow for reliably resolving ambiguities inherent in the vanishing point detection and in the repeating and symmetric structures present in most buildings. Furthermore, the manually measured points reduce the computational burden considerably, and can be used to guarantee the required overlap of at least one point between consecutive models needed to transfer scale from model to model.

The application on the CIPA reference data set of the three methods shortly outlined above is described in the next sections.

3.3.2 Image orientation based on single image reconstruction

The direct solution with rectangles in object space

The procedure for image orientation described in (Heuvel, 1997) is applied to four images of the CIPA data set. In each image the contours of two faces of the building are measured manually with lines (Figure 7).

Figure 7: Line measurements for the orientation procedure using rectangles in object space.

Model coordinates have been computed for each image. A parallelogram suffices for the direct solution used. Here a perpendicularity constraint is applied to the observations. The direct method is applied with the adjusted observations. The test results of four images (two rectangles each) of this perpendicularity constraint are summarized in Table 7 under "rectangularity test" (ratio test value / critical value, 0.1% significance level). The a priori precision was set to 1 pixel standard deviation for the image coordinates of the corner points. A constraint for the perpendicularity between two neighbouring faces was not applied. Each face is processed independently. However, the scale of the two faces reconstructed from one image is related, i.e. the average distance to the projection centre of common points is set equal for both faces. The remaining difference in depth direction in the model coordinates between two common points is called the discrepancy (Table 7). Without rectangularity constraints the maximum discrepancy is 0.12% of the average distance to the projection centre. After applying rectangularity constraints the maximum discrepancy reduces to 0.03% of this distance. Together with the reduction of the formal standard deviation, this demonstrates the improved consistency obtained by applying rectangularity constraints.

Image	Rectangularity test (Ratio with critical value) Long / short face	Coordinate discrepancy With / without rectangularity (% of distance)	Maximum σ in depth With / without rectangularity (% of depth)
11	1.11 / 0.10	0.032 / 0.109	0.035 / 0.045
6	0.04 / 0.87	0.030 / 0.025	0.055 / 0.080
3	0.45 / 0.66	0.013 / 0.007	0.032 / 0.036
16	0.27 / 0.28	0.005 / 0.119	0.116 / 0.219

Table 7: Summary of the model coordinate computation with the direct solution.

In the next step the camera coordinate systems of images 6, 3, and 16 are transformed to the system of image 11 through similarity transformations using the computed model coordinates. For each transformation only the four corner points of the common rectangle are available. Image 3 (located opposite of image 11) has four points of two different rectangles in overlap with image 11. Approximate values of the parameters are computed by a direct solution. With 7 parameters there are 5 degrees of freedom. The results of the transformations are summarized in (Table 8). All overall tests are rejected (critical value 2.9, 1.3% significance level). Possible reasons for the rejections are:

The software for the similarity transformation does not account for noise in the reference coordinate set.

- The correlations between the coordinates of different points are neglected.
- The a priori standard deviation (set to 1 pixel) is too optimistic.
- Possible imperfections present in the interior orientation data.

Transformation of Image	Overall test (Ratio with critical value)	Largest w-test	Differences with adjusted relative rotations x, y, z (Angles in degree)	Differences with adjusted relative position vector (Angle in degree)
6 3 (via 6)	5.8 23.4	7.2 14.4	1.02, 0.88, 0.55 1.06, 0.70, 1.73	0.30 1.35
16 3 (via 16)	6.8 4.8	6.4 5.5	1.72, 0.42, 1.73 3.96, 1.34, 3.72	0.12 1.74
3	6.4	8.4	0.84, 0.90, 0.33	0.74

Table 8: Summary of the relative orientation computation by similarity transformation of model coordinates.

The results of the relative orientation are compared with the relative orientation information present in the exterior orientation files that resulted from the final line-photogrammetric bundle adjustment (see section 3.4). Most differences are in the order of 1 degree. The relative orientation of (or via) image 16 is less accurate due to an image configuration that is unfavourable. Figure 8 depicts the model that results as a by-product of the orientation procedure. The grey faces are reconstructed from image 11; the coloured faces from image 3. In section 3.4 it is shown that the approximate values obtained with the direct solution based on rectangles in object space are of sufficient quality to obtain convergence in the line-photogrammetric bundle adjustment.

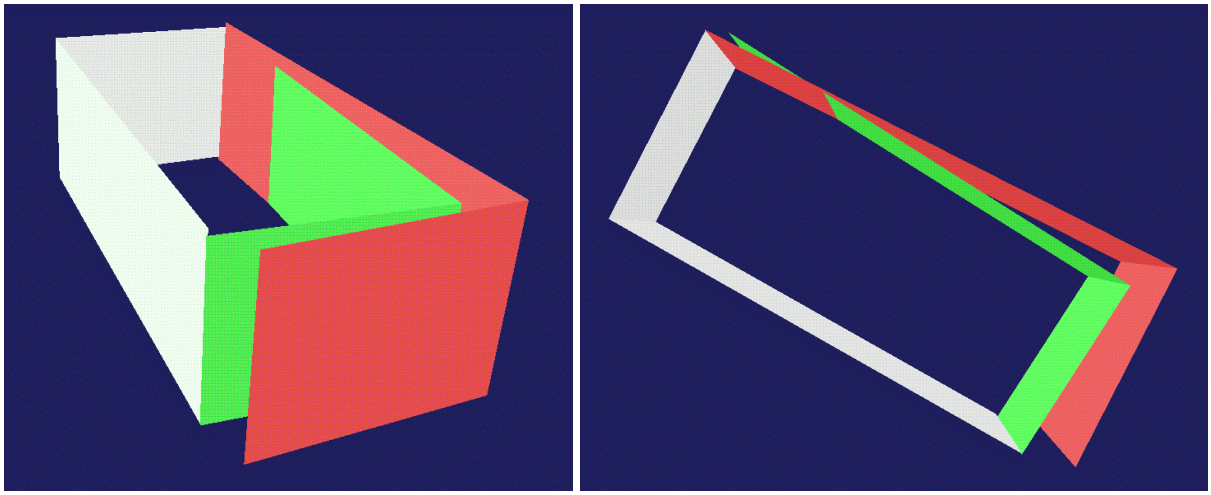

Figure 8: Two views of reconstructed and transformed model parts using the direct solution; grey; image 11, green: image 3 (via 6), red: image 3 (via 16).

Reconstruction after adjustment using condition equations

As described in the previous section the observations were adjusted using one rectangularity constraint before the direct solution was applied for reconstruction. The procedure of which results are shown in this section applies a complete set of constraints and a different method for the model coordinate computation. It is described in detail in (Heuvel, 1998). The adjustment of the constraints listed below results in a unique set of model coordinates per image computed from the adjusted observations. This is in contrast with the method applied in the previous section. The adjustment model is built with the following six constraints:

- One parallelism constraint (Three vertical lines intersect in one vanishing point)
- Three perpendicularity constraints (The three object orientations are assumed to be orthogonal)
- Two point intersection constraints (Three lines intersecting in one point in the image. Mathematically, this constraint is identical to the first one)

The results of the four adjustments are summarized in Table 9. Again, the a priori standard deviation of the image line end point coordinates is set to 1 pixel. The critical value for the overall test is 2.8 (1% significance level). There is a clear correlation with the results of the rectangularity test shown in Table 7.

Image	Overall test (Ratio with critical value)	Maximum residual (mm / pixel)
11	5.4	0.0368 / 5.7
6	3.3	0.0248 / 3.8
3	1.1	0.0150 / 2.3
16	0.2	0.0052 / 0.8

Table 9: Summary of the single image adjustment of six condition equations.

Transformation of Image	Overall test (Ratio with critical value)	Largest w-test	Differences with adjusted relative rotations x, y, z (Angles in degree)	Differences with adjusted relative position vector (Angle in degree)
6	1.1	3.2	0.60, 0.20, 0.62	0.47
3 (via 6)	6.2	5.8	1.02, 0.57, 0.85	0.53
16	3.1	4.0	1.71, 0.54, 1.65	3.15
3 (via 16)	1.03	2.7	0.99, 0.56, 0.82	0.34
3	0.36	1.6	0.38, 0.28, 0.30	0.64

Table 10: Summary of the relative orientation by similarity transformation of model coordinates.

The results of the model coordinate transformation to the system of image 11 are shown in Table 10. Because error propagation is not implemented, the a priori variance for the model coordinates was set equal for all coordinates and equivalent to 1 pixel in the image scaled to model space using the longest distance from the projection centre to a model point. Because of the differences in the stochastic model the test results of Table 8 and Table 10 are not comparable. The differences with the adjusted relative orientation data are smaller on average, compared to the results presented in the previous section. However, there are some exceptions (see results of image 16 for instance). The reconstructed model parts are depicted in Figure 9. Comparison with Figure 8 specially shows the effect of perpendicularity constraints between faces. The maximum residual of the similarity transformation directly from the model of image 3 to the model of image 11 (not shown in the figures) reduces from 0.24% to 0.16% of the largest distance in the model.

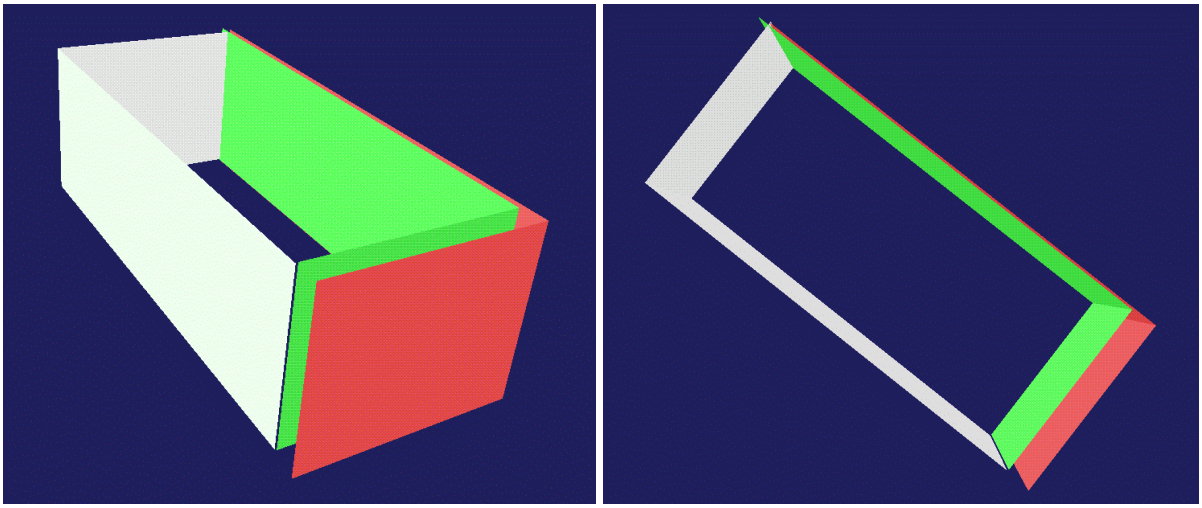

Figure 9: Two views of reconstructed and transformed model parts after adjustment of observations; grey: image 11, green: image 3 (via 6), red: image 3 (via 16).

3.3.3 Semi-automatic image orientation

Limitations to fully automated image orientation

The chance of success of the procedure for automated relative orientation is dependent on the following aspects:

- Building structure and characteristics:
  - Presence of straight, parallel, orthogonal, and coplanar edges
  - Presence of repeating structure or textures, such as the windows of the Zurich city hall
- Image configuration and characteristics:
  - Relative orientation of the images to the building.
    - Restriction to rotation around the optical axis and image tilt should be observed.
    - Considerable scale change along the façade is a disadvantage for the procedure.
    - In order to scale a model relative to a previous model, the same façade should be present in three consecutive images (this is not the case with the selected images).
  - Relative orientation between the images.
    - The larger the base – height (base – depth) ratio, the smaller the chance of successful relative orientation.
    - Large-scale difference between overlapping image parts have the same effect.
  - Image coverage of the overlapping part between images.
    - For larger image coverage, the chances of success are better.
    - If the building contains repeating structures, the same part of the façade (preferably the whole façade) should be visible in both images in order to find a correct match.

The CIPA reference data set shows several of the characteristics listed above. Two characteristics play a major role in prohibiting the procedure for automated relative orientation to be successful in all cases. The first one is the considerable differences in image scale between images. This is due to the obliqueness of the selected images, as well as the large differences in the object to image distance (image 16). Secondly, the repeating structures in the form of the many identical windows make the detection of the

correspondence ambiguous. To some extent it is possible to adapt the parameters to these characteristics. The parameters for the minimum line length and the minimum distance between lines for point creation are dependent on the image scale. However, in the case of large scale differences these parameters have to be set such that the number of lines and the number of created points becomes too large (i.e. a small minimum line length and a large minimum distance).

A computationally more efficient procedure such as RANSAC could be a solution to the problem above, but has not been investigated. However, it is expected that the repeating structures such as the windows could result in mismatches when not all likely correspondences are investigated in the search, as is the case in the procedure presented here. Therefore, the solution chosen is the manual measurement of one to three corresponding points in both images. The effectiveness of this solution, and the sensitivity of the fully automated procedure to the input parameters are demonstrated in the following three examples in which the procedure is applied to image pair 6-3:

1. Failure: 30 pixel minimum line length, 5 pixel maximum line distance for intersection (Figure 10 and Figure 11).
2. Success: the same parameters as for case 1, and two manually measured points in both images (Figure 12 and Figure 13).
3. Success: 40 pixel minimum line length, and 10 pixel maximum line distance (Figure 14 and Figure 15).

The figures can be found at the end of this section. In Table 11 the main statistics on the accepted solutions of the three cases are gathered.

Image 6 – Image 3	Case 1	Case 1	Case 2	Case 3
Permutation number (minimum 5 correspondences)	0	2	0	0
Minimum line length	30 pixel	30 pixel	30 pixel	40 pixel
Maximum distance for point creation	5 pixel	5 pixel	5 pixel	10 pixel
# manually measured points	0	0	2	0
# created points image 1 / 2	178 / 184	178 / 184	178/ 184	204 / 214
# correspondence hypotheses	1685	1347	1687	2378
# potential tests	821,386	599,678	1,396,973	1,182,214
# computed tests	98,879 (12%)	64,831 (10.8%)	196,957 (14.1%)	213,991 (18.1%)
# accepted tests	10,494 (1.3%)	4,975 (0.8%)	13,547 (1.0%)	26,063 (3.2%)
# clusters	1845	1243	14	3706
Maximum # correspondences	25	18	6	27
# clusters after testing	95	20	3	97
Maximum # correspondences	18	18	5	22
Test (ratio with critical value)	3.45	2.43	5.01	3.65

Table 11: Accepted solutions for the three tests for relative orientation of image 3 and image 6.

The ambiguity in the solution is not correctly resolved in case 1, although the two accepted solutions are very close. Both have 18 correspondences after applying statistical testing. However, the test value of the erroneous solution is lower than the one of the correct solution (2.43 versus 3.45). This demonstrates that it is not always possible to detect correct correspondence, especially for buildings with repeating structures.

With the manual measurement of two corresponding points (case 2), the erroneous solution (permutation 2) is eliminated. The a priori standard deviation of the manual measurements was set to 0.5 pixel. This relatively high precision in combination with imperfections in the relative rotations derived through the vanishing point detection lead to a reduction in the number of correspondences (from 18 to 5) and an increase of the test value (from 3.45 to 5.01).

Case 3 shows that automatic relative orientation is possible, but only with adapted parameter settings. A longer minimum line length results in fewer lines for the non-corresponding façades because of their smaller average image scale. An increase of the maximum distance between lines to be intersected leads to more points in the common façade.

Figures of case 1

Figure 10: Top: results of line extraction and vanishing point detection of images 6 (left) and 3 (right). Middle: points from line intersections. Bottom: result of erroneous correspondence detection.

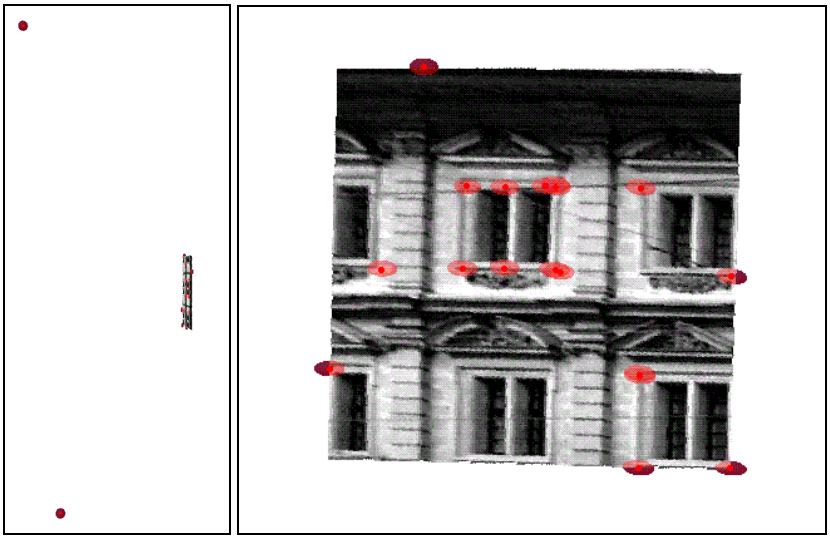

Figure 11: View of the 3D model with the two projection centres from the top (left) and the rectified part of the façade that contains the “corresponding” points (right). The red dots visualize the covariance matrix of the 3D co-ordinates.

Figures of case 2

Figure 12: Result of correct correspondence detection with two manually measured points (1001 and 1004). For the results of the vanishing point detection and point creation see Figure 10.

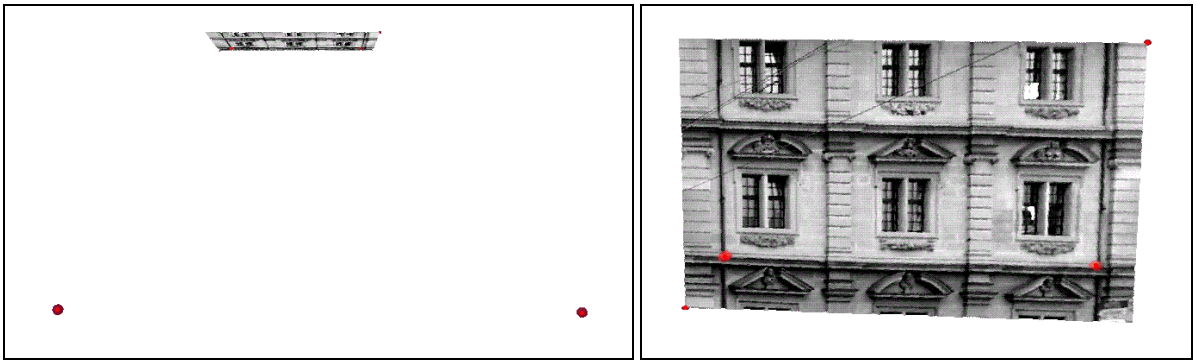

Figure 13: View of the 3D model from the top (left) and the rectified part of the façade that contains the five corresponding points (right). The manually measured points are in the lower-left and the top-right corner.

Figures of case 3

Figure 14: Top: results of line extraction and vanishing point detection of images 6 (left) and 3 (right). Middle: points from line intersections. Bottom: result of correct correspondence detection.

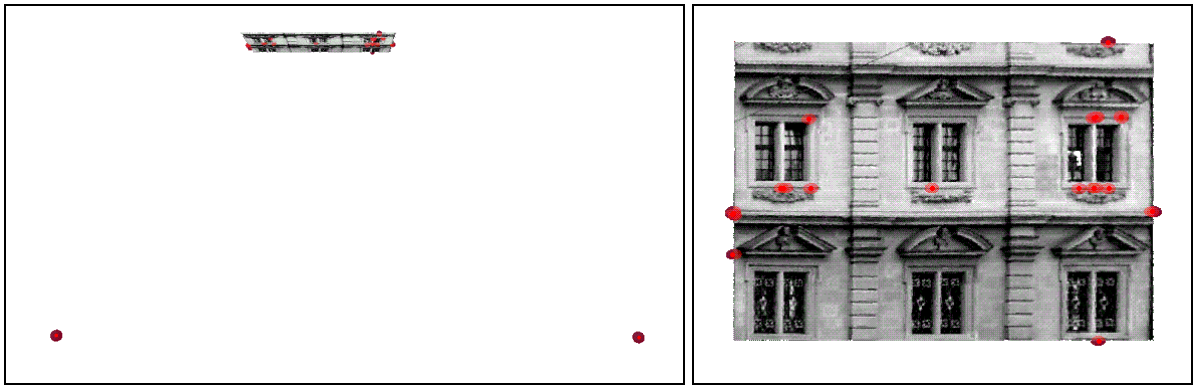

Figure 15: View of the 3D model from the top (left) and the rectified part of the façade that contains the 22 corresponding points.

In the next section it is shown that the semi-automatic approach also is an effective solution for transferring scale from one model to the next. Here three points are manually measured in each image for a successful orientation of all four images.

Semi-automatic image orientation for the CIPA data set
For all images, apart from image 16, the same set of parameters has been used (Table 12). The last three parameters are introduced to reduce the number of coplanarity tests that have to be evaluated. The reduction is typically between 80% and 90%. Image 16 has a considerably different image scale and therefore requires adaptation of the parameters. For image 16 the line extraction was limited to the part of the image that contains the building. Furthermore, the minimum line length was reduced to 15 pixels.

Parameter	Value
A priori standard deviation For all image point coordinates (pixel)	1.0
Minimum line length (pixel)	30 (15 for image 16)
Maximum line distance (pixel)	10
Angle epipole – vertical (degree)	90 +/- 10
Maximum scale difference	3.0
Minimum angle between epipolar planes (degree)	1

Table 12 : Input parameters

For each relative orientation of two images only one solution (i.e. permutation of the rotation matrix) was accepted. All solutions contain two manually measured points except the solution for image pair 11 / 6, which is based on three manually measured correspondences. No additional correspondences were found for this pair.

The threshold of 5 pixels for the distance between two lines to be intersected is chosen relatively low in order to reduce the computational burden. Increasing this parameter to 10 pixels leads to about three times as many points, an increase in the number of correspondence hypotheses with about a factor of 10, and an increase in the number of accepted tests with a factor in the order of 100 (Table 14). Results of vanishing point detection and point creation are shown in Figure 16.

As expected, the number of detected correspondences increases, except for image pair 11 / 6 where all correspondence hypotheses between line intersections are again being rejected. Apart from the test value for this pair, all test values increase due to the higher number of correspondences in the selected clusters. Note that these tests are all rejected (test ratio over 1.0), while all individual line tests are accepted for these clusters. The

individual line tests the hypothesis of an error in a single image line. The comparison with adjusted exterior orientations shows an angular difference between 1.1 and 5.4 degrees.

Images	11 / 6	6 / 3	3 / 16	16 / 11
Permutation	2	2	3	0
Minimum line length	30 / 30 pixel	30 / 30 pixel	30 / 15 pixel	15 / 30 pixel
# created points image 1 / 2	118 / 178	178 / 182	182 / 318	318 / 118
# correspondence hypotheses	859	1761	3872	751
# potential tests	358,496	1,524,111	7,377,195	271,577
# computed tests	114,393 (31.9%)	331,645 (21.8%)	1,165,881 (15.8%)	54,950 (20.2%)
# accepted tests	3,811 (1.1%)	18,470 (1.2%)	69,253 (0.9%)	2,390 (0.9%)
# clusters	6	15	45	11
Max. # correspondences	4	5	16	6
# clusters after testing	1	4	18	4
Max. # correspondences	3	5	12	6
Test (ratio with critical value)	6.35	2.14	2.91	0.69
Rotation differences with adjusted (angles in degree)	4.3, 2.5, 4.9	1.1, 1.4, 1.8	4.9, 1.1, 4.9	2.9, 2.2, 1.9
Position differences with adjusted (angle in degree)	2.5	5.4	2.9	3.0

Table 13: Results of relative orientation of four images with maximum line distance set to 5 pixels.

Images	11 / 6	6 / 3	3 / 16	16 / 11
Permutation	2	2	3	0
Minimum line length	30 / 30 pixel	30 / 30 pixel	30 / 15 pixel	15 / 30 pixel
# created points image 1 / 2	313 / 518	518 / 525	525 / 690	690 / 313
# correspondence hypotheses	7676	15,754	24,378	7,699
# potential tests	29,455,922	123,465,692	295,521,867	29,301,857
# computed tests	7,818,702 (26.5%)	28,017,900 (22.7%)	52,507,884 (17.8%)	5,090,893 (17.4%)
# accepted tests	242,471 (0.8%)	1,802,638 (1.5%)	4,534,611 (1.5%)	294,610 (1.0%)
# clusters	82	127	300	79
Maximum # correspondences	9	28	44	14
# clusters after testing	1	40	31	26
Maximum # correspondences	3	25	40	13
Test (ratio with critical value)	6.35	3.84	3.65	2.64
Rotation differences with adjusted (angles in degree)	4.3, 2.5, 4.9	1.1, 1.4, 1.8	4.9, 1.1, 4.9	2.9, 2.2, 1.9
Position differences with adjusted (angle in degree)	2.5	5.4	3.2	3.4

Table 14: Results of relative orientation of four images with maximum line distance set to 10 pixels.

The last image pair is added to be able to compare the initial exterior orientation data of image 11 with the data computed by “chaining” the four relative orientations. Note that the manually measured points on the corners of the building are essential in this process. The difference in position of image 11 is 5.4% of the largest distance in object space.

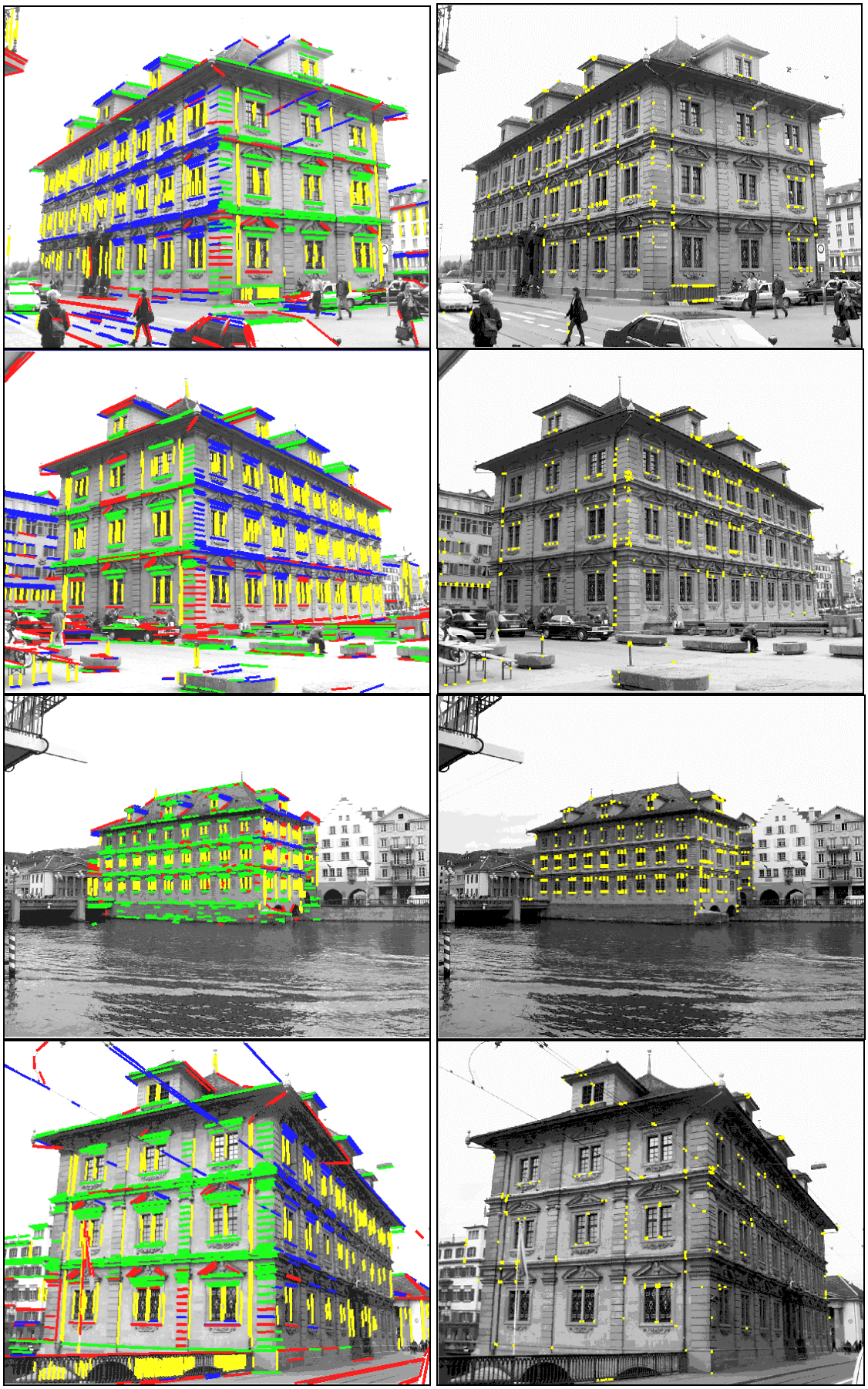

Figure 16: Results of the vanishing point detection for all four images (from top: image 6, 3, 16, 11).

In Figure 17 to Figure 20 the corresponding points are shown in overlay with the four image pairs.

Figure 17: Image pair 11 – 6. Three manually measured corresponding points.

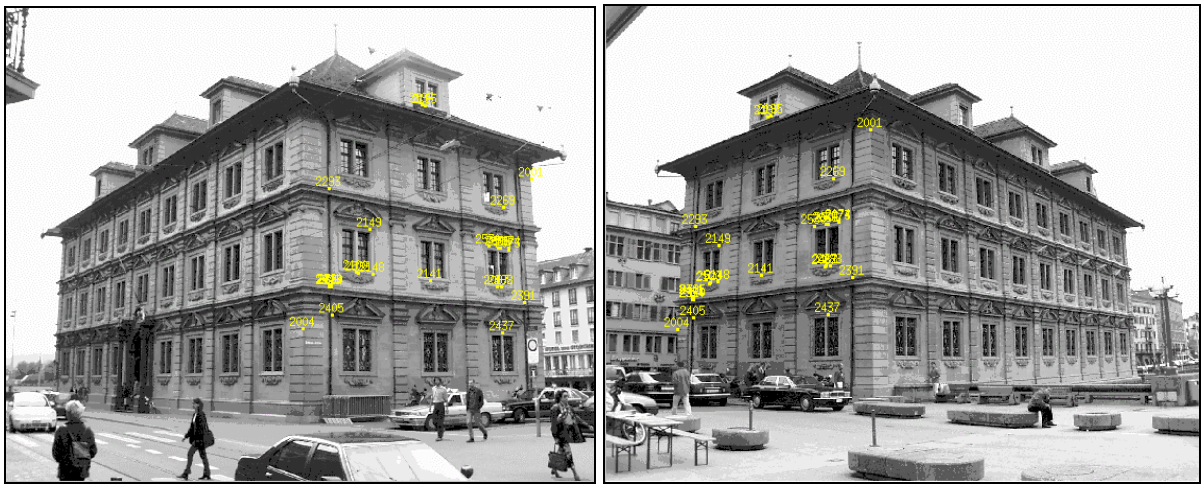

Figure 18: Image pair 6 – 3, 25 correspondences.

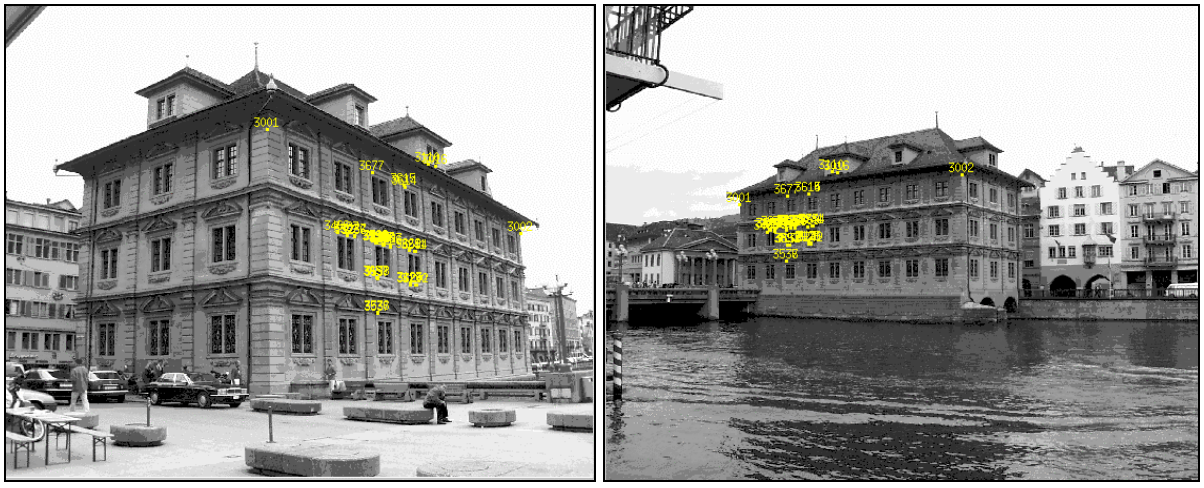

Figure 19: Image pair 3 – 16, 40 correspondences.

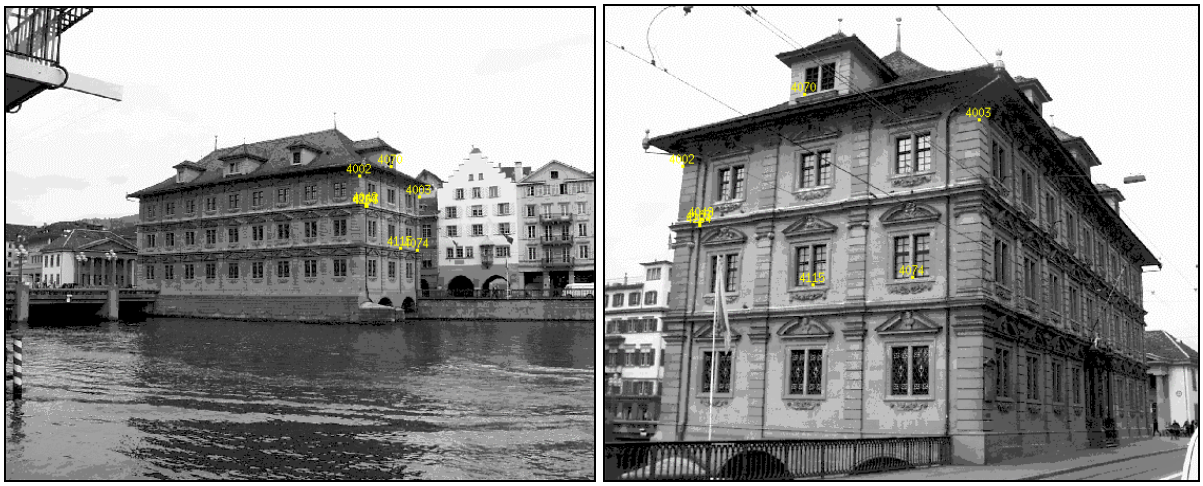

Figure 20: Image pair 16 – 11, 13 correspondences.

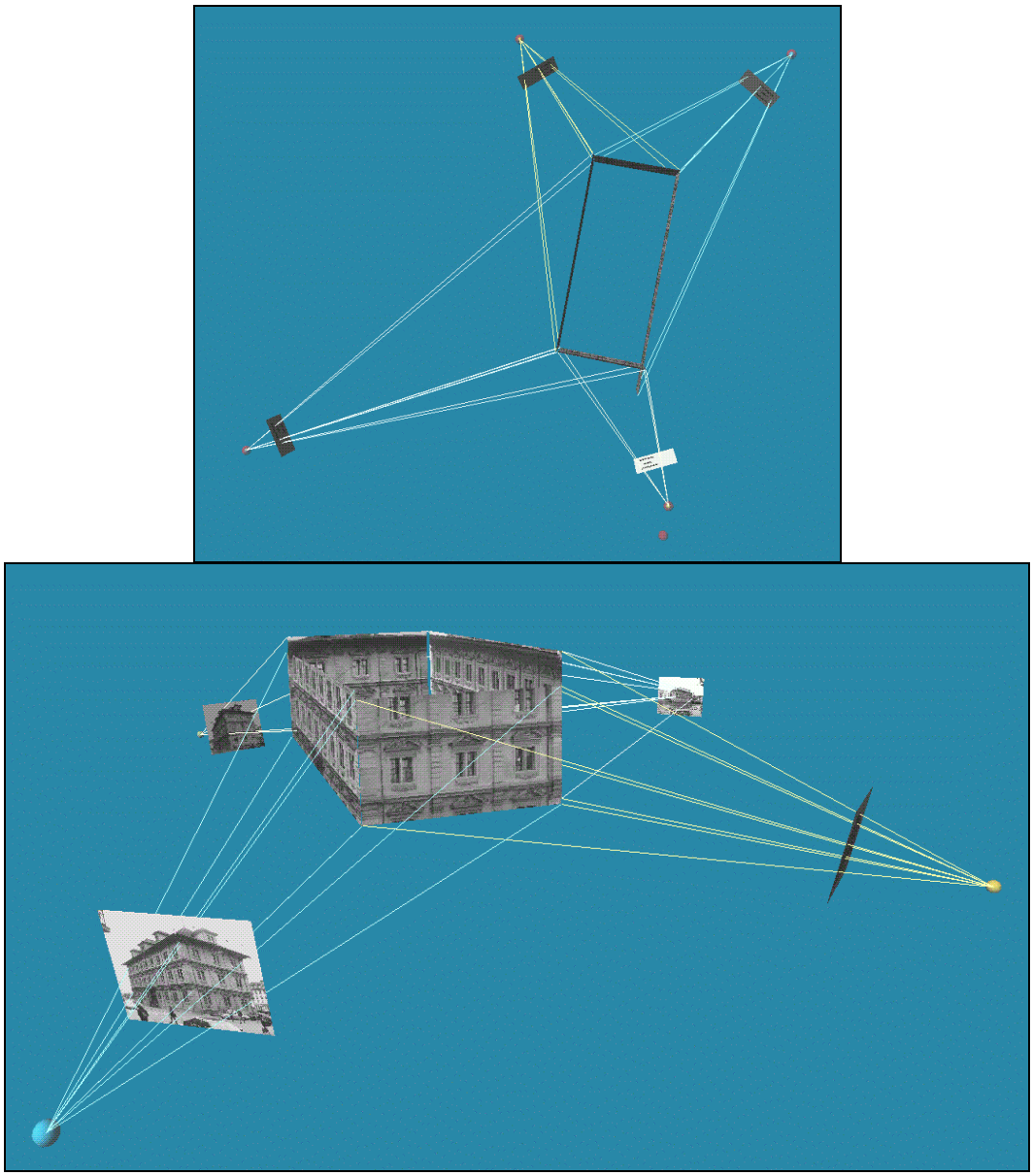

Figure 21: 3D model seen from the top (top), and an oblique view (bottom).

3.4 Object reconstruction

3.4.1 Procedure for object reconstruction

The object reconstruction is based on least-squares estimation of parameters that describe an object model. The model is represented by a surface description or B-rep of which not only 3D coordinates of vertices are estimated, but also object plane parameters and exterior orientation parameters. Parameterisation is singularity free. Approximate values are required for the exterior orientation parameters only. These parameters result from one of the procedures discussed in section 3.3.

The observations are manual line measurements of which the end points can be placed at any location on the edge. This allows edges to be partly occluded and gives the operator the freedom to select a location with good contrast. The object topology is also manually specified. The adjustment allows the incorporation of geometric constraints. Three types of constraints can be distinguished:

- Constraints required because of the over-parameterisation that avoids singularities.
- A set of coplanarity constraints is included that results from the topology of the B-rep.
- Additional constraints can be specified such as angle (parallelism) between planes (and others).

All geometric constraints are formulated as observation equations for which an appropriate weight is to be selected. The mathematical model is described in more detail in (Heuvel, 1999b).

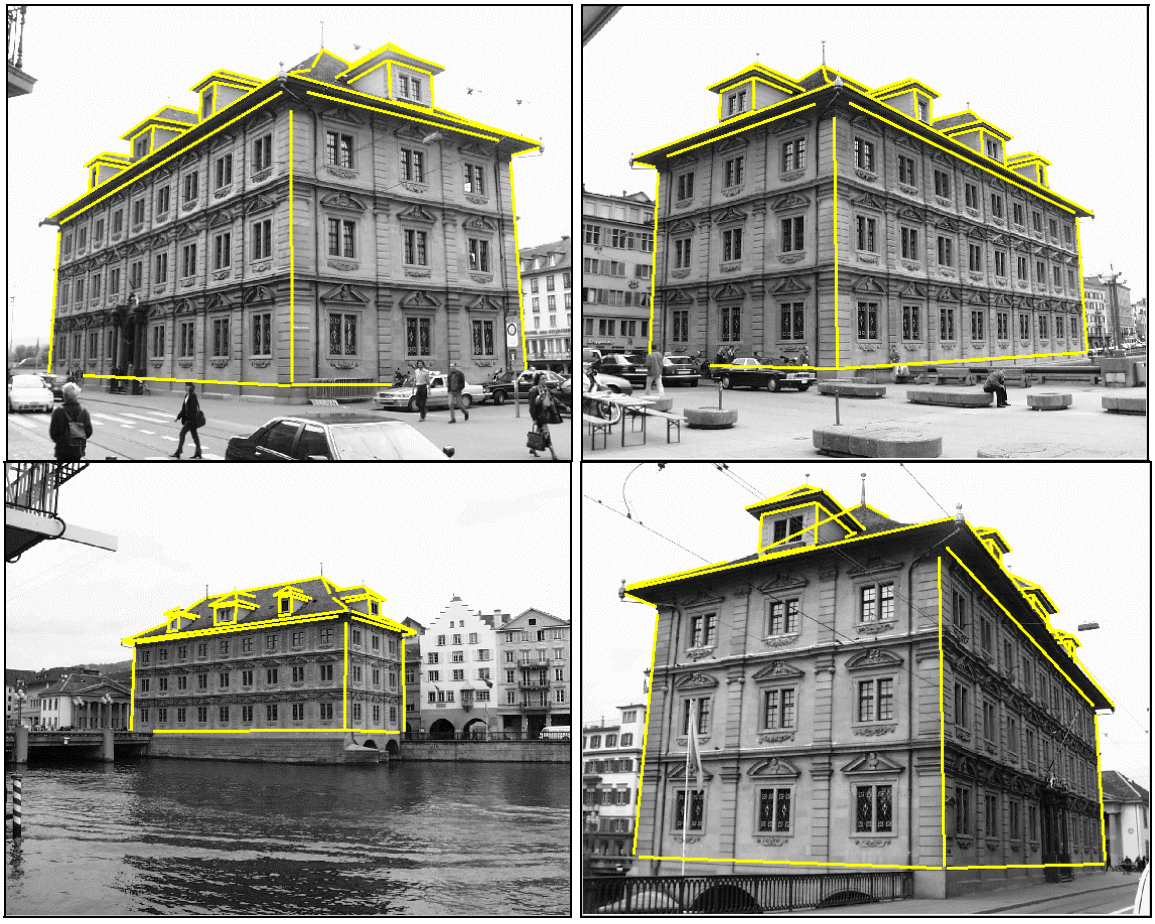

Figure 22: Line measurements for object reconstruction.

3.4.2 Object reconstruction of the Zurich city hall

Hrabacek has reconstructed the Zurich city hall as described in (Hrabacek and Heuvel, 2000). At that time, it was not known that the selected images were taken with two sets of camera settings as reported in (Rottensteiner et al., 2001). Therefore, the estimated variance factor was relatively high. Here, the same line measurements are adjusted (Figure 22). The two main differences with the adjustments by Hrabacek are the use of the calibration results described in section 3.2, and the use of approximate values as they resulted from the procedures described in section 3.3. The adjustment results are summarised in Table 15. The resulting model is shown in Figure 23.

	Number/Value	Parameters	Equations	σ_0 [2]
# image lines	199		393	1 pixel
# coplanarity constraints	246		246	$1e^{-3}$
# parallelogram constraints	30		90	$1e^{-3}$
# additional constraints	27		51	2 / 5 degree
# images	4	28	4 [3]	$1e^{-6}$
# planes	49	196	49 [3]	$1e^{-6}$
# points	74	222	7 (control)	$1e^{-4}$
Total		446	840	
Overall test	1.305			
Max. residual (lines)	0.0336 mm (5.2 pixel)			
Max. residual (constraints)	1.52 σ			

Table 15: Main statistics of the line-photogrammetric bundle adjustment.

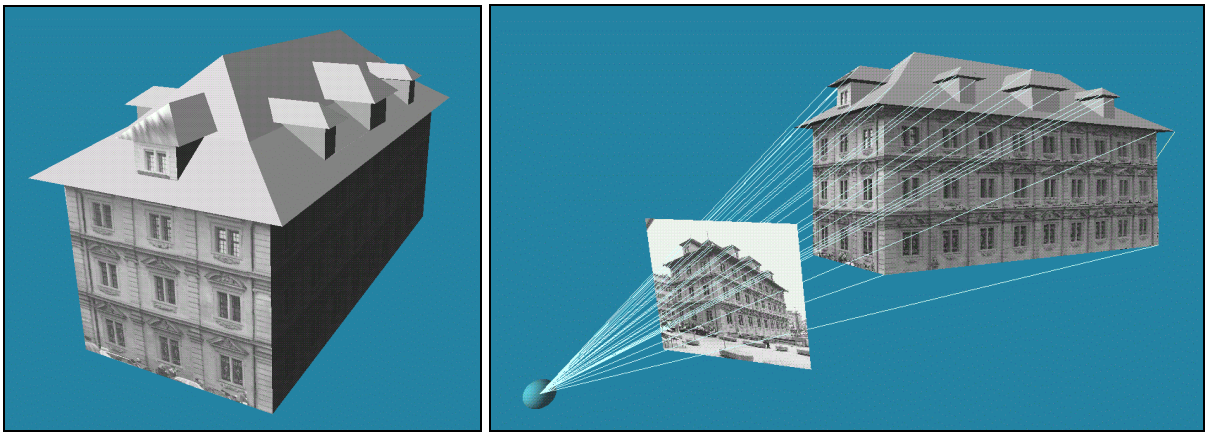

Figure 23: Reconstructed model (left) and model with image and rays (right).

The roof points of the window faces of the dorms are not visible in most images because they are occluded by the roofline itself (Figure 22). However, they could be reconstructed with the use of line measurements in combination with coplanarity constraints. Texture mapping by image rectification is only performed for faces of which all bordering edges are measured in one image (and the related image lines intersect at an angle larger than a threshold). For most faces of the roof and dorms this is not the case.

The additional geometric constraints consisted of three perpendicularity constraints and 24 plane parallelism constraints. Because a parallelism constraint involves two equations the total number of additional equations is 51 (=3+24x2). Halfway the roof there is an auxiliary horizontal plane established in order to make possible the reconstruction of the points where the roof bends. In Figure 24 the standard error ellipsoids of the points are shown. The three

[2] If not stated otherwise, units are at model scale. Note, the largest distance in the model is about 1.
[3] Equations added to eliminate the rank deficiency that results from over-parameterisation.

control points (seven coordinates fixed) are located at the bottom corners of the building. In the model on the left the parallelism constraint of the auxiliary face with the horizontal face at the bottom end of the roof was left out. As a result, the precision of the points degrades considerably.

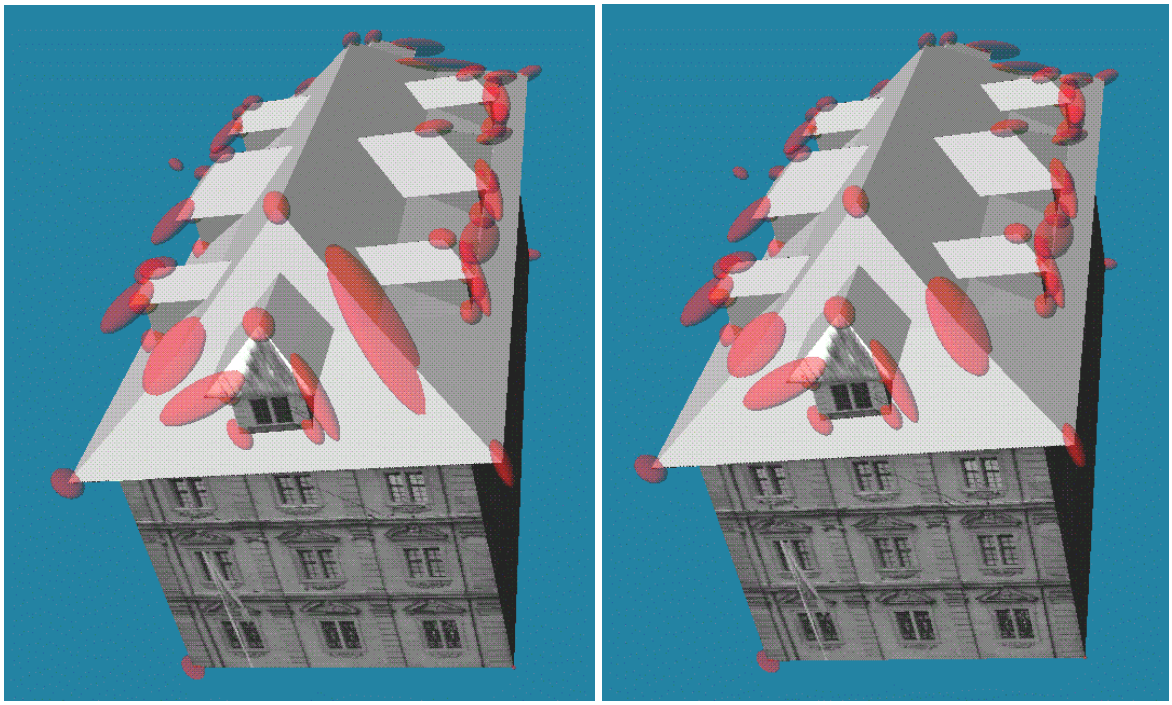

Figure 24: Standard ellipsoids of points enlarged with a factor 10 relative to the model. One plane parallelism constraint is removed for the reconstruction of the model on the left.

3.5 Conclusions

The processing of images of the CIPA reference data set has demonstrated the capabilities and limitations of the developed procedures for camera calibration, image orientation, and object reconstruction. The common characteristics of these procedures are:

- The incorporation of knowledge on the construction of the building
- Use of image line features, manually or automatically extracted
- The use of a limited number of images

Calibration of the camera was performed in a semi-automatic way with five images of the reference data set. A procedure for camera calibration from one or more images is outlined and applied. Interior orientation parameters were estimated using automatically and manually extracted lines in a single image. However, the quality of the results depends greatly on the image characteristics. For a full and accurate camera calibration, several images with different orientation relative the building are needed. Correspondence between the images is not required.

Two fundamentally different procedures for image orientation have been tested. The first one is based on partial model reconstruction from a single image followed by a similarity transformation between the models. The procedure is robust and in the tests performed resulting orientations differ less than 4 degrees from the adjusted values derived in a bundle adjustment. However, manual line measurements are needed. The second procedure aims at automation. Tests with images from the CIPA data set show that correct relative

orientation can be obtained, but as in the procedure for automated camera calibration, the chance of success greatly depends on the image configuration and characteristics. Especially the repeating structures (windows) in the façades lead to an ambiguous problem. Between two and three manually measured corresponding points were needed to obtain a correct and reliable solution, and at the same time allowed to determine the relative scale of consecutive models. Furthermore, the manual measurements reduce the computational burden considerably. The resulting relative orientations differed by up to 5 degrees form the values obtained with a bundle adjustment. A partial object model results as a by-product of the procedures for image orientation.

A full object model was reconstructed from manual line measurements in only four images taken at the building corners. The approximate values for the image orientations were obtained with the semi-automatic procedure for relative orientation. Approximate values of object point and plane parameters were obtained using the image line measurements. Geometric object constraints made possible the reconstruction of occluded object points, improved regularity of the object model as well as the quality of the network.

References

Heuvel, F.A. van den, 1997. Exterior Orientation using Coplanar Parallel Lines, 10th Scandinavian Conference on Image Analysis (SCIA'97), Lappeenranta, Finland, pp. 71-78.

Heuvel, F.A. van den, 1998. 3D reconstruction from a single image using geometric constraints. ISPRS J. of Photogrammetry and Remote Sensing, 53(6): 354-368.

Heuvel, F.A. van den, 1999a. Estimation of interior orientation parameters from constraints on line measurements in a single image. P. Patias (Editor). International Archives of Photogrammetry and Remote Sensing, Vol. 32 part 5W11, Thessaloniki, Greece, pp. 81-88.

Heuvel, F.A. van den, 1999b. A Line-photogrammetric mathematical model for the reconstruction of polyhedral objects. S.F. El-Hakim (Editor), Videometrics VI. proceedings of SPIE, Vol. 3641, San Jose, USA, pp. 60-71.

Heuvel, F.A. van den, 2002. Towards automatic relative orientation for architectural photogrammetry. P. Patias (Editor). International Archives of Photogrammetry and Remote Sensing, Vol. 34 part 5, Corfu, Greece, pp. 227-232.

Hrabacek, J. and Heuvel, F.A. van den, 2000. Weighted geometric object constraints integrated in a line-photogrammetric bundle adjustment, ISPRS congress. International Archives of Photogrammetry and Remote Sensing, Vol. 33, part B5, Amsterdam, pp. 380-387.

Rottensteiner, F., Grussenmeyer, P. and Geneva, M., 2001. Experiences with the digital photogrammetric program package Orpheus based on CIPA's "Zurich city hall" dataset for architectural photogrammetry, XVIII CIPA Int. symposium. proc, Potsdam, Germany, pp. 639-646.

Streilein, A., Grussenmeyer, P. and Hanke, K., 1999. "Zurich city hall" - A reference data set for digital close-range photogrammetry, XVII CIPA Symposium. proc, Olinda, Brazil, pp. CD.

Streilein, A., Hanke, K. and Grussenmeyer, P., 2000. First experiences with the "Zurich city hall" data set for architectural photogrammetry, ISPRS congress. International Archives of Photogrammetry and Remote Sensing, Vol. 33 part B5, Amsterdam, pp. 772-779.

4 Conclusions and future work

The papers on which this thesis is based present methods for the orientation of architectural images and their use for reconstruction. Orientation procedures have been developed for the interior as well as the relative, and the related exterior orientation. All the methods use image lines – manually or automatically extracted – as the principal type of observations and exploit generic knowledge of the object shape. Each procedure is to be regarded as a tool to be used in a system for photogrammetric reconstruction of architecture. This system is semi-automatic, aiming at minimising user interaction and keeping track of quality in all stages of the modelling process. Considerable efforts in research and development are still required to complete such a system. The author has concentrated on the research involved and does not aim at system development.

This chapter first addresses the envisaged integration of the methods presented in this thesis, then discusses the missing elements that supply the topics for future research, and finally draws conclusions.

4.1 Integration of the research results

Single image and multiple image processing have to be distinguished in a procedure for reconstruction using the methods presented in this thesis. Single image processing will be highly automated, while for multiple image reconstruction manual interaction is required. An integrated procedure is outlined as follows:

- Single image processing:
  - Image line extraction
  - Vanishing point detection, used for both interior and relative orientation (Heuvel, 1998b)
  - Approximate interior orientation, possibly from multiple images when these are acquired with the same camera and camera settings (Heuvel, 1999a)
- Multiple image processing:
  - Epipole detection (i.e. automated relative orientation) (Heuvel, 2002)
  - Manual line measurement for modelling, taking advantage of the (approximately) calibrated and oriented imagery, and collecting shape information
  - Integrated least-squares bundle adjustment (Heuvel, 1999b)

The last two steps are also applicable for reconstruction from a single image (Heuvel, 2001). During manual measurement, adjustment and testing of measurements can be performed and continuously updated to avoid the introduction of errors in an early stage of the modelling (Heuvel and Vosselman, 1997).

The procedure as outlined above is highly automatic, up to the stage of manual line measurements required for modelling. However, the results automatically obtained depend on the characteristics of the images. When automation fails, the methods allow user interaction for supplying additional information, or can be replaced by manual methods:

- Line extraction and vanishing point detection are replaced by manual line measurement and inference of object parallelism and orthogonality.
- Relative orientation is determined with the help of single image reconstructions based on the manual line measurements required for modelling (Heuvel, 1998a)

Final parameter estimation and assessment of their quality are performed through a least-squares bundle adjustment in which image line observations and object shape knowledge is integrated.

4.2 Future work

In the approach for reconstruction from a single or multiple uncalibrated images the camera calibration is separated from the reconstruction (Heuvel, 2001). This implies that uncertainty in the interior orientation parameters is not accounted for in the reconstruction. As a result the quality assessment resulting from the bundle adjustment is too optimistic. Approximate values for the interior orientation parameters are required for the adjustment. For finding these values a separate camera calibration step is suitable. However, these parameters should also be estimated in the bundle adjustment in which manual line measurements are used for the estimation of the object model parameters. The values found in the procedure using vanishing points can be introduced as weighted observations in order not to lose the information contained in the automatically extracted lines used for camera calibration. This self-calibration option is not implemented in the bundle adjustment.

For the estimation of lens distortion parameters it is disadvantageous that the current approach can only deal with straight image edges represented by their two endpoints. Currently long images lines, curved as a result of lens distortion, are approximated by several short straight edges. Estimation of lens distortion and image plane deformations is improved with the extraction and adjustment of curved image edges. An attractive approach for adjustment of measurements on curved image lines is presented in (Habib et al., 2002).

Adjustment of image line observations is part of most of the procedures presented in this thesis. The mathematical model adopted for parameter estimation is the so-called mixed model that is non-linear in both observations and parameters (Teunissen, 1999). The iterative procedure for obtaining the solution and especially the effects of errors and noise in the observations needs further investigation. The co-variance matrix of the parameters is computed using error propagation with a diagonal weight matrix for the original observations, i.e. endpoint co-ordinates of image lines. Statistical testing of the hypothesis of an error in an image line has been implemented for the vanishing point detection. It is recognised that in future work testing and reliability issues need to be studied in more detail.

The weighting of observations affects the computed precision of the parameters and is decisive for statistical testing. Some experiments with an image endpoint co-ordinate precision that depends on the line length have been performed (Heuvel, 1998b). More research on this topic is required. This is equally true for the weighting of the object shape constraints that have been implemented as observation equations (Heuvel, 1999b).

In the procedure for epipole detection relative orientation of two views is determined. Image points are created by intersecting lines of which the related object edges are assumed to be coplanar. At this point the purely line-based approach is abandoned. The main reason is the fact that a stronger geometry results from ray intersection than from intersection of interpretation planes. However, finding correspondence of image lines assuming the presence of coplanar object edges is worth investigating. Another option is to add a third image (Patias et al., 1995).

A logical next step is one towards fully automated reconstruction of buildings. As shown in (Heuvel, 2002) and chapter 3, the epipole detection results in a partial reconstruction as a by-product. The procedure has the potential to reconstruct unconnected parts of object faces. The challenge is to arrive at robust face detection and then gather evidence for the

intersection of the related planes in order to build the object topology. Image matching could play a role in the face detection. The results will improve with the use of more than two images, but greatly depend on the object structure and the presence of texture in the building faces. Related research on this topic is reported in (Werner and Zisserman, 2002).

4.3 Conclusions

In photogrammetry the procedures for camera calibration (i.e. interior orientation), relative, exterior (or absolute) orientation, and reconstruction are clearly distinguished and treated separately. In computer vision these steps are treated in a more integrated way in which only two steps are distinguished. The first step is the projective reconstruction in which image orientation and object reconstruction are combined. The second step is the rectification of the projective reconstruction into a metric one (Hartley and Zisserman, 2000). In the second step the interior orientation parameters are determined, while in photogrammetry camera calibration often is a first and separate step in which the interior orientation parameters are assumed not to vary from image to image. In many computer vision approaches each image introduces a new set of interior orientation parameters that weaken the solution in cases where several images are taken with the same sufficiently stable camera.

In this research orientation and reconstruction are intertwined. The basic reason is found in the use of object knowledge in all steps. The object knowledge is to be regarded as knowledge on the reconstruction and allows estimation of at least some interior orientation parameters, as well as partial object reconstruction from a single image. The latter can also be regarded as exterior orientation because the position and orientation of the image relative to the reconstruction is found at the same time.

In conclusion, the use of object knowledge results in an integration of the orientation and reconstruction procedures that are commonly separated in photogrammetry. In contrast to what is common in computer vision, the intermediate projective reconstruction is not established. The metric reconstruction implies determination of interior orientation as a pre-processing step as is common in photogrammetry. Approximate value computation is to be regarded as a near metric reconstruction when final interior orientation parameters are estimated in the bundle adjustment using self-calibration.

The research presented in this thesis mainly contributes to photogrammetry, but also to computer vision. It treats topics that seem to belong primarily to the field of computer vision in a photogrammetric way and offers new solutions. This photogrammetric approach is characterised by the development of robust direct solutions for approximate value computation, followed by integral least-squares adjustment. Quality control – implemented through statistical testing and precision computation of parameters – is part of both steps. Furthermore, the chosen approach is a semi-automatic one that aims at a reliable solution with a minimum of user interaction, while in computer vision one generally aims at full automation often under real-time constraints.

From a close-range photogrammetric standpoint the developed mathematical model for bundle adjustment using image lines, integrating shape constraints, and estimating the parameters of a polyhedral B-rep is an improvement compared to other approaches. These approaches often require corner point measurement, do not allow the use of shape constraints, or the topology of the B-rep cannot be taken into account in the adjustment. As shown in (Heuvel, 2001) this approach also allows a rigorous bundle adjustment and partial object reconstruction from line observations in a single image.

The developed bundle adjustment is applicable when a polyhedral B-rep is an appropriate object model. The methods that aim at automation are developed for architectural photogrammetry, although vanishing point detection has been successfully tested for image orientation in an industrial environment as well. A semi-automatic method has been developed for relative orientation of widely separated architectural images. This method has been demonstrated to be successful for angles between two optical axes of more than 60 degree, with repeating structure in the façades (Heuvel, 2002). The required manual interaction is limited to the measurement of a maximum of a few points, depending on the characteristics of the images and their configuration (chapter 3). The method results in a partial and approximate object reconstruction and therefore is to be regarded as a step towards automated reconstruction of structured object models of buildings.

References

Habib, A.F., Morgan, M. and Lee, Y.-R., 2002. Bundle adjustment with self-calibration using straight lines. Photogrammetric Record, 17(100): 635-650.

Hartley, R. and Zisserman, A., 2000. Multiple view geometry in computer vision. Cambridge University Press, Cambridge.

Heuvel, F.A. van den, 1998a. 3D reconstruction from a single image using geometric constraints. ISPRS J. of Photogrammetry and Remote Sensing, 53(6): 354-368.

Heuvel, F.A. van den, 1998b. Vanishing point detection for architectural photogrammetry. H. Chikatsu and E. Shimizu (Editors). International Archives of Photogrammetry and Remote Sensing, Vol. 32 part 5, Hakodate, Japan, pp. 652-659.

Heuvel, F.A. van den, 1999a. Estimation of interior orientation parameters from constraints on line measurements in a single image. P. Patias (Editor). International Archives of Photogrammetry and Remote Sensing, Vol. 32 part 5W11, Thessaloniki, Greece, pp. 81-88.

Heuvel, F.A. van den, 1999b. A Line-photogrammetric mathematical model for the reconstruction of polyhedral objects. S.F. El-Hakim (Editor), Videometrics VI. proceedings of SPIE, Vol. 3641, San Jose, USA, pp. 60-71.

Heuvel, F.A. van den, 2001. Object reconstruction from a single architectural image taken with an uncalibrated camera. Photogrammetrie Fernerkundung Geoinformation, 2001(4): 247-260.

Heuvel, F.A. van den, 2002. Towards automatic relative orientation for architectural photogrammetry. P. Patias (Editor). International Archives of Photogrammetry and Remote Sensing, Vol. 34 part 5, Corfu, Greece, pp. 227-232.

Heuvel, F.A. van den and Vosselman, G., 1997. Efficient 3D modeling of buildings using a priori geometric object information. S.F. El-Hakim (Editor), Videometrics V. proceedings of SPIE, Vol. 3174, San Diego, USA, pp. 38-49.

Patias, P., Petsa, E. and Streilein, A., 1995. Digital line photogrammetry - concepts, formulation, degeneracies, simulations, algorithms, practical examples, Eidgenössische Technische Hochschule (ETH), Zürich, Switserland.

Teunissen, P.J.G., 1999. Adjustment Theory, an Introduction. Delft University Press, Delft.

Werner, T. and Zisserman, A., 2002. New techniques for automated architectural reconstruction from photographs, ECCV 2002. Springer-Verlag, pp. 541-555.

Curriculum vitae

Frank van den Heuvel was born in 1959 in Heerlen. After completing his secondary education at “Het Nieuwe Lyceum” in Bilthoven in 1978, he started his studies in Geodetic Engineering at the Delft University of Technology. He obtained his degree “cum laude” in 1986. The title of his thesis was “Astrometric Satellite Hipparcos - Gridstep-Inconsistency Correction during Reduction on Circles”. In 1987 he was a research assistant for half a year at the University of New Brunswick in Canada, working on geodetic use of the Global Positioning System (GPS). From 1988 to 1994 he joined Ingenieursbureau Geodelta in Delft where he worked on numerous projects in close-range and aerial photogrammetry, GPS, and development of adjustment software for photogrammetry, surveying, and GPS. Furthermore, he conducted research in image matching and camera calibration. In 1994 he returned to the Department of Geodesy of the Delft University of Technology where he became an assistant professor. Until 1996 he contributed to a handbook for the Dutch Cadastre titled “Handleiding voor de Technische Werkzaamheden van het Kadaster”. At the Department of Geodesy he is responsible for education in close-range photogrammetry and has participated in many research projects in different application fields, such as industrial, medical, and architectural photogrammetry. He has authored and co-authored over 35 papers, mainly in the field of close-range photogrammetry. His work on architectural photogrammetry is presented in this PhD thesis.